FERMION MASSES AND MIXINGS, LEPTOGENESIS AND BARYON NUMBER VIOLATION IN UNIFIED THEORIES

By

Shaikh Saad

Bachelor of Science (Hons.) in Physics
University of Dhaka
Dhaka, Bangladesh
2009

M.Sc. in Theoretical Physics
University of Dhaka
Dhaka, Bangladesh
2010

Submitted to the Faculty of the
Graduate College of the
Oklahoma State University
in partial fulfillment of
the requirements for
the Degree of
DOCTOR OF PHILOSOPHY
July, 2017

FERMION MASSES AND MIXINGS, LEPTOGENESIS AND BARYON NUMBER VIOLATION IN UNIFIED THEORIES

Dissertation Approved:

Regents Prof. Kaladi S. Babu

Dissertation Advisor

Associate Prof. Alexander Khanov

Assistant Prof. Joseph Haley

Prof. Birne Binegar

ACKNOWLEDGMENTS

First, I would like to express my sincere gratitude to my thesis advisor Dr. Kaladi Babu for his valuable advice, patient guidance, inspiration, constructive criticism and continuous support all along my Ph.D. life. Besides my advisor, I can not thank enough to my committee members Dr. Alexander Khanov, Dr. Joseph Haley and Dr. Birne Binegar for critical insights and suggestions and for their interest in my work. I would also like to thank Dr. Satyanarayan Nandi and Dr. Jacques Perk who were initially a part of my committee for all their supports, valuable comments and showing intense interest in my research work. I would like to acknowledge my collaborators Dr. Borut Bajc and Dr. Alexander Khanov for their help, support and stimulating discussions. I would like to express my deepest appreciation to my former advisor Dr. Arshad Momen, who has been a great mentor for me during my Bachelor and Masters degree programs and for providing me inspiration and moral support till now. I would like to thank Dr. Talal Ahmed, who is a good friend of mine, for all the fascinating discussions and encouragement since my Bachelor program till now. I would like to thank our current Post-doc Dr. Tathagata Ghosh for useful discussions and ongoing collaboration. Special thank to Dr. Julio Julio, Dr. Ayon Patra and Dr. Saki Khan who are the fellow graduate students and Sudip Jana who is a current graduate student of the High Energy Group here at Oklahoma State University for interesting and helpful discussions.

I would like to thank the department of physics and the High Energy Physics Group, Oklahoma State University for providing me assistantship to carry out my degree program. I am also indebted to the staffs of the department of physics, specially to Susan Cantrell, for their endless supports and all sorts of helps. I would like to acknowledge the recipient of the Robberson Summer Fellowship 2016 from the Graduate College, Oklahoma State University. I would also like to thank the organizers of CETUP* 2015 and CETUP* 2017, specially to Barbara Szczerbinska for hospitality and giving me the opportunity to participate in the workshops which is full of creative and stimulating discussions.

Last but not the least, I would like to express my deepest gratitude to my mom Selina and my siblings Zeba, Tasneem and Shoaib, who have been providing me encouragement and moral support all through my life. No achievement would have been possible without the endless love and care of my family. I am also grateful to my friends, specially to my best friends, Sharmi and Sagar for always be there for inspiring me. [1]

[1] Acknowledgements reflect the views of the author and are not endorsed by committee members or Oklahoma State University

Name: Shaikh Saad

Date of Degree: JULY, 2017

Title of Study: **FERMION MASSES AND MIXINGS, LEPTOGENESIS AND BARYON NUMBER VIOLATION IN UNIFIED THEORIES**

Major Field: Physics

Abstract: In this dissertation, we study physics beyond the Standard Model (SM) of particle physics to incorporate some of its unexplained phenomenon. Grand Unified Theories (GUTs) are natural extensions of the SM, since gauge coupling unification can be realized in these theories. Also in GUTs, charged quantization can be explained, the hierarchical pattern of the charged fermion spectrum may be understood due to unification of quarks and leptons into same multiplet, extremely small neutrino mass naturally arises via the seesaw mechanism, the cosmological baryon asymmetry of the universe can be explained within the GUT framework and some of the unified theories naturally include Dark Matter candidates. Here, we study several different unified theories that are potential candidates for theories beyond the SM. First we study a class of unified models based on the $SO(10)$ gauge symmetry without the presence of the Higgs in the fundamental 10_H representation, as has been used in the literature for most of the $SO(10)$ constructions. Instead, a vector-like fermion in the spinorial representations $16 + \overline{16}$ is introduced to accommodate flavor mixing. In this new framework, two different non-supersymmetric models and four inequivalent supersymmetric models are studied. This framework provides insights into the fermion masses and mixings. Proton decay branching ratios are also analysed in this context. Then we study a non-supersymmetric $SO(10)$ model and show that the most economic Yukawa sector of such theories consists of a real 10_H, a real 120_H and a complex 126_H Higgs, provided that $SO(10)$ is the only symmetry of the theory. Usual constructions based on non-supersymmetric $SO(10)$ models complexify these Higgs fields, which require additional symmetry exterior to the original gauge symmetry. We show that, with $SO(10)$ being the only symmetry of the theory, a good fit to the full fermion spectrum can be achieved with the economic Higgs sector mentioned above. Furthermore, gauge coupling unification is studied and within this theory the leading proton decay branching ratios are found to be $p \to \overline{\nu}\pi^+$ and $p \to e^+\pi^0$. Then we study a class of unified models with $SU(5)$ gauge symmetry and follow statistical approach to predict the fermion spectrum from the theory. The Yukawa coupling matrices in this theory are assumed to be non-hierarchical, that is structure-less. The observed hierarchies in the fermion masses and mixings are reproduced with only three parameters of the theory that are assumed to be hierarchical. A detail Monte Carlo analysis shows that, with Yukawa couplings being uncorrelated random variables obeying Gaussian distributions, all observables in the fermion sector can be nicely reproduced. Then we study a minimal partial unified model based on the $SU(2)_L \times SU(2)_R \times SU(4)_C$ gauge symmetry. A good fit to the full fermion spectrum is achieved, where the seesaw mechanism is responsible for generating neutrino masses and Leptogenesis mechanism can account for the observed cosmological baryon asymmetry of the universe. On top of the gauge symmetry, an imposed global Peccei-Quinn symmetry $U(1)_{PQ}$ solves the strong CP problem and simultaneously provides the axion as the Dark Matter candidate. We also study nucleon decay modes and nuetron-antineutron oscillation in this framework.

TABLE OF CONTENTS

Chapter Page

LIST OF FIGURES

LIST OF TABLES

CHAPTER 1

INTRODUCTION

1.1 The Standard Model of Particle Physics

1.1.1 The Structure of the Standard Model

The Standard Model (SM) of particle physics is a highly successful theory to explain the nature at very short distances. Within our limitations of the technical ability, the SM so far is consistent with experimental observations and describing physics at the microscopic level. The SM describes the electromagnetic, the strong and the weak interactions. All the observed microscopic phenomena can be explained within these three forces. According to the SM, matter is made of two types of elementary particles, the quarks and the leptons. Elementary particle are the constituents that do not have any substructure. The quarks and the leptons are fermions, that is spin $\frac{1}{2}$ particles. In the SM, there are three lepton doublets, $\{\ell^-, \nu_\ell\}$ $(\ell = e, \mu, \tau)$ the electron with electric charge -1 and its associated neutrino which is electrically neutral. There exist two different types of quarks, the up-type quarks that carry electric charge of $+\frac{2}{3}$ and down-type quark with $-\frac{1}{3}$ charge. Like the leptons, three quark doublets are present in the SM, $\{q^{+\frac{2}{3}}, q^{-\frac{1}{3}}\}$ ($q^{+\frac{2}{3}} = u, c, t$ and $q^{-\frac{1}{3}} = d, s, b$). In addition to fermions (spin $\frac{1}{2}$), SM also contains bosons (particles with either zero or integer spin) of two different types, vector bosons (spin-1 particles) and scalar bosons (spin-0 particles). The force experienced between two fundamental matter particles are caused by the exchange of gauge (vector) bosons. For different types of forces, different gauge bosons need to be present. To explain our nature, the structure of the SM consists of the following gauge group:

$$SM \equiv SU(3)_C \times SU(2)_L \times U(1)_Y. \tag{1.1.1}$$

The strong interactions

The $SU(3)_C$ gauge group is responsible for the strong interactions. In addition to electric charge, particles that have strong interaction must be charged under $SU(3)$ group. This new quantum number is known as color charge. Not all elementary particles are charged under the color group. This strong dynamics described by $SU(3)_C$ gauge group is also known as Quantum Chromodynamics (QCD). Among the fermions, since quarks carry color charge, this group acts on the quarks. Each type of quark form a fundamental representation of $SU(3)_C$. The strong interaction between two colored particles are exchanged by the gauge bosons, called the

gluons, G^A_μ (μ is the Lorentz index). Since gauge bosons belong to the adjoint representation of the group, there exist eight gluons ($A = 1 - 8$) since $SU(3)$ group has eight generators.

The QCD is a renormalizable gauge theory described by the following Lagrangian:

$$\mathcal{L}_{QCD} = \overline{q}_j(i\gamma^\mu D_\mu - m_j)q_j - \frac{1}{4}F^{A\,\mu\nu}F^A_{\mu\nu}, \tag{1.1.2}$$

where, q_j are the quark fields in the triplet representation and $j = 1 - 3$ is the generation index. m_j represents the mass of the quark q_j (we will briefly discuss about the mass generation at the later part of this section) and the covariant derivative is given by:

$$D_\mu = \partial_\mu - ig_s t^A G^A_\mu. \tag{1.1.3}$$

Here, g_s is the gauge coupling constant, that determines the strength of the strong interaction and t^A ($A = 1-8$) are the $SU(3)$ generators. These generators obey the usual $SU(3)$ commutation relation $[t^A, t^B] = if_{ABC}t^C$, where f_{ABC} are the group structure constants. And the field strength, $F^A_{\mu\nu}$ is given by

$$F^A_{\mu\nu} = \partial_\mu G^A_\nu - \partial_\nu G^A_\mu - g_s f_{ABC} G^B_\nu G^C_\nu. \tag{1.1.4}$$

From this Lagrangian Eq. (1.1.2), it is clear that, just like Quantum Eelectrodynamics (QED), the usual physical vertex fermion-antifermion-gauge boson is present (here gauge bosons are the gluons, instead of photons in QED). The dynamics of QCD is richer than QED, which is due to the non-abelian nature of the group. From Eqs. (1.1.2) and (1.1.4), one can see that, 3-gluon and 4-gluon vertices are possible (unlike QED). It is due to the presence of the G^2 term in Eq. (1.1.4), that leads to cubic and quartic interactions in the QCD Lagrangian.

The electroweak interactions

The $SU(2)_L \times U(1)_Y$ part of the SM describes the unified weak and electromagnetic interactions. $SU(2)_L$ is the weak isospin group, acting on the left-chiral fermions and $U(1)_Y$ represents the hypercharge group. The interactions of $SU(2)_L$ group is carried by three gauge bosons W^a_μ ($a = 1 - 3$), whereas the gauge boson corresponding to $U(1)_Y$ group is B_μ. Left-chiral fermions are in the doublet representation of $SU(2)_L$, where as the right-chiral fermions are the singlets and all the fermions of the SM carry non-zero charge under $U(1)_Y$. In Table 1.1, we show the quantum numbers of all the fermions in the SM.

The dynamics of the $SU(2)_L \times U(1)_Y$ interactions is given by the following Lagrangian:

$$\mathcal{L}_{ew} = \overline{\psi}_L i\gamma^\mu D_\mu \psi_L + \overline{\psi}_R L i\gamma^\mu D_\mu \psi_R - \frac{1}{4}F^{a\,\mu\nu}F^a_{\mu\nu} - \frac{1}{4}B^{\mu\nu}B_{\mu\nu}. \tag{1.1.5}$$

With the field strengths,

$$B_{\mu\nu} = \partial_\mu B_\nu - \partial_\nu B_\mu \;\text{ and }\; F^a_{\mu\nu} = \partial_\mu W^a_\nu - \partial_\nu W^a_\mu - g\epsilon_{abc}W^b_\nu W^c_\nu. \tag{1.1.6}$$

$\begin{pmatrix} u_L \\ d_L \end{pmatrix}, \begin{pmatrix} c_L \\ s_L \end{pmatrix}, \begin{pmatrix} t_L \\ b_L \end{pmatrix}$	: (3,2, $\frac{1}{6}$)
u_R, c_R, t_R	: (3,1, $\frac{2}{3}$)
d_R, s_R, b_R	: (3,1, -$\frac{1}{3}$)
$\begin{pmatrix} \nu_L^e \\ e_L \end{pmatrix}, \begin{pmatrix} \nu_L^\mu \\ \mu_L \end{pmatrix}, \begin{pmatrix} \nu_L^\tau \\ \tau_L \end{pmatrix}$	: (1,2, -$\frac{1}{2}$)
e_R, μ_R, τ_R	: (1,1, -1)

Table 1.1: Quantum numbers of the fermions (spin $\frac{1}{2}$) under $SU(3)_C \times SU(2)_L \times U(1)_Y$.

Here ϵ_{abc}, the Levi-Civita tensor (completely antisymmetric) are the structure constants of the group $SU(2)$ and g being the gauge coupling constant of $SU(2)_L$ group. The covariant derivative is given by:

$$D_\mu = \partial_\mu - igt^a W_\mu^a - \frac{i}{2} g' Y B_\mu. \tag{1.1.7}$$

Where, g' is the gauge coupling constant associated with the hypercharge group $U(1)_Y$. The generators of the groups $SU(2)_L$ and $U(1)_Y$ are represented by t^a $(a = 1-3)$ and $\frac{1}{2}Y$ respectively. The $SU(2)$ generators follow the same commutation relation as mentioned above for $SU(3)$ group, with the structure constants f_{ABC} being replaced by ϵ_{abc}. Now, using the normalization of the generators as follows:

$$Tr[t^a t^b] = \frac{1}{2}\delta^{ab}, \tag{1.1.8}$$

the electric charge operator, Q can be written as:

$$Q = t^3 + \frac{1}{2}Y. \tag{1.1.9}$$

The hypercharge of the particles are presented in Table 1.1, so one can straightforwardly compute the electric charge of these particles.

From the charged-current interactions in the Lagrangian Eq. (1.1.5), it is straightforward to show that the eigenstates of the charged gauge bosons are

$$W^\pm = (W^1 \pm iW^2)/\sqrt{2}, \tag{1.1.10}$$

and from the neutral-current interactions, the eigenstates of the two neutral gauge bosons are given by

$$A_\mu = \cos\theta_W B_\mu + \sin\theta_W W_\mu^3, \tag{1.1.11}$$

$$Z_\mu = -\sin\theta_W B_\mu + \cos\theta_W W_\mu^3. \tag{1.1.12}$$

A_μ is the photon field and Z_μ mediates the weak neutral-current interactions. Here, θ_W represents the Weinberg angle defined as:

$$\tan\theta_W = \frac{g'}{g}. \tag{1.1.13}$$

As usual, in the Lagrangian Eq. (1.1.5) the left-chiral (ψ_L) and the right-chiral (ψ_R) fermion fields are obtained by using the left and right projection operators defined as:

$$L = \frac{1-\gamma_5}{2}; \quad R = \frac{1+\gamma_5}{2}. \tag{1.1.14}$$

As explicitly shown in Table 1.1, the left-chiral and right-chiral fermions in the SM have different transformation properties under the gauge group, hence their interactions are different. This is why the bare mass term, which is of the form $m\overline{\psi}_L\psi_R$ is forbidden in the Lagrangian, since this combination is not gauge invariant. This is why the SM is a chiral theory, since the left-chiral and right-chiral fields behave differently under the SM gauge group. The gauge bosons of the SM are also massless in the symmetric limit. It will be pointed out below that, the mechanism that generates the fermion mass, is also responsible for generating gauge boson masses.

At low energy the $SU(2)_L \times U(1)_Y$ group spontaneously breaks down to $U(1)_{em}$, that explains the electromagnetic interactions. To realize such breaking pattern, the SM should contain another type of particle known as the Higgs field, ϕ_α ($\alpha = 1, 2$) which is a scalar boson (spin-0 particle). This Higgs field is in the doublet (fundamental) representation of $SU(2)_L$ and has hypercharge of $\frac{1}{2}$ under $U(1)_Y$.

$$\phi = \begin{pmatrix} \phi^+ \\ \phi^0 \end{pmatrix} : (2, \frac{1}{2}). \tag{1.1.15}$$

This spontaneously symmetry breaking scenario is know as the Brout-Englert-Higgs-Kibble mechanism [1–4] (Higgs mechanism for short) and the electro-weak theory, based on the spontaneous broken of $SU(2)_L \times U(1)_Y$ symmetry down to $U(1)_{em}$ symmetry is known as the Glashow-Salam-Weinberg (GSW) model [5–7].

The Higgs mechanism

Now we will explain the Higgs mechanism very briefly. The part of the SM Lagrangian that contains the interactions involving the Higgs field is given by:

$$\mathcal{L}_{Higgs} = (D_\mu\phi)^\dagger(D^\mu\phi) - V(\phi) - (\overline{\psi}_{Li}y_{ij}\psi_{Rj}\phi + h.c.). \tag{1.1.16}$$

Here, y_{ij} are the Yukawa coupling constants that represnt the interaction of the fermion with the Higgs field. The most general gauge invariant renormalizable potential can be written as

$$V(\phi) = -\frac{1}{2}\mu^2\phi^\dagger\phi + \frac{1}{4}\lambda(\phi^\dagger\phi)^2. \tag{1.1.17}$$

When the Higgs field acquires a vacuum expectation value (VEV), $\langle\phi^0\rangle = v \neq 0$, the SM gauge group is spontaneously broken down to $U(1)_{em}$ group.

Due to this symmetry breaking, three of the four gauge bosons will acquire mass due to Goldstone-Nambu theorem [8–11]. The remaining massless gauge boson corresponds to the photon. The mass of the gauge bosons

can be computed from the Higgs Lagrangian Eq. (1.1.16) in a straightforward way. Using the definitions of the eigenstates of the gauge bosons given in Eqs. (1.1.10) and (1.1.11), it can be easily shown that the Higgs kinetic term contains the following terms

$$\mathcal{L}_{Higgs} \supset \frac{1}{2} g^2 v^2 W_\mu^+ W^{-\mu} + \frac{1}{2} g^2 v^2 / \cos^2\theta_W Z^\mu Z_\mu \tag{1.1.18}$$

$$= \frac{1}{2} m_W^2 W_\mu^+ W^{-\mu} + \frac{1}{2} m_Z^2 Z^\mu Z_\mu. \tag{1.1.19}$$

As mentioned earlier, this same mechanism is responsible for generating fermion masses as well. Which can be seen from the Lagrangian Eq. (1.1.16). This is obvious, since ϕ will be reaplced by its VEV, v. Due to the symmetry breaking, the fermions get mass which is proportionality to the corresponding Yukawa coupling strength ($m_f = v\ y_f$). In the SM these Yukawa couplings are not determined, rather needs to be measured experimentally.

In the SM, there exist only one Higgs doublet. Its mass can also be computed form the Lagrangian Eq. (1.1.16), and is given by $m_H^2 = \lambda v^2$, where the quartic coupling λ in the SM is also a free parameter. Even though the existence of the Higgs field was predicted many years ago, only recently it has been discovered in the experiments at the Large Hadron Collider (LHC) [12, 13] and its mass is measured to be 126 GeV. All the elementary particles predicted by the SM have been discovered and the prediction of the SM are experimentally verified. So far all the measurements are completely consistent with theory.

1.1.2 Shortcomings of the Standard Model

Despite of the extreme success of the SM, still there are some observed phenomena, that can not be explained by the SM. In the SM, the neutrinos are assumed to be massless. However, non-vanishing mass of the neutrinos have been firmly confirmed through the oscillations experiments [121–123]. The Yukawa couplings in the SM are completely arbitrary parameters. Among the nineteen free parameters in the SM, fourteen of them are associated with the flavor sector, six quark masses, three charged lepton masses, four quark mixing parameters (three mixing angles and a Dirac type CP violating phase). Since neutrinos are observed to have mass, it adds another nine parameter into the theory, the three masses, three mixing angles and three CP-violating phases. Due to this enormous freedom available in the Yukawa sector, the SM is completely unable to provide any insight into the fermion masses and mixings. This shortcoming of the SM is known as the falvor puzzle. The other parameter lies in the strong sector, known as the θ parameter. The θ parameter is associated with an additional term in the QCD Lagrangian given by:

$$\mathcal{L}_\theta = \frac{\theta}{16\pi^2} F_{\mu\nu}^A \widetilde{F}^{A\mu\nu}, \tag{1.1.20}$$

where, $\widetilde{F}^A_{\mu\nu\rho\sigma} = \frac{1}{2}\epsilon\mu\nu\rho\sigma F^{A\rho\sigma}$. This operator violates CP and through loop diagram, this term contributes to

the neutron electric dipole moment. From the experimental constraints on the neutron electric dipole moment, θ parameter needs to be very small, $\theta \ll 10^{-9}$. Whereas, due to naturalness, this parameter is expected to be of the order of one. Theoretically, there is no understanding, why this needs to be so small and this is known as the strong CP problem.

Also, charge quantization is not self-explanatory within the SM. Experimentally, the charge of the electron and the proton are the same, $|1 - Q_e/Q_p| < 10^{-21}$. Proton is not an elementary particle and it consists of three quarks, two up-type quarks and a down-type quark. In principle there is no reason for the charges of electron and the proton to be the same. The electric charge of the fundamental particles are computed from the formula given in Eq. 1.1.9. Since electric charge is an experimentally measured quantity, the hypercharges in the SM are assigned accordingly to match with the observed electric charge. In short, fundamental understanding of the charge quantization is lacking in the SM.

Furthermore, other phenomenological observations, such as the existence of Dark Matter (DM) and Baryon asymmetry of the universe can not be incorporated in the SM. The existence of the DM in the universe was a really surprising result. It is found that only 4.9% of the total mass-energy of the known universe is made up of ordinary matter. Among the rest, 26.8% consists of DM and rest is contributed by the dark energy. The most convincing, as well as one of the earliest evidence of DM was discovered from the galactic rotation curves [17]. The most recent accurate critical density determination of DM is obtained from the global fits of cosmological parameters [18]. The density of cold, non-baryonic matter and the density of baryonic matter, using the measurements of the partial distributions of the galaxies and the anisotropy of the cosmic microwave background are found to be:

$$\Omega_{DM} h^2 \sim 0.1186 \pm 0.0020, \tag{1.1.21}$$

$$\Omega_{BM} h^2 \sim 0.02226 \pm 0.00023, \tag{1.1.22}$$

where, h represents the Hubble constant in the units of $100 km/s.Mpc$.

The matter-antimatter asymmetry of the universe is another mystery which can not be solved within the SM. Our observed universe is matter dominated and the presence of the animatter is almost negligible. At the very early stages of the history of the universe after the big bang, matter and antimatter were present with the creation and the annihilation reactions in thermal equilibrium. The energies in the cooling plasma at some later times started to become small enough for pair production to take place and hence, matter and antimatter annihilated with a small portion of the matter left in the plasma. Detonating n_b and $n_{\bar{b}}$ as the baryon and antibaryon numbers, the baryon asymmetry of the universe is defined as:

$$\eta = [\frac{n_b - n_{\bar{b}}}{n_\gamma}]_{T=3K}, \tag{1.1.23}$$

where, n_γ is the photon number. The baryon asymmetric parameter in today's universe is measured [19, 20] to be:

$$\eta \sim 6 \times 10^{-10}. \tag{1.1.24}$$

Theoretically, this asymmetry in the baryon number may be generated dynamically and known as baryogenesis. There exist three necessary conditions to accommodate successful baryogenesis, known as the Sakharov conditions [21], that are: (i) baryon number violation, (ii) C and CP violation and (iii) deviation from thermal equilibrium. Within the SM there is not enough CP-violation that can incorporate the observed baryon asymmetry given in Eq. 1.1.24, new source of CP-violation is needed beyond the SM.

These are some clear indications that the SM is not a complete theory and begs for extension for a more complete theory and for better understanding of the nature.

1.1.3 Organization of this Dissertation

The purpose of this dissertation is to incorporate some of the unexplained phenomena of the SM. This is certainly done by extending the SM. Particular attention is paid to explain the flavor puzzle, baryon asymmetry and baryon number violation. To solve these shortcoming of the SM, the attempt taken in this dissertation is by embedding the SM in to unified theories. In chapter 2, we study a new class of unified theories based on the $SO(10)$ gauge symmetry. These proposed new models provide insights into the fermion masses and mixings, both the charged fermions and the neutrinos. Unlike the conventional $SO(10)$ models, the Higgs boson belonging to the fundamental representation, 10_H is not present in this new class of models. Instead a vector-like fermions in the $16 + \overline{16}$ representation is introduced to induce the flavor mixing. A variety of scenarios, both non-supersymmetric and supersymmetric, are studied within this framework. For symmetry breaking purpose, $\overline{126}_H$ Higgs is accompanied by either a 45_H or a 210_H of Higgs boson. Our analysis shows that this framework, by utilizing either type-I or type-II seesaw mechanism, an excellent fit to the fermion masses and mixings can be obtained with a limited number of parameters. To test and distinguish these flavor models, proton decay branching ratios are also computed.

In chapter 3, we construct a realistic model, based on the $SO(10)$ gauge group with the most economic Yukawa sector. Here we work in the non-supersymmetric framework. The group theory of the $SO(10)$ demands that the Higgs fields belonging to the 10_H and 120_H representations are real (126_H is inherently complex), whereas most constructions seem to compleixify these fields, this complexification is done to reduce the number of the parameters of the theory for the sake of predictability. However, this complxification demands additional symmetry into the theory which is exterior to the original $SO(10)$ gauge symmetry, either discrete or continuous symmetry. In this work, we prove that, a realistic model can be built without extending the symmetry of the

theory and the minimal Higgs sector of such a theory consists of a real 10_H, a real 120_H and a complex 126_H. A good fit to the fermion masses and mixings, including the neutrino sector is found. We also study the gauge coupling unification and proton decay branching ratios that can be tested experimentally.

In chapter 4, we attempt to solve the flavor puzzle in light of anarchy hypothesis. Here, we develop a class of unified models based on the $SU(5)$ gauge symmetry. In these theories, the fundamental Yukawa coupling matrices are assumed to be completely structure-less, that is, no hierarchy among the different entries is assumed. The observed hierarchies of the fermion masses and mixings are incorporated by the only three model parameters, that are assumed to be hierarchical. The Yukawa couplings are treated to be completely uncorrelated random variables that follow Gaussian distributions. In our statistical analysis, we follow Monte Carlo simulations and show that, the observed fermion masses and mixings in the charged fermion and the neutrino sector can be reproduced that is in good agreement with the experimental data.

In chapter 5, we build a model based on a partial unified theory, known as the Pati-Salam model. The gauge symmetry of this model is $SU(2)_L \times SU(2)_R \times SU(4)_C$, and we work in the non-supersymmetric framework. We build a minimal model and show that, it can explain the flavor data. To explain the neutrino mass, seesaw mechanism is assumed, which together with Leptogenesis scenario can explain the baryon asymmetry of the universe. Pati-Salam model, extended by the global $U(1)_{PQ}$ Peccei-Quinn symmetry can simultaneously solve the strong CP problem and provide a Dark Matter candidate, which is the axion. Even though the gauge bosons of the Pati-Salam theory do not mediate proton decay, nucleon decay can be originated due to the presence of scalar diquarks and leptoquarks. Possible nucleon decay modes and neutron-antineutron oscillation are studied. In chapter 6, we conclude.

CHAPTER 2

NEW CLASS OF $SO(10)$ MODELS FOR FLAVOR

2.1 Introduction

Grand unified theories [22–24] based on $SO(10)$ gauge symmetry [25] are attractive candidates for physics beyond the Standard Model (SM). These theories predict the existence of right-handed neutrinos needed for the seesaw mechanism, and unify all fermions of a given family into a single irreducible multiplet, the 16–dimensional spinor representation. Quarks and leptons are thus unified, as are the three gauge interactions of the SM. The unification of fermions into multiplets suggests that $SO(10)$ may serve as a fertile ground for understanding the flavor puzzle. There are challenges involved, since in particular, large neutrino mixing angles should emerge from the same underlying Yukawa structure that allows for small quark mixing angles. This indeed has been realized in a class of $SO(10)$ models with a minimal set of Yukawa coupling matrices [26–34], and we shall provide a new class of models that achieves this in this paper. Since $SO(10)$ admits an intermediate symmetry, the Pati-Salam symmetry $SU(4)_c \times SU(2)_L \times SU(2)_R$ or one of its subgroups, unification of gauge couplings can occur consistently even without low energy supersymmetry. Of course, $SO(10)$ may be realized in the supersymmetric context as well, in which case the intermediate symmetry breaking scale may be the same as the unification scale. As far as the Yukawa sector of the theory is concerned, the two scenarios (non-SUSY versus SUSY) are not all that different. In this paper we shall study a new class of $SO(10)$ models addressing the flavor puzzle both in the non-supersymmetric and in the SUSY contexts.

One of our motivations for the present study is the difficulty faced by a widely studied minimal renormalizable supersymmetric SO(10) [35–37] grand unified theory. This theory has attracted much attention in the past due to several attractive features which include:

- natural generation of neutrino masses and mixings through type I [38] and type II [39] seesaw mechanism;
- relation between neutrino and charged fermion mass matrices [26];
- good fit of fermion masses and mixings with an economic Yukawa sector with only two symmetric Yukawa matrices [26–34];
- automatic and exact low energy R-parity conservation leading to a compelling dark matter candidate

[40–44];

- connection of the $b-\tau$ Yukawa unification and large atmospheric mixing angle in scenarios with dominant type II seesaw mechanism [45–47].

The Yukawa sector of this theory has only two symmetric matrices (in flavor space), involving a 10_H and a $\overline{126}_H$ of Higgs bosons. It is natural to include a 210_H for completing the symmetry breaking. In such a scenario, unfortunately, once the constraints from the Higgs sector are properly taken into account, the model can be ruled out [48–51], assuming that the low energy supersymmetric threshold corrections to the fermion masses are negligible. With the relatively large Higgs mass $m_H = 125$ GeV, the split supersymmetric scenario [52, 53] of the minimal $SO(10)$ model [54] is also found to be inconsistent [56, 57][1].

One should not abandon the whole elegant grand unified program simply because the simplest supersymmetric realization does not work perfectly. The usual way to rule in a theory that was ruled out is to increase the particle content and thus the number of model parameters. This was the approach of [58], where a new 120-dimensional Higgs representation has been added to the minimal model.[2] In this way the Yukawa sector increases by one antisymmetric matrix, which gives sufficient freedom to fit the data.

In this paper [59] we will go, surprisingly, in the opposite direction, and ask ourselves, if it is possible to fit the data with less, not more, Yukawa matrices. This paradoxical question has obviously a hidden proviso, otherwise we would get no mixing at all. To account for the correct low energy mass spectrum, mixings, and CP violation we will thus make use of an extra vector-like generation $16 + \overline{16}$, similar to the one used in [60]. The difference with [60] is that we will assume the bilinear spinors 16_a to be coupled with $\overline{126}_H$ instead of 10_H. In this way we may hope to describe neutrino masses and mixings in a pattern similar to the charged fermions, which is one of the great achievements of the $SO(10)$ framework.

We shall see that this decreasing of the number of Yukawa matrices at the expense of an extra vector-like family can be successful and we will show several examples where it works. Although we will consider different possible Higgs sectors and take some of their constraints seriously, we will not consider a combined fit of the Higgs and Yukawa parameters, which can obviously pose extra restrictions. This more modest approach nevertheless shows that $SO(10)$ Yukawa sectors with a single Yukawa matrix can be realistic.

The rest of the paper is organized as follows. In Sec. II we present the key features of the new class of $SO(10)$ models. In Sec. III we set up the framework and the formalism. In Sec. IV we adopt a specific basis that removes redundancies, which is well suited for numerical analysis of the flavor observables. Sec. V discusses

[1] BB thanks Ketan Patel for pointing this out.

[2] Another possibility, not yet fully explored, is to increase the Higgs sector parameters, for example with a 54_H, see Ref [28] for fermion fits.

the constraints imposed on the SUSY models from the minimization of the Higgs potential. Sec. VI has our numerical fits to the fermion masses and mixings for the six models analyzed. Finally, in Sec. VII we conclude.

2.2 New class of $SO(10)$ models

The key feature of the new proposed models is the absence of 10_H. In its place we introduce a $16+\overline{16}$ vector-like fermions. In addition to a $\overline{126}_H$, we employ either a 45_H or a 210_H for symmetry breaking. These fields have non-trivial couplings to the vector-like fermions, which is needed to avoid certain unwanted relations among down-type quark and charged lepton masses. Additional Higgs fields (e.g. 54_H) are needed for consistent GUT symmetry breaking, but these fields do not enter into the Yukawa sector. The Yukawa Lagrangian of our models has a very simple form,

$$\mathcal{L}_{\rm Yuk} = \overline{16}\,(m_a + \eta_a 45_H)\,16_a + 16_a\,\mathcal{Y}_{ab}\,\overline{126}_H\,16_b + \overline{16}\,\bar{y}\,126_H\,\overline{16} + h.c. \tag{2.2.1}$$

corresponding to the use of 45_H as the symmetry breaking field (in addition to the $\overline{126}_H$ field). Here $a,\, b = 1-4$ are the generation indices which include a 16 from the vector-like family. We thus see that the Yukawa sector has one 4×4 matrix $\mathcal{Y}_{ab}$, and two four-vectors m_a and η_a. Since $\mathcal{Y}_{ab}$ can be chosen to be diagonal and real, this amounts to $4+4+4$ flavor mixing parameters. The Yukawa coupling $\overline{16}\,\bar{y}\,126_H$ does not have any effect on the light fermion masses and mixings. While in the diagonal and real basis for $\mathcal{Y}_{ab}$ the vectors m_a and η_a are in general complex, these being related to GUT scale masses, one complex combination disappears from low energy masses and mixings. One should add to this set two (real) VEV ratios (one from the two SM singlets of 45_H and one for the up-type and down-type Higgs doublet VEV ratio from the $\overline{126}_H$), and an overall scale for the right-handed neutrino masses. We thus see that the model has 14 real parameters and 7 phases to fit 18 observed values among quark masses, quark mixings and CP violation, charged fermion masses, neutrino mass-squard differences and mixing angles. Thus these models are rather constrained, yet we show that excellent fits are obtained. It may be noted that the minimal supersymmetric $SO(10)$ models with two symmetric Yukawa coupling matrices involving 10_H and $\overline{126}_H$ have 12 real parameters and 7 phases that enter into the flavor sector.

The basic structure of Eq. (2.2.1) can be realized in several other ways. We study all such $SO(10)$ models in this paper. The Higgs field 45_H in Eq. (2.2.1) may be replaced by a 210_H. In this case, since the 210_H contains three SM singlet fields, there are two ratios of VEVs from the 210_H, which would increase the number of parameters by one. These models may be realized with or without low energy supersymmetry. In the non-SUSY models, the VEVs of 45_H and 210_H are real, while in SUSY models they are in general complex (thus increasing the phase parameters to 8). In the SUSY models we find that although the 210_H has two associated VEV ratios, only one of the two is independent, due to symmetry breaking constraints arising from the superpotential. In

SUSY versions, additional fields other than $\overline{126}_H$ and 210_H used in the Yukawa sector are often required, in order to avoid new chiral supermultiplets that remain light and spoil unification of gauge couplings. A summary of the models that fit into this classification and studied here is given below. All models contain a $\overline{126}_H$ (plus a 126_H in the case of SUSY), in addition to the Higgs fields shown below.

A. Non-SUSY Model with $45_H + 54_H$
B. Non-SUSY Model with $210_H + 54_H$ or $210_H + 16_H$
C. SUSY Model with $45_H + 54_H + 16_H + \overline{16}_H$
D. SUSY Model with $210_H + 54_H$
E. SUSY Model with $210_H + 16_H + \overline{16}_H$
F. SUSY Model with $210_H + 54_H + 16_H + \overline{16}_H$

The VEV of the SM singlet in $\overline{126}_H$ will be found *a posteriori* to be around $10^{13} - 10^{14}$ GeV in all models. This has an effect on the choice of Higgs fields, especially in the SUSY models: Very simple Higgs systems used for GUT symmetry breaking would lead to certain sub-multiplets having mass of order 10^{11} GeV, which would spoil perturbative unification of gauge couplings in SUSY $SO(10)$. The choice of "other Higgs fields" shown above are in part guided by this not happening. Furthermore, in some simplistic SUSY cases, the Higgs doublet mass matrix becomes proportional to other color sector mass matrix. Making a pair of Higgs doublets light would then lead to making a pair of colored states light as well, which affects perturbative unification. Such cases are avoided in the scenarios shown above. In each of the models listed above, seesaw mechanism may be realized via either type-I or type-II chain. Such sub-classes will be denoted by a label I or II when needed. Thus **AI** would refer to type-I seesaw in Model **A**, and likewise **AII** for type-II seesaw in the same model.

Models **A** and **B** are nonsupersymmetric, while models **C**–**F** are supersymmetric. For model **A**, in addition to 45_H, a 54_H is needed to break $SO(10)$ down to the SM without going through an intermediate $SU(5)$-symmetric limit. In Model **B** which uses a 210_H, an additional field, either a 54_H or a 16_H is needed for the following reason. As noted already, 126_H acquires a VEV of order $10^{13} - 10^{14}$ GeV, which can be ignored for the study of GUT symmetry breaking at around 10^{16} GeV. A single 210_H would break $SO(10)$ down to one of its maximal little groups, such as $SU(5) \times U(1)$, $SU(4)_C \times SU(2)_L \times SU(2)_R$ etc. The fermion mass matrix would then reflect this unbroken symmetry, which is not realistic in the light fermion spectrum. Addition of a 54_H (or a 16_H) with a GUT VEV would reduce the surviving symmetry and help with realistic fermion masses. For SUSY $SO(10)$, it is not a viable model if the symmetry is only broken by $45_H + 54_H$, since in this case, the Higgs doublet (1,2,1/2) and the Higgs octet (8,2,1/2) mass matrices become identical. So one cannot make the MSSM doublet fields light without also making the octet fields light. To break this degeneracy one needs to extend the Higgs sector. For this purpose in model **C**, we enlarge the Higgs sector by adding $16_H + \overline{16}_H$. SUSY $SO(10)$ model with $210_H + 126_H + \overline{126}_H$ is also not a consistent model, because with the requirement $v_R \sim 10^{13-14}$

GeV, the octet $(8,3,0)$ Higgs field becomes light with a mass of order $\sim 10^{10-11}$ GeV, so the theory does not remain perturbative up to the GUT scale. Thus, in order to avoid this, in model **D**, we include 54_H Higgs and in model **E**, we include a $16_H + \overline{16}_H$. It will be shown later in Sec. V that, in all these SUSY $SO(10)$ models with a 210_H, there is only one independent VEV ratio involving the 210_H field, owing to symmetry breaking constraints. Including more Higgs multiplets, one can break such relationships among VEVs which can lead to two independent VEV ratios for 210_H. We also consider this general case which is labeled as model **F**, where in addition to 210_H, one has both 54_H and $16_H + \overline{16}_H$ (or some unspecified) multiplets. It is to be mentioned that, we do not consider any model where both the 45_H and 210_H are present simultaneously, which would lead to more parameters and thus less predictions in the fermion sector. Details of the symmetry breaking schemes will be explained further in Sec. V.

2.3 The set-up and formalism

All models we study have one vector like $16 + \overline{16}$ pair plus 3 generations of chiral 16's. Their mass terms and couplings to a 45_H given in Eq. (2.2.1) can be expanded to yield

$$\begin{aligned}
\overline{16}\,(m_a + \eta_a 45_H)\,16_a &= \bar{L}\,(m_a + \eta_a(3v_1))\,L_a + \bar{Q}\,(m_a + \eta_a(-v_1))\,Q_a \\
&+ e^c_a\,(m_a + \eta_a(-3v_1 - v_2))\,\bar{e}^c + \nu^c_a\,(m_a + \eta_a(-3v_1 + v_2))\,\bar{\nu}^c \\
&+ d^c_a\,(m_a + \eta_a(v_1 - v_2))\,\bar{d}^c + u^c_a\,(m_a + \eta_a(v_1 + v_2))\,\bar{u}^c, \qquad (2.3.2)
\end{aligned}$$

where $a = 1, \ldots, 4$ and

$$v_1 = \langle 45_H \rangle_{(1,1,15)} \quad , \quad v_2 = \langle 45_H \rangle_{(1,3,1)}. \qquad (2.3.3)$$

These are the SM singlet components of 45_H which acquire GUT scale VEVs denoted here as $v_{1,2}$.

The mass terms are of the general form

$$\bar{\psi} M_a \psi_a. \qquad (2.3.4)$$

Although by redefining the phases of ψ_a we can make all these M_a real, we will keep them complex in general. Then we project to the heavy states as usual by

$$\psi_a \to U_{ab}\psi_b, \qquad (2.3.5)$$

with

$$U = \begin{pmatrix} \Lambda & \Lambda x^* \\ -x^T\Lambda & \bar{\Lambda} \end{pmatrix} \qquad (U^\dagger = U^{-1}) \qquad (2.3.6)$$

$$\Lambda = 1 - \frac{x^* x^T}{\sqrt{1+|x|^2}(\sqrt{1+|x|^2}+1)} \qquad (\Lambda^\dagger = \Lambda) \qquad (2.3.7)$$

$$x^T = \frac{1}{M_4}(M_1, M_2, M_3) \quad , \quad \bar{\Lambda} = \frac{1}{\sqrt{1+|x|^2}}. \qquad (2.3.8)$$

To this we add the Yukawa couplings to $\overline{126}_H$. Although we are free to choose this 4×4 Yukawa matrix to be diagonal and real (in the original basis, i.e. before (2.3.5)), we will keep it to be complex symmetric and choose a convenient basis later on. The $\overline{16}$ has coupling to the 126_H, but this will turn out to not affect light fermion masses. The relevant Yukawa couplings are (see Eq. (2.2.1))

$$16_a \, \mathcal{Y}_{ab} \, \overline{126}_H \, 16_b + \overline{16} \, \bar{y} \, 126_H \, \overline{16}. \tag{2.3.9}$$

In this original basis we put all together:

$$\begin{aligned}
& \begin{pmatrix} d_a^c & \overline{d} \end{pmatrix} \begin{pmatrix} \mathcal{Y}_{ab} v_d & m_a + \eta_a (v_1 - v_2) \\ m_b + \eta_b (-v_1) & \bar{y} v_d \end{pmatrix} \begin{pmatrix} d_b \\ \bar{d}^c \end{pmatrix} \\
+ & \begin{pmatrix} u_a^c & \overline{u} \end{pmatrix} \begin{pmatrix} \mathcal{Y}_{ab} v_u & m_a + \eta_a (v_1 + v_2) \\ m_b + \eta_b (-v_1) & \bar{y} v_u \end{pmatrix} \begin{pmatrix} u_b \\ \bar{u}^c \end{pmatrix} \\
+ & \begin{pmatrix} e_a^c & \overline{e} \end{pmatrix} \begin{pmatrix} -3\mathcal{Y}_{ab} v_d & m_a + \eta_a (-3v_1 - v_2) \\ m_b + \eta_b (3v_1) & -3\bar{y} v_d \end{pmatrix} \begin{pmatrix} e_b \\ \bar{e}^c \end{pmatrix} \\
+ & \begin{pmatrix} \nu_a^c & \overline{\nu} \end{pmatrix} \begin{pmatrix} -3\mathcal{Y}_{ab} v_u & m_a + \eta_a (-3v_1 + v_2) \\ m_b + \eta_b (3v_1) & -3\bar{y} v_u \end{pmatrix} \begin{pmatrix} \nu_b \\ \bar{\nu}^c \end{pmatrix} \\
+ & \frac{1}{2} \begin{pmatrix} \nu_a^c & \bar{\nu} \end{pmatrix} \begin{pmatrix} \mathcal{Y}_{ab} v_R & 0 \\ 0 & \bar{y} \bar{v}_L \end{pmatrix} \begin{pmatrix} \nu_b^c \\ \bar{\nu} \end{pmatrix} + \frac{1}{2} \begin{pmatrix} \nu_a & \bar{\nu}^c \end{pmatrix} \begin{pmatrix} \mathcal{Y}_{ab} v_L & 0 \\ 0 & \bar{y} \bar{v}_R \end{pmatrix} \begin{pmatrix} \nu_b \\ \bar{\nu}^c \end{pmatrix},
\end{aligned} \tag{2.3.10}$$

where

$$\begin{aligned}
v_R &= \langle \overline{126}_H \rangle_{(1,3,10)} \quad , \quad v_L = \langle \overline{126}_H \rangle_{(3,1,\overline{10})} \\
\bar{v}_R &= \langle 126_H \rangle_{(1,3,\overline{10})} \quad , \quad \bar{v}_L = \langle 126_H \rangle_{(3,1,10)} \\
v_u &= \langle \overline{126}_H \rangle_{(2,2,15)_u} \quad , \quad v_d = \langle \overline{126}_H \rangle_{(2,2,15)_d}.
\end{aligned} \tag{2.3.11}$$

Here v_R and $\bar{v}_R$ are close to, but somewhat below the GUT scale, while $v_{u,d}$ are the VEVs of the electroweak Higgs doublets arising from the $\overline{126}_H$. v_L and $\bar{v}_L$ denote the induced VEVs of the $SU(2)_L$ triplets from 126_H and $\overline{126}_H$. In non-supersymmetric models, we have $\bar{v}_R = v_R^*$, $v_d = v_u^*$ and $\bar{v}_L = v_L^*$.

After the transformation given in Eq. (2.3.5) the matrices Eq. (2.3.10) become

$$
\begin{aligned}
\to \quad & \begin{pmatrix} d_a^c & \overline{d} \end{pmatrix} \begin{pmatrix} (U_{d^c}^T)_{ae}\mathcal{Y}_{ef}v_d(U_Q)_{fb} & M_{d^c}\delta_{a4} \\ M_Q\delta_{b4} & \bar{y}v_d \end{pmatrix} \begin{pmatrix} d_b \\ \bar{d}^c \end{pmatrix} \\
+ \quad & \begin{pmatrix} u_a^c & \overline{u} \end{pmatrix} \begin{pmatrix} (U_{u^c}^T)_{ae}\mathcal{Y}_{ef}v_u(U_Q)_{fb} & M_{u^c}\delta_{a4} \\ M_Q\delta_{b4} & \bar{y}v_u \end{pmatrix} \begin{pmatrix} u_b \\ \bar{u}^c \end{pmatrix} \\
+ \quad & \begin{pmatrix} e_a^c & \overline{e} \end{pmatrix} \begin{pmatrix} (U_{e^c}^T)_{ae}(-3)\mathcal{Y}_{ef}v_d(U_L)_{fb} & M_{e^c}\delta_{a4} \\ M_L\delta_{b4} & -3\bar{y}v_d \end{pmatrix} \begin{pmatrix} e_b \\ \bar{e}^c \end{pmatrix} \\
+ \quad & \begin{pmatrix} \nu_a^c & \overline{\nu} \end{pmatrix} \begin{pmatrix} (U_{\nu^c}^T)_{ae}(-3)\mathcal{Y}_{ef}v_u(U_L)_{fb} & M_{\nu^c}\delta_{a4} \\ M_L\delta_{b4} & -3\bar{y}v_u \end{pmatrix} \begin{pmatrix} \nu_b \\ \bar{\nu}^c \end{pmatrix} \\
+ \quad & \frac{1}{2}\begin{pmatrix} \nu_a^c & \bar{\nu} \end{pmatrix} \begin{pmatrix} (U_{\nu^c}^T)_{ae}\mathcal{Y}_{ef}v_R(U_{\nu^c})_{fb} & 0 \\ 0 & \bar{y}\bar{v}_L \end{pmatrix} \begin{pmatrix} \nu_b^c \\ \bar{\nu} \end{pmatrix} \\
+ \quad & \frac{1}{2}\begin{pmatrix} \nu_a & \bar{\nu}^c \end{pmatrix} \begin{pmatrix} (U_L^T)_{ae}\mathcal{Y}_{ef}v_L(U_L)_{fb} & 0 \\ 0 & \bar{y}\bar{v}_R \end{pmatrix} \begin{pmatrix} \nu_b \\ \bar{\nu}^c \end{pmatrix}.
\end{aligned}
\tag{2.3.12}
$$

To get the light fermion mass matrices defined as

$$
\mathcal{L} = d^{cT}M_D d + u^{cT}M_U u + e^{cT}M_E e + \frac{1}{2}\nu^T M_N \nu + h.c. \tag{2.3.13}
$$

we have to project to the light generations. In doing so we need to evaluate ($\mathcal{Y}$ is a 4×4 matrix, while Y is its 3×3 submatrix)

$$
\begin{aligned}
U_1^T\mathcal{Y}U_2 &= \begin{pmatrix} \Lambda_1^T & -\Lambda_1^T x_1 \\ x_1^\dagger\Lambda_1^T & \bar{\Lambda}_1 \end{pmatrix} \begin{pmatrix} Y & y \\ y^T & y_4 \end{pmatrix} \begin{pmatrix} \Lambda_2 & \Lambda_2 x_2^* \\ -x_2^T\Lambda_2 & \bar{\Lambda}_2 \end{pmatrix} \\
&= \begin{pmatrix} \Lambda_1^T(Y - yx_2^T - x_1y^T + y_4x_1x_2^T)\Lambda_2 & \Lambda_1^T(Yx_2^* + y - x_1y^Tx_2^* - y_4x_1)\bar{\Lambda}_2 \\ \bar{\Lambda}_1(x_1^\dagger Y + y^T - x_1^\dagger yx_2^T - y_4x_2^T)\Lambda_2 & \bar{\Lambda}_1(x_1^\dagger Yx_2^* + y^Tx_2^* + x_1^\dagger Y + y_4)\bar{\Lambda}_2 \end{pmatrix},
\end{aligned}
\tag{2.3.14}
$$

where we used $\Lambda x^* = \bar{\Lambda}x^*$.

For charged fermions this is enough, and we get (mass matrices are defined as $\psi^c M_\Psi \psi$)

$$
M_D = v_d\Lambda_{d^c}^T\left(Y - yx_Q^T - x_{d^c}y^T + y_4x_{d^c}x_Q^T\right)\Lambda_Q \tag{2.3.15}
$$

$$
M_U = v_u\Lambda_{u^c}^T\left(Y - yx_Q^T - x_{u^c}y^T + y_4x_{u^c}x_Q^T\right)\Lambda_Q \tag{2.3.16}
$$

$$
M_E = -3v_d\Lambda_{e^c}^T\left(Y - yx_L^T - x_{e^c}y^T + y_4x_{e^c}x_L^T\right)\Lambda_L. \tag{2.3.17}
$$

For neutrinos things are slightly more involved, since there are two kinds of heavy neutrinos, the usual right-handed ones, plus the new vector-like ones. The full symmetric Majorana mass matrix is 10×10. However, in the leading order in $yv_R/M_{L,\nu^c}$ (M_{L,ν^c} denote the masses of vector-like leptons), the situation returns to ordinary with

$$M_{\nu_D} = -3v_u\Lambda_{\nu^c}^T(Y - yx_L^T - x_{\nu^c}y^T + y_4x_{\nu^c}x_L^T)\Lambda_L \tag{2.3.18}$$

$$M_{\nu_R} = v_R\Lambda_{\nu^c}^T(Y - yx_{\nu^c}^T - x_{\nu^c}y^T + y_4x_{\nu^c}x_{\nu^c}^T)\Lambda_{\nu^c} \tag{2.3.19}$$

$$M_{\nu_L} = v_L\Lambda_L^T(Y - yx_L^T - x_Ly^T + y_4x_Lx_L^T)\Lambda_L, \tag{2.3.20}$$

so that as usual by using the seesaw [38] formula we arrive at the 3×3 light neutrino mass matrix as

$$M_N = M_{\nu_L} - M_{\nu_D}^T M_{\nu_R}^{-1} M_{\nu_D}. \tag{2.3.21}$$

If the approximation $yv_R/M_{L,\nu^c} \ll 1$ is not good, we write the full symmetric matrix for $(\nu_i, \nu_i^c, \nu_4, \bar{\nu}^c, \nu_4^c, \bar{\nu})$:

$$\begin{pmatrix}
(U_L^T(v_L\mathcal{Y})U_L)_{ij} & (U_L^T(-3v_u\mathcal{Y})U_{\nu^c})_{ij} & (U_L^T(v_L\mathcal{Y})U_L)_{i4} & 0 & (U_L^T(-3v_u\mathcal{Y})U_{\nu^c})_{i4} & 0 \\
(U_{\nu^c}^T(-3v_u\mathcal{Y})U_L)_{ij} & (U_{\nu^c}^T(v_R\mathcal{Y})U_{\nu^c})_{ij} & (U_{\nu^c}^T(-3v_u\mathcal{Y})U_L)_{i4} & 0 & (U_{\nu^c}^T(v_R\mathcal{Y})U_{\nu^c})_{i4} & 0 \\
(U_L^T(v_L\mathcal{Y})U_L)_{4j} & (U_L^T(-3v_u\mathcal{Y})U_{\nu^c})_{4j} & (U_L^T(v_L\mathcal{Y})U_L)_{44} & 0 & (U_L^T(-3v_u\mathcal{Y})U_{\nu^c})_{44} & M_L \\
0 & 0 & 0 & \bar{v}_Ry & M_{\nu^c} & -3v_uy \\
(U_{\nu^c}^T(-3v_u\mathcal{Y})U_L)_{4j} & (U_{\nu^c}^T(v_R\mathcal{Y})U_{\nu^c})_{4j} & (U_{\nu^c}^T(-3v_u\mathcal{Y})U_L)_{44} & M_{\nu^c} & (U_{\nu^c}^T(v_R\mathcal{Y})U_{\nu^c})_{44} & 0 \\
0 & 0 & M_L & -3v_uy & 0 & \bar{v}_Ly
\end{pmatrix}. \tag{2.3.22}$$

One can integrate out ν_4 and $\bar{\nu}$ without any trace, since they mix through a large M_L, but otherwise feel just the small VEVs. What remains is for $(\nu_i, \nu_i^c, \bar{\nu}^c, \nu_4^c)$:

$$\begin{pmatrix}
(U_L^T(v_L\mathcal{Y})U_L)_{ij} & (U_L^T(-3v_u\mathcal{Y})U_{\nu^c})_{ij} & 0 & (U_L^T(-3v_u\mathcal{Y})U_{\nu^c})_{i4} \\
(U_{\nu^c}^T(-3v_u\mathcal{Y})U_L)_{ij} & (U_{\nu^c}^T(v_R\mathcal{Y})U_{\nu^c})_{ij} & 0 & (U_{\nu^c}^T(v_R\mathcal{Y})U_{\nu^c})_{i4} \\
0 & 0 & \bar{v}_Ry & M_{\nu^c} \\
(U_{\nu^c}^T(-3v_u\mathcal{Y})U_L)_{4j} & (U_{\nu^c}^T(v_R\mathcal{Y})U_{\nu^c})_{4j} & M_{\nu^c} & (U_{\nu^c}^T(v_R\mathcal{Y})U_{\nu^c})_{44}
\end{pmatrix}. \tag{2.3.23}$$

This has again the form

$$\begin{pmatrix}
M_{\nu_L} & M_{\nu_D}^T \\
M_{\nu_D} & M_{\nu_R}
\end{pmatrix}. \tag{2.3.24}$$

and thus Eq. (2.3.21) applies with M_{ν_L} given by Eq. (2.3.20), but now for 5 right-handed neutrinos with a 5×3 matrix M_{ν_D} and a 5×5 symmetric matrix M_{ν_R}:

$$M_{\nu_D} = (-3v_u)\begin{pmatrix} \Lambda_{\nu^c}(Y - yx_L^T - x_{\nu^c}y^T + y_4 x_{\nu^c}x_L^T)\Lambda_L \\ 0 \\ \bar{\Lambda}_{\nu^c}(x_{\nu^c}^T Y + y^T - x_{\nu^c}^T y x_L^T - x_L^T y_4)\Lambda_L \end{pmatrix} \tag{2.3.25}$$

$$M_{\nu_R} = \begin{pmatrix} v_R\Lambda_{\nu^c}(Y - yx_{\nu^c}^T - x_{\nu^c}y^T + y_4 x_{\nu^c}x_{\nu^c}^T)\Lambda_{\nu^c} & 0 & v_R\Lambda_{\nu^c}(Yx_{\nu^c} + y - x_{\nu^c}y^T x_{\nu^c} - y_4 x_{\nu^c})\bar{\Lambda}_{\nu^c} \\ 0 & \bar{v}_R y & M_{\nu^c} \\ v_R\bar{\Lambda}_{\nu^c}(x_{\nu^c}^T Y + y^T - x_{\nu^c}^T y x_{\nu^c}^T - y_4 x_{\nu^c}^T)\Lambda_{\nu^c} & M_{\nu^c} & v_R\bar{\Lambda}_{\nu^c}(x_{\nu^c}^T Y x_{\nu^c} + y^T x_{\nu^c} + x_{\nu^c}^T y + y_4)\bar{\Lambda}_{\nu^c} \end{pmatrix}. \tag{2.3.26}$$

To conclude, let's write down explicitly the various $\vec{x}$'s:

$$\vec{x}_L = \frac{\vec{m} + \vec{\eta}(3v_1)}{m_4 + \eta_4(3v_1)} \quad , \quad \vec{x}_Q = \frac{\vec{m} + \vec{\eta}(-v_1)}{m_4 + \eta_4(-v_1)}, \tag{2.3.27}$$

$$\vec{x}_{e^c} = \frac{\vec{m} + \vec{\eta}(-3v_1 - v_2)}{m_4 + \eta_4(-3v_1 - v_2)} \quad , \quad \vec{x}_{\nu^c} = \frac{\vec{m} + \vec{\eta}(-3v_1 + v_2)}{m_4 + \eta_4(-3v_1 + v_2)}, \tag{2.3.28}$$

$$\vec{x}_{d^c} = \frac{\vec{m} + \vec{\eta}(v_1 - v_2)}{m_4 + \eta_4(v_1 - v_2)} \quad , \quad \vec{x}_{u^c} = \frac{\vec{m} + \vec{\eta}(v_1 + v_2)}{m_4 + \eta_4(v_1 + v_2)}. \tag{2.3.29}$$

Defining

$$\vec{x} = \frac{\vec{m}}{m_4} \quad , \quad u_{1,2} = \eta_4 \frac{v_{1,2}}{m_4} \quad , \quad \vec{z} = \frac{\vec{\eta}}{\eta_4}, \tag{2.3.30}$$

we can rewrite the above as

$$\begin{aligned} \vec{x}_L &= \frac{\vec{x} + \vec{z}(3u_1)}{1 + (3u_1)} \quad , \quad \vec{x}_Q = \frac{\vec{x} + \vec{z}(-u_1)}{1 + (-u_1)}, \\ \vec{x}_{e^c} &= \frac{\vec{x} + \vec{z}(-3u_1 - u_2)}{1 + (-3u_1 - u_2)} \quad , \quad \vec{x}_{\nu^c} = \frac{\vec{x} + \vec{z}(-3u_1 + u_2)}{1 + (-3u_1 + u_2)}, \\ \vec{x}_{d^c} &= \frac{\vec{x} + \vec{z}(u_1 - u_2)}{1 + (u_1 - u_2)} \quad , \quad \vec{x}_{u^c} = \frac{\vec{x} + \vec{z}(u_1 + u_2)}{1 + (u_1 + u_2)}. \end{aligned} \tag{2.3.31}$$

To get the masses and mixings we change the basis

$$x \to X_L x \quad , \quad x^c \to X_R^* x^c \tag{2.3.32}$$

for $x = d, u, e, \nu$ and $X = D, U, E, N$. This means that (for $X = N$, $X_R = X_L^*$)

$$M_X = X_R M_X^d X_L^\dagger \tag{2.3.33}$$

so that the CKM and PMNS matrices are defined as

$$V_{CKM} = U_L^\dagger D_L \tag{2.3.34}$$

$$V_{PMNS} = E_L^\dagger N_L. \tag{2.3.35}$$

So far we have been very general. However, there are redundancies that are present, which should be removed for an efficient numerical fitting algorithm. In the next section we shall choose a specific basis, which may appear at first to be less intuitive but which is well-suited for our numerical minimization. There are two

obvious basis choices, one where $\mathcal{Y}_{ab}$ is diagonal, and a second one where the vectors m_a and η_a have simple forms. It is the second one that is used in the next section. For further use we give here the relations between the two sets of parameters.

$$\begin{aligned}
\vec{x} &= (0, 0, \tan\theta e^{-i\phi}) && (2.3.36)\\
\vec{z} &= (0, 0, 0) && (2.3.37)\\
Y_{ij} &= a_{ij} && (2.3.38)\\
y &= (a_{41}, a_{42}, a_{43}) && (2.3.39)\\
y_4 &= a_{44} && (2.3.40)
\end{aligned}$$

and

$$\begin{aligned}
u_1 &= -\frac{Te^{-i\phi}}{\cos\theta}\frac{\epsilon}{5} && (2.3.41)\\
u_2 &= -\frac{Te^{-i\phi}}{\cos\theta}\left(1+\frac{3\epsilon}{5}\right). && (2.3.42)
\end{aligned}$$

2.3.1 210_H instead of 45_H

If the 45_H is replaced by a 210_H, we simply change Eq. (2.3.2) into:

$$\begin{aligned}
\overline{16}\,(m_a + \eta_a 210)\,16_a &= \bar{L}\,(m_a + \eta_a(\phi_1 - 3\phi_2))\,L_a\\
&+ \bar{Q}\,(m_a + \eta_a(\phi_1 + \phi_2))\,Q_a\\
&+ e^c_a\,(m_a + \eta_a(-\phi_1 - 3\phi_2 + 3\phi_3))\,\bar{e}^c\\
&+ \nu^c_a\,(m_a + \eta_a(-\phi_1 - 3\phi_2 - 3\phi_3))\,\bar{\nu}^c\\
&+ d^c_a\,(m_a + \eta_a(-\phi_1 + \phi_2 - \phi_3))\,\bar{d}^c\\
&+ u^c_a\,(m_a + \eta_a(-\phi_1 + \phi_2 + \phi_3))\,\bar{u}^c
\end{aligned} \qquad (2.3.43)$$

where

$$\phi_1 = \langle 210_H\rangle_{(1,1,1)} \quad , \quad \phi_2 = \langle 210_H\rangle_{(1,1,15)} \quad , \quad \phi_3 = \langle 210_H\rangle_{(1,3,15)} \qquad (2.3.44)$$

are the VEVs of the three SM singlets of 210_H.

This then changes Eq. (2.3.31) into

$$\begin{aligned}
\vec{x}_L = \frac{\vec{x}+\vec{z}(u_1-3u_2)}{1+(u_1-3u_2)} \quad &, \quad \vec{x}_Q = \frac{\vec{x}+\vec{z}(u_1+u_2)}{1+(u_1+u_2)},\\
\vec{x}_{e^c} = \frac{\vec{x}+\vec{z}(-u_1-3u_2+3u_3)}{1+(-u_1-3u_2+3u_3)} \quad &, \quad \vec{x}_{\nu^c} = \frac{\vec{x}+\vec{z}(-u_1-3u_2-3u_3)}{1+(-u_1-3u_2-3u_3)},\\
\vec{x}_{d^c} = \frac{\vec{x}+\vec{z}(-u_1+u_2-u_3)}{1+(-u_1+u_2-u_3)} \quad &, \quad \vec{x}_{u^c} = \frac{\vec{x}+\vec{z}(-u_1+u_2+u_3)}{1+(-u_1+u_2+u_3)},
\end{aligned} \qquad (2.3.45)$$

where now

$$u_{1,2,3} = \eta_4 \frac{\phi_{1,2,3}}{m_4}. \tag{2.3.46}$$

For correspondence with the specific basis chosen in the next section, we still have Eqs. (2.3.36)- (2.3.40), but Eqs. (2.3.41)-(2.3.42) are replaced by

$$u_1 = \frac{T e^{-i\phi}}{\cos\theta} \tag{2.3.47}$$

$$u_2 = \frac{T e^{-i\phi}}{\cos\theta} \frac{\epsilon_1}{\sqrt{3}} \tag{2.3.48}$$

$$u_3 = \frac{T e^{-i\phi}}{\cos\theta} \epsilon_2 \sqrt{\frac{2}{3}} \ . \tag{2.3.49}$$

2.4 Analysis in a specific basis

The general formulas given in the previous section for the light fermion mass matrices have built-in redundancies. Here we choose a specific basis where these redundancies are removed. We choose a basis where the four-vectors in Eq. (2.2.1) have simple forms:

$$\eta_a = (0, 0, 0, 1)\, b, \quad m_a = (0, 0, \sin\theta, e^{i\phi}\cos\theta)\, M \ . \tag{2.4.50}$$

These simple forms are achieved by 4×4 family rotation, which makes the vector $\vec{\eta}$ to have the form shown, and a subsequent 3×3 family rotation that brings the vector $\vec{m}$ to this form. A further rotation in the first two family space can be made, we choose this rotation to make the 4×4 Yukawa matrix, denoted as a_{ij} in this specific basis, to be diagonal in the 1-2 subspace, i.e., $a_{12} = a_{21} = 0$. The correspondence given in Eqs. (2.3.36)-(2.3.40) as well as Eqs. (2.3.41)-(2.3.42) for the case of 45_H arise from this choice of basis. (The parameters T and ϵ will be defined shortly.) Let us denote $\Phi = 45_H$ or 210_H and the VEV of Φ to be $\langle\Phi\rangle = \Omega$ which has two components (for $\Phi = 45_H$) or three components (for $\Phi = 210_H$). The Yukawa Lagrangian in this specific basis takes the form:

$$\mathcal{L}_{\rm Yuk} = \sum_{i,j=1}^{4} a_{ij}\ 16_i\ 16_j\ \overline{126}_H + \bar{y}\ \overline{16}\ \overline{16}\ 126_H + b\ \overline{16}\ 16_4\ \Phi + M\ \overline{16}\ (\sin\theta\ 16_3 + e^{i\phi}\cos\theta\ 16_4). \tag{2.4.51}$$

The effective mass terms that arise after the VEV of Φ is inserted would depend on the VEV ratio of the two SM singlets in 45_H and on two VEV ratios of the three SM singlets in the case of 210_H. For the former, we can define an unbroken charge Q, which is not the electric charge, but a linear combination of hypercharge Y and the $U(1)_X$ charge contained in $SO(10) \to SU(5) \times U(1)_X$ – the 45_H leaves this charge Q unbroken. A parameter ϵ can be introduced in terms of which the unbroken charge Q can be defined for each of the SM fermions [60]:

$$Q = -\frac{1}{5}X + \frac{6(\epsilon+1)}{5}\frac{Y}{2} = 2I_{3R} + \frac{6\epsilon}{5}\frac{Y}{2}, \tag{2.4.52}$$

where X is normalized so that $X_{10\in16}=1$, $X_{\overline{5}\in16}=-3$ and $X_{1\in16}=5$. Thus the charges of fermions $\in 16$ of $SO(10)$ for the case of 45_H are:

$$\begin{aligned} Q_{u,d}=\frac{1}{5}\epsilon;\ Q_{u^c}=-1-\frac{4}{5}\epsilon;\ Q_{d^c}=1+\frac{2}{5}\epsilon;\\ Q_{e,\nu}=-\frac{3}{5}\epsilon;\ Q_{e^c}=1+\frac{6}{5}\epsilon;\ Q_{\nu^c}=-1. \end{aligned} \tag{2.4.53}$$

For 210_H case the fermion charges are given in terms of two parameters $\epsilon_{1,2}$:

$$\begin{aligned} Q_{u,d}=1+\frac{\epsilon_1}{\sqrt{3}};\ Q_{u^c}=-1+\frac{\epsilon_1}{\sqrt{3}}+\sqrt{\frac{2}{3}}\epsilon_2;\ Q_{d^c}=-1+\frac{\epsilon_1}{\sqrt{3}}-\sqrt{\frac{2}{3}}\epsilon_2;\\ Q_{e,\nu}=1-\sqrt{3}\epsilon_1;\ Q_{e^c}=-1-\sqrt{3}\epsilon_1+\sqrt{6}\epsilon_2;\ Q_{\nu^c}=-1-\sqrt{3}\epsilon_1-\sqrt{6}\epsilon_2. \end{aligned} \tag{2.4.54}$$

These charges are obtained from Eq. (2.3.43) by setting $\phi_1=1$, $\phi_2=\epsilon_1/\sqrt{3}$ and $\phi_3=\sqrt{2/3}\,\epsilon_2$.

For non-SUSY case, $Q_f=Q_f^*$ as Φ is a real field in this case, while Q_f is complex in the case of SUSY. Now, writing $b\,\overline{16}\,16_4\,\langle\Phi\rangle=b\Omega(\overline{f}Q_f f_4+\overline{f}^c Q_{f^c}f_4^c)$, the last two terms of the Yukawa Lagrangian in Eq. (2.4.51) can be written as

$$\mathcal{L}_{\rm Yuk}\supseteq\overline{f}[(M\sin\theta)f_3+(Me^{i\phi}\cos\theta+b\Omega Q_f)f_4]+\overline{f}^c[(M\sin\theta)f_3^c+(Me^{i\phi}\cos\theta+b\Omega Q_{f^c})f_4^c]. \tag{2.4.55}$$

Then defining

$$T\equiv b\Omega/M;\ N_{f,f^c}\equiv\sqrt{1+T^2|Q_{f,f^c}|^2+T\cos\theta(e^{-i\phi}Q_{f,f^c}+e^{i\phi}Q^*_{f,f^c})}, \tag{2.4.56}$$

the heavy (GUT scale) fields $(\hat{f}_4,\hat{f}_4^c)$ and the light SM fields $(\hat{f}_3,\hat{f}_3^c)$ can be identified as

$$\frac{(\sin\theta)f_3+(e^{i\phi}\cos\theta+TQ_f)f_4}{N_f}\equiv\hat{f}_4\ ;\ \frac{(e^{-i\phi}\cos\theta+TQ_f^*)f_3-(\sin\theta)f_4}{N_f}\equiv\hat{f}_3; \tag{2.4.57}$$

$$\frac{(\sin\theta)f_3^c+(e^{i\phi}\cos\theta+TQ_{f^c})f_4^c}{N_{f^c}}\equiv\hat{f}_4^c\ ;\ \frac{(e^{-i\phi}\cos\theta+TQ_{f^c}^*)f_3^c-(\sin\theta)f_4^c}{N_{f^c}}\equiv\hat{f}_3^c. \tag{2.4.58}$$

These expressions are valid for $f=u,d,e,\nu$ and $f^c=u^c,d^c,e^c,\nu^c$. Then from the full Yukawa Lagrangian one can compute the charged fermion and Dirac neutrino mass matrices for the light fermions written as f^cM_ff as:

$$M_f^T=v_fk_f\begin{bmatrix}a_{11}^f & 0 & a_{13}^f\\ 0 & a_{22}^f & a_{23}^f\\ a_{31}^f & a_{32}^f & a_{33}^f\end{bmatrix}, \tag{2.4.59}$$

where $f=U,D,E,\nu_D$, $v_e=v_d$, $v_\nu=v_u$, $k_{u,d}=1$ and $k_{e,\nu}=-3$. We define the ratio $v_u/v_d\equiv r$. Note that this ratio is not exactly equal to $\tan\beta$ of MSSM, but is closely related to it. If we ignore the mixing of the up and down-type Higgs doublets from $\overline{126}_H$ with other doublets present in the theory, r would be equal to $\tan\beta$ in MSSM. The following relations are then readily obtained:

$$a^f_{11} = a_{11} \ , \tag{2.4.60}$$

$$a^f_{13} = \frac{a_{13}(e^{i\phi}\cos\theta + TQ_{f^c}) - a_{14}\sin\theta}{N_{f^c}} \ , \tag{2.4.61}$$

$$a^f_{22} = a_{22} \ , \tag{2.4.62}$$

$$a^f_{23} = \frac{a_{23}(e^{i\phi}\cos\theta + TQ_{f^c}) - a_{24}\sin\theta}{N_{f^c}} \ , \tag{2.4.63}$$

$$a^f_{31} = \frac{a_{13}(e^{i\phi}\cos\theta + TQ_{f}) - a_{14}\sin\theta}{N_{f}} \ , \tag{2.4.64}$$

$$a^f_{32} = \frac{a_{23}(e^{i\phi}\cos\theta + TQ_{f}) - a_{24}\sin\theta}{N_{f}} \ , \tag{2.4.65}$$

$$a^f_{33} = \frac{a_{33}(e^{i\phi}\cos\theta + TQ_{f})(e^{i\phi}\cos\theta + TQ_{f^c}) + a_{44}\sin^2\theta - a_{34}\sin\theta[2e^{i\phi}\cos\theta + T(Q_f + Q_{f^c})]}{N_f N_{f^c}} \ . \tag{2.4.66}$$

Note that a rotation in the 1-2 sector has been made which makes $a^f_{12} = a^f_{21} = a_{12} = 0$. These mass matrices are not symmetric, since $a^f_{ij} \neq a^f_{ji}$, although the original matrix obeyes $a_{ij} = a_{ji}$. These four mass matrices for $f = U, D, D, \nu_D$ are given in terms of the parameters $\epsilon, T, \theta, \phi$ and a_{ij} (with $i, j = 1 - 4$ and $a_{12} = a_{21} = 0$). We choose to take elements of M_E to be independent. One can then solve for a_{13} and a_{14} in terms of a^e_{13} and a^e_{31}; similarly a_{23} and a_{24} in terms of a^e_{23} and a^e_{32}. From Eqs.(2.4.61), (2.4.63), (2.4.64), (2.4.65) and (2.4.53) one sees that this is a valid choice provided that $\epsilon \neq -5/9$ for $\Phi = 45_H$. (If $\epsilon = -5/9$, $a^e_{13} = a^e_{31}$ and $a^e_{23} = a^e_{32}$, which does not lead to realistic fermion masses.) Similarly for the case of $\Phi = 210_H$, the restriction is $\epsilon_2 \neq 0$ is required as can be seen from Eq. (2.4.54). All these mass matrices have the same 1-2 sector and one can choose $a_{11} = a^e_{11}$ and $a_{22} = a^e_{22}$. In addition, $a^e_{33}, a^u_{33}, a^d_{33}$ depend on 3 independent parameters a_{33}, a_{34}, a_{44} that appear only in the (3,3) sector of the light mass matrices. Since this linear system is invertible, one can treat $a^e_{33}, a^u_{33}, a^d_{33}$ as independent parameters. The (3,3) element of the right-handed neutrino Majorana matrix is then not free, and is determined in terms of $a^e_{33}, a^u_{33}, a^d_{33}$. Expressions for a_{ij} in terms of the independent parameters chosen are given below:

$$a_{13} = \frac{N_{e^c} a^e_{13} - N_e a^e_{31}}{T(Q_{e^c} - Q_e)} \ , \tag{2.4.67}$$

$$a_{14} = \frac{N_{e^c} a^e_{13}(e^{i\phi}\cos\theta + TQ_e) - N_e a^e_{31}(e^{i\phi}\cos\theta + TQ_{e^c})}{\sin\theta T(Q_{e^c} - Q_e)} \ , \tag{2.4.68}$$

$$a_{23} = \frac{N_{e^c} a^e_{23} - N_e a^e_{32}}{T(Q_{e^c} - Q_e)} \ , \tag{2.4.69}$$

$$a_{24} = \frac{N_{e^c} a^e_{23}(e^{i\phi}\cos\theta + TQ_e) - N_e a^e_{32}(e^{i\phi}\cos\theta + TQ_{e^c})}{\sin\theta T(Q_{e^c} - Q_e)} \ , \tag{2.4.70}$$

$$a_{33} = (a^u_{33} N_u N_{u^c} C_1 + a^d_{33} N_d N_{d^c} C_2 + a^e_{33} N_e N_{e^c} C_3)/(T^2 D_1) \ , \tag{2.4.71}$$

$$a_{34} = (a^u_{33} N_u N_{u^c} C_4 + a^d_{33} N_d N_{d^c} C_5 - a^e_{33} N_e N_{e^c} C_6)/(T^2 D_1) \ , \tag{2.4.72}$$

$$a_{44} = (a^u_{33} N_u N_{u^c} C_7 + a^d_{33} N_d N_{d^c} C_8 - a^e_{33} N_e N_{e^c} C_9)/(T^2 D_1) \ , \tag{2.4.73}$$

with

$$C_1 = Q_{d^c} - Q_{e^c} + Q_d - Q_e; \tag{2.4.74}$$

$$C_2 = Q_{e^c} - Q_{u^c} + Q_e - Q_u; \tag{2.4.75}$$

$$C_3 = -Q_{d^c} + Q_{u^c} - Q_d + Q_u; \tag{2.4.76}$$

$$C_4 = \csc\theta \left(e^{i\phi}\cos\theta\,(Q_{d^c} - Q_{e^c}) + Q_d\left(TQ_{d^c} + e^{i\phi}\cos\theta\right) - Q_e\left(TQ_{e^c} + e^{i\phi}\cos\theta\right)\right); \tag{2.4.77}$$

$$C_5 = \csc\theta \left(Q_e\left(TQ_{e^c} + e^{i\phi}\cos\theta\right) + e^{i\phi}\cos\theta\,(Q_{e^c} - Q_{u^c}) - Q_u\left(TQ_{u^c} + e^{i\phi}\cos\theta\right)\right); \tag{2.4.78}$$

$$C_6 = \csc\theta \left(Q_d\left(TQ_{d^c} + e^{i\phi}\cos\theta\right) + e^{i\phi}\cos\theta\,(Q_{d^c} - Q_{u^c}) - Q_u\left(TQ_{u^c} + e^{i\phi}\cos\theta\right)\right); \tag{2.4.79}$$

$$\begin{aligned} C_7 = {} & T^2 Q_d Q_e \csc^2\theta Q_{d^c} - T^2 Q_d Q_e \csc^2\theta Q_{e^c} + T^2 Q_d \csc^2\theta Q_{d^c} Q_{e^c} - T^2 Q_e \csc^2\theta Q_{d^c} Q_{e^c} \\ & + e^{2i\phi}\cot^2\theta Q_{d^c} + 2Te^{i\phi} Q_d \cot\theta\csc\theta Q_{d^c} - e^{2i\phi}\cot^2\theta Q_{e^c} \\ & - 2Te^{i\phi} Q_e \cot\theta\csc\theta Q_{e^c} + e^{2i\phi} Q_d \cot^2\theta - e^{2i\phi} Q_e \cot^2\theta; \end{aligned} \tag{2.4.80}$$

$$\begin{aligned} C_8 = {} & e^{2i\phi}\cot^2\theta Q_{e^c} + T^2 Q_e \csc^2\theta Q_u Q_{e^c} - T^2 Q_e \csc^2\theta Q_u Q_{u^c} + T^2 Q_e \csc^2\theta Q_{e^c} Q_{u^c} \\ & - T^2 \csc^2\theta Q_u Q_{e^c} Q_{u^c} + 2Te^{i\phi} Q_e \cot\theta\csc\theta Q_{e^c} - 2Te^{i\phi}\cot\theta\csc\theta Q_u Q_{u^c} \\ & - e^{2i\phi}\cot^2\theta Q_{u^c} + e^{2i\phi} Q_e \cot^2\theta - e^{2i\phi}\cot^2\theta Q_u; \end{aligned} \tag{2.4.81}$$

$$\begin{aligned} C_9 = {} & e^{2i\phi}\cot^2\theta Q_{d^c} + T^2 Q_d \csc^2\theta Q_u Q_{d^c} - T^2 Q_d \csc^2\theta Q_u Q_{u^c} + T^2 Q_d \csc^2\theta Q_{d^c} Q_{u^c} \\ & - T^2 \csc^2\theta Q_u Q_{d^c} Q_{u^c} + 2Te^{i\phi} Q_d \cot\theta\csc\theta Q_{d^c} - 2Te^{i\phi}\cot\theta\csc\theta Q_u Q_{u^c} \\ & - e^{2i\phi}\cot^2\theta Q_{u^c} + e^{2i\phi} Q_d \cot^2\theta - e^{2i\phi}\cot^2\theta Q_u; \end{aligned} \tag{2.4.82}$$

$$\begin{aligned} D_1 = {} & Q_d Q_e Q_{d^c} + Q_d Q_{d^c} Q_{e^c} - Q_e Q_{d^c} Q_{e^c} - Q_d Q_e Q_{e^c} - Q_d Q_u Q_{d^c} - Q_d Q_{d^c} Q_{u^c} \\ & + Q_u Q_{d^c} Q_{u^c} + Q_d Q_u Q_{u^c} + Q_e Q_u Q_{e^c} - Q_e Q_u Q_{u^c} + Q_e Q_{e^c} Q_{u^c} - Q_u Q_{e^c} Q_{u^c}. \end{aligned} \tag{2.4.83}$$

The elements of M_E are independent parameters. We can express M_U and M_D in terms of $T, \theta, \phi, a^u_{33}, a^d_{33}, a^e_{ij}$ and ϵ (or $\epsilon_{1,2}$) for the case of 45_H (or 210_H), so in this basis the charged fermion mass matrices are:

$$M_E^T = -3v_d \begin{bmatrix} a^e_{11} & 0 & a^e_{13} \\ 0 & a^e_{22} & a^e_{23} \\ a^e_{31} & a^e_{32} & a^e_{33} \end{bmatrix} ; \tag{2.4.84}$$

$$M_U^T = v_u \begin{bmatrix} a^e_{11} & 0 & \frac{a^e_{13}N_{e^c}(Q_e-Q_{u^c})+a^e_{31}N_e(-Q_{e^c}+Q_{u^c})}{N_{u^c}(Q_e-Q_{e^c})} \\ 0 & a^e_{22} & \frac{a^e_{23}N_{e^c}(Q_e-Q_{u^c})+a^e_{32}N_e(-Q_{e^c}+Q_{u^c})}{N_{u^c}(Q_e-Q_{e^c})} \\ \frac{a^e_{13}N_{e^c}(Q_e-Q_u)+a^e_{31}N_e(-Q_{e^c}+Q_u)}{N_u(Q_e-Q_{e^c})} & \frac{a^e_{23}N_{e^c}(Q_e-Q_u)+a^e_{32}N_e(-Q_{e^c}+Q_u)}{N_u(Q_e-Q_{e^c})} & a^u_{33} \end{bmatrix} ; \tag{2.4.85}$$

$$M_D^T = v_d \begin{bmatrix} a^e_{11} & 0 & \frac{a^e_{13}N_{e^c}(Q_e-Q_{d^c})+a^e_{31}N_e(-Q_{e^c}+Q_{d^c})}{N_{d^c}(Q_e-Q_{e^c})} \\ 0 & a^e_{22} & \frac{a^e_{23}N_{e^c}(Q_e-Q_{d^c})+a^e_{32}N_e(-Q_{e^c}+Q_{d^c})}{N_{d^c}(Q_e-Q_{e^c})} \\ \frac{a^e_{13}N_{e^c}(Q_e-Q_u)+a^e_{31}N_e(-Q_{e^c}+Q_u)}{N_u(Q_e-Q_{e^c})} & \frac{a^e_{23}N_{e^c}(Q_e-Q_u)+a^e_{32}N_e(-Q_{e^c}+Q_u)}{N_u(Q_e-Q_{e^c})} & a^d_{33} \end{bmatrix} . \tag{2.4.86}$$

Since $Q_u = Q_d$, we have $a^d_{31} = a^u_{31}$ and $a^d_{32} = a^u_{32}$, see Eqs. (2.4.64) and (2.4.65).

Now, the rotation that was made in the 1-2 sector to set $a_{12} = 0$ simultaneously can make a^e_{11} and a^e_{22} real. This rotation will alter the column $\{(M_E)_{13}, (M_E)_{23}\}^T$ and the row $\{(M_E)_{31}, (M_E)_{32}\}$ in such a way that the forms of M_U Eq. (2.4.85) and M_D Eq. (2.4.86) are preserved. All parameters are complex, except that one among $a^{u,d,e}_{33}$ can be made real (we choose a^d_{33} to be real), and that T can be chosen real. So the parameter set is

$$\{\epsilon, r, T, \theta, \phi, a^e_{11}, a^e_{22}, a^e_{13}, a^e_{31}, a^e_{23}, a^e_{32}, a^e_{33}, a^u_{33}, a^d_{33}\} \text{ for } 45_{\rm H} \text{ or}$$

$$\{\epsilon_1, \epsilon_2, r, T, \theta, \phi, a^e_{11}, a^e_{22}, a^e_{13}, a^e_{31}, a^e_{23}, a^e_{32}, a^e_{33}, a^u_{33}, a^d_{33}\} \text{ for } 210_{\rm H}.$$

Of these sets, $\{a^e_{13}, a^e_{31}, a^e_{23}, a^e_{32}, a^e_{33}, a^u_{33}\}$ are complex (with a^d_{33} chosen to be real). For $\Phi = 45_H$, there are 13 magnitudes and 7 phases (in total 20 parameters) for non-SUSY case. In the case of SUSY, ϵ is complex, so one additional phase enters (for a total 21 parameters). For $\Phi = 210_H$ in the SUSY context with minimal Higgs content, ϵ_1 and ϵ_2 are not independent of each other (see later), so there are again 13 magnitudes and 8 phases (in total 21 parameters). Later we will also consider a case with non-minimal Higgs sector where both these VEV ratios $\epsilon_{1,2}$ can be in general independent of each other. In the neutrino sector (discussed in the next subsection) the mass matrix is given by these same parameters except for an overall scale ($v_{R,L}$ for type-I and type-II seesaw scenarios respectively) that adds one new parameter.

2.4.1 The neutrino sector

Type-I seesaw

To write down the mass matrix in the neutrino sector, we make the assumption that $M, b\Omega \gg v_R$, which is a valid approximation provided that $M, b\Omega \sim M_{GUT} \sim 10^{16}$ GeV. Note that in order to generate light neutrino

masses by using the seesaw mechanism, one roughly needs $v_R \sim 10^{12-14}$ GeV. In this approximation, no new parameter comes into play in the neutrino mass matrix except the scale v_R. For type-I seesaw mechanism the Dirac neutrino mass matrix can be read off from Eq. (2.4.59):

$$M_{\nu_D}^T = -3v_u \begin{bmatrix} a_{11}^e & 0 & \frac{a_{13}^e N_{e^c}(Q_e - Q_{\nu^c}) + a_{31}^e N_e(-Q_{e^c} + Q_{\nu^c})}{N_{\nu^c}(Q_e - Q_{e^c})} \\ 0 & a_{22}^e & \frac{a_{23}^e N_{e^c}(Q_e - Q_{\nu^c}) + a_{32}^e N_e(-Q_{e^c} + Q_{\nu^c})}{N_{\nu^c}(Q_e - Q_{e^c})} \\ a_{31}^e & a_{32}^e & a_{33}^\nu \end{bmatrix} . \tag{2.4.87}$$

Since $Q_e = Q_\nu$, $a_{31}^\nu = a_{31}^e$ and $a_{32}^\nu = a_{32}^e$. The expressions for a_{33}^ν are given in Eqs. (2.4.88) and (2.4.89) for $\Phi = 45_H$ and 210_H respectively are given by:

$$a_{33}^\nu = a_{33}^u \frac{N_u N_{u^c}}{N_\nu N_{\nu^c}} + a_{33}^d \frac{N_d N_{d^c}}{N_\nu N_{\nu^c}} \frac{1 + \epsilon/5}{1 + \epsilon} - a_{33}^e \frac{N_e N_{e^c}}{N_\nu N_{\nu^c}} \frac{1 + \epsilon/5}{1 + \epsilon}. \tag{2.4.88}$$

And for the case of 210_H we find:

$$a_{33}^\nu = a_{33}^u \frac{N_u N_{u^c}}{N_\nu N_{\nu^c}} \frac{C_{10}}{D_2} + a_{33}^d \frac{N_d N_{d^c}}{N_\nu N_{\nu^c}} \frac{C_{11}}{D_2} + a_{33}^e \frac{N_e N_{e^c}}{N_\nu N_{\nu^c}} \frac{C_{12}}{D_2}, \tag{2.4.89}$$

with

$$C_{10} = 3\left(8\sqrt{6}\epsilon_1^2 - 4\left(2\sqrt{3}\epsilon_2 + 3\sqrt{2}\right)\epsilon_1 + \epsilon_2\left(\sqrt{6}\epsilon_2 + 6\right)\right), \tag{2.4.90}$$

$$C_{11} = 3\left(-8\sqrt{6}\epsilon_1^2 + 12\sqrt{2}\epsilon_1 + \epsilon_2\left(\sqrt{6}\epsilon_2 - 6\right)\right), \tag{2.4.91}$$

$$C_{12} = 8\sqrt{6}\epsilon_1^2 + 4\left(2\sqrt{3}\epsilon_2 + 3\sqrt{2}\right)\epsilon_1 - 3\epsilon_2\left(\sqrt{6}\epsilon_2 + 2\right), \tag{2.4.92}$$

$$D_2 = \left(4\epsilon_1 - \sqrt{2}\epsilon_2\right)\left(2\sqrt{6}\epsilon_1 - 3\sqrt{3}\epsilon_2 + 3\sqrt{2}\right). \tag{2.4.93}$$

One can derive the right-handed neutrino Majorana mass matrix to be

$$\frac{M_{\nu_R}}{v_R} = \begin{bmatrix} a_{11}^e & 0 & \frac{a_{13}^e N_{e^c}(Q_e - Q_{\nu^c}) + a_{31}^e N_e(-Q_{e^c} + Q_{\nu^c})}{N_{\nu^c}(Q_e - Q_{e^c})} \\ 0 & a_{22}^e & \frac{a_{23}^e N_{e^c}(Q_e - Q_{\nu^c}) + a_{32}^e N_e(-Q_{e^c} + Q_{\nu^c})}{N_{\nu^c}(Q_e - Q_{e^c})} \\ \frac{a_{13}^e N_{e^c}(Q_e - Q_{\nu^c}) + a_{31}^e N_e(-Q_{e^c} + Q_{\nu^c})}{N_{\nu^c}(Q_e - Q_{e^c})} & \frac{a_{23}^e N_{e^c}(Q_e - Q_{\nu^c}) + a_{32}^e N_e(-Q_{e^c} + Q_{\nu^c})}{N_{\nu^c}(Q_e - Q_{e^c})} & a_{33}^R \end{bmatrix}, \tag{2.4.94}$$

The expressions for a_{33}^R are given in Eqs. (2.4.95) and (2.4.96) for $\Phi = 45_H$ and 210_H respectively are given below. Using Eqs. (2.4.71), (2.4.72) and (2.4.73) for the 45_H-case we have:

$$a_{33}^R = \frac{3}{2} a_{33}^u \frac{N_u N_{u^c}}{N_{\nu^c}^2} \frac{1 + \epsilon/5}{1 + 3\epsilon/5} - \frac{5}{4} a_{33}^e \frac{N_e N_{e^c}}{N_{\nu^c}^2} \frac{(1 + \epsilon/5)^2}{\epsilon(1 + \epsilon)} + \frac{5}{4} a_{33}^d \frac{N_d N_{d^c}}{N_{\nu^c}^2} \frac{1 + \frac{3}{5}\epsilon + \frac{3}{25}\epsilon^2 + \frac{33}{125}\epsilon^3}{\epsilon(1 + \epsilon)(1 + 3\epsilon/5)}. \tag{2.4.95}$$

And for 210_H-case we have:

$$a_{33}^R = a_{33}^u \frac{N_u N_{u^c}}{N_{\nu^c}^2} \frac{C_{13}}{D_3} - a_{33}^d \frac{N_d N_{d^c}}{N_{\nu^c}^2} \frac{C_{14}}{D_3} + a_{33}^e \frac{N_e N_{e^c}}{N_{\nu^c}^2} \frac{C_{15}}{D_3}, \tag{2.4.96}$$

with

$$C_{13} = 18\sqrt{3}\epsilon_2^4 + 36\sqrt{2}\epsilon_2^3 - 45\sqrt{6}\epsilon_1\epsilon_2^3 + 12\sqrt{3}\epsilon_2^2 - 156\epsilon_1\epsilon_2^2 + 72\sqrt{6}\epsilon_1^3\epsilon_2 + 12\sqrt{2}\epsilon_1^2\epsilon_2 - 30\sqrt{6}\epsilon_1\epsilon_2 + 48\epsilon_1^3 + 24\sqrt{3}\epsilon_1^2, \tag{2.4.97}$$

$$C_{14} = 9\sqrt{3}\epsilon_2^4 + 18\sqrt{2}\epsilon_2^3 - 45\sqrt{6}\epsilon_1\epsilon_2^3 + 72\sqrt{3}\epsilon_1^2\epsilon_2^2 + 6\sqrt{3}\epsilon_2^2 - 96\epsilon_1\epsilon_2^2 + 72\sqrt{6}\epsilon_1^3\epsilon_2 + 36\sqrt{2}\epsilon_1^2\epsilon_2 - 18\sqrt{6}\epsilon_1\epsilon_2 + 48\epsilon_1^3 + 24\sqrt{3}\epsilon_1^2, \tag{2.4.98}$$

$$C_{15} = 16\sqrt{6}\epsilon_1^3 + 8\left(5\sqrt{3}\epsilon_2 + 6\sqrt{2}\right)\epsilon_1^2 + 6\left(\sqrt{6}\epsilon_2^2 + 8\epsilon_2 + 2\sqrt{6}\right)\epsilon_1 - 3\epsilon_2\left(3\sqrt{3}\epsilon_2^2 + 6\sqrt{2}\epsilon_2 + 2\sqrt{3}\right), \tag{2.4.99}$$

$$D_3 = 2\epsilon_1\left(4\epsilon_1 - \sqrt{2}\epsilon_2\right)\left(2\sqrt{6}\epsilon_1 - 3\sqrt{3}\epsilon_2 + 3\sqrt{2}\right). \tag{2.4.100}$$

Then, the light neutrino mass matrix in the type-I seesaw scenario is given by

$$M_N = -M_{\nu_D}^T M_{\nu_R}^{-1} M_{\nu_D}. \tag{2.4.101}$$

Type-II seesaw

In analogy to the the analysis done in Sec. 2.4.1 one can derive the type-II seesaw contributions to the the neutrino mass matrix by replacing $v_R \to v_L$ and $\nu^c \to \nu$. In this type-II seesaw scenario the neutrino mass matrix is then given by

$$M_{\nu_L} = v_L \begin{bmatrix} a_{11}^e & 0 & a_{31}^e \\ 0 & a_{22}^e & a_{32}^e \\ a_{31}^e & a_{32}^e & a_{33}^L \end{bmatrix}. \tag{2.4.102}$$

The expressions for a_{33}^L are given in Eqs. (2.4.103) and (2.4.104) for $\Phi = 45_H$ and 210_H respectively are given by:

$$a_{33}^L = \frac{-4}{5} a_{33}^e \frac{N_{e^c}}{N_\nu} \frac{\epsilon}{1+\epsilon} + \frac{1}{2} a_{33}^u \frac{N_u N_{u^c}}{N_\nu^2} \frac{5+9\epsilon}{5+3\epsilon} + \frac{1}{10} a_{33}^d \frac{N_d N_{d^c}}{N_\nu^2} \frac{25+50\epsilon+9\epsilon^2}{(1+\epsilon)(5+3\epsilon)}. \tag{2.4.103}$$

And for the case of 210_H we have:

$$a_{33}^L = a_{33}^u \frac{N_u N_{u^c}}{N_\nu^2} \frac{C_{16}}{D_4} + a_{33}^d \frac{N_d N_{d^c}}{N_\nu^2} \frac{C_{17}}{D_4} + a_{33}^e \frac{N_e N_{e^c}}{N_\nu^2} \frac{C_{18}}{D_4}, \tag{2.4.104}$$

with

$$C_{16} = 3\left(8\left(\sqrt{6}\epsilon_2 - 2\right)\epsilon_1^2 - 4\left(2\sqrt{3}\epsilon_2^2 + \sqrt{2}\epsilon_2 - 2\sqrt{3}\right)\epsilon_1 + \epsilon_2\left(\sqrt{6}\epsilon_2^2 + 4\epsilon_2 - 2\sqrt{6}\right)\right), \tag{2.4.105}$$

$$C_{17} = 3\left(-8\left(\sqrt{6}\epsilon_2 - 2\right)\epsilon_1^2 + \left(12\sqrt{2}\epsilon_2 - 8\sqrt{3}\right)\epsilon_1 + \epsilon_2\left(\sqrt{6}\epsilon_2^2 - 8\epsilon_2 + 2\sqrt{6}\right)\right), \tag{2.4.106}$$

$$C_{18} = 8\sqrt{3}\epsilon_1\epsilon_2\left(2\sqrt{2}\epsilon_1 - \epsilon_2\right), \tag{2.4.107}$$

$$D_4 = 2\epsilon_2\left(\sqrt{2}\epsilon_2 - 4\epsilon_1\right)\left(-2\sqrt{6}\epsilon_1 + 3\sqrt{3}\epsilon_2 - 3\sqrt{2}\right). \tag{2.4.108}$$

2.5 Symmetry breaking constraints

In all models studied here, there is no 10_H Higgs and matter fields couple to $126_H + \overline{126}_H$ and 45_H or 210_H scalars. There are considerations as outlined in Sec. II that would require additional Higgs fields to be present for consistent symmetry breaking. While there are no constraints on the VEV ratios when a 210_H is employed in the non-SUSY framework, these ratios are determined in the case of SUSY. We consider the various constraints on the symmetry breaking sector in this section.

2.5.1 Non-SUSY $SO(10)$ models A and B

Model **A** employs 126_H, 45_H and a 54_H. Breaking of $SO(10)$ down to SM via $SU(5)$ channel is not viable due to gauge coupling unification and proton decay limits. If only 45_H and 126_H (or 16_H) Higgs multiplets are used to break $SO(10)$, breaking takes place through the $SU(5)$-symmetric channel [61–63]. The other two breaking channels $SO(10) \to SU(3)_c \times SU(2)_L \times SU(2)_R \times U(1)_{B-L} \to SM$ and $SO(10) \to SU(4)_c \times SU(2)_L \times U(1)_R \to SM$ do not have stable vacuum at the tree-level. Recently quantum corrections to the tree-level potential have been taken into account [64, 65] and the validity of such breaking channels has been shown. However, we do not rely on quantum corrections in this paper. This is why the Higgs sector needs to be extended with a 54_H for consistent $SO(10)$ breaking down to SM [66, 67]. Note that a Higgs system consisting of 126_H and 54_H is sufficient for symmetry breaking purposes if also a 10_H is used [68], but without the 10_H as in our case, a 45_H is necessary.

Since the SM Higgs doublet is part of the 126_H in this model, a question arises as to the negativity of its squared mass. Consistency of the GUT scale symmetry breaking would require all physical scalar squared masses to be positive, which includes the SM Higgs doublet. There must then be a source that turns this positive mass to negative value. It has been shown in Ref. [69] that indeed such a turn-around is possible, provided that some scalar from any GUT multiplet remains light and has non-negligible couplings to the SM Higgs doublet. The context in Ref. [69] is similar to our present case, where a 144_H of $SO(10)$ is used to break the GUT symmetry as well as the electroweak symmetry. Since our present non-SUSY model has an intermediate scale, we expect some of the scalars to survive down to the intermediate scale, which would enable turning the Higgs mass-squared to negative value so as to trigger electroweak symmetry breaking.

In Model **B** we employ a 210_H in addition to the 126_H. This is not however sufficient for our purpose. Since the VEV of 126_H is much smaller than the GUT scale, a single 210_H would break the GUT symmetry to one of its maximal little groups, such as $SU(5) \times U(1)$ or $SU(4)_c \times SU(2)_L \times SU(2)_R$ [70]. The fermion mass matrices will then carry traces of this unbroken symmetry, which would lead to unwanted mass relations. This is why we extend the scalar sector by adding a 54_H or 16_H. For non-SUSY $SO(10)$ model with Higgs multiplets

$210_H + 54_H$, since $54^2 \ni 1_s + 54_s + 770_s$ and $210^2 \ni 1_s + 54_s + 770_s$, the scalar potential contains 2 non-trivial quartic couplings between $210_H - 54_H$. In addition, 210_H has 3 non-trivial quartic couplings and 54_H has one cubic and one non-trivial quartic couplings. This counting of non-trivial couplings dictates that in general the two VEV ratios $\epsilon_{1,2}$ from the 210_H are free parameters. Similar argument can be provided if 54_H is replaced by 16_H Higgs.

2.5.2 SUSY $SO(10)$ Models C–F

The Higgs sector of Model **D** consists of $210_H + 54_H + 126_H + \overline{126}_H$. This system is a subset of the SUSY $SO(10)$ models studied in Ref. [71]. The relevant part of the superpotential with only 210_H, 54_H and $126_H + \overline{126}_H$ is:

$$\begin{aligned} W = &\frac{1}{2}m_1\Phi^2 + m_2\Delta\overline{\Delta} + \frac{1}{2}m_5E^2 + \lambda_1\Phi^3 + \lambda_8E^3 \\ &+ \lambda_2\Phi\Delta\overline{\Delta} + \lambda_{10}\Phi^2E + \lambda_{11}\Delta^2E + \lambda_{12}\overline{\Delta}^2E. \end{aligned} \tag{2.5.109}$$

Since the VEV of 126_H is required to be in the intermediate scale $\sim 10^{13-14}$ GeV range from a fit to light neutrino masses arising via the seesaw mechanism, in this analysis of the superpotential one can neglect the contribution coming from this field as the other scalars $210_H + 54_H$ will get much larger VEVs of order the GUT scale $\sim 10^{16}$ GeV. Then the relevant stationary equations are

$$\begin{aligned} 0 &= m_1V_1 + \frac{\lambda_1}{2\sqrt{6}}V_3^2 + \sqrt{\frac{3}{5}}V_1V_E, \\ 0 &= m_1V_2 + \frac{\lambda_1}{3\sqrt{2}}(V_2^2 + V_3^2) - \frac{2\lambda_{10}}{\sqrt{15}}V_2V_E, \\ 0 &= m_1V_3 + \frac{\lambda_1}{\sqrt{6}}V_1V_3 + \frac{\sqrt{2}\lambda_1}{3}V_2V_3 + \frac{\lambda_{10}}{2\sqrt{15}}V_3V_E, \\ 0 &= m_5V_E + \frac{\sqrt{3}\lambda_8}{2\sqrt{5}}V_E^2 + \frac{\sqrt{3}\lambda_{10}}{2\sqrt{5}}V_1^2 - \frac{\lambda_{10}}{\sqrt{15}}V_2^2 + \frac{\lambda_{10}}{4\sqrt{15}}V_3^2. \end{aligned} \tag{2.5.110}$$

Here the $V_1 = \langle(1,1,1)\rangle$, $V_2 = \langle(1,1,15)\rangle$ and $V_3 = \langle(1,3,15)\rangle$ are the VEVs of $\Phi(210_H)$ and the 54_H VEV is $V_E = \langle(1,1,1)\rangle$ under the Pati-Salam group $SU(2)_L \times SU(2)_R \times SU(4)_C$ decomposition. Compared to Eqs. (2.3.44), here a different normalization is used and one can make the identifications $V_1 = \phi_1, V_2 = \sqrt{3}\phi_2, V_3 = \sqrt{3/2}\phi_3$.

The last relation in Eq. (2.5.110) can be solved for the free mass parameter m_5. Taking differences of the other three twice, we obtain two independent solutions,

$$V_1 = -\frac{\sqrt{3}V_2}{2} \quad \text{or,} \quad \mathrm{V_1} = \frac{\mathrm{V_3^2}}{2\sqrt{3}\mathrm{V_2}}. \tag{2.5.111}$$

These correspond to the VEV ratios ($\epsilon_1 = V_2/V_1, \epsilon_2 = V_3/V_1$) given as

$$\epsilon_1 = -\frac{2}{\sqrt{3}} \quad \text{or,} \quad \epsilon_1 = \frac{\epsilon_2^2}{2\sqrt{3}}. \tag{2.5.112}$$

While studing the fermions masses and mixing numerically, we will consider both these cases. These models are labelled as $\mathbf{D}^{\rm a}$ for the solution $\epsilon_1 = -\frac{2}{\sqrt{3}}$ and $\mathbf{D}^{\rm b}$ for solution $\epsilon_1 = \frac{\epsilon_2^2}{2\sqrt{3}}$.

In Model **E**, we use a 210_H along with a $16_H + \overline{16}_H$ for symmetry breaking purpose. These fields are in addition to the $126_H + \overline{126}_H$ fields present. Just like the previous case, since the $SO(10)$ breaking VEV of the Higgs scalars 210_H and $16_H + \overline{16}_H$ are $\sim M_{GUT}$, one can neglect the terms involving the scalar 126_H which has a much lower VEV. The form of the superpotantial is identical to Eq. (2.5.109) with the $126_H(\overline{126}_H)$ replaced by $16_H(\overline{16}_H)$. Denoting the $16_H(\overline{16}_H)$ VEV as $V_\psi(\overline{V}_\psi)$ and its mass by m_ψ, the relevant stationary equations in this case are

$$\begin{aligned}
0 &= m_1 V_1 + \frac{\lambda_1}{2\sqrt{6}} V_3^2 + \frac{\lambda_2}{10\sqrt{6}} V_\psi \overline{V}_\psi, \\
0 &= m_1 V_2 + \frac{\lambda_1}{3\sqrt{2}} (V_2^2 + V_3^2) + \frac{\lambda_2}{10\sqrt{2}} V_\psi \overline{V}_\psi, \\
0 &= m_1 V_3 + \frac{\lambda_1}{\sqrt{6}} V_1 V_3 + \frac{\sqrt{2}\lambda_1}{3} V_2 V_3 + \frac{\lambda_2}{10} V_\psi \overline{V}_\psi, \\
0 &= V_\psi \overline{V}_\psi [m_\psi + \frac{\lambda_2}{10\sqrt{6}} V_1 + \frac{\lambda_2}{10\sqrt{2}} V_2 + \frac{\lambda_2}{10} V_3].
\end{aligned} \tag{2.5.113}$$

There are two different solutions of this system of stationary equations

$$\begin{aligned}
& V_1 = \frac{V_3}{\sqrt{6}}, \;\; V_2 = \frac{V_3}{\sqrt{2}}; \\
\text{or,} \;\; & \mathrm{V}_1 = \frac{-36 m_1^2 V_3 + 5 V_3^3 \lambda_1^2}{\sqrt{6}(-6 m_1 + V_3 \lambda_1)^2}, \;\; V_2 = -\frac{-36 m_1^2 + 12 m_1 V_3 \lambda_1 + V_3^2 \lambda_1^2}{\sqrt{2}\lambda_1(-6 m_1 + V_3 \lambda_1)}.
\end{aligned} \tag{2.5.114}$$

So the VEV ratios are given by

$$\begin{aligned}
& \epsilon_1 = \sqrt{3}, \;\; \epsilon_2 = \sqrt{6}; \\
\text{or,} \;\; & \epsilon_1 = \frac{\sqrt{3}(-6+\epsilon)(-36+12\epsilon+\epsilon^2)}{\epsilon(36-5\epsilon^2)}, \;\; \epsilon_2 = \frac{\sqrt{6}(-6+\epsilon)^2}{-36+5\epsilon^2} \;\; ; \quad \text{with} \;\; \epsilon \equiv \mathrm{V}_3 \frac{\lambda_1}{\mathrm{m}_1},
\end{aligned} \tag{2.5.115}$$

where ϵ is a free parameter. We discard the first solution since this corresponds to $SU(5)$-symmetric case. The surviving model will be labeled **E**.

By adding more Higgs multiplets in either of the models **D** or **E**, as for example $16_H + \overline{16}_H$ or adding another 54_H to model **D**, these relations for VEV ratios can be made invalid and $\epsilon_{1,2}$ can be made independent parameters. We will also study this general case. We choose to add $16_H + \overline{16}_H$ in model **D** and 54_H in model **E** and label these classes of model as **F**. Finally, for SUSY model **C**, consisting of $126_H + \overline{126}_H + 45_H + 54_H + 16_H + \overline{16}_H$, we stress that the $16_H + \overline{16}_H$ are needed for successfully tuning the MSSM doublets light without making simultaneously any other submultiplet light. The parameter ϵ is arbitrary in this case.

2.6 Numerical analysis of fermion masses and mixings

In this section we show our fit results of fermion masses and mixings for different $SO(10)$ models described in Sections II and V. We do the fitting for both non-SUSY and SUSY cases, each with type-I and type-II seesaw

scenarios. For optimization purpose we do a χ^2-analysis. The pull and χ^2-function are defined as:

$$P_i = \frac{O_{i\ \mathrm{th}} - E_{i\ \mathrm{exp}}}{\sigma_i}, \tag{2.6.116}$$

$$\chi^2 = \sum_i P_i^2, \tag{2.6.117}$$

where σ_i represent experimental 1σ uncertainty and $O_{i\ \mathrm{th}}$, $E_{i\ \mathrm{exp}}$ and P_i represent the theoretical prediction, experimental central value and pull of observable i. We fit the values of the observables at the GUT scale, $M_{GUT} = 2 \times 10^{16}$ GeV. To get the GUT scale values of the observables, for non-SUSY case, we take the central values at the M_Z scale from Table-1 of Ref. [72] and use the renormalization group equation (RGE) running factors given in Ref. [73] to get the GUT scale inputs. For the associated one sigma uncertainties of the observables at the GUT scale, we keep the same percentage uncertainty with respect to the central value of each quantity as that at the M_Z scale. For SUSY case, the low scale values of the observables are taken from Table-2 of [72] at $\mu = 1$ TeV where the values are converted to the $\overline{\mathrm{DR}}$ scheme and then using the renormalization group equation running for MSSM [74, 75] we get the GUT scale inputs. For all different SUSY $SO(10)$ models, we do the fitting for $\tan\beta = 10$. For the charged lepton masses, a relative uncertainty of 0.1% is assumed in order to take into account the theoretical uncertainties arising for example from threshold effects. The inputs in the neutrino sector are taken from Ref. [76]. For neutrino observables, we do not run the RGE from low scale to the GUT scale, which is a relatively small effect, except for an overall rescaling on the neutrino masses that can be absorbed in the corresponding scale v_R or v_L. In the case of inverted hierarchical neutrino mass spectrum, RGE effects can be important, whereas for all our cases the spectrum turns out to be normal hierarchical. Since the right-handed neutrino masses are extremely heavy, threshold corrections might also have effects on the neutrino observables if the Dirac neutrino matrix elements are of order one, but in our case the elements are much smaller than one. All these inputs are shown in the tables where the fit results are presented. Below we present our best fit results and the corresponding parameters for different $SO(10)$ GUT models as discussed above.

Model A: Non-SUSY $SO(10)$: $45_H + 54_H + \overline{126}_H$

The fit results and the predictions for model **A** are shown in Table 3.3 and 3.4 respectively. For model **AI** (Model **A** with type-I seesaw) the parameter set is:

$$\begin{aligned}\{a^u_{33}, a^d_{33}, \epsilon, T, \theta, \phi, v_R, r\} =& \{0.415986 + 0.0944114i, 0.0246549, -1.24753, 8.68487,\\ & 0.560999, -0.0127783, 1.58339 \cdot 10^{13}\mathrm{GeV}, 6.76689\}\end{aligned}$$

and

$$a^e_{ij} = 10^{-2} \begin{pmatrix} 0.0959072 & 0 & -1.47328 - 0.508307i \\ 0 & -0.00693205 & -0.302045 - 0.119282i \\ 0.149467 + 0.0128315i & 0.0534903 - 0.0345252i & 0.461306 - 1.4512i \end{pmatrix}. \quad (2.6.118)$$

Masses (in GeV) and Mixing parameters	Inputs (at $\mu = M_{GUT}$)	Fitted values (**AI**) (at $\mu = M_{GUT}$)	pulls (**AI**)	Fitted values (**AII**) (at $\mu = M_{GUT}$)	pulls (**AII**)
$m_u/10^{-3}$	0.437±0.147	0.441	0.03	0.469	0.21
m_c	0.236±0.007	0.236	0.003	0.236	0.02
m_t	73.82±0.64	73.82	0.01	73.81	-0.01
$m_d/10^{-3}$	1.12±0.11	1.14	0.16	1.12	-0.01
$m_s/10^{-3}$	21.93±1.07	21.82	-0.10	21.98	0.04
m_b	0.987±0.008	0.987	-0.003	0.987	-0.003
$m_e/10^{-3}$	0.469658±0.000469	0.469649	-0.01	0.469757	0.21
$m_\mu/10^{-3}$	99.1474±0.0991	99.1555	0.08	99.0913	-0.56
m_τ	1.68551±0.00168	1.68542	-0.05	1.68602	0.29
$\|V_{us}\|/10^{-2}$	22.54±0.06	22.53	-0.01	22.54	0.005
$\|V_{cb}\|/10^{-2}$	4.856±0.06	4.856	0.001	4.853	-0.03
$\|V_{ub}\|/10^{-2}$	0.420±0.013	0.420	0.07	0.420	0.02
δ_{CKM}	1.207±0.054	1.205	-0.03	1.205	-0.03
$\Delta m^2_{sol}/10^{-5}(\text{eV}^2)$	7.56±0.24	7.56	0.01	7.54	-0.06
$\Delta m^2_{atm}/10^{-3}(\text{eV}^2)$	2.41±0.08	2.40	-0.004	2.41	0.05
$\sin^2\theta^{PMNS}_{12}$	0.308±0.017	0.308	0.01	0.302	-0.29
$\sin^2\theta^{PMNS}_{23}$	0.387±0.0225	0.388	0.03	0.396	0.42
$\sin^2\theta^{PMNS}_{13}$	0.0241±0.0025	0.0238	-0.11	0.0239	-0.04

Table 2.1: Fitted values of the observables correspond to $\chi^2 = 7 \cdot 10^{-2}$ and 0.78 for models **AI** and **AII** respectively. These fittings correspond to $|a_{ij}|_{max} = |a_{44}|$ =1.9 and 3.3 for the type-I and type-II cases respectively (see text for details). For the charged lepton masses, a relative uncertainty of 0.1% is assumed in order to take into account the theoretical uncertainties arising for example from threshold effects.

For model **AII** (Model **A** with type-II seesaw) the parameter set is:

$$\{a^u_{33}, a^d_{33}, \epsilon, T, \theta, \phi, v_L, r\} = \{0.152744 + 0.399269i, -0.0244755, -0.393925, 11.4001, 0.560999,$$
$$0.105066, 1.69937 \cdot 10^{-8}\text{GeV}, 6.75824\}$$

and

Quantity	Predicted Value (**AI**)	Predicted Value (**AII**)
$\{m_1, m_2, m_3\}$ (in eV)	$\{3.72 \cdot 10^{-3}, 9.45 \cdot 10^{-3}, 4.99 \cdot 10^{-2}\}$	$\{4.38 \cdot 10^{-3}, 9.72 \cdot 10^{-3}, 5.00 \cdot 10^{-2}\}$
$\{\delta^{PMNS}, \alpha_{21}^{PMNS}, \alpha_{31}^{PMNS}\}$	$\{120.03^\circ, 144.92^\circ, -168.49^\circ\}$	$\{104.80^\circ, 159.32^\circ, 95.05^\circ\}$
$\{m_{cos}, m_\beta, m_{\beta\beta}\}$ (in eV)	$\{6.31 \cdot 10^{-2}, 6.55 \cdot 10^{-3}, 1.22 \cdot 10^{-3}\}$	$\{6.42 \cdot 10^{-2}, 7.05 \cdot 10^{-3}, 2.24 \cdot 10^{-4}\}$
$\{M_1, M_2, M_3\}$ (in GeV)	$\{8.65 \cdot 10^{7}, 2.66 \cdot 10^{10}, 6.99 \cdot 10^{11}\}$	-

Table 2.2: Predictions of the models **A**. m_i are the light neutrino masses, M_i are the right-handed neutrino masses, $\alpha_{21,31}$ are the Majorana phases following the PDG parametrization, $m_{cos} = \sum_i m_i$, $m_\beta = \sum_i |U_{ei}|^2 m_i$ is the effective mass parameter for beta-decay and $m_{\beta\beta} = |\sum_i U_{ei}^2 m_i|$ is the effective mass parameter for neutrinoless double beta decay.

$$a_{ij}^e = 10^{-2} \begin{pmatrix} 0.127684 & 0 & -0.0742479 + 0.0532305i \\ 0 & -0.00055042 & 0.0264824 + 0.0152045i \\ 0.136072 + 0.0070994i & 0.0582979 + 0.00164043i & -0.398502 - 2.1619i \end{pmatrix}. \quad (2.6.119)$$

In performing such optimization, solutions with lower values of χ^2 exist but we are only interested in the solutions for which the original couplings a_{ij} are also in the perturbative range. In the optimization process we restrict ourselves to the case of $(a_{ij})_{max} \lesssim 2$. For all the solutions that are presented, we did find good fits with this cut-off except for model **AII** where $|a_{44}| = 3.3$ as can be seen from Eq. 2.6.132 . The original coupling matrices a_{ij} can be computed with the parameter sets that result due to the minimization process.

In Table 3.4, the predicted quantities correspond to the best fit values. For example, for model **AI**, the predicted value of the Dirac type CP violating phase in the neutrino sector is $\delta^{PMNS} = 2\pi/3$. The fit result presented in this case is very good since $\chi^2 = 7 \cdot 10^{-2}$. We have investigated the robustness of the predicted value of δ_{PMNS} and found it to be not very robust. Since the χ^2 for the best fit is extremely small, it is quite fine to deviate from the minimum χ^2 are still find acceptable fits. We find that the variation of δ_{PMNS} from the predicted value can be quite large. In Fig. 2.1, we show the variation of δ^{PMNS} with χ^2/n_{obs}. Most of the fit results presented in this work have small total χ^2, so this conclusion on the robustness of δ^{PMNS} prediction is valid for the other models as well. We present the variation plot only for model **AI**.

Model B: Non-SUSY $SO(10)$: $\mathbf{210_H + 54_H + \overline{126}_H}$ (or $\mathbf{210_H + 16_H + \overline{126}_H}$)

The fit results and the predictions for models **B** are shown in Table 3.5 and 3.1 respectively. The parameter set for model **BI** is:

$$\{a_{33}^u, a_{33}^d, \epsilon_1, \epsilon_2, T, \theta, \phi, v_R, r\} = \{-0.0380751 - 0.424441i, 0.0244949, 1.61753, 1.67225, 0.764487,$$
$$0.541654, -2.91319, 2.23915 \cdot 10^{13}\text{GeV}, 6.74578\}$$

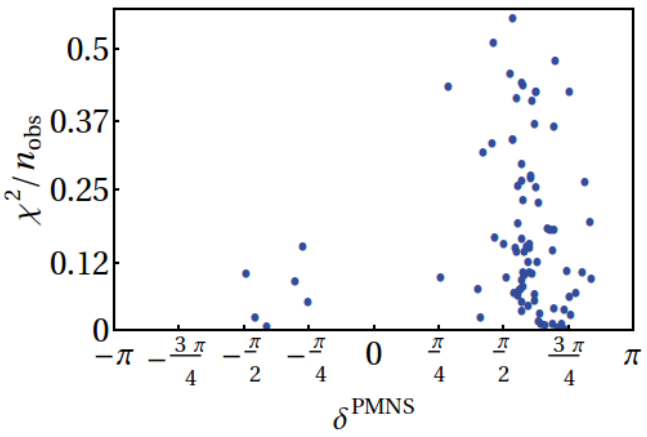

Figure 2.1: Variation of δ^{PMNS} with χ^2/n_{obs} for the model **AI**. In plotting this, we restrict to the regime for which $\chi^2 \leq 10$.

and

$$a^e_{ij} = 10^{-2} \begin{pmatrix} -0.122115 & 0 & 0.899426 + 1.16951i \\ 0 & 0.00569753 & -0.104101 - 0.15069i \\ -0.175821 - 0.103765i & 0.0325028 + 0.0638096i & 1.46544 + 0.663581i \end{pmatrix}. \tag{2.6.120}$$

The parameter set for model **BII** is:

$$\{a^u_{33}, a^d_{33}, \epsilon_1, \epsilon_2, T, \theta, \phi, v_R, r\} = \{0.174446 + 0.389832i, 0.0244585, 1.07061, 0.666248, 0.526787, 0.713998, 0.295856, 1.32386 \cdot 10^{-8}\text{GeV}, 6.74635\}$$

and

$$a^e_{ij} = 10^{-2} \begin{pmatrix} 0.00424453 & 0 & 0.130198 - 0.0532261i \\ 0 & 0.0963929 & -0.386912 - 0.75915i \\ -0.0711623 - 0.0235054i & 0.0531238 + 0.181145i & -1.64856 - 1.16034i \end{pmatrix}. \tag{2.6.121}$$

Masses (in GeV) and Mixing parameters	Inputs (at $\mu = M_{GUT}$)	Fitted values (**B I**) (at $\mu = M_{GUT}$)	pulls (**B I**)	Fitted values (**B II**) (at $\mu = M_{GUT}$)	pulls (**B II**)
$m_u/10^{-3}$	0.437±0.147	0.436	-0.0007	0.437	0.0002
m_c	0.236±0.007	0.236	0.006	0.236	-0.00009
m_t	73.82±0.64	73.82	0.003	73.82	-0.00005
$m_d/10^{-3}$	1.12±0.11	1.12	0.0	1.12	-0.0005
$m_s/10^{-3}$	21.93±1.07	21.95	0.01	21.93	-0.0003
m_b	0.987±0.008	0.987	0.005	0.987	0.0003
$m_e/10^{-3}$	0.469658±0.000469	0.469654	-0.008	0.469658	-0.0004
$m_\mu/10^{-3}$	99.1474±0.0991	99.1412	-0.06	99.1476	0.002
m_τ	1.68551±0.00168	1.68555	0.02	1.68551	-0.002
$\|V_{us}\|/10^{-2}$	22.54±0.06	22.54	0.0009	22.54	-0.00004
$\|V_{cb}\|/10^{-2}$	4.856±0.06	4.856	0.0001	4.856	0.0002
$\|V_{ub}\|/10^{-2}$	0.420±0.013	0.419	-0.001	0.419	-0.0001
δ_{CKM}	1.207±0.054	1.207	0.003	1.207	0.0005
$\Delta m^2_{sol}/10^{-5}(\mathrm{eV}^2)$	7.56±0.24	7.55	-0.001	7.56	0.00005
$\Delta m^2_{atm}/10^{-3}(\mathrm{eV}^2)$	2.41±0.08	2.40	0.004	2.41	0.0001
$\sin^2\theta_{12}^{PMNS}$	0.308±0.017	0.307	-0.004	0.307	-0.0003
$\sin^2\theta_{23}^{PMNS}$	0.387±0.0225	0.387	-0.002	0.387	0.00004
$\sin^2\theta_{13}^{PMNS}$	0.0241±0.0025	0.0241	0.01	0.0241	0.00009

Table 2.3: Best fit values of the observables correspond to $\chi^2 = 5 \cdot 10^{-3}$ and $1 \cdot 10^{-5}$ for models **BI** and **BII** respectively. These fittings correspond to $|a_{ij}|_{max} = |a_{44}|$ =0.56 and 0.26 for the type-I and type-II cases respectively. For the charged lepton masses, a relative uncertainty of 0.1% is assumed in order to take into account the theoretical uncertainties arising for example from threshold effects.

Model C: SUSY $SO(10)$: $\mathbf{45_H + 54_H + 16_H + \overline{16}_H + 126_H + \overline{126}_H}$

The fit results and the predictions for models **C** are shown in Table 2.5 and 2.6 respectively. The parameter set for model **CI** is:

$$\{a^u_{33}, a^d_{33}, \epsilon, T, \theta, \phi, v_R, r\} = \{-0.22531 + 0.467722i, 0.0317632, -1.10245 + 0.269791i,$$
$$5.51352, 0.560999, 0.448339, 1.39544 \cdot 10^{13}\mathrm{GeV}, 9.14437\}$$

and

$$a^e_{ij} = 10^{-2} \begin{pmatrix} 0.113952 & 0 & -1.52545 - 0.861024i \\ 0 & 0.0066433 & 0.103718 - 0.25156i \\ 0.103242 - 0.07705i & 0.0528824 + 0.0275714i & -0.300714 - 1.23388i \end{pmatrix}. \quad (2.6.122)$$

Quantity	Predicted Value (**BI**)	Predicted Value (**BII**)
$\{m_1, m_2, m_3\}$ (in eV)	$\{2.58 \cdot 10^{-3}, 9.07 \cdot 10^{-3}, 4.99 \cdot 10^{-2}\}$	$\{2.61 \cdot 10^{-3}, 9.07 \cdot 10^{-3}, 4.99 \cdot 10^{-2}\}$
$\{\delta^{PMNS}, \alpha_{21}^{PMNS}, \alpha_{31}^{PMNS}\}$	$\{-38.38°, 175.84°, -131.48°\}$	$\{-65.38°, -158.28°, -96.19°\}$
$\{m_{cos}, m_\beta, m_{\beta\beta}\}$ (in eV)	$\{6.15 \cdot 10^{-2}, 5.67 \cdot 10^{-3}, 8.33 \cdot 10^{-4}\}$	$\{6.16 \cdot 10^{-2}, 5.69 \cdot 10^{-3}, 3.93 \cdot 10^{-4}\}$
$\{M_1, M_2, M_3\}$ (in GeV)	$\{5.47 \cdot 10^{8}, 3.48 \cdot 10^{10}, 5.73 \cdot 10^{11}\}$	-

Table 2.4: Predictions of models **B**. m_i are the light neutrino masses, M_i are the right handed neutrino masses, $\alpha_{21,31}$ are the Majorana phases following the PDG parametrization, $m_{cos} = \sum_i m_i$, $m_\beta = \sum_i |U_{ei}|^2 m_i$ is the effective mass parameter for beta-decay and $m_{\beta\beta} = |\sum_i U_{ei}^2 m_i|$ is the effective mass parameter for neutrinoless double beta decay.

The parameter set for model **CII** is:

$$\begin{aligned}\{a_{33}^u, a_{33}^d, \epsilon, T, \theta, \phi, v_L, r\} =& \{0.0307775 + 0.518792i, -0.0317378, -0.75526 - 0.237386i, \\ & 4.66699, 0.713998, -0.0578946, 1.55237 \cdot 10^{-8}\text{GeV}, 9.1424\}\end{aligned}$$

and

$$a_{ij}^e = 10^{-2} \begin{pmatrix} -0.104302 & 0 & 0.88437 - 0.647303i \\ 0 & 0.00422339 & 0.0628707 - 0.166004i \\ -0.0805026 - 0.140317i & -0.0449238 - 0.0524454i & -0.793384 + 1.69782i \end{pmatrix}. \quad (2.6.123)$$

Masses (in GeV) and Mixing parameters	Inputs (at $\mu = M_{GUT}$)	Fitted values (**CI**) (at $\mu = M_{GUT}$)	pulls (**CI**)	Fitted values (**CII**) (at $\mu = M_{GUT}$)	pulls (**CII**)
$m_u/10^{-3}$	0.502±0.155	0.502	0.001	0.501	-0.0005
m_c	0.245±0.007	0.245	0.002	0.245	0.001
m_t	90.28±0.90	90.28	-0.0005	90.28	-0.002
$m_d/10^{-3}$	0.839±0.084	0.838	-0.006	0.839	-0.001
$m_s/10^{-3}$	16.62±0.90	16.62	-0.00005	16.62	0.002
m_b	0.938±0.009	0.938	-0.001	0.938	-0.001
$m_e/10^{-3}$	0.344021±0.000344	0.344021	0.0001	0.344018	-0.008
$m_\mu/10^{-3}$	72.6256±0.0726	72.6273	0.02	72.6240	-0.02
m_τ	1.24038±0.00124	1.24036	-0.01	1.24038	-0.001
$\|V_{us}\|/10^{-2}$	22.53±0.07	22.53	0.002	22.53	0.001
$\|V_{cb}\|/10^{-2}$	3.934±0.06	3.933	-0.001	3.934	0.001
$\|V_{ub}\|/10^{-2}$	0.340±0.011	0.340	-0.001	0.340	-0.004
δ_{CKM}	1.208±0.054	1.208	0.004	1.208	0.001
$\Delta m^2_{sol}/10^{-5}(\mathrm{eV}^2)$	7.56±0.24	7.56	0.001	7.55	-0.001
$\Delta m^2_{atm}/10^{-3}(\mathrm{eV}^2)$	2.41±0.08	2.41	0.001	2.40	-0.0006
$\sin^2\theta_{12}^{PMNS}$	0.308±0.017	0.308	0.005	0.308	0.003
$\sin^2\theta_{23}^{PMNS}$	0.387±0.0225	0.387	-0.0001	0.387	-0.002
$\sin^2\theta_{13}^{PMNS}$	0.0241±0.0025	0.0240	-0.002	0.0240	-0.003

Table 2.5: Best fit result for models **C** with inputs correspond to $\tan\beta = 10$. The fitted values correspond to $\chi^2 = 7 \cdot 10^{-4}$ for model **CI** and $6 \cdot 10^{-4}$ for model **CII**. These fittings correspond to $|a_{ij}|_{max} = |a_{44}|$ =1.5 and 1.03 for the type-I and type-II cases respectively. For the charged lepton masses, a relative uncertainty of 0.1% is assumed in order to take into account the theoretical uncertainties arising for example from threshold effects.

Quantity	Predicted Value (**CI**)	Predicted Value (**CII**)
$\{m_1, m_2, m_3\}$ (in eV)	$\{5.36 \cdot 10^{-3}, 1.02 \cdot 10^{-2}, 5.01 \cdot 10^{-2}\}$	$\{3.68 \cdot 10^{-3}, 9.44 \cdot 10^{-3}, 4.99 \cdot 10^{-2}\}$
$\{\delta^{PMNS}, \alpha_{21}^{PMNS}, \alpha_{31}^{PMNS}\}$	$\{157.92°, 158.41°, -104.87°\}$	$\{85.15°, 165.93°, 138.22°\}$
$\{m_{cos}, m_\beta, m_{\beta\beta}\}$ (in eV)	$\{6.57 \cdot 10^{-2}, 7.90 \cdot 10^{-3}, 1.35 \cdot 10^{-3}\}$	$\{6.31 \cdot 10^{-2}, 6.53 \cdot 10^{-3}, 7.55 \cdot 10^{-4}\}$
$\{M_1, M_2, M_3\}$ (in GeV)	$\{1.91 \cdot 10^{8}, 1.63 \cdot 10^{10}, 1.33 \cdot 10^{12}\}$	-

Table 2.6: Predictions of the models **C**. m_i are the light neutrino masses, M_i are the right handed neutrino masses, $\alpha_{21,31}$ are the Majorana phases following the PDG parametrization, $m_{cos} = \sum_i m_i$, $m_\beta = \sum_i |U_{ei}|^2 m_i$ is the effective mass parameter for beta-decay and $m_{\beta\beta} = |\sum_i U_{ei}^2 m_i|$ is the effective mass parameter for neutrinoless double beta decay.

Model D: SUSY $SO(10)$: $\mathbf{210_H + 54_H + 126_H + \overline{126}_H}$

The fit results and the predictions for model $\mathbf{D^aI}$ are shown in Table 2.7 and 2.8 respectively. The parameter set for this fit of model $\mathbf{D^aI}$ is:

$$\{a_{33}^u, a_{33}^d, \epsilon_2, T, \theta, \phi, v_R, r\} = \{-0.343904 + 0.38917i, 0.0318629, -5.89976 - 0.158839i, 0.77736,$$
$$0.532473, 2.76646, 1.95768 \cdot 10^{13}\text{GeV}, 9.15103\}$$

and

$$a_{ij}^e = 10^{-10} \begin{pmatrix} -0.00696426 & 0 & 0.289526 - 0.387539i \\ 0 & -0.0703536 & 1.4192 + 0.447705i \\ 0.00893467 - 0.0548221i & 0.11474 + 0.140445i & 1.06975 - 1.07627i \end{pmatrix}. \quad (2.6.124)$$

Masses (in GeV) and Mixing parameters	Inputs (at $\mu = M_{GUT}$)	Fitted values ($\mathbf{D^aI}$) (at $\mu = M_{GUT}$)	pulls ($\mathbf{D^aI}$)
$m_u/10^{-3}$	0.502±0.155	0.520	0.12
m_c	0.245±0.007	0.243	-0.20
m_t	90.28±0.90	90.17	-0.11
$m_d/10^{-3}$	0.839±0.084	0.967	1.51
$m_s/10^{-3}$	16.62±0.90	16.49	-0.14
m_b	0.938±0.009	0.939	0.14
$m_e/10^{-3}$	0.344021±0.000344	0.343834	-0.54
$m_\mu/10^{-3}$	72.6256±0.0726	72.4978	-1.75
m_τ	1.24038±0.00124	1.23997	-0.32
$\lvert V_{us}\rvert/10^{-2}$	22.53±0.07	22.53	-0.09
$\lvert V_{cb}\rvert/10^{-2}$	3.934±0.06	3.920	-0.22
$\lvert V_{ub}\rvert/10^{-2}$	0.340±0.011	0.341	0.10
δ_{CKM}	1.208±0.054	1.192	-0.28
$\Delta m^2_{sol}/10^{-5}(\mathrm{eV}^2)$	7.56±0.24	7.52	-0.15
$\Delta m^2_{atm}/10^{-3}(\mathrm{eV}^2)$	2.41±0.08	2.42	0.13
$\sin^2\theta_{12}^{PMNS}$	0.308±0.017	0.290	-1.00
$\sin^2\theta_{23}^{PMNS}$	0.387±0.0225	0.399	0.55
$\sin^2\theta_{13}^{PMNS}$	0.0241±0.0025	0.0235	-0.20

Table 2.7: Fitting result for model $\mathbf{D^aI}$ with inputs correspond to $\tan\beta = 10$. The fitted values correspond to $\chi^2 = 7.4$ for type-I. It should be mentioned that, among all the fit results presented in this work, this specific fit has the largest value of χ^2 which is 7.4 for 18 observables. This fit correspond to $|a_{ij}|_{max} = |a_{44}| = 1.55$. For the charged lepton masses, a relative uncertainty of 0.1% is assumed in order to take into account theoretical uncertainties arising for example from threshold effects. We did not find any acceptable fit within the perturbative range for model $\mathbf{D^aII}$.

Quantity	Predicted Value ($\mathbf{D}^{\mathrm{a}}\mathbf{I}$)
$\{m_1, m_2, m_3\}$ (in eV)	$\{1.58 \cdot 10^{-3}, 8.81 \cdot 10^{-3}, 4.99 \cdot 10^{-2}\}$
$\{\delta^{PMNS}, \alpha_{21}^{PMNS}, \alpha_{31}^{PMNS}\}$	$\{85.64°, 139.76°, 149.60°\}$
$\{m_{cos}, m_\beta, m_{\beta\beta}\}$ (in eV)	$\{6.03 \cdot 10^{-2}, 4.78 \cdot 10^{-3}, 1.21 \cdot 10^{-3}\}$
$\{M_1, M_2, M_3\}$ (in GeV)	$\{8.89 \cdot 10^{7}, 2.14 \cdot 10^{10}, 2.63 \cdot 10^{12}\}$

Table 2.8: Predictions of the model $\mathbf{D}^{\mathrm{a}}\mathbf{I}$. m_i are the light neutrino masses, M_i are the right handed neutrino masses, $\alpha_{21,31}$ are the Majorana phases following the PDG parametrization, $m_{cos} = \sum_i m_i$, $m_\beta = \sum_i |U_{ei}|^2 m_i$ is the effective mass parameter for beta-decay and $m_{\beta\beta} = |\sum_i U_{ei}^2 m_i|$ is the effective mass parameter for neutrinoless double beta decay.

The fit results and the predictions for models $\mathbf{D}^{\mathrm{b}}$ are shown in Table 2.9 and 2.10 respectively. The parameter set for $\mathbf{D}^{\mathrm{b}}\mathbf{I}$ is:

$$\{a_{33}^u, a_{33}^d, \epsilon_2, T, \theta, \phi, v_R, r\} = \{-0.416619 - 0.310425i, -0.0317247, 3.76592 + 0.0145385i, 0.310345,$$
$$2.84818, 0.132797, 2.21257 \cdot 10^{13}\mathrm{GeV}, 9.14124\}$$

and

$$a_{ij}^e = 10^{-2} \begin{pmatrix} 0.0964978 & 0 & -0.0230964 + 1.18352i \\ 0 & -0.00493562 & 0.00684639 - 0.202567i \\ -0.0394903 - 0.200904i & 0.055507 + 0.0481135i & 0.753644 + 1.64867i \end{pmatrix}. \quad (2.6.125)$$

And the parameter set for model $\mathbf{D}^{\mathrm{b}}\mathbf{II}$ is:

$$\{a_{33}^u, a_{33}^d, \epsilon_2, T, \theta, \phi, v_L, r\} = \{-0.365477 - 0.36971i, 0.0316996, 3.53671 - 0.311658i, 0.343597,$$
$$- 2.95969, -0.131357, 1.58947 \cdot 10^{-8}\mathrm{GeV}, 9.14446\}$$

and

$$a_{ij}^e = 10^{-2} \begin{pmatrix} 0.00324628 & 0 & -0.026757 + 0.083972i \\ 0 & -0.148375 & 0.450875 + 0.843973i \\ -0.0190056 - 0.0577497i & -0.129264 - 0.0587799i & 1.86523 + 0.58344i \end{pmatrix}. \quad (2.6.126)$$

Masses (in GeV) and Mixing parameters	Inputs (at $\mu = M_{GUT}$)	Fitted values ($\mathbf{D}^{\mathrm{b}}\mathbf{I}$) (at $\mu = M_{GUT}$)	pulls ($\mathbf{D}^{\mathrm{b}}\mathbf{I}$)	Fitted values ($\mathbf{D}^{\mathrm{b}}\mathbf{II}$) (at $\mu = M_{GUT}$)	pulls ($\mathbf{D}^{\mathrm{b}}\mathbf{II}$)
$m_u/10^{-3}$	0.502±0.155	0.501	-0.0006	0.502	0.001
m_c	0.245±0.007	0.245	-0.004	0.245	0.003
m_t	90.28±0.90	90.28	0.002	90.28	-0.00009
$m_d/10^{-3}$	0.839±0.084	0.839	0.001	0.838	-0.004
$m_s/10^{-3}$	16.62±0.90	16.62	-0.001	16.62	-0.0001
m_b	0.938±0.009	0.938	-0.001	0.938	0.001
$m_e/10^{-3}$	0.344021±0.000344	0.344016	-0.01	0.344019	-0.007
$m_\mu/10^{-3}$	72.6256±0.0726	72.6279	0.03	72.62249	-0.01
m_τ	1.24038±0.00124	1.24035	-0.02	1.24039	0.004
$\lvert V_{us}\rvert/10^{-2}$	22.53±0.07	22.53	0.0004	22.53	-0.0003
$\lvert V_{cb}\rvert/10^{-2}$	3.934±0.06	3.934	0.002	3.933	-0.0005
$\lvert V_{ub}\rvert/10^{-2}$	0.340±0.011	0.340	-0.001	0.340	-0.0005
δ_{CKM}	1.208±0.054	1.208	0.002	1.208	-0.001
$\Delta m^2_{sol}/10^{-5}(\mathrm{eV}^2)$	7.55±0.24	7.56	-0.0004	7.55	-0.0003
$\Delta m^2_{atm}/10^{-3}(\mathrm{eV}^2)$	2.41±0.08	2.41	0.0008	2.40	-0.0003
$\sin^2\theta_{12}^{PMNS}$	0.308±0.017	0.308	-0.001	0.308	-0.0003
$\sin^2\theta_{23}^{PMNS}$	0.387±0.0225	0.387	0.0007	0.387	0.001
$\sin^2\theta_{13}^{PMNS}$	0.0241±0.0025	0.0241	0.001	0.02409	-0.001

Table 2.9: Fitting result for model $\mathbf{D}^{\mathrm{b}}$ with inputs correspond to $\tan\beta = 10$. The fitted values correspond to $\chi^2 = 1.9{\cdot}10^{-3}$ and $2{\cdot}10^{-4}$ for models $\mathbf{D}^{\mathrm{b}}\mathbf{I}$ and $\mathbf{D}^{\mathrm{b}}\mathbf{II}$ respectively. These fits correspond to $|a_{ij}|_{max} = |a_{44}| = 0.81$ and 0.99 for the two cases respectively. For the charged lepton masses, a relative uncertainty of 0.1% is assumed in order to take into account theoretical uncertainties arising for example from threshold effects.

Model E: SUSY $SO(10)$: $\mathbf{210_H + 16_H + \overline{16}_H + 126_H + \overline{126}_H}$

The fit results and the predictions for models **E** are shown in Table 2.11 and 2.12 respectively. For model **EI**, the parameter set is:

$$\{a^u_{33}, a^d_{33}, \epsilon, T, \theta, \phi, v_R, r\} = \{0.0873809 + 0.511807i, 0.0316596, 3.21783 + 0.31637i, 0.762371,$$
$$0.747998, 2.38528, 2.26917 \cdot 10^{13}\mathrm{GeV}, 9.13917\}$$

and

$$a^e_{ij} = 10^{-2}\begin{pmatrix} 0.00565532 & 0 & 0.0242668 + 0.230491i \\ 0 & 0.10865 & 1.42287 - 0.445238i \\ -0.0636824 - 0.00136495i & -0.154896 + 0.137372i & -1.56252 + 0.079592i \end{pmatrix}. \quad (2.6.127)$$

Quantity	Predicted Value ($\mathbf{D}^{\mathrm{b}}\mathbf{I}$)	Predicted Value ($\mathbf{D}^{\mathrm{b}}\mathbf{II}$)
$\{m_1, m_2, m_3\}$ (in eV)	$\{2.20 \cdot 10^{-3}, 8.96 \cdot 10^{-3}, 4.99 \cdot 10^{-2}\}$	$\{4.72 \cdot 10^{-3}, 9.89 \cdot 10^{-3}, 5.00 \cdot 10^{-2}\}$
$\{\delta^{PMNS}, \alpha_{21}^{PMNS}, \alpha_{31}^{PMNS}\}$	$\{50.24°, 169.13°, 111.61°\}$	$\{66.63°, 161.63°, 0.41°\}$
$\{m_{cos}, m_\beta, m_{\beta\beta}\}$ (in eV)	$\{6.10 \cdot 10^{-2}, 5.38 \cdot 10^{-3}, 7.40 \cdot 10^{-4}\}$	$\{6.47 \cdot 10^{-2}, 7.37 \cdot 10^{-3}, 4.54 \cdot 10^{-4}\}$
$\{M_1, M_2, M_3\}$ (in GeV)	$\{9.40 \cdot 10^{8}, 3.13 \cdot 10^{10}, 2.44 \cdot 10^{11}\}$	-

Table 2.10: Predictions of models $\mathbf{D}^{\mathrm{b}}$. m_i are the light neutrino masses, M_i are the right handed neutrino masses, $\alpha_{21,31}$ are the Majorana phases following the PDG parametrization, $m_{cos} = \sum_i m_i$, $m_\beta = \sum_i |U_{ei}|^2 m_i$ is the effective mass parameter for beta-decay and $m_{\beta\beta} = |\sum_i U_{ei}^2 m_i|$ is the effective mass parameter for neutrinoless double beta decay.

For model **EII**, the parameter set is:

$$\{a_{33}^u, a_{33}^d, \epsilon, T, \theta, \phi, v_L, r\} = \{-0.43609 + 0.282193i, -0.0316974, 3.21172 + 0.154721i, 0.54795,$$
$$0.682955, 2.41863, 1.26299 \cdot 10^{-8}\mathrm{GeV}, 9.1442\}$$

and

$$a_{ij}^e = 10^{-2} \begin{pmatrix} -0.00491523 & 0 & 0.0991935 + 0.158945i \\ 0 & -0.0989956 & 1.00507 - 0.775818i \\ -0.0677936 - 0.0254017i & 0.0688011 + 0.186132i & -1.33307 + 1.14438i \end{pmatrix}. \quad (2.6.128)$$

Masses (in GeV) and Mixing parameters	Inputs (at $\mu = M_{GUT}$)	Fitted values (**EI**) (at $\mu = M_{GUT}$)	pulls (**EI**)	Fitted values (**EII**) (at $\mu = M_{GUT}$)	pulls (**EII**)
$m_u/10^{-3}$	0.502±0.155	0.501	-0.001	0.502	0.0005
m_c	0.245±0.007	0.245	-0.007	0.245	0.001
m_t	90.28±0.90	90.28	0.001	90.28	-0.002
$m_d/10^{-3}$	0.839±0.084	0.839	0.001	0.839	-0.0005
$m_s/10^{-3}$	16.62±0.90	16.62	0.00009	16.62	-0.0001
m_b	0.938±0.009	0.938	-0.0002	0.938	-0.001
$m_e/10^{-3}$	0.344021±0.000344	0.344022	0.004	0.344023	0.005
$m_\mu/10^{-3}$	72.6256±0.0726	72.6250	-0.007	72.62641	0.01
m_τ	1.24038±0.00124	1.24036	-0.01	1.24037	-0.009
$\|V_{us}\|/10^{-2}$	22.53±0.07	22.53	0.001	22.53	-0.0001
$\|V_{cb}\|/10^{-2}$	3.934±0.06	3.934	0.005	3.933	-0.0003
$\|V_{ub}\|/10^{-2}$	0.340±0.011	0.340	-0.007	0.340	0.0006
δ_{CKM}	1.208±0.054	1.208	0.007	1.208	0.004
$\Delta m^2_{sol}/10^{-5}(\mathrm{eV}^2)$	7.56±0.24	7.56	0.001	7.55	-0.0002
$\Delta m^2_{atm}/10^{-3}(\mathrm{eV}^2)$	2.41±0.08	2.409	-0.0007	2.41	0.0003
$\sin^2\theta_{12}^{PMNS}$	0.308±0.017	0.308	0.006	0.307	-0.002
$\sin^2\theta_{23}^{PMNS}$	0.387±0.0225	0.387	0.002	0.387	0.0008
$\sin^2\theta_{13}^{PMNS}$	0.0241±0.0025	0.0240	0.0001	0.0241	0.001

Table 2.11: Fitting result for models **E** with inputs correspond to $\tan\beta = 10$. The fitted values correspond to $\chi^2 = 4 \cdot 10^{-4}$ for model **EI** and $2 \cdot 10^{-4}$ for model **EII** respectively. These fittings correspond to $|a_{ij}|_{max} = |a_{44}|$ =0.76 and 0.89 for the type-I and type-II cases respectively. For the charged lepton masses, a relative uncertainty of 0.1% is assumed in order to take into account theoretical uncertainties arising for example from threshold effects.

Quantity	Predicted Value (**EI**)	Predicted Value (**EII**)
$\{m_1, m_2, m_3\}$ (in eV)	$\{2.06 \cdot 10^{-3}, 8.93 \cdot 10^{-3}, 4.98 \cdot 10^{-2}\}$	$\{2.46 \cdot 10^{-3}, 9.03 \cdot 10^{-3}, 4.99 \cdot 10^{-2}\}$
$\{\delta^{PMNS}, \alpha_{21}^{PMNS}, \alpha_{31}^{PMNS}\}$	$\{46.84°, -178.55°, 141.46°\}$	$\{-53.69°, -172.46°, -123.70°\}$
$\{m_{cos}, m_\beta, m_{\beta\beta}\}$ (in eV)	$\{6.08 \cdot 10^{-2}, 5.28 \cdot 10^{-3}, 9.54 \cdot 10^{-4}\}$	$\{6.14 \cdot 10^{-2}, 5.58 \cdot 10^{-3}, 7.05 \cdot 10^{-4}\}$
$\{M_1, M_2, M_3\}$ (in GeV)	$\{2.79 \cdot 10^{8}, 2.15 \cdot 10^{10}, 1.82 \cdot 10^{12}\}$	-

Table 2.12: Predictions of models **E**. m_i are the light neutrino masses, M_i are the right handed neutrino masses, $\alpha_{21,31}$ are the Majorana phases following the PDG parametrization, $m_{cos} = \sum_i m_i$, $m_\beta = \sum_i |U_{ei}|^2 m_i$ is the effective mass parameter for beta-decay and $m_{\beta\beta} = |\sum_i U_{ei}^2 m_i|$ is the effective mass parameter for neutrinoless double beta decay.

Model F: SUSY $SO(10)$: $\mathbf{210_H + 54_H + 16_H + \overline{16}_H + 126_H + \overline{126}_H}$

The fit results and the predictions for models **F** are shown in Table 2.13 and 2.14 respectively. The parameter set for model **FI** is:

$$\begin{aligned}\{a_{33}^u, a_{33}^d, \epsilon_1, \epsilon_2, T, \theta, \phi, v_R, r\} =& \{-0.508413 + 0.106596i, 0.0317542, 1.21369 + 0.393457i, 1.11752 \\ &+ 1.12726i, 0.652924, 0.682955, -2.69221, 2.17249 \cdot 10^{13}\text{GeV}, 9.14433\}\end{aligned}$$

and

$$a_{ij}^e = 10^{-2} \begin{pmatrix} -0.101322 & 0 & 1.50945 + 0.641937i \\ 0 & 0.00628798 & -0.311418 - 0.017807i \\ -0.0659206 - 0.186996i & -0.0254875 + 0.0490826i & 0.979206 + 0.994616i \end{pmatrix}. \quad (2.6.129)$$

And the parameter set for model **FII** is:

$$\begin{aligned}\{a_{33}^u, a_{33}^d, \epsilon_1, \epsilon_2, T, \theta, \phi, v_L, r\} = \{&-0.0175831 - 0.518919i, -0.0317748, 1.13488 - 0.537296i, \\ &0.934779 - 0.810325i, 0.577852, 0.541654, 2.37836, 1.17202 \cdot 10^{-8}\text{GeV}, 9.14329\}\end{aligned}$$

and

$$a_{ij}^e = 10^{-2} \begin{pmatrix} 0.00631171 & 0 & -0.244096 - 0.0355119i \\ 0 & -0.106855 & 1.42499 - 0.0405503i \\ -0.00203514 - 0.0627216i & -0.159398 + 0.138939i & 1.56233 + 0.439752i \end{pmatrix}. \quad (2.6.130)$$

Masses (in GeV) and Mixing parameters	Inputs (at $\mu = M_{GUT}$)	Fitted values (**FI**) (at $\mu = M_{GUT}$)	pulls (**FI**)	Fitted values (**FII**) (at $\mu = M_{GUT}$)	pulls (**FII**)
$m_u/10^{-3}$	0.502±0.155	0.501	-0.003	0.501	-0.0005
m_c	0.245±0.007	0.245	0.006	0.245	0.001
m_t	90.28±0.90	90.28	0.003	90.28	0.001
$m_d/10^{-3}$	0.839±0.084	0.839	0.004	0.839	0.001
$m_s/10^{-3}$	16.62±0.90	16.62	-0.001	16.62	0.001
m_b	0.938±0.009	0.938	0.0001	0.938	-0.0001
$m_e/10^{-3}$	0.344021±0.000344	0.344022	0.001	0.344022	0.002
$m_\mu/10^{-3}$	72.6256±0.0726	72.6237	-0.02	72.62539	-0.002
m_τ	1.24038±0.00124	1.24039	0.007	1.24038	0.0003
$\lvert V_{us}\rvert/10^{-2}$	22.53±0.07	22.53	0.0002	22.53	0.0001
$\lvert V_{cb}\rvert/10^{-2}$	3.934±0.06	3.933	-0.001	3.934	0.0001
$\lvert V_{ub}\rvert/10^{-2}$	0.340±0.011	0.340	-0.007	0.340	-0.001
δ_{CKM}	1.208±0.054	1.208	0.001	1.208	0.004
$\Delta m^2_{sol}/10^{-5}(\mathrm{eV}^2)$	7.56±0.24	7.56	0.00003	7.55	-0.0002
$\Delta m^2_{atm}/10^{-3}(\mathrm{eV}^2)$	2.41±0.08	2.41	0.0005	2.41	0.0001
$\sin^2\theta_{12}^{PMNS}$	0.308±0.017	0.308	0.0004	0.308	0.0004
$\sin^2\theta_{23}^{PMNS}$	0.387±0.0225	0.387	-0.001	0.387	0.001
$\sin^2\theta_{13}^{PMNS}$	0.0241±0.0025	0.0240	-0.0009	0.02409	-0.002

Table 2.13: Fitting result for models **F** with inputs correspond to $\tan\beta = 10$. The fitted values correspond to $\chi^2 = 9\cdot10^{-4}$ and $3\cdot10^{-5}$ for models **FI** and **FII** respectively. These fittings correspond to $|a_{ij}|_{max} = |a_{44}|$ =0.67 and 1.08 for the type-I and type-II cases respectively. For the charged lepton masses, a relative uncertainty of 0.1% is assumed in order to take into account theoretical uncertainties arising for example from threshold effects.

Quantity	Predicted Value (**FI**)	Predicted Value (**FII**)
$\{m_1, m_2, m_3\}$ (in eV)	$\{1.84 \cdot 10^{-3}, 8.88 \cdot 10^{-3}, 4.98 \cdot 10^{-2}\}$	$\{2.00 \cdot 10^{-3}, 8.92 \cdot 10^{-3}, 4.98 \cdot 10^{-2}\}$
$\{\delta^{PMNS}, \alpha_{21}^{PMNS}, \alpha_{31}^{PMNS}\}$	$\{-60.72°, -175.43°, -164.89°\}$	$\{44.97°, 179.45°, 133.12°\}$
$\{m_{cos}, m_\beta, m_{\beta\beta}\}$ (in eV)	$\{6.06 \cdot 10^{-2}, 5.11 \cdot 10^{-3}, 1.17 \cdot 10^{-3}\}$	$\{6.08 \cdot 10^{-2}, 5.23 \cdot 10^{-3}, 9.61 \cdot 10^{-4}\}$
$\{M_1, M_2, M_3\}$ (in GeV)	$\{3.92 \cdot 10^{8}, 1.97 \cdot 10^{10}, 1.27 \cdot 10^{12}\}$	-

Table 2.14: Predictions of models **F**. m_i are the light neutrino masses, M_i are the right handed neutrino masses, $\alpha_{21,31}$ are the Majorana phases following the PDG parametrization, $m_{cos} = \sum_i m_i$, $m_\beta = \sum_i |U_{ei}|^2 m_i$ is the effective mass parameter for beta-decay and $m_{\beta\beta} = |\sum_i U_{ei}^2 m_i|$ is the effective mass parameter for neutrinoless double beta decay.

For all the fits to the different models presented in this work, these matrices are shown below:

Model **AI**:

$$a_{ij} = 10^{-2} \begin{pmatrix} 0.0959072 & 0 & 0.579907 + 0.173698i & 5.94255 + 2.20933i \\ 0 & -0.00693205 & 0.134449 + 0.0151987i & 1.11642 + 0.685207i \\ 0.579907 + 0.173698i & 0.134449 + 0.0151987i & 0.343854 + 2.01413i & 16.4068 + 0.693589i \\ 5.94255 + 2.20933i & 1.11642 + 0.685207i & 16.4068 + 0.693589i & 192.42 + 53.2691i \end{pmatrix}. \tag{2.6.131}$$

Model **AII**:

$$a_{ij} = 10^{-2} \begin{pmatrix} 0.127684 & 0 & -0.300661 + 0.102672i & -2.93065 + 0.584561i \\ 0 & -0.00055042 & -0.00799172 + 0.0297446i & -0.450085 + 0.185354i \\ -0.300661 + 0.102672i & -0.00799172 + 0.0297446i & 0.164493 - 2.14188i & 8.08605 + 16.5832i \\ -2.93065 + 0.584561i & -0.450085 + 0.185354i & 8.08605 + 16.5832i & 96.688 + 321.511i \end{pmatrix}. \tag{2.6.132}$$

Model **BI**:

$$a_{ij} = 10^{-2} \begin{pmatrix} -0.122115 & 0 & 0.711183 + 0.747142i & -1.99272 - 3.01439i \\ 0 & 0.00569753 & -0.0996008 - 0.168017i & 0.22039 + 0.476214i \\ 0.711183 + 0.747142i & -0.0996008 - 0.168017i & -1.6329 - 3.89159i & 2.08313 + 14.9094i \\ -1.99272 - 3.01439i & 0.22039 + 0.476214i & 2.08313 + 14.9094i & 10.1819 - 55.9358i \end{pmatrix}. \tag{2.6.133}$$

Model **BII**:

$$a_{ij} = 10^{-2} \begin{pmatrix} 0.00424453 & 0 & -0.739696 + 0.100859i & -0.261416 - 0.180202i \\ 0 & 0.0963929 & 1.59142 + 3.41719i & -0.546982 + 1.75381i \\ -0.739696 + 0.100859i & 1.59142 + 3.41719i & 35.6473 + 92.8117i & -22.3139 + 45.2696i \\ -0.261416 - 0.180202i & -0.546982 + 1.75381i & -22.3139 + 45.2696i & -25.416 + 7.30749i \end{pmatrix}. \tag{2.6.134}$$

Model **CI**:

$$a_{ij} = 10^{-2} \begin{pmatrix} 0.113952 & 0 & 0.491463 + 0.565896i & 3.76471 + 4.85316i \\ 0 & 0.0066433 & -0.0563066 + 0.107998i & -0.804669 + 0.719013i \\ 0.491463 + 0.565896i & -0.0563066 + 0.107998i & -1.4383 + 2.14192i & -6.53535 + 21.208i \\ 3.76471 + 4.85316i & -0.804669 + 0.719013i & -6.53535 + 21.208i & -59.2957 + 144.035i \end{pmatrix}. \tag{2.6.135}$$

Model **CII**:

$$a_{ij} = 10^{-2} \begin{pmatrix} -0.104302 & 0 & -0.23862 + 0.777714i & -1.41328 + 3.82589i \\ 0 & 0.00422339 & -0.0155148 + 0.115636i & 0.0287095 + 0.732858i \\ -0.23862 + 0.777714i & -0.0155148 + 0.115636i & -0.0699652 + 2.31316i & 0.347507 + 16.8414i \\ -1.41328 + 3.82589i & 0.0287095 + 0.732858i & 0.347507 + 16.8414i & -5.81915 + 103.489i \end{pmatrix}. \tag{2.6.136}$$

Model $\mathbf{D^aI}$:

$$a_{ij} = 10^{-10} \begin{pmatrix} -0.00696426 & 0 & -0.245942 + 0.340282i & -0.981934 + 1.05034i \\ 0 & -0.0703536 & -1.2441 - 0.347061i & -3.9061 - 2.2744i \\ -0.245942 + 0.340282i & -1.2441 - 0.347061i & -11.3476 + 13.1125i & -38.737 + 28.5679i \\ -0.981934 + 1.05034i & -3.9061 - 2.2744i & -38.737 + 28.5679i & -137.986 + 71.4185i \end{pmatrix}. \tag{2.6.137}$$

Model $\mathbf{D^bI}$:

$$a_{ij} = 10^{-2} \begin{pmatrix} 0.0964978 & 0 & 0.0463804 + 0.612925i & 0.23948 - 4.0549i \\ 0 & -0.00493562 & -0.0692766 - 0.122098i & 0.0709726 + 0.757652i \\ 0.0463804 + 0.612925i & -0.0692766 - 0.122098i & -1.50677 - 1.28146i & 9.26908 + 9.93996i \\ 0.23948 - 4.0549i & 0.0709726 + 0.757652i & 9.26908 + 9.93996i & -60.1029 - 54.8455i \end{pmatrix}. \tag{2.6.138}$$

Model $\mathbf{D^bII}$:

$$a_{ij} = 10^{-2} \begin{pmatrix} 0.00324628 & 0 & 0.00619872 + 0.0924098i & 0.0581533 + 0.495523i \\ 0 & -0.148375 & 0.234817 + 0.306995i & 2.43678 + 3.11641i \\ 0.00619872 + 0.0924098i & 0.234817 + 0.306995i & -0.940024 - 1.19953i & -10.2704 - 9.213i \\ 0.0581533 + 0.495523i & 2.43678 + 3.11641i & -10.2704 - 9.213i & -63.9596 - 76.7709i \end{pmatrix}. \tag{2.6.139}$$

Model **EI**:

$$a_{ij} = 10^{-2} \begin{pmatrix} 0.00565532 & 0 & -0.266188 + 0.0701303i & 0.518805 - 0.533918i \\ 0 & 0.10865 & 0.425618 + 1.82085i & -3.18677 - 2.87341i \\ -0.266188 + 0.0701303i & 0.425618 + 1.82085i & -14.7905 + 7.46579i & 14.094 - 32.9412i \\ 0.518805 - 0.533918i & -3.18677 - 2.87341i & 14.094 - 32.9412i & 19.4372 + 73.7643i \end{pmatrix}. \tag{2.6.140}$$

Model **EII**:

$$a_{ij} = 10^{-2} \begin{pmatrix} -0.00491523 & 0 & -0.113267 + 0.379235i & -0.0710291 - 0.772947i \\ 0 & -0.0989956 & 1.91708 + 0.433922i & -4.21969 + 0.992353i \\ -0.113267 + 0.379235i & 1.91708 + 0.433922i & -14.9942 + 2.32607i & 31.5765 - 18.8751i \\ -0.0710291 - 0.772947i & -4.21969 + 0.992353i & 31.5765 - 18.8751i & -50.6035 + 73.4838i \end{pmatrix}. \tag{2.6.141}$$

Model **FI**:

$$a_{ij} = 10^{-2} \begin{pmatrix} -0.101322 & 0 & 1.00796 - 1.0692i & -3.40853 + 1.66912i \\ 0 & 0.00628798 & -0.117644 + 0.20702i & 0.5911 - 0.454689i \\ 1.00796 - 1.0692i & -0.117644 + 0.20702i & -3.59013 + 11.2045i & 20.5757 - 20.2831i \\ -3.40853 + 1.66912i & 0.5911 - 0.454689i & 20.5757 - 20.2831i & -63.553 + 23.8071i \end{pmatrix}. \tag{2.6.142}$$

Model **FII**:

$$a_{ij} = 10^{-2} \begin{pmatrix} 0.00631171 & 0 & -0.0913116 - 0.224948i & 0.708328 + 0.52168i \\ 0 & -0.106855 & 0.477564 + 1.57686i & -4.01776 - 3.01492i \\ -0.0913116 - 0.224948i & 0.477564 + 1.57686i & 12.5721 - 5.02818i & -18.1583 + 34.5582i \\ 0.708328 + 0.52168i & -4.01776 - 3.01492i & -18.1583 + 34.5582i & -22.102 - 106.709i \end{pmatrix}. \tag{2.6.143}$$

2.7 $d = 5$ proton decay

Since the flavor dynamics occurs at the GUT scale in this class of models, the best hope for testing this idea is by studying proton decay, in particular, its branching ratios into different modes. While such an analysis can be done for both non-SUSY and SUSY models, here we confine our discussion to the more dominant $d = 5$ decay modes in SUSY mediated by the color-triplet Higgsinos.

We will bound ourselves to the (presumably) dominant $d = 5$ (charged) wino mediated mode, so that only $\mathrm{SU}(2)_L$ non-singlets will appear in the effective operators:

$$W \propto (Y_{QQ})_{ij} (Y_{QL})_{kl} (Q_i Q_j) (Q_k L_l) \tag{2.7.144}$$

with

$$Y_{QQ} = \Lambda_Q^T \left(Y - y x_Q^T - x_Q y^T + y_4 x_Q x_Q^T \right) \Lambda_Q \tag{2.7.145}$$

$$Y_{QL} = \Lambda_Q^T \left(Y - y x_L^T - x_Q y^T + y_4 x_Q x_L^T \right) \Lambda_L \tag{2.7.146}$$

We have to project them to the mass eigenstates defined by the unitary matrices $X = U, D, E, N$ which diagonalize the mass matrices as

$$M_X = X_R M_X^d X_L^\dagger \tag{2.7.147}$$

We will use the notation $(X = U, D)$

$$Y_{XZ} = X_L^T Y_{QQ} Z_L \ \ (\text{for } \ Z = U, D) \tag{2.7.148}$$

$$= X_L^T Y_{QL} Z_L \ \ (\text{for } \ Z = E, N) \tag{2.7.149}$$

After 1-loop $\tilde{w}^{\pm}$ dressing and assuming degeneracy and negligible left-right sfermion mixing the normalized amplitudes for different channels [77] are, in the mass eigenbasis,

$$\begin{aligned} A(K^+\bar{\nu}_l) &= \langle K^+| \, (ud)_L \, s_L |p\rangle \, [(Y_{UD})_{11} \, (Y_{DN})_{2l} - (Y_{DD})_{21} \, (Y_{UN})_{1l}] \\ &+ \langle K^+| \, (us)_L \, d_L |p\rangle \, [(Y_{UD})_{12} \, (Y_{DN})_{1l} - (Y_{DD})_{12} \, (Y_{UN})_{1l}] \end{aligned} \tag{2.7.150}$$

$$A(\pi^+\bar{\nu}_l) = \langle \pi^+| \, (ud)_L \, d_L |p\rangle \, [(Y_{UD})_{11} \, (Y_{DN})_{1l} - (Y_{DD})_{11} \, (Y_{UN})_{1l}] \tag{2.7.151}$$

$$A(K^0 e_l^+) = \langle K^0| \, (us)_L \, u_L |p\rangle \, [(Y_{UU})_{11} \, (Y_{DE})_{2l} - (Y_{UD})_{12} \, (Y_{UE})_{1l}] \tag{2.7.152}$$

$$A(\pi^0 e_l^+) = \langle \pi^0| \, (ud)_L \, u_L |p\rangle \, [(Y_{UU})_{11} \, (Y_{DE})_{1l} - (Y_{UD})_{11} \, (Y_{UE})_{1l}] \tag{2.7.153}$$

$$A(\eta e_l^+) = \langle \eta| \, (ud)_L \, u_L |p\rangle \, [(Y_{UU})_{11} \, (Y_{DE})_{1l} - (Y_{UD})_{11} \, (Y_{UE})_{1l}] \tag{2.7.154}$$

where the numerical values (with maximal error around 30%) of the hadron matrix elements can be found in [78].

The unitary matrices X and the Yukawa matrix elements $Y_{QQ,QL}$ are outputs of each successful fit done. As an example, for model $\mathbf{D}^{\mathrm{a}}\mathbf{I}$ we find

$$Y_{QQ} = \begin{pmatrix} -0.0000696426 & 0 & -0.0105713 + 0.00524935i \\ 0 & -0.000703536 & -0.0237115 - 0.0274144i \\ -0.0105713 + 0.00524935i & -0.0237115 - 0.0274144i & -1.05171 - 0.204611i \end{pmatrix} \tag{2.7.155}$$

$$Y_{QL} = \begin{pmatrix} -0.0000696426 & 0 & -0.0000232394 - 0.000554968i \\ 0 & -0.000703536 & 0.00140745 + 0.00114372i \\ -0.0105713 + 0.00524935i & -0.0237115 - 0.0274144i & 0.00550524 - 0.00420826i \end{pmatrix} \tag{2.7.156}$$

$$U_L = \begin{pmatrix} 0.947932 + 0.154511i & 0.0250533 - 0.277159i & -0.00483953 - 0.00916537i \\ 0.0236485 + 0.277423i & -0.948101 + 0.150221i & -0.0314764 + 0.00505612i \\ -0.00438488 - 0.00319527i & 0.0288651 + 0.0161593i & -0.895175 - 0.444452i \end{pmatrix} \tag{2.7.157}$$

$$D_L = \begin{pmatrix} 0.44376 + 0.785783i & -0.114306 - 0.415343i & -0.00683343 + 0.0000682437i \\ -0.135958 + 0.408742i & -0.484535 + 0.761308i & 0.00448262 - 0.00785931i \\ -0.00402935 - 0.00717747i & -0.00772054 - 0.00109752i & -0.895597 - 0.444722i \end{pmatrix} \tag{2.7.158}$$

$$E_L = \begin{pmatrix} -0.914868 + 0.192948i & -0.182083 - 0.209497i & -0.00368156 + 0.220751i \\ 0.16774 - 0.285354i & -0.612359 - 0.228437i & 0.639383 + 0.233362i \\ -0.0189384 - 0.125958i & -0.00319539 + 0.704116i & -0.0568573 + 0.696242i \end{pmatrix} \tag{2.7.159}$$

$$N_L = \begin{pmatrix} -0.502397 + 0.721475i & -0.139083 - 0.437348i & 0.047407 + 0.119192i \\ -0.43546 + 0.122682i & -0.243261 + 0.682259i & 0.24818 - 0.45725i \\ -0.0953668 + 0.115327i & 0.0333823 + 0.513435i & -0.0502508 + 0.842822i \end{pmatrix} \tag{2.7.160}$$

After squaring (2.7.150)-(2.7.154) and multiplying by the appropriate phase space factor (m_P, m_L, m_p are the pseudo-scalar, lepton and proton mass, respectively)

$$\left(1 - 2\left(\frac{m_P^2 + m_L^2}{m_p^2}\right) + \left(\frac{m_P^2 - m_L^2}{m_p^2}\right)^2\right) \tag{2.7.161}$$

one can calculate the branching fractions for different channels (for neutrino final states we sum over all 3 flavors), the results are given for the different models in table 2.15. While as expected, the $K^+\overline{\nu}$ mode dominates, other sub-leading modes, notably $p \to \pi^+\overline{\nu}$, can be used to test and distinguish various models.

2.8 Conclusion

We have presented in this paper a new class of $SO(10)$ models that can successfully address the flavor puzzle. The key ingredient of our models is the absence of 10_H that is conventionally used in most $SO(10)$ models. Its

	CI	**CII**	**D^{a} I**	**D^{b}I**	**D^{b}II**	**EI**	**EII**	**FI**	**FII**
$K^+\bar{\nu}$	88.39	94.36	50.39	92.71	75.26	89.03	77.91	94.78	90.65
$\pi^+\bar{\nu}$	10.85	5.55	48.33	7.12	24.62	10.48	21.58	4.95	9.17
K^0e^+	0.00	0.00	0.00	0.00	0.00	0.00	0.00	0.00	0.00
$K^0\mu^+$	0.35	0.04	0.49	0.08	0.05	0.23	0.21	0.13	0.09
π^0e^+	0.00	0.00	0.00	0.00	0.00	0.00	0.00	0.00	0.00
$\pi^0\mu^+$	0.34	0.04	0.66	0.08	0.06	0.21	0.25	0.12	0.08
ηe^+	0.00	0.00	0.00	0.00	0.00	0.00	0.00	0.00	0.00
$\eta\mu^+$	0.06	0.01	0.12	0.01	0.01	0.04	0.05	0.02	0.01

Table 2.15: Branching ratios for the main decay modes of the proton mediated by colored Higgsinos in SUSY $SO(10)$ models with successful fermion fits.

absence is compensated by the introduction of a vector-like family in the $16 + \overline{16}$ representation. The Yukawa sector of these models has just a single 4×4 matrix, along with two four-vectors. As a consequence, there are only 14 flavor parameters and 7 phases to fit all fermion masses and mixings, including the neutrino sector.

While the Yukawa system is highly nonlinear, by numerical optimization we have found excellent fits to the fermion observables in a variety of models. A $\overline{126}_H$ is present in all models, to generate large right-handed neutrino Majorana masses as well as to provide the SM Higgs doublet. The vector-like fermions have couplings to either a 45_H or a 210_H that is used to complete the symmetry breaking. A total of six models, four supersymmetric and two non-supersymmetric, have been studied. In each case type-I or type-II seesaw mechanism was analyzed. In one case (Model **D**) with SUSY, minimization of the Higgs potential led to a two-fold solution set, with each providing an excellent fit to flavor observables.

While this class of high scale models cannot be easily tested at collider experiments, proton decay provides an avenue to probe such models. We have investigate the branching ratios for proton decay in the SUSY models, with the results presented in Table 2.15. While it is an ambitious goal to test flavor models in proton decay discovery, even without such a discovery it is heartening to learn that a large class of models can shed light on the various puzzles of fermion masses observed in nature. In particular, starting from a highly symmetrical quark and lepton sector these models produce large neutrino mixing simultaneously with small quark mixing, a highly nontrivial achievement.

CHAPTER 3

YUKAWA SECTOR OF MINIMAL $SO(10)$ UNIFICATION

3.1 Introduction

Grand unified theories (GUTs) [79–81] based on the gauge group $SO(10)$ [25] are very attractive candidates to unify the strong, weak and electromagnetic forces into a single force, as well as to shed light on some of the open questions of the Standard Model (SM). Quarks and leptons of each family are unified into a single irreducible representations of $SO(10)$ group, the 16-dimensional spinor, which also contains the right-handed neutrino. The presence of the right-handed neutrino makes the seesaw mechanism [38, 82] for generating small neutrino masses very compelling in these theories. Since $SO(10)$ gauge symmetry is automatically anomaly-free [25], it provides a nice explanation for the miraculous cancelation of anomalies that occurs within each fermion family. The observed quantization of electric charges is also understood in these theories owing to their non-Abelian nature. Unifying all fermions into a single multiplet gives us the hope of understanding some aspects of the flavor puzzle in these theories. Unification of gauge couplings occurs naturally at an energy scale of $\sim 10^{15-16}$ GeV [64, 65, 68, 83–91], as $SO(10)$ admits an intermediate symmetry group – unlike theories based on $SU(5)$ which must break directly to the SM. It is of course well known that if supersymmetry is assumed to be present in its minimal version at the TeV scale, one-step breaking of $SO(10)$ directly down to the SM can be realized at an energy scale of 2×10^{16} GeV [92]. The focus of this paper [93] is, however, $SO(10)$ theories without the assumption of supersymmetry.

We wish to inquire what an economic Yukawa sector would look like in renormalizable $SO(10)$ theories. This may appear to be a well understood issue, but as we suggest here, this question has not been properly resolved. Economy may be viewed as having the least number of Higgs fields as well as Yukawa parameters while being realistic. Assuming that there are no new fermions beyond the three families of chiral 16s[1] the answer to this question may be found in the group theory of fermion bilinears:

$$16 \times 16 = 10_s + 120_a + 126_s. \tag{3.1.1}$$

Here the subscripts s and a stand for symmetric and antisymmetric components (in family space). The 10 and

[1] If vector-like fermions belonging to $16 + \overline{16}$ (or other real representations) with GUT scale masses exist and mix with the chiral 16s, new possibilities are available, see for e.g., Ref. [**?**, 94].

the 120 are real representations in $SO(10)$, while the 126 is complex. The most general renormalizable Yukawa couplings in $SO(10)$ theories then would take the form

$$\mathcal{L}_{yuk} = 16_F(Y^i_{10}10^i_H + Y^j_{120}120^j_H + Y^k_{126}\overline{126}^k_H)16_F. \tag{3.1.2}$$

Here the index i takes values $i = 1, 2, ..n_{10}$ where n_{10} is the number of 10_H fields employed, and similarly the index $j = 1, 2, ..n_{120}$ and $k = 1, 2, ..n_{126}$ with n_{120} and n_{126} being the number of 120_H and $\overline{126}_H$ present in the theory. The Yukawa coupling matrices Y^i_{10} and Y^k_{126} are 3×3 complex symmetric matrices in family space, while Y^j_{120} are complex antisymmetric matrices. We wish to identify the smallest possible set of $\{n_{10}, n_{120}, n_{126}\}$ that would lead to a realistic spectrum of quark and lepton masses as well as mixing angles. This set will turn out to be the choice $n_{10} = n_{120} = n_{126} = 1$, as we shall see. This result is satisfying, as it suggests that nature has utilized each possible Higgs field for fermion mass generation exactly once, without any replication.

Before establishing this assertion, which will be done in the next section, let us note that *a complex* 10 can be constructed from *two real* 10s in $SO(10)$: $10_c = (10_1 + i10_2)/\sqrt{2}$. Similarly, *a complex* 120_c may be constructed from *two real* 120s. In these cases, the Yukawa couplings will involve terms of the type $16_F10_c16_F$ as well as $16_F10^*_c16_F$ with completely independent Yukawa coupling matrices, and similarly for the 120_c field. It is possible to assign a charge exterior to $SO(10)$ to these fields – such as the Peccei–Quinn $U(1)$ motivated on other grounds – so that the Yukawa couplings contain only the $16_F10_c16_F$ term, and not the $16_F10^*_c16_F$ term. These restricted class of Yukawa couplings in $SO(10)$ have been studied extensively [26, 32–34, 95–99]. While interesting, the predictions of such models are those of $SO(10)\times G$ where G is a symmetry exterior to $SO(10)$, and not of the true grand unified symmetry $SO(10)$ itself. Our inquiry relates to the minimal Yukawa sector in theories where only the $SO(10)$ gauge symmetry plays a role.

It should be noted that in theories which assume supersymmetry (SUSY), which is not the focus of the present work, chiral superfields are necessarily complex, thus requiring the complexification of 10 and 120 Higgs fields. Holomorphy of the superpotential would imply that the coupling $16_F10^*_c16_F$ is not present simultaneously with the superpotential term $16_F10_c16_F$. These models share some of the features of non-SUSY models based on $SO(10)\times U(1)_{PQ}$, although the renormalization group evolution of the fermion mass parameters between the weak scale and the GUT scale would be different in the two classes of theories. Supersymmetric $SO(10)$ models have been studied extensively, and it has been shown that economic models where only a (complex) 10_H and a $\overline{126}_H$ couple to fermions can be predictive and consistent with all fermion masses and mixings [26–29, 31, 32, 34, 45, 46, 51, 54, 55]. If the additional Higgs fields needed for symmetry breaking are restricted to a 126_H and a 210_H, split supersymmetry may be required for consistency [54]. Alternatively, a (complex) 120_H may be introduced to relax some of the restrictions imposed by the symmetry breaking sector [30, 100–102].[2]

[2]Symmetries external to $SO(10)$ have also been applied in the context of renormalizable SUSY $SO(10)$ with some success in

Our goal in this paper is to identify the analog of the minimal SUSY $SO(10)$ Yukawa sector, but for $SO(10)$ theories without supersymmetry.

The rest of the paper is organized as follows. In Sec. 2 we present our proof that the economic Higgs sector will have $n_{10} = n_{120} = n_{126} = 1$. In Sec. 3 we analyze the predictions of this model for quark and lepton masses and mixings. Here we present our numerical study which shows full consistency with experimental data. In Sec. 4 we present the constraints on these models from the unification of gauge couplings; in Sec. 5 we calculate the proton decay branching ratios. In Sec. 6 we conclude.

3.2 Economic Yukawa Sector in $SO(10)$

In this section we establish the assertion that $n_{10} = n_{120} = n_{126} = 1$ is the economic choice of Yukawa sector in non-supersymmetric $SO(10)$ theories. This corresponds to choosing one real 10_H, one real 120_H and a complex $\overline{126}_H$ of Higgs bosons that have Yukawa couplings with the three chiral families of 16_F. An additional Higgs filed belonging to 45_H, 54_H or 210_H would be needed for completing the symmetry breaking. These fields, however, do not have Yukawa couplings with the 16_F, and the precise choice is not so important for now. A proof of our assertion would require that the choice $n_{10} = n_{120} = n_{126} = 1$ leads to a realistic fermion spectrum, and no other simpler choice exists consistent with realism. The former part of the proof is delegated to Sec. 3 where we perform a numerical analysis of this economic Yukawa sector; here we address the latter part.

If only one Higgs field among 10_H, 120_H and $\overline{126}_H$ is present in a theory, there would be no flavor mixing – as the Yukawa coupling matrix of this single Higgs field can be diagonalized using an $SO(10)$ rotation. Thus at least two Higgs fields are needed for realistic fermion spectrum. One of the fields used must be a 126_H, since it gives large Majorana masses to the righ-handed neutrinos directly. This field also plays a role in the symmetry breaking sector, as it breaks $SO(10)$ down to $SU(5)$, reducing the rank. One could consider replacing the 126_H with a 16_H which can play a similar role in rank reduction. In such a case the right-handed neutrino can acquire a large Majorana mass via the two-loop Witten diagram [108] involving gauge boson and scalar loops. The induced Majorana mass can be estimated [109] to be of order

$$M_{\nu^c} \approx \left(\frac{\alpha_{10}}{4\pi}\right)^2 Y_{10} \frac{v_R^2}{M_{\rm GUT}} \tag{3.2.3}$$

where α_{10} is the $SO(10)$ gauge coupling, Y_{10} is the Yukawa coupling of 10_H, and v_R is the $B-L$ breaking vacuum expectation value (VEV) of the 16_H. In a nonsupersymmetric $SO(10)$ theory v_R is well below the GUT scale for consistency with gauge coupling unification, with its range being $v_R \approx (10^{11} - 10^{14})$ GeV depending on the surviving intermediate symmetry. M_{ν^c} is then of order 10^8 GeV or less, which is too small to reproduce

explaining the fermion spectrum. See for example Ref. [103–107].

the correct order of magnitude for the light neutrino masses.[3]

Keeping one 126_H field in the theory, we seek if a realistic fermion spectrum can be generated with the addition of a second Higgs field. This turns out to be not possible. If the second Higgs field is a 126_H, the mass relations $m_\tau = -3m_b, m_\mu = -3m_s$ and $m_e = -3m_d$ will result at the GUT scale, which are inconsistent with observations. The ratio m_τ/m_b is found to be about 1.7 at the GUT scale (with small input errors) when the low energy mass parameters are evolved up to the GUT scale using SM renormalization group equations. We found that this ratio is more realistically in the range $(1.4 - 1.7)$, when intermediate scale threshold effects arising from the right-handed neutrino sector and the gauge bosons of $SU(4)_c$ are included. Each of the two threshold effects causes a decrease in the ratio m_τ/m_b at the GUT scale. We conclude that the relation $m_\tau = 3m_b$ is clearly excluded. The relation $m_\mu = 3m_s$ is not too far off (our RGE evolution shows the ratio m_μ/m_s to be about 4 at the GUT scale), while $m_e = 3m_d$ is off by an order of magnitude. Thus a minimal Yukawa sector consisting of two copies of $\overline{126}_H$ is not realistic.

If the second Higgs field is a real 10_H, two complex symmetric Yukawa matrices can be written down, one with the 10_H, and one with the $\overline{126}_H$. However, the Higgs doublet in the 10_H is self-conjugate, and is contained in the $(2, 2, 1)$ representation of the Pati-Salam subgroup $SU(2)_L \times SU(2)_R \times SU(4)_c$. This field can be written as

$$\Phi^* = \tau_2 \Phi \tau_2 \Rightarrow \Phi = \begin{pmatrix} \phi_0 & \phi^+ \\ -\phi^- & \phi_0^* \end{pmatrix}. \tag{3.2.4}$$

In general, if the (1,1) element of Φ is independent from the (2,2) element, we can denote their respective vacuum expectation values to be v_u and v_d with v_u giving mass to the up-quarks and Dirac neutrinos, while v_d generates down-quark and charged lepton masses. The reality of 10_H implies that $v_u = v_d^* \equiv v_{10}$, and thus the ratio $r = |v_u/v_d| = 1$. With $r = 1$, the needed splitting between the top and bottom quark masses cannot be achieved. Note that $r = 1$ is a special case of the general $SO(10) \times U(1)_{PQ}$ models with $v_u \neq v_d^*$. Such models have been studied, which find the phenomenological requirement $r \sim m_t/m_b$. A three generation analysis of fermion masses and mixings with a complex 10_H in Ref. [32] shows that a realistic fit requires $r \sim 70$, which is well outside of the prediction of $r = 1$ in the case of real 10_H. Thus we conclude that one $\overline{126}_H$ and one real 10_H is not realistic [99].

What about using one $\overline{126}_H$ and one 120_H? As shown in Ref. [99], this case also cannot reproduce fermion masses correctly. The ratio m_t/m_b comes out to be of order one, rather than the phenomenological value of ~ 70. In addition, as we shall show, this model predicts the GUT scale mass ratio $m_\tau/m_b \simeq 3$, with any

[3]This issue with the Witten mechanism may be resolved in split supersymmetry, where $v_R = M_{\rm GUT}$ [109]. The SUSY particle masses should be of order the GUT scale to prevent additional suppression factor of $M_{\rm SUSY}/M_{\rm GUT}$ in Eq. (3.2.3), which may cause a problem with generating a Higgs boson mass of 125 GeV [56].

deviation of order $m_s/m_b \sim 5\%$. As already noted, the ratio $m_\tau/m_b = (1.4 - 1.7)$ at the GUT scale in $SO(10)$ models under discussion. Thus we conclude that only two Higgs fields being responsible for Yukawa couplings cannot be realistic.

When three Higgs fields are introduced, the choice of one 10_H, one 120_H and one $\overline{126}_H$ appears attractive, as there in no replication here. This choice can indeed lead to a realistic fermion mass spectrum, as we elaborate in the next section. There would be two complex symmetric Yukawa coupling matrices in this case, along with one complex antisymmetric matrix. If an alternative choice of one $\overline{126}_H$ and two copies of 120_H can lead to a realistic spectrum, that would have less parameters with one symmetric and two antisymmetric Yukawa matrices. However, as we show in a subsection 3.2.1 below, this choice would lead to the relation $m_\tau = 3m_b$ with corrections of order 5%, even when one allows for large off-diagonal contributions to the mass matrices from the 120_H. Models with one $\overline{126}_H$ and two copies of 10_H would be realistic; however, these models would have three complex symmetric Yukawa matrices which have more parameters compared to the case of one 10_H, one 120_H and one $\overline{126}_H$. This completes the first part of the proof that $n_{10} = n_{120} = n_{126} = 1$ is the economic choice for the Yukawa sector. To complete the proof we establish in the next section that this choice is indeed realistic.

3.2.1 Proof of $m_\tau \simeq 3m_b$ in models with 126_H and $2 \times 120_H$

Without loss of generality, we can diagonalize the Yukawa coupling of 126_H. We focus on the second and third generation down quarks and charged leptons. Their mass matrices can be written down as

$$M_D = \begin{pmatrix} a & c \\ -c & b \end{pmatrix}, \quad M_E = \begin{pmatrix} -3a & c' \\ -c' & -3b \end{pmatrix}. \tag{3.2.5}$$

This form persists even when many of 120_H fields are used, with their mass contribution going into the off-diagonal entries differently in M_D and M_E. The exact invariants of these matrices are then

$$m_s^2 + m_b^2 = |a|^2 + |b|^2 + 2\,|c|^2 \tag{3.2.6}$$

$$m_\mu^2 + m_\tau^2 = 9\,(|a|^2 + |b|^2) + 2\,|c'|^2 \tag{3.2.7}$$

$$m_s m_b = |ab + c^2| \tag{3.2.8}$$

$$m_\mu m_\tau = |9\,ab + c'^2| \tag{3.2.9}$$

From these relations it follows that

$$m_\mu^2 + m_\tau^2 = 9\,(m_s^2 + m_b^2) + 18\,\left[\left|c^2 - m_s m_b e^{i\alpha} + \frac{m_\mu m_\tau}{9} e^{i\beta}\right| - |c|^2\right]\,. \tag{3.2.10}$$

The undetermined parameter c is bounded by Eq. (3.2.6), and no matter how we vary c, the deviation from 3 in the ratio m_τ/m_b is of order $m_s/m_b \sim 5\%$. The inclusion of the first family is not expected to change

considerably this result. This proves that a Higgs sector consisting of one 126_H and two or any number of copies of real 120_H cannot lead to realistic fermion masses.

3.2.2 A comment on doublet-triplet splitting

As is well known, any grand unified theory has to address the question of making one Higgs doublet light, while its color triplet GUT partner remains superheavy so as to not cause rapid proton decay. This doublet-triplet splitting problem is present in both SUSY and non-SUSY minimal GUTs. If the Higgs doublet mass is not split from the color triplet mass, either the electroweak symmetry would break at the GUT scale, or not break at all, or the light color-triplet would lead to far too fast proton decay. A fine-tuning is necessary to bring the Higgs doublet mass down to the weak scale. In supersymmetric versions, this fine-tuning is done at the tree level, SUSY would guarantee its stability against quantum corrections. In non-supersymmetric $SO(10)$ theories, the tuning must be done after taking account of loop corrections to a very high order. The induced Higgs mass from quantum loops would be at the n-loop level of order $\Delta m_H^{(n)} \sim M_{\rm GUT}(\alpha/4\pi)^{n/2}$. For $m_H \sim 125$ GeV, the tuning must be done after $n = 12$ loop corrections are included. We note that this is nevertheless only one fine-tuning, albeit not easily enforceable by actual calculations. The Hermitian Higgs doublet mass matrix is tuned to have near-zero determinant. In contrast, in minimal SUSY GUTs, the needed tree level tuning requires the determinant of the complex doublet Higgsino mass matrix to be near zero. Recall that in SUSY all mass parameters in the superpotential are complex in general. Such a tuning amounts to two conditions, unlike the non-supersymmetric tuning, which requires only one such condition. Although the Higgs mass can be ensured only after including very high order corrections in non-SUSY $SO(10)$, we find it intriguing that the fine-tuning condition is more minimal here compared to minimal SUSY $SO(10)$.

3.3 Realistic Fermion Spectrum with Minimal Yukawa Sector

As argued in the previous section, the minimal Yukawa sector of $SO(10)$ makes use of one real 10_H, one real 120_H and one complex $\overline{126}_H$ of Higgs bosons that couple to the three families of fermions in the 16_F representation. Here we proceed to establish the consistency of such a theory with observed fermion masses and mixings.

With no symmetry other than the gauge symmetry of $SO(10)$ imposed, the most general Yukawa interactions of the model can be written down as

$$\mathcal{L}_{yuk} = 16_F(Y_{10}10_H + Y_{120}120_H + Y_{126}\overline{126}_H)16_F. \tag{3.3.11}$$

Here Y_{10} and Y_{126} are complex symmetric Yukawa matrices, while Y_{120} is a complex antisymmetric matrix.

Under the Pati-Salam subgroup $G_{PS} \equiv SU(2)_L \times SU(2)_R \times SU(4)_c$, these fields decompose as

$$16 = (2,1,4) + (1,2,\overline{4}) \tag{3.3.12}$$

$$10 = (2,2,1) + (1,1,6) \tag{3.3.13}$$

$$120 = (2,2,1) + (1,1,10) + (1,1,\overline{10}) + (3,1,6) + (1,3,6) + (2,2,15) \tag{3.3.14}$$

$$126 = (1,1,6) + (3,1,10) + (1,3,\overline{10}) + (2,2,15). \tag{3.3.15}$$

The 10_H has one SM doublet Higgs field contained in the bidoublet (2,2,1), while the 120_H has two SM Higgs doublets, one each belonging to (2,2,1) and (2,2,15). The reality condition for the (2,2,1) from 10_H is listed in Eq. (3.2.4), while those from the 120_H would imply $v_u^{(1)} = v_d^{(1)*} \equiv v_{120}^{(1)}$ and $v_u^{(15)} = v_d^{(15)*} \equiv v_{120}^{(15)}$ with the superscripts (1) and (15) denoting the (2,2,1) and the (2,2,15) fragments. The 126_H contains two SM Higgs fields contained in the complex bidoublet (2,2,15) fragment, which is not subject to the reality condition. We denote the up-type and down-type electroweak VEVs of the $\overline{126}_H$ as v_{126}^u and v_{126}^d respectively. Note also that the $(1,3,10)$ fragment of $\overline{126}_H$ contains a SM singlet field which generates large Majorana masses for the right-handed neutrinos once it acquires a VEV.

The up-quark, down-quark, charged leptons, Dirac neutrino and Majorana neutrino mass matrices derived from Eq. (5.3.24)can be now written down:

$$M_U = v_{10}Y_{10} + v_{126}^u Y_{126} + (v_{120}^{(1)} + v_{120}^{(15)})Y_{120}, \tag{3.3.16}$$

$$M_D = v_{10}^* Y_{10} + v_{126}^d Y_{126} + (v_{120}^{(1)*} + v_{120}^{(15)*})Y_{120}, \tag{3.3.17}$$

$$M_E = v_{10}^* Y_{10} - 3v_{126}^d Y_{126} + (v_{120}^{(1)*} - 3v_{120}^{(15)*})Y_{120}, \tag{3.3.18}$$

$$M_{\nu_D} = v_{10}Y_{10} - 3v_{126}^u Y_{126} + (v_{120}^{(1)} - 3v_{120}^{(15)})Y_{120}, \tag{3.3.19}$$

$$M_{\nu_{R,L}} = v_{R,L}Y_{126}. \tag{3.3.20}$$

Now defining

$$D = v_{10}Y_{10}, \;\; A = (v_{120}^{(1)} + v_{120}^{(15)})Y_{120}, \;\; S = v_{126}^u Y_{126}, \tag{3.3.21}$$

$$r_1 = \frac{v_{126}^d}{v_{126}^u}, \;\; r_2 = \frac{v_{120}^{(1)*} - 3v_{120}^{(15)*}}{v_{120}^{(1)} + v_{120}^{(15)}}, \;\; e^{i\phi} = \frac{v_{120}^{(1)*} + v_{120}^{(15)*}}{v_{120}^{(1)} + v_{120}^{(15)}}, \;\; c_{R,L} = \frac{v_{R,L}}{v_{126}^u}, \tag{3.3.22}$$

and going into a phase convention where v_{10} is real (this can be done by an $SU(2)_L$ rotation), we get

$$M_U = D + S + A, \tag{3.3.23}$$

$$M_D = D + r_1 S + e^{i\phi} A, \tag{3.3.24}$$

$$M_E = D - 3r_1 S + r_2 A, \tag{3.3.25}$$

$$M_{\nu_D} = D - 3S + r_2^* e^{i\phi} A, \tag{3.3.26}$$

$$M_{\nu_{R,L}} = c_{R,L} S. \tag{3.3.27}$$

These matrices are written in a basis $f_i M_{ij} f_j^c$. The light neutrino mass matrix, obtained from the see-saw formula, is given by

$$M_N = M_{\nu_L} - M_{\nu_D} M_{\nu_R}^{-1} M_{\nu_D}^T. \tag{3.3.28}$$

Without loss of generality one can choose a basis where S is real, positive and diagonal. In this basis, S would have 3 real parameters while D has 6 complex parameters. Since the matrix A is antisymmetric, it has 3 complex parameters. There are 4 additional complex parameters in $r_{1,2}, c_{R,L}$ and one phase ϕ. An overall phase either from c_L or c_R will be irrelevant in the matrix M_N. Altogether there are then 16 real parameters and 13 phases. With these parameters one should fit 18 observables: 6 quark masses, 3 quark mixing angles, 1 CKM phase, 3 charged lepton masses, 2 neutrino mass squared differences, and 3 mixing angles in the neutrino sector. If we assume dominance of either type-I or type-II seesaw, then the parameter set is reduced by 1 magnitude and 1 phase. Although the number of model parameters is larger than the number of observables, it is nontrivial to find an acceptable fit owing to the fact that 12 or 13 parameters are phases which cannot be manipulated much.

The type-II contribution to the light neutrino mass matrix originates in the model from terms such as $10_H^2 126_H^2$ in the scalar potential. When decomposed into the the Pati-Salam symmetry group, this term would contain terms of the type $(3,1,10)(2,2,1)^2(1,3,\overline{10})$. When the singlet VEV of $(1,3,\overline{10})$ and the doublet VEV of $(2,2,1)$ are inserted in this term, a linear term in $(3,1,10)$ would result, which leads to an induced VEV for its neutral component: $v_L \sim v_R v^2/M_{\rm GUT}^2$. We note that with the right-handed neutrino mass given as in (5.3.33), the mass of the (X',Y') gauge bosons which are outside of $SU(5)$ but mediate proton decay is given as $M_{X',Y'} = \sqrt{2} g v_R$, where g is the $SO(10)$ gauge coupling.

3.3.1 Numerical analysis of the fermion masses and mixings

In this section we discuss the procedure we follow for the numerical analysis to the fermion masses and mixings and present our fit results. For optimization purpose we do a χ^2-analysis. The pull and χ^2-function are defined as:

$$P_i = \frac{O_{i\ \mathrm{th}} - E_{i\ \mathrm{exp}}}{\sigma_i}, \tag{3.3.29}$$

$$\chi^2 = \sum_i P_i^2, \tag{3.3.30}$$

where σ_i represent experimental 1σ uncertainty and $O_{i\ \mathrm{th}}$, $E_{i\ \mathrm{exp}}$ and P_i represent the theoretical prediction, experimental central value and pull of observable i. We fit the values of the observables at the GUT scale, $M_{GUT} = 2 \times 10^{16}$ GeV. To get the GUT scale values of the observables we take the central values at the M_Z scale from Table-1 of Ref. [72]. With this input we do the renormalization group equation (RGE) running of the Yukawa couplings [110] and the CKM parameters [111] within the SM up to the GUT scale. For the associated one sigma uncertainties of the observables at the GUT scale, we keep the same percentage uncertainty with respect to the central value of each quantity as that at the M_Z scale. For the charged lepton masses, a relative uncertainty of 0.1% is assumed in order to take into account the theoretical uncertainties arising for example from threshold effects. All these inputs are presented in Table 3.1. The RGE running factors for the Yukawa couplings $\eta_i = y_i(M_{GUT})/y_i(M_Z)$ and for the CKM mixing angles $\eta_{ij}^{\mathrm{CKM}} = \theta_{ij}^{\mathrm{CKM}}(M_{GUT})/\theta_{ij}^{\mathrm{CKM}}(M_Z)$ are taken to be:

$$(\eta_u, \eta_c, \eta_t) = (0.382, 0.382, 0.434) \tag{3.3.31}$$

$$(\eta_d, \eta_s, \eta_b) = (0.399, 0.399, 0.348) \tag{3.3.32}$$

$$(\eta_e, \eta_\mu, \eta_\tau) = (0.967, 0.967, 0.967) \tag{3.3.33}$$

$$(\eta_{12}^{\mathrm{CKM}}, \eta_{23}^{\mathrm{CKM}}, \eta_{13}^{\mathrm{CKM}}) = (1.000, 1.154, 1.154) \tag{3.3.34}$$

The low scale inputs as shown in Table 4.2.10 in the neutrino sector are taken from Ref. [76]. For neutrino observables, we run the RGE for the dimension five operator from low scale to the v_R scale [112] and use these new values during the fitting produce. For this running purpose, we have assumed hierarchical structure of the neutrinos and used the approximations $m_2 = \sqrt{\Delta m^2_{sol}}$ and $m_3 = \sqrt{\Delta m^2_{atm}}$. The running values of the observables at the high scale depend on the scale v_R, this is why we present the neutrino mass squared differences resulting from running in Table 3.3 at the relevant scale v_R corresponding to two different fits (type-I dominance and type-I+II case), while all the other inputs are at $M_{\mathrm{GUT}} = 2 \times 10^{16}$ GeV.

In $SO(10)$ GUT models such as the one we are considering, the (3,3) entry of the Dirac neutrino Yukawa coupling matrix $Y_{\nu D}$ is expected to be of the order of unity, and thus RGE corrections proportional to $Y_{\nu D}$ can be important in the momentum range $M_{\nu^c} \leq \mu \leq M_{\mathrm{GUT}}$. This effect could have a sizeable contribution to the tau lepton mass only, since for the first and second generation Dirac Yukawa couplings turn out to be small. Including this effect of the heavy right-handed neutrinos thresholds, the Dirac neutrino mass matrix gets modified at the GUT scale as

Yukawa Couplings & CKM parameters	$\mu = M_Z$	$\mu = M_{GUT}$
$y_u/10^{-6}$	6.65 ± 2.25	2.54 ± 0.86
$y_c/10^{-3}$	3.60 ± 0.11	1.37 ± 0.04
y_t	0.9860 ± 0.00865	0.428 ± 0.003
$y_d/10^{-5}$	1.645 ± 0.165	6.56 ± 0.65
$y_s/10^{-4}$	3.125 ± 0.165	1.24 ± 0.06
$y_b/10^{-2}$	1.639 ± 0.015	0.57 ± 0.005
$y_e/10^{-6}$	2.79475 ± 0.0000155	2.70341 ± 0.00270
$y_\mu/10^{-4}$	5.89986 ± 0.0000185	5.70705 ± 0.00570
$y_\tau/10^{-2}$	1.00295 ± 0.0000905	0.97020 ± 0.00097
$\theta_{12}^{\rm CKM}$	0.22735 ± 0.00072	0.22739 ± 0.0006
$\theta_{23}^{\rm CKM}/10^{-2}$	4.208 ± 0.064	4.858 ± 0.06
$\theta_{13}^{\rm CKM}/10^{-3}$	3.64 ± 0.13	4.202 ± 0.13
$\delta^{\rm CKM}$	1.208 ± 0.054	1.207 ± 0.054

Table 3.1: Values of observables at M_Z scale from Ref. [72]. Here experimental central values with associated 1σ uncertainties are quoted. The masses of fermions are given by the relations $m_i = v\ y_i$ with $v = 174.104$ GeV. The corresponding values at the GUT scale are obtained by RGE evolution. For the associated one sigma uncertainties of the observables at the GUT scale, we keep the same percentage uncertainty with respect to the central value of each quantity as that at the M_Z scale. For the charged lepton Yukawa couplings at the GUT scale, a relative uncertainty of 0.1% is assumed in order to take into account the theoretical uncertainties arising for example from threshold effects.

$$M'_{\nu_D} = \left[1 - \frac{3}{2(16\pi^2)} Y_{\nu D} \log(\frac{M_{GUT}}{c_R S}) Y^\dagger_{\nu D}\right] M_{\nu_D}. \tag{3.3.35}$$

while the modified charged lepton mass matrix becomes

$$M'_E = \left[1 + \frac{3}{2(16\pi^2)} Y'_{\nu D} \log(\frac{M_{GUT}}{c_R S}) Y'^\dagger_{\nu D}\right] M_E. \tag{3.3.36}$$

To be clear, the tau lepton mass decreases in going from the ν_R mass scale to the GUT scale due to the Dirac neutrino Yukawa correction. In the fitting procedure it was thus M'_E from Eq. (3.3.36) to be compared to the experimental values at M_{GUT}, while in (3.3.28) $M_{\nu D}$ has been replaced by $M'_{\nu D}$ (3.3.35). Notice that M_E and $Y_{\nu D} = M_{\nu D}/v$ in Eqs. (3.3.36) and (3.3.35) are defined in Eqs. (3.3.25) and (5.5.52).

We investigate three different scenarios, type-I dominance, type-II dominance and the general scenario where both contributions are present, type-I+II. The fit results corresponding to our numerical analysis is presented in Table 3.3. We found good solutions for both type-I and type-I+II with total $\chi^2 = 0.45$ and 0.004 respectively, but not for type-II scenario (the total $\chi^2 \sim 1000$ in this case). For the type-II case, our numerical analysis shows that, for the best fit, the worst fitted quantity corresponds to Δm^2_{sol} that comes out to be $\sim 10^3$ times

smaller (with pull $\sim$ -32) than the experimental data. The other discrepancy is of the quantity θ_{23}^{PMNS} that is $\sim$1.5 times smaller compared to the experimental central value. With these fit results the predictions of the model for these two scenarios are listed in Table 3.4. The parameter set corresponding to these best fit results for type-I and type-I+II cases respectively are given below. We conclude that the model gives an excellent fit to all observables in the fermion sector. This completes our proof of the minimality of the Yukawa sector in $SO(10)$ models.

Quantity	Central Value
$\Delta m^2_{sol}/10^{-5}eV^2$	7.56±0.24
$\Delta m^2_{atm}/10^{-3}eV^2$	2.41±0.08
$\sin^2\theta_{12}^{\rm PMNS}/10^{-1}$	3.08±0.17
$\sin^2\theta_{23}^{\rm PMNS}/10^{-1}$	3.875±0.225
$\sin^2\theta_{13}^{\rm PMNS}/10^{-2}$	2.41±0.25

Table 3.2: Observables in the neutrino sector used in our fits taken from Ref. [76].

From the best fit results presented in Table 3.3 one can see that the right-handed breaking scale for the type-I and type- I+II solutions are very different. From Eq (3.3.22) $v_R = c_R\ v^u_{126}$ with $c_R = 5.8\times10^{12}$ and 4.2×10^{10} respectively. Assuming $v^u_{126}\sim 174$ GeV, for the type-I scenario $v_R\sim 10^{15}$ GeV, which corresponds to high value for the heaviest right-handed neutrino mass $M_3\sim 5\times10^{14}$ GeV (see Table 3.4) that naturally can incorporate the extremely light neutrino masses. To see this, consider the basis we are working where the matrix S is real and diagonal. Parameters corresponding to the best fit solutions for both the cases (type-I and type-I+II) the $(3,3)$ entry of the Dirac type neutrino mass matrix is 3 times the $(3,3)$ entry of S matrix, $S_{33} = m_t$ ($A_{33} = 0$ and D_{33} is negligible). Then the heaviest light neutrino mass is given by the approximate relation $m_3 \sim {M_{\nu_D}}_{33}{}^2/(c_R S_{33}) = 9m_t/c_R = 0.1$ eV which is roughly the correct order. On the contrary, the best fit solution corresponding to type-I+II scenario has v_R scale which is about two orders of magnitude smaller compared to the former case. As a consequence the heaviest right-handed neutrino mass is also smaller by two orders of magnitude that overshoots the light neutrino mass. Naive estimation gives $m_3\sim 9m_t/c_R = 16$ eV which is too large. Hence, to reproduce the light neutrino spectrum in this case some cancellations must take place, so some degree of fine tuning in the setup Eqs (3.3.23)-(3.3.27) is needed to be consistent with the neutrino data.

Masses (in GeV) and Mixing parameters	Inputs (at $\mu = M_{GUT}$)	Fitted values (**type-I**) (at $\mu = M_{GUT}$)	pulls (**type-I**)	Fitted values (**type-I+II**) (at $\mu = M_{GUT}$)	pulls (**type-I+II**)
$m_u/10^{-3}$	0.442±0.149	0.444	0.009	0.442	-0.0002
m_c	0.238±0.007	0.238	-0.002	0.238	0.0001
m_t	74.51±0.65	74.52	0.009	74.52	-0.005
$m_d/10^{-3}$	1.14±0.11	1.14	-0.0002	1.14	-0.00006
$m_s/10^{-3}$	21.58±1.14	21.60	0.007	21.59	0.0001
m_b	0.994±0.009	0.994	0.002	0.994	0.000005
$m_e/10^{-3}$	0.470692±0.000470	0.470674	-0.03	0.470675	-0.003
$m_\mu/10^{-3}$	99.3658±0.0993	99.3618	-0.04	99.3621	-0.003
m_τ	1.68923±0.00168	1.68925	0.01	1.68925	0.001
$\lvert V_{us}\rvert/10^{-2}$	22.54±0.06	22.54	0.002	22.54	0.00008
$\lvert V_{cb}\rvert/10^{-2}$	4.856±0.06	4.856	0.001	4.856	0.0007
$\lvert V_{ub}\rvert/10^{-2}$	0.420±0.013	0.420	-0.007	0.420	-0.0001
δ_{CKM}	1.207±0.054	1.207	0.01	1.207	0.005
$\Delta m^2_{sol}/10^{-4}(\text{eV}^2)$	1.29±0.04 (1×10^{15}GeV) 1.27±0.04 (7.3×10^{12}GeV)	1.27	-0.48	1.27	0.04
$\Delta m^2_{atm}/10^{-3}(\text{eV}^2)$	4.12±0.13 (1×10^{15}GeV) 4.05±0.13 (7.3×10^{12}GeV)	4.06	- 0.46	4.06	0.04
$\sin^2\theta_{12}^{\text{PMNS}}$	0.308±0.017	0.308	-0.01	0.308	0.00001
$\sin^2\theta_{23}^{\text{PMNS}}$	0.387±0.0225	0.387	-0.01	0.387	-0.00006
$\sin^2\theta_{13}^{\text{PMNS}}$	0.0241±0.0025	0.0241	0.01	0.0241	-0.0003

Table 3.3: Best fit values of the observables correspond to $\chi^2 = 0.45$ and 0.004 for **type-I** and **type-I+II** scenarios respectively for 18 observables. For the charged lepton masses, a relative uncertainty of 0.1% is assumed in order to take into account the theoretical uncertainties arising for example from threshold effects. The neutrino mass squared differences are fitted at the v_R scale, which for our solutions are $\sim 1\times10^{15}$ GeV and $\sim 7.3\times10^{12}$ GeV for **type-I** and **type-I+II** respectively. Here the v_R scale is determined by using the relation $v_R = c_R v^u_{126}$ given in Eq. (3.3.22), we have taken $v^u_{126} = 174.104$ GeV. One should note that due to the right-handed neutrino threshold corrections the charged lepton mass matrix gets modified and is given in Eq. (3.3.36). The fitted masses for the charged leptons presented in this table are the eigenvalues of this modified matrix, M'_E. The effect of the right-handed neutrinos is to decrease the tau lepton mass in going from ν_R scale to the GUT scale. For the fits presented in the table, the actual fitted mass of the tau lepton is $m_\tau = 1.617$ GeV (1.573 GeV) at the GUT scale for the **type-I** (**type-I+II**) scenario, which matches correctly with the input value when the right-handed neutrino threshold correction is taken into account. For **type-II** scenario, we have not found any acceptable solution as mentioned in the text.

Quantity	Predicted Value (**type-I**)	Predicted Value (**type-I+II**)
$\{m_1, m_2, m_3\}$ (in eV)	$\{1.51 \cdot 10^{-4}, 1.12 \cdot 10^{-2}, 6.47 \cdot 10^{-2}\}$	$\{1.02 \cdot 10^{-2}, 1.52 \cdot 10^{-2}, 6.55 \cdot 10^{-2}\}$
$\{\delta^{PMNS}, \alpha_{21}^{PMNS}, \alpha_{31}^{PMNS}\}$	$\{2.81°, 169.61°, 27.25°\}$	$\{-150.82°, -136.92°, -106.50°\}$
$\{m_{cos}, m_\beta, m_{\beta\beta}\}$ (in eV)	$\{7.61 \cdot 10^{-2}, 5.05 \cdot 10^{-3}, 2.13 \cdot 10^{-3}\}$	$\{9.10 \cdot 10^{-2}, 1.30 \cdot 10^{-2}, 4.09 \cdot 10^{-3}\}$
$\{M_1, M_2, M_3\}$ (in GeV)	$\{1.04 \cdot 10^{5}, 1.23 \cdot 10^{12}, 4.34 \cdot 10^{14}\}$	$\{6.14 \cdot 10^{6}, 1.12 \cdot 10^{10}, 3.14 \cdot 10^{12}\}$

Table 3.4: Predictions of the minimal non-SUSY $SO(10)$ model for **type-I** and **type-I+II** scenarios. m_i are the light neutrino masses, M_i are the right handed neutrino masses, $\alpha_{21,31}$ are the Majorana phases following the PDG parametrization, $m_{cos} = \sum_i m_i$, $m_\beta = \sum_i |U_{ei}|^2 m_i$ is the effective mass parameter for beta-decay and $m_{\beta\beta} = |\sum_i U_{ei}^2 m_i|$ is the effective mass parameter for neutrinoless double beta decay.

Now we present the parameter set corresponding to the χ^2 best fit for the type-I scenario. [4].

The parameter set corresponding to the χ^2 best fit for the type-I scenario is:

$$r_1 = -3.5178190 \times 10^{-3} - 5.1827520 \times 10^{-3} i \tag{3.3.37}$$

$$r_2 = -1.0441669 + 1.6253165 \times 10^{-1} i \tag{3.3.38}$$

$$\phi = -7.9459769 \times 10^{-1} \tag{3.3.39}$$

$$c_R = 5.8035176 \times 10^{12} \tag{3.3.40}$$

$$S = \begin{pmatrix} 1.7926501 \times 10^{-8} & 0 & 0 \\ 0 & 2.1219581 \times 10^{-1} & 0 \\ 0 & 0 & 7.4949627 \times 10^{1} \end{pmatrix} \text{GeV} \tag{3.3.41}$$

$$D = \begin{pmatrix} 2.8344746 \times 10^{-4} - 5.3097883 \times 10^{-4} i & 4.501669 \times 10^{-3} - 1.7083332 \times 10^{-3} i & 6.0343793 \times 10^{-2} + 7.8900202 \times 10^{-3} i \\ 4.501669 \times 10^{-3} - 1.7083332 \times 10^{-3} i & 2.7783311 \times 10^{-2} - 1.5722435 \times 10^{-2} i & 3.0561540 \times 10^{-1} + 9.6327579 \times 10^{-2} i \\ 6.0343793 \times 10^{-2} + 7.8900202 \times 10^{-3} i & 3.0561540 \times 10^{-1} + 9.6327579 \times 10^{-2} i & -4.304058 \times 10^{-1} + 2.4126529 \times 10^{-1} i \end{pmatrix} \text{GeV} \tag{3.3.42}$$

$$A = \begin{pmatrix} 0 & -3.9710310 \times 10^{-3} - 1.6550999 \times 10^{-3} i & -4.0391236 \times 10^{-2} - 4.2504129 \times 10^{-2} i \\ 3.9710310 \times 10^{-3} + 1.6550999 \times 10^{-3} i & 0 & -1.7267986 \times 10^{-1} - 3.2019088 \times 10^{-1} i \\ 4.0391236 \times 10^{-2} + 4.2504129 \times 10^{-2} i & 1.7267986 \times 10^{-1} + 3.2019088 \times 10^{-1} i & 0 \end{pmatrix} \text{GeV} \tag{3.3.43}$$

[4] To reproduce the observables presented in Table. 3.3 for both the type-I and type-I+II scenarios, one must keep all the significant digits of the parameters presented in here. This high level of accuracy is needed to reproduce the neutrino observables; it is due to the fact that the right-handed neutrino mass spectrum in both cases shows extreme hierarchy among the generations, see Table. 3.4. Since this hierarchy between the first and the second generations is extreme, chopping-off digits effects mainly the quantity Δm^2_{sol}.

The parameter set corresponding to the χ^2 best fit for the type-I+II scenario is:

$$r_1 = 4.1628007 \times 10^{-3} - 3.1705843 \times 10^{-3} i \tag{3.3.44}$$

$$r_2 = -7.4367427 \times 10^{-1} + 3.5915531 \times 10^{-1} i \tag{3.3.45}$$

$$\phi = -6.4632781 \times 10^{-1} \tag{3.3.46}$$

$$c_R = 4.2254013 \times 10^{10} \tag{3.3.47}$$

$$c_L = 1.5155879 \times 10^{-10} - 1.4499546 \times 10^{-11} i \tag{3.3.48}$$

$$S = \begin{pmatrix} 1.4547716 \times 10^{-4} & 0 & 0 \\ 0 & 2.6693088 \times 10^{-1} & 0 \\ 0 & 0 & 7.4473135 \times 10^{1} \end{pmatrix} \text{GeV} \tag{3.3.49}$$

$$D = \begin{pmatrix} 4.8953934 \times 10^{-4} - 2.6113522 \times 10^{-4} i & -1.6504521 \times 10^{-5} + 1.1420336 \times 10^{-2} i & -2.151214 \times 10^{-1} + 1.7234983 \times 10^{-2} i \\ -1.6504521 \times 10^{-5} + 1.1420336 \times 10^{-2} i & -2.8562186 \times 10^{-2} + 2.8403787 \times 10^{-2} i & -3.7065300 \times 10^{-1} - 2.0521574 \times 10^{-1} i \\ -2.151214 \times 10^{-1} + 1.7234983 \times 10^{-2} i & -3.7065300 \times 10^{-1} - 2.0521574 \times 10^{-1} i & 3.6722700 \times 10^{-2} + 2.6598904 \times 10^{-1} i \end{pmatrix} \text{GeV} \tag{3.3.50}$$

$$A = \begin{pmatrix} 0 & 2.518929 \times 10^{-3} - 1.1393329 \times 10^{-2} i & 1.7915567 \times 10^{-1} + 1.1538080 \times 10^{-1} i \\ -2.518929 \times 10^{-3} + 1.1393329 \times 10^{-2} i & 0 & 1.6923025 \times 10^{-1} + 3.6425489 \times 10^{-1} i \\ -1.7915567 \times 10^{-1} - 1.1538080 \times 10^{-1} i & -1.6923025 \times 10^{-1} - 3.6425489 \times 10^{-1} i & 0 \end{pmatrix} \text{GeV} \tag{3.3.51}$$

3.4 Gauge Coupling Unification

As is well known, the three gauge couplings of the SM do not unify at a common scale. $SO(10)$ models provide a way to achieve coupling unification by virtue of an intermediate scale. In our proposed framework, the first stage of symmetry breaking can be achieved by employing a real 45_H, or a real 54_H or a real 210_H, along with a complex 126_H. Employing 45_H Higgs would require relying on the quantum corrections in the Higgs potential [64, 65, 91], while there is no such problem with the use of 210_H. In both cases the discrete D Parity symmetry would be broken at the GUT scale [85]. The intermediate gauge symmetry may be $SU(2)_L \times SU(2)_R \times SU(4)_c$ when a 210_H is used, while it is $SU(2)_L \times SU(2)_R \times SU(3)_c \times U(1)_{B-L}$ if the 45_H is used. Alternatively, a 54_H can break $SO(10)$ down to Pati-Salam symmetry preserving D parity. In this case the unification scale tends to be lower, of order 2×10^{15} GeV, if threshold effects arising from the scalar multiplets are ignored. This can potentially be in conflict with proton decay limits. It has been recently shown in Ref. [68] that symmetry breaking with a 54_H and a 126_H can lead to higher values of $M_{\rm GUT}$ consistent with proton lifetime, when

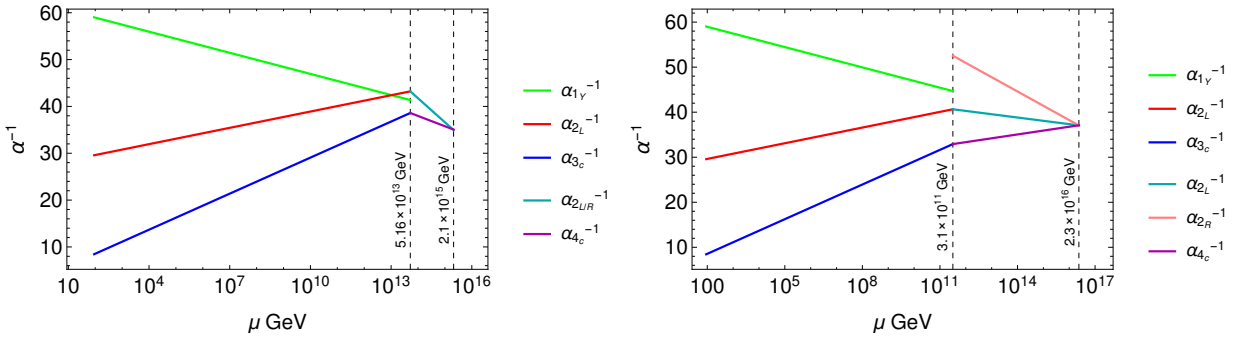

Figure 3.1: 1-loop gauge coupling running of the three SM gauge couplings from low scale to intermediate PS scale and from PS scale to GUT scale for minimal non-SUSY $SO(10)$ model. The left plot corresponds to the case when the GUT symmetry is broken by 54_H Higgs that leaves the discrete symmetry $g_L = g_R$ unbroken. The right plot is for the case when 54_H is replaced by 210_H Higgs that does not preserve the discrete symmetry.

threshold effects are properly included. Here we present for completeness our results on the unification of gauge couplings assuming the intermediate symmetry to be $SU(2)_L \times SU(2)_R \times SU(4)_c$ with or without D parity.

Since breaking $SO(10)$ gauge group by 54_H Higgs preserves the discrete parity, that demands the equality of the $SU(2)_L$ and $SU(2)_R$ gauge couplings ($g_L = g_R$) at the PS intermediate scale. The low energy data completely determines the value of this scale as well as the GUT scale with the assumption of survival hypothesis [113–115]. The one-loop beta function coefficients for the evolution of the $U(1)$, $SU(2)_L$ and $SU(3)_c$ gauge couplings are $b_i = \{41/10, -19/6, -7\}$ [116]. To determine the intermediate scale, we use the low energy values from Ref. [72]: $\alpha_1^{-1}(M_Z) = 59.02$, $\alpha_2^{-1}(M_Z) = 29.57$ and $\alpha_3^{-1}(M_Z) = 8.44$ (only the central values are quoted here). Then from the intermediate scale to the GUT scale we run the RGEs with one-loop coefficients $b_i = \{67/6, 67/6, 10/3\}$ for the group G_{224} that determines the GUT scale. The existence of the multiplets $(2,2,1) \subset 10_H$, $(2,2,1) + (2,2,15) \subset 120_H$ and $(2,2,15) + (3,1,10) + (1,3,\overline{10}) \subset 126_H$ is assumed at the intermediate scale while the rest of the multiplets are assumed to have GUT scale mass following the survival hypothesis. One-loop running of the RGEs of the gauge couplings are shown in Fig. 3.1 (left plot).

From this Fig. 3.1 one sees that the GUT scale is $\sim 2 \times 10^{15}$ GeV, which is about a factor of 2.5 smaller compared to what is needed to save the theory from the experimental proton decay limit $\tau_p \gtrsim 1.29 \times 10^{34}$ yrs [117]. Certainly the assumption made that all scalar particles have a common mass at the assumed scale is too restrictive: the Higgs multiplets are likely to have non-degenerate mass spectrum with masses scattered around each scale under consideration. If one includes this threshold correction arising from the Higgses, the unification scale can be raised as shown in an explicit calculation in Ref. [68]. There is no strict guideline, however, on how much the mass spectrum may be scattered; this would lead to significant uncertainty in proton lifetime estimate. As we show in the next section, the branching ratios for proton decay are much more stable

and can be used to test these theories.

If instead of a 54_H a 210_H is used to break the GUT symmetry, then the unification scale is naturally raised to about 2×10^{16} GeV. This is because D parity is broken by the VEV of 210_H, and as a result, with the assumption of survival hypothesis, the intermediate scale scalar spectrum is left-right asymmetric. Although 210_H allows for other intermediate symmetries, here we focus on the Pati-Salam symmetry. The gauge coupling evolution with the PS intermediate symmetry is presented in Fig. 3.1 (right plot). Following survival hypothesis, we consider the multiplets $(2,2,1) \subset 10_H$, $(2,2,1) \subset 120_H$ and $(2,2,15) + (1,3,\overline{10}) \subset 126_H$ at the intermediate scale with the rest of the multiplets lying at the GUT scale. With these multiplets, the one-loop RGE coefficients are $b_i = \{2, 26/3, -7/3\}$ for the group G_{224}. This plot clearly shows that the GUT scale can be raised by about an order of magnitude compared to the 54_H scenario and one does not need to rely on the threshold correction to save the theory from rapid proton decay. It should be noted that the scenario with 210_H has a drawback that the intermediate scale is relatively low $\sim 10^{11}$ GeV, which does not fit the right-handed neutrino mass spectrum as well as the 54_H model where this scale is around $(10^{13} - 10^{14})$ GeV. A look at the heaviest right-handed neutrino mass from Table 3.4 suggests that the case of type-I seesaw prefers symmetry breaking by a 54_H, while the type I + type II scenario can accommodate breaking by a 210_H.

3.5 Proton Decay Branching Ratios

In non-SUSY $SO(10)$ models, proton decay mediated by the gauge bosons are the most important. The lifetime of the proton is extremely sensitive to the superheavy gauge bosons masses ($M_{(X,Y)}$) since the lifetime goes as $\tau_p \sim M^4_{(X,Y)}/(g^4 m_p^5)$, where m_p is the proton mass and g is the unified gauge coupling. As noted in the previous section, there is a large uncertainty in the determination of M_X from low energy data, owing to unknown high scale threshold effects. On the other hand, proton decay branching ratios are less sensitive to these threshold effects, and so we focus on the predictions of the model for branching ratios.

The gauge bosons of $SO(10)$ belong to the adjoint 45. The decomposition of this field under the SM gauge symmetry is given by:

$$\begin{aligned} 45 = &(1,1,1) + (1,1,0) + (1,1,-1) + (1,3,0) + (3,2,\frac{1}{6}) + (3,2,-\frac{5}{6}) + (\overline{3},2,\frac{1}{6}) + (\overline{3},2,\frac{5}{6}) \\ &+ (1,1,0) + (3,1,\frac{2}{3}) + (\overline{3},1,-\frac{2}{3}) + (8,1,0). \end{aligned} \tag{3.5.52}$$

The gauge bosons responsible for proton decay are the $(X,Y)(3,2,-5/6)$ and $(X',Y')(3,2,1/6)$. The gauge

interaction Lagrangian of these bosons with the fermions in the current eigenstate basis is given by [118]:

$$\begin{aligned}\mathcal{L}_{int} = \frac{g}{\sqrt{2}}\{&[-\overline{e}_L\gamma^\mu \overline{X}^i_\mu d^C_{Li}] + [\overline{\nu}_L\gamma^\mu \overline{Y}^i_\mu d^C_{Li}] + [\overline{d}_{Li}\gamma^\mu \overline{X}^i_\mu e^C_L + \epsilon_{ijk}\overline{u}^{Ck}_L\gamma^\mu \overline{X}^i_\mu u^j_L] \\ &+ [-\overline{u}_{Li}\gamma^\mu \overline{Y}^i_\mu e^C_L + \epsilon_{ijk}\overline{u}^{Ck}_L\gamma^\mu \overline{Y}^i_\mu d^j_L] + [-\epsilon_{ijk}\overline{d}^{Ck}_L\gamma^\mu \overline{X}'^i_\mu d^j_L] + [-\overline{u}_{Ri}\gamma^\mu \overline{X}'^i_\mu \nu^C_R] + [-\overline{u}_{Li}\gamma^\mu \overline{X}'^i_\mu \nu^C_L] \\ &+ [\epsilon_{ijk}\overline{d}^{Ck}_L\gamma^\mu \overline{Y}'^i_\mu u^j_L] + [-\overline{u}_{Ri}\gamma^\mu \overline{Y}'^i_\mu e^+_R] + [-\overline{d}_{Li}\gamma^\mu \overline{Y}'^i_\mu \nu^C_L] + h.c.\},\end{aligned} \tag{3.5.53}$$

where i, j, k are color indices and we have suppressed the family indices and $SU(2)_L$ indices.

The resulting $d = 6$ effective operators of the form $QQQL$ responsible for proton decay can be constructed from this Lagrangian [119, 120]:

$$\mathcal{O}^{B-L}_I = k_1^2\ \epsilon_{ijk}\ \epsilon_{\alpha\beta}\ \overline{u^C_{iaL}}\ \gamma^\mu\ Q_{j\alpha aL}\ \overline{e^C_{b\ L}}\ \gamma_\mu\ Q_{k\beta bL}; \tag{3.5.54}$$

$$\mathcal{O}^{B-L}_{II} = k_1^2\ \epsilon_{ijk}\ \epsilon_{\alpha\beta}\ \overline{u^C_{iaL}}\ \gamma^\mu\ Q_{j\alpha aL}\ \overline{d^C_{kbL}}\ \gamma_\mu\ L_{\beta bL}; \tag{3.5.55}$$

$$\mathcal{O}^{B-L}_{III} = k_2^2\ \epsilon_{ijk}\ \epsilon_{\alpha\beta}\ \overline{d^C_{iaL}}\ \gamma^\mu\ Q_{j\beta aL}\ \overline{u^C_{kbL}}\ \gamma_\mu\ L_{\alpha bL}; \tag{3.5.56}$$

$$\mathcal{O}^{B-L}_{IV} = k_2^2\ \epsilon_{ijk}\ \epsilon_{\alpha\beta}\ \overline{d^C_{iaL}}\ \gamma^\mu\ Q_{j\beta aL}\ \overline{\nu^C_{b\ L}}\ \gamma_\mu\ Q_{k\alpha bL}. \tag{3.5.57}$$

Here, $k_1 = g_u/(\sqrt{2}M_{(X,Y)})$ and $k_2 = g_u/(\sqrt{2}M_{(X',Y')}$, $Q_L = (u_L, d_L)$ and $L_L = (\nu_L, e_L)$. The indices i, j, k are color indices, a, b are family indices and α, β are $SU(2)_L$ indices. In the physical basis these operators will be modified as:

$$\mathcal{O}(e^C_\alpha, d_\beta) = c(e^C_\alpha, d_\beta)\ \epsilon_{ijk}\ \overline{u^C_{i\ L}}\ \gamma^\mu u_{jL}\ \overline{e^C_{\alpha\ L}}\ \gamma_\mu\ d_{k\beta L}; \tag{3.5.58}$$

$$\mathcal{O}(e_\alpha, d^C_\beta) = c(e_\alpha, d^C_\beta)\ \epsilon_{ijk}\ \overline{u^C_{i\ L}}\ \gamma^\mu u_{jL}\ \overline{d^C_{k\beta\ L}}\ \gamma_\mu\ e_{\alpha L}; \tag{3.5.59}$$

$$\mathcal{O}(\nu_l, d_\alpha, d^C_\beta) = c(\nu_l, d_\alpha, d^C_\beta)\ \epsilon_{ijk}\ \overline{u^C_{i\ L}}\ \gamma^\mu\ d_{j\alpha L}\ \overline{d^C_{k\beta\ L}}\ \gamma_\mu\ \nu_{lL}; \tag{3.5.60}$$

$$\mathcal{O}(\nu^C_l, d_\alpha, d^C_\beta) = c(\nu^C_l, d_\alpha, d^C_\beta)\ \epsilon_{ijk}\ \overline{d^C_{i\beta\ L}}\ \gamma^\mu\ u_{jL}\ \overline{\nu^C_{l\ L}}\ \gamma_\mu\ d_{k\alpha L}; \tag{3.5.61}$$

where

$$c(e^C_\alpha, d_\beta) = k_1^2\left[V_1^{11}V_2^{\alpha\beta} + (V_1V_{UD})^{1\beta}\left(V_2V_{UD}^\dagger\right)^{\alpha 1}\right]; \tag{3.5.62}$$

$$c(e_\alpha, d^C_\beta) = k_1^2V_1^{11}V_3^{\beta\alpha} + k_2^2\left(V_4V_{UD}^\dagger\right)^{\beta 1}\left(V_1V_{UD}V_4^\dagger V_3\right)^{1\alpha}; \tag{3.5.63}$$

$$c(\nu_l, d_\alpha, d^C_\beta) = k_1^2\left(V_1V_{UD}\right)^{1\alpha}\left(V_3V_{EN}\right)^{\beta l} + k_2^2V_4^{\beta\alpha}\left(V_1V_{UD}V_4^\dagger V_3V_{EN}\right)^{1l}; \tag{3.5.64}$$

$$c(\nu^C_l, d_\alpha, d^C_\beta) = k_2^2\left[\left(V_4V_{UD}^\dagger\right)^{\beta 1}\left(U_{EN}^\dagger V_2\right)^{l\alpha} + V_4^{\beta\alpha}\left(U_{EN}^\dagger V_2V_{UD}^\dagger\right)^{l1}\right]; \alpha = \beta \neq 2. \tag{3.5.65}$$

In the above V_1, V_2 etc are mixing matrices defined so that $V_1 = U_L^TU_R$, $V_2 = E_L^TD_R$, $V_3 = D_L^TE_R$, $V_4 = D_L^TD_R$, $V_{UD} = U_R^\dagger D_R$, $V_{EN} = E_R^\dagger N$ and $U_{EN} = E_L^TN$, where U, D, E define the diagonalizing matrices given by

$$U_L^\dagger\ M_U\ U_R \;=\; M_U^{diag} \tag{3.5.66}$$

$$D_L^\dagger\ M_D\ D_R \;=\; M_D^{diag} \tag{3.5.67}$$

$$E_L^\dagger\ M_E\ E_R \;=\; M_E^{diag} \tag{3.5.68}$$

$$N^T\ M_N\ N \;=\; M_N^{diag}. \tag{3.5.69}$$

Then the partial decay width of the decay $N \to P + \bar{l}$ ($N = p, n$, $P = (\pi, K, \eta)$ and $\bar{l}$ is anti-lepton) is given by:

$$\Gamma(N \to P + \bar{l}) = \frac{m_N}{32\pi}[1 - (\frac{m_P}{m_N})^2]^2 \left| \sum_I C^I W_0^I(N \to P) \right|^2, \tag{3.5.70}$$

where the coefficients C^I are given in Eqs. (3.5.62)-(3.5.65) and the relevant form factors W_0 are obtained by using lattice QCD computations [78]:

$$\langle \pi^0|(u,d)_R u_L|p\rangle_0 = -0.103, \langle \pi^+|(u,d)_R u_L|p\rangle_0 = -0.103, \langle K^0|(u,s)_R u_L|p\rangle_0 = 0.098,$$

$$\langle K^+|(u,s)_R d_L|p\rangle_0 = -0.054, \langle K^+|(u,d)_R s_L|p\rangle_0 = -0.093, \langle \eta|(u,d)_R u_L|p\rangle_0 = 0.015.$$

In Table 3.5 we present the $d = 6$ proton decay branching ratios calculated for our best fit parameter sets. We find that the two dominant modes are $p \to \overline{\nu}\pi^+$ and $p \to e^+\pi^0$. A comparison of these modes with those of more general $d = 6$ proton decay studies [120] shows similarity. The near dominance of the $\overline{\nu}\pi^+$ mode may be taken as a test of the Yukawa sector presented here.

p decay modes	**type-I**	**type-I+II**
$p \to \overline{\nu} + \pi^+$	49.07%	48.77%
$p \to e^+\pi^0$	42.57%	35.16%
$p \to \mu^+ K^0$	4.13%	5.12%
$p \to \mu^+\pi^0$	1.60%	5.62%
$p \to \overline{\nu} K^+$	1.19%	2.64%
$p \to e^+ K^0$	0.99%	2.28%
$p \to e^+\eta$	0.40%	0.33%
$p \to \mu^+\eta$	0.01%	0.05%

Table 3.5: Proton decay branching ratios in minimal non-SUSY $SO(10)$ GUT in **type-I** and **type-I+II** cases. For neutrino final states, we sum over all three flavors.

3.6 Conclusion

In this work, we have presented an economic Yukawa sector for $SO(10)$ models. The main feature of this construction is that only the $SO(10)$ symmetry is used to constrain the Yukawa parameters. The Higgs system consists of a *real* 10_H, a *real* 120_H and a complex $\overline{126}_H$ that have Yukawa couplings. In most nonsupersymmetric $SO(10)$ models in the literature symmetries outside of $SO(10)$ – such as a Peccei-Quinn $U(1)$ – are used to constrain the Yukawa sector. That would require the complexification of the *real* 10_H and *real* 120_H. The model presented here deviates from this, and yet is quite constraining. We showed that, with a limited number of Yukawa parameters, a good fit to all fermion masses and mixings, including the neutrino sector is possible. Once the flavor sector is fixed, we are able to calculate the proton decay branching ratios. The dominant decays of the proton are found to be $p \to \overline{\nu}\pi^+$ and $p \to e^+\pi^0$, which may provide partial tests of the model.

CHAPTER 4

ANARCHY WITH HIERARCHY: A PROBABILISTIC APPRAISAL

4.1 Introduction

Although the Standard Model (SM) of particle physics has been highly successful, it does not address some of the observed phenomena. For example, neutrinos in the SM are strictly massless. Non-zero masses for the neutrinos have been firmly established through oscillations experiments conducted with atmospheric [121], solar [122], accelerator [123] and reactor [124] neutrinos, requiring modification of the minimal model. An aesthetic shortcoming of the SM, arising from the enormous freedom available in the Yukawa Lagrangian, is that it provides very little insight into the masses and mixings of quarks and leptons. This shortcoming is often dubbed as the "flavor puzzle" and many extensions of the SM are constructed to address this issue. The purpose of this paper is to interpret the apparently diverse set of flavor parameters – quark masses, quark mixing angles, charged fermion masses, neutrino masses and leptonic mixing angles – in a unified fashion probabilistically.

The observed masses in the charged fermion sector show a hierarchical structure, with the strongest hierarchy seen in the up-type quark sector, and a somewhat milder hierarchy seen in the down-type quark and charged lepton sectors. These mass parameters, at the momentum scale $\mu = \mathrm{M_Z}$, are approximately given by (in units of $m_t = 1$):

$$\begin{aligned} m_u \sim 7.5 \times 10^{-6};\ m_c \sim 3.6 \times 10^{-3};\ m_t \sim 1; \\ m_d \sim 1.6 \times 10^{-5};\ m_s \sim 3 \times 10^{-4};\ m_b \sim 1.6 \times 10^{-2}; \\ m_e \sim 3 \times 10^{-6};\ m_\mu \sim 6 \times 10^{-4};\ m_\tau \sim 1 \times 10^{-2}. \end{aligned} \tag{4.1.1}$$

In contrast, the two neutrino squared-mass differences measured in oscillation experiments yield values given by [125]

$$\Delta m^2_{\mathrm{sol}} \sim 7.5 \times 10^{-5}\ \mathrm{eV}^2 \text{ and } \Delta m^2_{\mathrm{atm}} \sim 2.5 \times 10^{-3}\ \mathrm{eV}^2. \tag{4.1.2}$$

Adopting a normal ordering of the mass spectrum with $m_1 < m_2 \ll m_3$ with m_i being the neutrino masses, these values would indicate a mild or almost no hierarchy with $m_2/m_3 \sim 1/5$, quite different from the hierarchy seen in the other sectors (Cf: Eq. (4.1.1)). Additionally, the inter-generational mixing angles in the quark

sector are found to be small, while the leptonic mixing angles are measured to be large:

$$\begin{aligned} &\theta_{12}^{\rm CKM} \sim 13^\circ;\ \theta_{23}^{\rm CKM} \sim 2.4^\circ;\ \theta_{13}^{\rm CKM} \sim 0.2^\circ; \\ &\theta_{12}^{\rm PMNS} \sim 34^\circ;\ \theta_{23}^{\rm PMNS} \sim 38^\circ;\ \theta_{13}^{\rm PMNS} \sim 9^\circ. \end{aligned} \tag{4.1.3}$$

Understanding these patterns observed in the fermion spectrum is a fundamental unresolved problem in particle physics. Various attempts have been made to explain the hierarchy in the charged fermion masses and mixings, adopting highly regulated mass matrices supported by flavor symmetries (for a review see Ref. [126]). On the other hand, random structure-less matrices may be better suited to explain the non-hierarchical mass spectrum and the large mixing angles observed in the neutrino sector [127]. The use of such random matrices to explain neutrino mixing angles has been termed "anarchy hypothesis". A probability measure should be specified for these random matrices such that the matrix elements remain random after a basis transformation. For random unitary matrices this is achieved uniquely by the Haar measure [128]. Such matrices have been shown to be successful in explaining the observed large mixing angles in the neutrino sector [127–135]. When basis independence of the random matrix is combined with the requirement that each entry of the matrix has a distribution independent of other entries, the measure gets determined uniquely to be Gaussian [136–139]. Anarchical neutrino mixing angles as well as mass ratios have been analyzed with the Gaussian measure in Ref. [139].

In this paper [141] we unify the anarchy hypothesis in the neutrino sector with the hierarchy observed in the quark and charged lepton sectors [140], [142], [143], [128] and analyze the resulting models from a probabilistic perspective. Such a unification is achieved in the framework of $SU(5)$ grand unified theories, which treat quarks and leptons on similar footing. For concreteness we adopt a supersymmetric framework, which admits a one step symmetry breaking of $SU(5)$ down to the MSSM. These models have at most three parameters which are hierarchical and determined from a fit to data. They also contain five complex Yukawa coupling matrices which are taken to be structure-less or anarchical. Elements of these Yukawa coupling matrices are treated as uncorrelated random variables obeying Gaussian distributions. We perform Monte Carlo simulations of this framework and compare theoretical expectations with experimental data, which show good agreement.

Our main analysis is focused on the Yukawa coupling structure obtained in SUSY $SU(5)$ unified theories where the three families of 10_i fermions mix with vector-like fermions belonging to $10_\alpha + \overline{10}_\alpha$ representations that have GUT scale masses [140]. A variant of this model using the Froggatt-Nielsen mechanism [144], where the three families of 10_i fermions are distinguished by a flavor $U(1)$ symmetry while the three families of $\overline{5}_i$ are universal, is also analyzed allowing for effective non-renormalizable operators [128]. This class of models is a special case of the general class, with only two hierarchical input parameters. A second variant, also using a similar $U(1)$ flavor symmetry, which now distinguishes the first family $\overline{5}_1$ from the $\overline{5}_{2,3}$ fields is also analyzed,

with a single hierarchy parameter as input [145, 146]. Good fit to the entire fermion spectrum is obtained in all cases with the Yukawa couplings taking on uncorrelated Gaussian distributions.

It should be noted that ways to understand the neutrino mass anarchy along with charged fermion mass hierarchy has been explored in extra dimensional models with some success [147–150]. These models have not yet been subject to a detailed Monte Carlo analysis for testing quantitatively the goodness of the fit. The (renormalizable) models we discuss here share some common qualitative features with these extra dimensional models.

We also develop a constrained Monte Carlo simulation method to evaluate the figure of merit of the uncorrelated Gaussian distributions adopted for the random variables. In this method we calculate a specific projection of the probability density distribution of the original random parameters onto a surface that corresponds to random parameters that satisfy the experimental constraints. The figure of merit that is optimized in this simulation is the distortion of the distributions of the random parameters with respect to their original (unconstrained) distributions. This constrained Monte Carlo result can be thought of as a multi-dimensional analog of the Kolmogorov-Smirnov statistical test for a single variable. Our analysis shows that the distortions from the original Gaussian distributions are not much, suggesting a good quality fit.

While the class of models studied here cannot be tested in their precise predictions, they may become strongly favored or disfavored once we know more about the neutrino mass and mixing parameters. With an anarchical structure the CP-violating parameter $\sin\delta$ in the neutrino sector is found to be peaked at maximal values (± 1), although variations from these peak values are not excluded. The probability distribution of the neutrino mass ratio m_1/m_2 is peaked around 0.3, with the probability of measuring it below $1/100$ found to be about 4%.

This paper is organized as follows. In Sec. 2 we present our unified SUSY $SU(5)$ model which allows for the mixing of the three families of 10_i with vector-like fermions in the $10_\alpha + \overline{10}_\alpha$ representations. Here we also present special cases of this general framework making use of flavor $U(1)$ symmetries. In Sec. 3 we present the results of our Monte Carlo simulations for the fermion mass and mixing parameters for the main model as well as for its variants. In Sec. 4 we develop a new constrained Monte Carlo method to evaluate the goodness of the fits and compare the distortions of these new distributions from the original Gaussian distributions. In Sec. 5 we conclude.

4.2 Unifying Anarchy with Hierarchy in $SU(5)$

As noted in the introduction, grand unified theories based on $SU(5)$ allow for a unified description of anarchy in the neutrino sector and hierarchy in the quark sector. We work in the context of SUSY $SU(5)$. The GUT

symmetry breaks spontaneously down to the MSSM at an energy scale of 2×10^{16} GeV. The effective low energy theory is the MSSM. Our focus is the Yukawa couplings of the quarks and leptons in these theories. At the MSSM level, the Yukawa coupling matrices for the up quarks, down quarks, charged leptons, Dirac neutrinos and the right-handed Majorana neutrinos derived from these models will take the form [140]:

$$Y_U = H^T Y_U^0 H, \tag{4.2.4}$$

$$Y_D = \epsilon_4 \, Y_D^0 H, \tag{4.2.5}$$

$$Y_L = \epsilon_4 \, H^T Y_L^0, \tag{4.2.6}$$

$$Y_N = Y_N^0, \tag{4.2.7}$$

$$Y_R = Y_R^0. \tag{4.2.8}$$

Here the superpotential couplings are written as $(f_i^c (Y_f)_{ij} f_j) \, H_f$ with H_u and H_d denoting the two Higgs fields of MSSM. The fermion mass matrices obtained from Eqs. (4.2.4)-(4.2.8) have the form

$$M_U = Y_U v_u, \; M_D = Y_D v_d, \; M_L = Y_L v_d, \text{ and } M_N = Y_N v_u, \; M_R = Y_R v_R \tag{4.2.9}$$

with v_u and v_d being the VEVs of H_u and H_d. We have assumed the right-handed Majorana neutrino masses arise through the vacuum expectation value (VEV) v_R of a SM singlet field. In $SU(5)$ unified theories, bare Majorana masses for the gauge singlet right-handed neutrinos may be written down. If such bare masses are adopted, the scale v_R should be treated as an overall scale in the Majorana mass matrix. The light neutrino mass matrix, obtained via the seesaw mechanism [38], has the form:

$$M_\nu = \left(Y_N^T Y_R^{-1} Y_N \right) \frac{v_u^2}{v_R} \; . \tag{4.2.10}$$

An explicit derivation of the Yukawa matrices of Eqs. (4.2.4)-(4.2.8) based on $SU(5)$ will be given in the next subsection. Here we note their salient features which enable the unification of hierarchy and anarchy.

The matrix H in Eqs. (4.2.4)-(4.2.6) is Hermitian, which may be chosen to be diagonal, real and positive:

$$H = \text{diag}(\epsilon_1, \, \epsilon_2, \, \epsilon_3). \tag{4.2.11}$$

Here $\epsilon_1 \ll \epsilon_2 \ll \epsilon_3 \sim 1$ are input parameters of the model which take hierarchical values [140]. $\epsilon_3 = 1$ can be chosen by redefining other parameters of the model. These parameters arise in the model by virtue of mixing between the three chiral 10_i-plets of fermions with vector-like $10_\alpha + \overline{10}_\alpha$ of fermions with GUT scale masses. Y_f^0 in Eqs. (4.2.4)-(4.2.8) are the "bare" Yukawa coupling matrices – coupling matrices in the absence of mixing with the vector-like $10_\alpha + \overline{10}_\alpha$ fermions – which will be assumed to have no specific structure. $SU(5)$ invariance implies that the same H multiplies all the bare Yukawa coupling matrices in Eqs. (4.2.4)-(4.2.6). Note that

H appears on the right of Y_D^0, while it appears on the left of Y_L^0. This occurs in $SU(5)$ since the d^c field – the $SU(2)_L$ singlet down-type anti-quark – is unified with the left-handed lepton doublet in a $\overline{5}$ representation. As a consequence, the left-handed lepton mixing angles will be of order unity, simultaneously with order one mixing in the right-handed down quark sector (which are unobservable). Note also that the mass matrices for down quarks and charged leptons are "lopsided" [140, 151–154]. Furthermore, H appears on both sides of Y_U^0 in Eq. (4.2.4) (while it appears only on one side of Y_D^0 and Y_E^0 in Eqs. (4.2.5)-(4.2.6)), which is due to the presence of u and u^c fields in the same 10-plet of $SU(5)$. As a result, the mass hierarchy in the up-quark sector would be stronger compared to the hierarchy in the down-quark and charged lepton sectors:

$$m_d : m_s : m_b \sim \epsilon_1 : \epsilon_2 : 1 \tag{4.2.12}$$

$$m_e : m_\mu : m_\tau \sim \epsilon_1 : \epsilon_2 : 1 \tag{4.2.13}$$

$$m_u : m_c : m_t \sim \epsilon_1^2 : \epsilon_2^2 : 1 \tag{4.2.14}$$

Such a pattern is consistent with observations.

As for the mixing angles, Eqs. (4.2.4)-(4.2.8) will lead to

$$\begin{aligned} V_{ij}^{CKM} &\sim \frac{\epsilon_i}{\epsilon_j},\ i < j; \\ V_{ij}^{lepton} &\sim 1,\ i < j. \end{aligned} \tag{4.2.15}$$

That is, small quark mixings are realized along with large leptonic mixings in these models.

The parameter ϵ_4 in Eqs. (4.2.5)-(4.2.6) is a third hierarchy parameter, corresponding to an overall suppression of Y_D and Y_L compared to Y_U, which has its origin in the mixing of Higgs doublets at the GUT scale. (In certain minimal models such mixings may be absent, in which case $\epsilon_4 = 1$. We have investigated this scenario and found that the goodness of the fit to data is poor.) Since there is no hierarchy parameter in Y_N and Y_R in Eqs. (4.2.7)-(4.2.8), the light neutrino masses do not exhibit any hierarchy in this construction, see Eq. (4.2.10)).

The form of the Yukawa matrices given in Eqs. (4.2.4)-(4.2.8) may also be obtained in other ways in the context of $SU(5)$ unification. It has been suggested that these forms may follow if the 10-plet fermions are composite, while the $\overline{5}$-plet fermions are elementary [142]. Alternatively, if there is a flavor symmetry that distinguishes the three families of 10-plets, with the $\overline{5}$-plets being indistinguishable by this symmetry [128], the forms of Eqs. (4.2.4)-(4.2.8) may follow with the restriction that $\epsilon_1 \simeq \epsilon_2^2$. A flavor-dependent $U(1)$ symmetry that distinguishes $\overline{5}_1$ from $\overline{5}_{2,3}$ can lead to yet another constrained model, which may have only a single hierarchy parameter [145, 146]. We shall analyze these special cases as well.

4.2.1 Anarchy and hierarchy via mixing with vector-like fermions

In this subsection we provide an explicit construction of the fermion Yukawa matrices of Eqs. (4.2.4)-(4.2.8) based on $SU(5)$ symmetry. The setup that we present here is quite general, we will discuss some of its special cases in subsequent subsections. The construction involves mixing of the chiral families in the 10_i representations of $SU(5)$ with vector-like $10_\alpha + \overline{10}_\alpha$ fermions which have GUT scale masses. Such mixings provide the needed hierarchy factors to explain the charged fermion masses and quark mixing angles. All the Yukawa couplings of the model will be assumed to be structure-less or anarchical. This applies to the Yukawa couplings in the quark sector, charged lepton sector, and the neutrino sector universally. Thus, in the spirit of anarchy, these Yukawa coupling matrix elements will all be taken as uncorrelated random variables with Gaussian distributions.

The three families of fermions belong to the $10_i + \overline{5}_i$ multiplets of $SU(5)$ ($i = 1-3$ is the generation index). Quarks and leptons are unified in these multiplets as $10_i = \{e_i^c, u_i^c, Q_i\}$ and $\overline{5}_i = \{L_i, d_i^c\}$, where $Q_i = (u_i\ d_i)^T$ and $L_i = (\nu_i\ e_i)^T$. To generate small neutrino masses via the seesaw mechanism three $SU(5)$ singlet fermions 1_i (ν_i^c) are introduced. If only a $5_H + \overline{5}_H$ Higgs pair is involved in the Yukawa couplings as usually assumed in minimal SUSY $SU(5)$, the relation $M_L = M_D^T$ will result among the down-type quark and charged lepton mass matrices, which is unacceptable. To correct for this at the renormalizable level, we extend the Higgs sector by introducing a $45_H + \overline{45}_H$ pair [155]. Then the Yukawa superpotential is given by (assuming the usual R-parity)

$$\begin{aligned} \mathcal{W}_Y &= 10_i Y^5_{ij} 10_j 5_H + 10_i Y^{45}_{ij} 10_j 45_H + \overline{5}_i Y^{\overline{5}}_{ij} 10_j \overline{5}_H + \overline{5}_i Y^{\overline{45}}_{ij} 10_j \overline{45}_H \\ &+ \overline{5}_i Y^1_{ij} 1_j 5_H + \frac{1}{2}(M_R)_{ij} 1_i 1_j, \end{aligned} \tag{4.2.16}$$

where $Y^{\overline{5}}$, $Y^{\overline{45}}$ and Y^1 are general complex matrices, while Y^5 and Y^{45} are complex symmetric and antisymmetric matrices. These "bare" Yukawa coupling matrix elements (as well as the Majorana mass terms M_R for the right-handed neutrinos, up to an overall scale) will all be taken to be random variables obeying Gaussian distributions.

The model also contains a set of vector-like fermions belonging to $10_\alpha + \overline{10}_\alpha$ representations, where $\alpha = 1, 2, ..n$ where n is the number of copies used. The choice of $n = 3$ is natural, in which case there would be 3 pairs of such fields. The superpotential now admits additional mass terms given by

$$\mathcal{W}_Y \supset m_{\alpha j} \overline{10}_\alpha 10_j + M_{\alpha\beta} \overline{10}_\alpha 10_\beta, \tag{4.2.17}$$

where the first term represents the mixing of the ordinary fermions with the vector-like fermions and the second term generates bare masses for these vector-like fermions. Other possible gauge invariant couplings are assumed to be absent due to additional symmetries. An example of such a symmetry is a $Z_2 \times Z_2$ with the vector-like fermions $\overline{10}_\alpha$ being odd under the first Z_2, and the rest of the fields being even. This choice will prevent unwanted terms of the type $\overline{10}_\alpha 10_\beta 24_H$ and $\overline{10}_\alpha 10_i 24_H$, involving the $SU(5)$ breaking Higgs field 24_H. Such a

Z_2 is broken by the terms in Eq. (4.2.17), but only softly. Under the second Z_2, both 10_α and $\overline{10}_\alpha$ fields are odd, while the remaining fields are even. This Z_2, which is also broken softly by the first term in Eq. (4.2.17), will prevent mixed Yukawa coupling of the type $10_i 10_\alpha 5_H$. (This second Z_2 is optional, since the presence of mixed Yukawa couplings of the type $10_i 10_\alpha 5_H$ do not have any effect on our analysis.)

In Eq. (4.2.17) the mass terms m and M are SM singlets, and will be assumed to be of order the GUT scale. The presence of these terms in the Yukawa Lagrangian modifies the structure of the mass matrices of the SM fermions. From Eq. (4.2.17), the heavy states are found to be $10^H_\alpha \propto m_{\alpha i} 10_i + M_{\alpha\beta} 10_\beta$, with the light states 10^L_i being orthogonal to the 10^H_α states. This system can be inverted to express 10_i and 10_α in terms of $10^{L,H}$ states: $10_i = (H\ 10^L + H'\ 10^H)_i$ with

$$H = (I + mM^{-1}M^{-1^\dagger}m^\dagger)^{-\frac{1}{2}}. \tag{4.2.18}$$

Substituting this form of 10_i in Eq. (4.2.16), one can write down the light quark and light lepton mass matrices as [140]:

$$M_U = H^T M_U^0 H, \tag{4.2.19}$$

$$M_D = M_D^0 H, \tag{4.2.20}$$

$$M_L = H^T M_L^0, \tag{4.2.21}$$

$$M_N = M_N^0, \tag{4.2.22}$$

$$M_R = M_R^0, \tag{4.2.23}$$

where $M_{U,D}$ are the up-type and down-type quark mass matrices, M_L is the charged lepton mass matrix, M_N is the Dirac type neutrino mass matrix and M_R is the right-handed neutrino Majorana mass matrix. In writing these mass matrices we have defined [156]

$$M_U^0 = \langle 5_H \rangle Y^5 + \langle 45_H \rangle Y^{45}, \tag{4.2.24}$$

$$M_D^0 = \langle \overline{5}_H \rangle Y^{\overline{5}} + \langle \overline{45}_H \rangle Y^{\overline{45}}, \tag{4.2.25}$$

$$M_L^0 = \langle \overline{5}_H \rangle Y^{\overline{5}^T} - 3\langle \overline{45}_H \rangle Y^{\overline{45}^T}, \tag{4.2.26}$$

$$M_N^0 = \langle 5_H \rangle\ Y^1, \tag{4.2.27}$$

$$M_R^0 = v_R\ Y_R^0. \tag{4.2.28}$$

Note that all matrices in Eqs. (4.2.24)-(4.2.27) are general complex, while M_R^0 in Eq. (4.2.28) is complex symmetric. (M_U^0 has symmetric contributions from $\langle 5_H \rangle$ as well as antisymmetric contributions from $\langle 45_H \rangle$, with the sum being neither symmetric nor antisymmetric.)

The Hermitian matrix H in Eq. (4.2.18) can be written as $H = U^\dagger \mathrm{diag}\{\epsilon_1, \epsilon_2, \epsilon_3\} U$, with U being a unitary matrix and ϵ_i's being real and positive ($i = 1, 2, 3$). Substituting this form of H in Eqs. (4.2.19)-(4.2.21)

and redefining the quark and lepton fields, one can absorb the unitary matrix U into the non-hierarchical matrices $M^0_{U,D,L}$ without affecting the numerical results. Thus, we choose $H = \text{diag}\{\epsilon_1, \epsilon_2, \epsilon_3\}$. A hierarchy $\epsilon_1 \ll \epsilon_2 \ll \epsilon_3 \sim 1$ can be generated within the model by arranging for unequal mixings between the 10_i and 10_α for different families. For example, for the third family, we may take $M_3 \gg m_3$ (ignoring generation mixing for simplicity of explaining) while for the second and first families we may take $M_2 \ll m_2$ and $M_1 \lll m_1$, see Eq. (4.2.18) [140]. We shall set $\epsilon_3 = 1$, since this parameter is of order one, and redefining other parameters of the theory enables this choice. Consequently, we will choose

$$H = \text{diag}\{\epsilon_1, \epsilon_2, 1\} \tag{4.2.29}$$

for our analysis.

The MSSM up-type Higgs doublet H_u that remains light to low energies is a linear combination of up-type doublets from the 5_H, 45_H and other possible up-type Higgs doublets present in the $SU(5)$ model. Similarly the light MSSM field H_d is a linear combination of down-type Higgs doublets from $\overline{5}_H$, $\overline{45}_H$ and other possible down-type Higgs doublets in the model. An example of such additional up-type and down-type Higgs doublets is a pair of $5'_H + \overline{5}'_H$ fields with no Yukawa couplings to the fermions. We then have

$$H_u = \alpha_u \, h^u_5 + \beta_u \, h^u_{45} + \sum_i \gamma^u_i h'^u_i \tag{4.2.30}$$

$$H_d = \alpha_d \, h^d_{\overline{5}} + \beta_d \, h^d_{\overline{45}} + \sum_i \gamma^d_i h'^d_i \tag{4.2.31}$$

with $|\alpha_u|^2 + |\beta_u|^2 + \sum_i |\gamma^u_i|^2 = 1 = |\alpha_d|^2 + |\beta_d|^2 + \sum_i |\gamma^d_i|^2$. Here $h^u_5 = (1, 2, \frac{1}{2}) \subset 5_H$, $h^u_{45} = (1, 2, \frac{1}{2}) \subset 45_H$, $h^d_{\overline{5}} = (1, 2, -\frac{1}{2}) \subset \overline{5}_H$ and $h^d_{\overline{45}} = (1, 2, -\frac{1}{2}) \subset \overline{45}_H$, where the quantum numbers under the SM gauge symmetry are indicated. The fields h'^u_i and h'^d_i are $(1, 2, \frac{1}{2})$ and $(1, 2, -\frac{1}{2})$ fields from additional Higgs multiplets, such as $5'_H + \overline{5}'_H$ pairs. All fields orthogonal to H_u and H_d remain superheavy. The VEVs of the doublet components of the various fields are related to the VEVs v_u and v_d of the MSSM fields H_u and H_d as

$$v_5 = \alpha^*_u v_u, \quad v_{45} = \beta^*_u v_u, \tag{4.2.32}$$

$$v_{\overline{5}} = \alpha^*_d v_d, \quad v_{\overline{45}} = \beta^*_d v_u. \tag{4.2.33}$$

Substituting these relations, one can rewrite the effective mass matrices Eqs. (4.2.19)-(4.2.23) for the fermions as:

$$M_U = v_u\, H^T Y_U^0 H \equiv v_u\, Y_U, \tag{4.2.34}$$

$$M_D = v_d\, \epsilon_4\, Y_D^0 H \equiv v_d\, Y_D, \tag{4.2.35}$$

$$M_L = v_d\, \epsilon_4\, H^T Y_L^0 \equiv v_d\, Y_L, \tag{4.2.36}$$

$$M_N = v_u\, Y_N^0 \equiv v_u\, Y_N, \tag{4.2.37}$$

$$M_R = v_R\, Y_R^0 \equiv v_R\, Y_R. \tag{4.2.38}$$

Here Y_U^0, Y_D^0 etc are the bare Yukawa coupling matrices derived from Eqs. (4.2.24)-(4.2.27), using the definitions given in Eq. (4.2.33):

$$Y_U^0 = \alpha_u^*\, Y^5 + \beta_u^*\, Y^{45}, \tag{4.2.39}$$

$$Y_D^0 = \alpha_d^*\, Y^{\overline{5}} + \beta_d^*\, Y^{\overline{45}}, \tag{4.2.40}$$

$$Y_L^0 = \alpha_d^*\, Y^{\overline{5}^T} - 3\beta_d^*\, Y^{\overline{45}^T}, \tag{4.2.41}$$

$$Y_N^0 = \alpha_u^*\, Y^1\ . \tag{4.2.42}$$

Thus, we see that the effective Yukawa coupling matrices of the quarks and leptons with the MSSM Higgs fields as given in Eqs. (4.2.4)-(4.2.8) are generated. The bare Yukawa couplings $Y^0_{U,D,L,N,R}$ in these equations will be treated as random variables obeying Gaussian distributions in our numerical analysis. The parameter ϵ_4 appearing in Eqs. (4.2.35)-(4.2.36) arises from the Higgs doublet mixing expressed in terms of ($\alpha_{u,d}$, $\beta_{u,d}$). To realize values of ϵ_4 in the range $\epsilon_4 = (0.04 - 0.1)$ as our fits would prefer, it is sufficient to take α_d and β_d somewhat smaller than one. Unitarity of the Higgs mixing matrix is maintained due to the presence of additional Higgs doublets such as $5'_H + \overline{5}'_H$ in the model. The model also has $\tan\beta = v_u/v_d$ as an input parameter. A relation between the $\tan\beta = v_u/v_d$ and ϵ_4 can be obtained from Eqs. (4.2.34)-(4.2.35):

$$\epsilon_4 \simeq \frac{m_b}{m_t} \tan\beta \frac{(Y_U^0)_{33}}{|(\overrightarrow{d_0})_3|} \tag{4.2.43}$$

where we have defined $(\overrightarrow{d_0})_3 = \{(Y_D^0)_{13}, (Y_D^0)_{23}, (Y_D^0)_{33}\}$. Note that to set $\epsilon_3 = 1$ which we have adopted, we redefine ϵ_4 in Eqs.(4.2.35)-(4.2.36), and also redefine v_u in Eq. (4.2.34).

Since the masses of the vector-like fermions are of the order of GUT scale, any effect of these particles at low energies will be suppressed by a factor of $1/M_{GUT}$, except for the dimension four fermion mass operators as discussed in the text. Hence their presence does not change the phenomenology of the MSSM or the Higgs boson mass. Even though the super-heavy vector-like fermions decouple, they may leave imprints on the SUSY flavor structure at low energies. However, SUSY models with large superpartner masses or gauge-mediated SUSY breaking models can potentially suppress any such flavor violating effects.

As noted previously, there are other ways of generating the Yukawa structure shown in Eqs. (4.2.4)-(4.2.8) by assuming $U(1)$ flavor symmetry that distinguishes the three families of 10_i [128], and/or the first family of $\overline{5}_1$ from $\overline{5}_{2,3}$ [145, 146], by hypothesizing that the 10_i-plets are composite [142, 157], or postulating extra dimensions [147, 148, 150]. Another interesting class of models proposed recently in Ref. [158, 159] has a very similar structure for the mass matrices, which we shall not investigate here. We do analyze the flavor $U(1)$ models as special cases of the general class of models described here, which are described next.

4.2.2 $SU(5)$-inspired models with $U(1)$ flavor symmetry

In this subsection we briefly describe a class of $SU(5)$-inspired models with $U(1)$ flavor symmetry. Models of this type can explain the hierarchical structure in the fermion masses and mixings by using the Fraggatt-Nielsen mechanism [144]. Smaller entries in the mass matrices are induced as higher dimensional operators suppressed by differing inverse powers of a fundamental mass scale. Assigning different charges to different families will lead to a hierarchy in masses and mixings.

The models we study here are inspired by SUSY $SU(5)$ unification – in the sense that the flavor $U(1)$ charge assignment will be compatible with $SU(5)$ – but we can work just within the framework of MSSM. We shall use the language of $SU(5)$, however, for simplicity. The three fermion families are assigned to $10_i + \overline{5}_i$, and we include three families of SM singlet 1_i (ν_i^c) fields for the seesaw mechanism. In order to reproduce the observed hierarchical structure in fermion masses, we make specific $U(1)$ charge assignment to the fermion fields as shown in Table 4.1. The integer charges q_1, q_2 and p are left unspecified in the table, two different choices will be presented below.

Field	$U_A(1)$ charge
$10_1, 10_2, 10_3$	$2q_1,\ q_1,\ 0$
$\overline{5}_1, \overline{5}_2, \overline{5}_3$	$q_2 + p,\ p,\ p$
$1_1, 1_2, 1_3$	$q_2,\ 0,\ 0$

Table 4.1: The flavor $U(1)$ charge assignment of the fermion fields in $SU(5)$ notation. The Yukawa matrices of Eqs. (4.2.4)-(4.2.8) will be induced with the choice $q_1 = 1$, $q_2 = p = 0$. Yukawa couplings given in Eqs. (4.2.46)- (4.2.48) will result with the choice $q_1 = 2$, $q_2 = 1$, $p = 0, 1$ or 2, corresponding to large, medium and small $\tan\beta$. These models also contain a flavon field S with $U(1)$ charge of -1 that acquires a VEV. The Higgs doublets H_u and H_d of MSSM are neutral under this $U(1)$.

In these models, the $U(1)$ flavor symmetry is broken by a single parameter $\epsilon = \langle S\rangle/M_*$, where $\langle S\rangle$ is the

VEV of an $SU(5)$ singlet flavon field S with $U(1)$ charge -1 and $M_* > M_{GUT}$ is a fundamental scale such as the string scale. The Yukawa superpotential contains higher dimensional terms suppressed by inverse powers of M_*, with coefficients which are all of order one. These couplings have the form

$$\mathcal{W}_Y \supset Y^u_{ij} Q_i u^c_j H_u \left(\frac{S}{M_*}\right)^{n^u_{ij}} + Y^d_{ij} Q_i d^c_j H_d \left(\frac{S}{M_*}\right)^{n^d_{ij}} + Y^\ell_{ij} L_i e^c_j H_d \left(\frac{S}{M_*}\right)^{n^\ell_{ij}} + Y^\nu_{ij} L_i \nu^c_j H_u \left(\frac{S}{M_*}\right)^{n^\nu_{ij}} + v_R Y^R_{ij} \nu^c_i \nu^c_j \left(\frac{S}{M_*}\right)^{n^{\nu^c}_{ij}} . \tag{4.2.44}$$

Here the integers n^u_{ij} etc are chosen such that the corresponding Yukawa coupling Y^u_{ij} is charge neutral. The couplings Y^u_{ij} etc are all taken to be of order unity. Still hierarchical masses and mixings are induced since the (ij) entry in the mass matrix has a suppression factor $\epsilon^{n_{ij}}$.

In our first flavor $U(1)$ model we choose the $U(1)$ charges of Table 4.1 to be $\{q_1 = 1, q_2 = 0, p = 0\}$ [128]. In this case the Yukawa coupling matrices will have the same form as in Eqs. (4.2.4)-(4.2.8). Note that in this model the three families of $\overline{5}_i$ are neutral under $U(1)$, while the 10_i carry differing charges given as (2, 1, 0). Since the $U(1)$ symmetry is broken by a single parameter, the Hermitian matrix H appearing in Eqs. (4.2.4)-(4.2.8) is now given by

$$H = \begin{pmatrix} \epsilon^2 & 0 & 0 \\ 0 & \epsilon & 0 \\ 0 & 0 & 1 \end{pmatrix} . \tag{4.2.45}$$

The only difference from the general model of the previous subsection is that here $\epsilon_2 \equiv \epsilon$ and $\epsilon_1 = \epsilon^2$.[1] This model will be analyzed separately, with the assumption that the Yukawa couplings entering Eq. (4.2.44) are random variables taking Gaussian distributions. The light neutrino mass matrix retains exactly the same structure-less pattern as before, since the ν^c fields as well as the L_i fields are all neutral under the $U(1)$. If the model is embedded in $SU(5)$ minimally, the wrong relation $Y_L = Y_D^T$ would result. This would require the extension of the scalar sector by a $45_H + \overline{45}_H$ pair. As before, the parameter ϵ_4 has the same definition as in Eqs. (4.2.4)-(4.2.8), and such models have two hierarchical parameters $\{\epsilon, \epsilon_4\}$.

A second flavor $U(1)$ model is obtained by the choice of $U(1)$ charges in Table 4.1 as $\{q_1 = 2, q_2 = 1, p =$ 0, 1, or 2$\}$ along with the charges of the scalar fields given by $\{H_u, H_d, S\} = \{0, 0, -1\}$. Here the first family $\overline{5}_1$ has a shifted charge compared to $\overline{5}_{2,3}$. This is the only difference of this model compared to the first flavor $U(1)$ model just discussed. Such a model has been studied in Ref. [145, 146], where the Yukawa coupling matrices written in the basis $f^c_i (Y_f)_{ij} f_j$ are shown to take the form:

[1] Strictly, $\epsilon_1 = O(1)\epsilon^2$, but this $O(1)$ coefficient may be absorbed into other $O(1)$ Yukawa couplings, which is what we shall do.

$$Y_U \sim \begin{pmatrix} \epsilon^8 & \epsilon^6 & \epsilon^4 \\ \epsilon^6 & \epsilon^4 & \epsilon^2 \\ \epsilon^4 & \epsilon^2 & 1 \end{pmatrix}, \quad Y_D \sim \epsilon^p \begin{pmatrix} \epsilon^5 & \epsilon^3 & \epsilon \\ \epsilon^4 & \epsilon^2 & 1 \\ \epsilon^4 & \epsilon^2 & 1 \end{pmatrix}, \tag{4.2.46}$$

$$Y_L \sim \epsilon^p \begin{pmatrix} \epsilon^5 & \epsilon^4 & \epsilon^4 \\ \epsilon^3 & \epsilon^2 & \epsilon^2 \\ \epsilon & 1 & 1 \end{pmatrix}, \; Y_N \sim \epsilon^p \begin{pmatrix} \epsilon^2 & \epsilon & \epsilon \\ \epsilon & 1 & 1 \\ \epsilon & 1 & 1 \end{pmatrix}, \tag{4.2.47}$$

$$Y_R \sim \begin{pmatrix} \epsilon^2 & \epsilon & \epsilon \\ \epsilon & 1 & 1 \\ \epsilon & 1 & 1 \end{pmatrix}, \qquad \mathcal{Y}_\nu \sim \epsilon^{2p} \begin{pmatrix} \epsilon^2 & \epsilon & \epsilon \\ \epsilon & 1 & 1 \\ \epsilon & 1 & 1 \end{pmatrix}. \tag{4.2.48}$$

Here $\mathcal{Y}_\nu$ determines the light neutrino mass matrix via the seesaw relation $M_\nu = \mathcal{Y}_\nu v_u^2/v_R$. The integer p is allowed to take three different values, $p = 0, 1$ or 2, corresponding to large, medium, and small values of $\tan\beta$. In Eqs. (4.2.46)-(4.2.48), each matrix element has an $O(1)$ coefficient c_{ij}^f that is not explicitly shown. These entries are taken to be of order unity. For our statistical analysis of the model, we shall take these c_{ij}^f to be random variables obeying uncorrelated Gaussian distributions. One clearly sees that although the charged fermion mass matrices here are quite similar to the previously discussed models, the light neutrino mass matrix is significantly different. Unlike the previous cases, it is no longer given by a matrix with order unity entries everywhere; rather it has somewhat of a hierarchical structure. In this model, it is possible to correct the $SU(5)$ relation $M_L = M_D^T$ via higher dimensional operators involving the 24_H field, and therefore, a parameter analogous to ϵ_4 is not required. As we shall see, a good fit to all data is obtained in this model with a single hierarchy parameter ϵ.

4.3 Statistical Analysis of Flavor Parameters in $SU(5)$-based Models

In this section we perform a statistical analysis of the general class of unified theories based on $SU(5)$. The general model described in Sec. 4.2.1 contains three hierarchical input parameters $\{\epsilon_1, \epsilon_2, \epsilon_4\}$ as well as $\tan\beta$ in the flavor sector. In addition, these models have five complex Yukawa coupling matrices, see Eqs. (4.2.4)-(4.2.8), the elements of which are treated as uncorrelated random variables with Gaussian distributions. After a detailed analysis of this general setup, we repeat the analysis for the two $SU(5)$-inspired flavor $U(1)$ variants. These variants have either two set of hierarchical parameters $\{\epsilon, \epsilon_4\}$, or a single parameter ϵ.

The primary goal of this section is to investigate how well the theoretical predictions of this class of models agree with the experimentally observed quantities on average. We perform a Monte Carlo simulation and derive the theoretical expectations for these models. We start with the MSSM Yukawa coupling matrices given in

Eqs. (4.2.4)-(4.2.8). As noted before, the matrices Y_F^0 in Eqs. (4.2.4)-(4.2.8) are random matrices with all elements of order $O(1)$. The matrices Y_F^0 for $F = U, D, L, N$ are of the Dirac-type and in general complex matrices. The right-handed neutrino Yukawa coupling matrix Y_R^0 in Eq. (4.2.8) is of the Majorana-type which is complex symmetric. We assume that each of these matrix elements is a random variable independent of other elements. The probability distributions of the matrix elements are assumed to be completely independent of the hierarchical model parameters $\{\epsilon_1, \epsilon_2, \epsilon_4\}$. Basis independence as well as absence of correlation between various matrix elements determine uniquely the probability measures for these random variables to be Gaussian [137, 139]:

$$\begin{aligned} dY_{\rm D}^0 &= \prod_{ij} dY_{ij}^0 \; e^{-|Y_{ij}^0|^2}, \\ dY_{\rm M}^0 &= \prod_{i} dY_{ii}^0 \; e^{-|Y_{ii}^0|^2} \; \prod_{i<j} dY_{ij}^0 \; e^{-2|Y_{ij}^0|^2}, \end{aligned} \tag{4.3.49}$$

Here the subscripts D and M represent Dirac-type and Majorana-type respectively. These measures are defined up to a scale factor e^{-c}, which has been set equal to 1. (When Gaussian distributions are applied to mass matrices, this scale factor can be used to fix the overall scale of the VEV, see Ref. [139] for details). From Eq. (4.3.49), all the elements of a general complex random matrix are independently generated with Gaussian distribution of variance 0.5 for both the real and imaginary parts separately. Similarly, for the complex symmetric random matrix, the real and imaginary parts are generated independently with Gaussian distribution of variance 0.5 and 0.25 for diagonal and off-diagonal entries respectively.

The class of models with Yukawa matrices given in Eqs. (4.2.4)-(4.2.8) has three input parameters, ϵ_i (i=1,2,4) and 84 random variables (72 in four general complex random matrices and 12 in one random complex symmetric matrix). In this section we present a Monte Carlo analysis of these models adopting Gaussian measure for the random matrix elements. The parameters ϵ_i are however not random, instead they are fixed by χ^2-function minimization. We have seen previously that these parameters do not enter in the neutrino sector. Thus, in order to fix the numerical values of these parameters we only include in the χ^2-minimization the observables in the charged fermion sector. The minimization is carried out at the GUT scale with 3 input parameters to fit 13 observables.

To perform the χ^2-minimization at the GUT scale we take the experimentally observed values of the charged fermion observables at the $\rm M_Z$ scale from Ref. [72]. These values are quoted in Table 5.2. We use the renormalization group running factors corresponding to MSSM, $\eta_i = m_i(\rm M_{GUT})/m_i(\rm M_Z)$, taken from Ref. [73] for the evolution of the Yukawa couplings from the $\rm M_Z$ scale to the GUT scale. These running factors are listed in Table 4.3. We perform the Monte Carlo analysis for two values of the parameter $\tan\beta$, 10 and 50. The Yukawa couplings at the GUT scale are obtained from the couplings determined at $\mu = \rm M_Z$ with the help of these

Yukawa Couplings and CKM parameters	$\mu = \mathrm{M_Z}$
$y_u/10^{-6}$	6.65 ± 2.25
$y_c/10^{-3}$	3.60 ± 0.11
y_t	0.9860 ± 0.00865
$y_d/10^{-5}$	1.645 ± 0.165
$y_s/10^{-4}$	3.125 ± 0.165
$y_b/10^{-2}$	1.639 ± 0.015
$y_e/10^{-6}$	2.79475 ± 0.0000155
$y_\mu/10^{-4}$	5.89986 ± 0.0000185
$y_\tau/10^{-2}$	1.00295 ± 0.0000905
θ_{12}^{CKM}	0.22735 ± 0.000072
$\theta_{23}^{CKM}/10^{-2}$	4.208 ± 0.064
$\theta_{13}^{CKM}/10^{-3}$	3.64 ± 0.13
δ^{CKM}	1.208 ± 0.054

Table 4.2: Observables in the charged fermion sector at the $\mathrm{M_Z}$ scale taken from Ref. [72]. For quantities with asymmetrical error bars, we have symmetrized and presented the experimental central values with associated 1 σ uncertainties. The fermion masses are given by the relations $m_i(\mathrm{M_Z}) = v\ y_i^{\mathrm{SM}}(\mathrm{M_Z})$, with $v = 174$ GeV.

renormalization running factors by using the relations $y_{u_i}^{\mathrm{MSSM}}(\mathrm{M_{GUT}}) = y_{u_i}^{\mathrm{SM}}(\mathrm{M_Z})\eta_{u_i}/\sin\beta$ for up-type quarks and $y_{d_i,e_i}^{\mathrm{MSSM}}(\mathrm{M_{GUT}}) = y_{d_i,e_i}^{\mathrm{SM}}(\mathrm{M_Z})\eta_{d_i,e_i}/\cos\beta$ for down-type quarks and charged leptons. We also run the CKM mixing parameters from $\mathrm{M_Z}$ to the GUT scale using the MSSM renormalization group equations [75, 111]. The renormalization running factors of the CKM matrix elements are presented in Table 4.3. The Yukawa couplings and the CKM mixing parameters at the GUT scale are presented in Table 5.3. For the associated one sigma uncertainties of these observables at the GUT scale, we take the same percentage uncertainty with respect to the central value of each quantity as that at the $\mathrm{M_Z}$ scale. For the charged lepton Yukawa couplings, a relative uncertainty of 1% is assumed, instead of smaller experimental statistical errors, in order to take into account the theoretical uncertainties such as SUSY and GUT scale threshold effects.

With these GUT scale inputs, using the Eqs. (4.2.4)-(4.2.8), we perform χ^2 minimization by treating ϵ_1, ϵ_2 and ϵ_4 as parameters and fit the data in the charged fermion sector. Here $n_{obs} = 13$ is the number of observables, with 3 parameters to fit them. The elements of the random matrices pick up random values independently according to Gaussian distribution. For our analysis the error, pull and χ^2-function are defined as follows:

$\tan\beta$	10	50
(η_u, η_c, η_t)	(0.385, 0.381, 0.536)	(0.377, 0.382, 0.551)
(η_d, η_s, η_b)	(0.241, 0.236, 0.273)	(0.175, 0.181, 0.211)
$(\eta_e, \eta_\mu, \eta_\tau)$	(0.583, 0.583, 0.585)	(0.423, 0.423, 0.442)
$(\eta_{us}^{CKM}, \eta_{cb}^{CKM}, \eta_{ub}^{CKM})$	(0.999, 0.890, 0.890)	(0.999, 0.826, 0.826)

Table 4.3: Renormalization group running factors for the masses, $\eta_i = m_i(\mathrm{M_{GUT}})/m_i(\mathrm{M_Z})$ (taken from Ref. [73]). These values are obtained with two-loop MSSM renormalization group evolution with appropriate one-loop matching conditions. In the last row the renormalization group running factors $\eta_{ij}^{CKM} = V_{ij}(\mathrm{M_{GUT}})/V_{ij}(\mathrm{M_Z})$ of the CKM matrix elements are listed, which are obtained by evolving the RGEs for these parameters [75, 111] from low energy to $\mathrm{M_{GUT}}$.

$$\begin{aligned} \sigma_i &= \sqrt{\sigma_{i\,\mathrm{th}}^2 + \sigma_{i\,\mathrm{exp}}^2}, \\ P_i &= \frac{O_{i\,\mathrm{th}} - E_{i\,\mathrm{exp}}}{\sigma_i}, \\ \chi^2 &= \sum_i P_i^2, \end{aligned} \tag{4.3.50}$$

where $\sigma_{i\,\mathrm{th}}$ and $\sigma_{i\,\mathrm{exp}}$ represent the theoretical standard deviation (TSD) and experimental 1σ uncertainty respectively and $O_{i\,\mathrm{th}}$, $E_{i\,\mathrm{exp}}$ and P_i represent the theoretical mean value (TMV), experimental central value (ECV) and pull of an observable i.

We find the minimum with $\chi^2/n_{obs} \sim 1$ along with the model parameters shown in Table 4.5. The best fit values of the observables obtained with these fixed model parameters resulting from our Monte Carlo optimization are shown in Table 4.6. In Fig. 5.2 we plot the histogram distributions of the observables in the quark and the charged lepton sectors corresponding to the fixed model parameters given in Table 4.5 for the case where $\tan\beta = 10$ (plots for the case $\tan\beta = 50$ are similar). In producing these distributions we have taken the sample size to be 10^4 and chose the bin size (N bins) to be 50.

The blue plots in Fig. 5.2 show histograms of the theoretical distributions of the up-type quark Yukawa couplings. Overlaid on these distributions are the experimental values of these couplings. We find very good agreement between theoretical expectations and observations. Among all the charged fermions, the eigenvalue spectrum of the up-type quarks shows the most hierarchical structure which is nicely reproduced. This is not surprising, as the stronger hierarchy is built into the model, see Eqs. (4.2.4)-(4.2.8).

For the down-type quark Yukawa couplings, theoretical distributions are shown in green in Fig. 5.2. Overlaid on these distributions are the experimental values of these parameters. These are in good agreement with observations for down-quark and bottom-quark, whereas for the strange-quark, the theoretical mean value

Yukawa Couplings and CKM mixing parameters	$\tan\beta = 10$ (at $\mu = \mathrm{M_{GUT}}$)	$\tan\beta = 50$ (at $\mu = \mathrm{M_{GUT}}$)
$y_u/10^{-6}$	2.57 ± 0.86	2.51 ± 0.84
$y_c/10^{-3}$	1.37 ± 0.04	1.37 ± 0.04
$y_t/10^{-1}$	5.31 ± 0.04	5.43 ± 0.04
$y_d/10^{-4}$	0.39 ± 0.04	1.44 ± 0.14
$y_s/10^{-3}$	0.74 ± 0.03	2.84 ± 0.14
$y_b/10^{-2}$	4.49 ± 0.04	17.29 ± 0.15
$y_e/10^{-5}$	1.63 ± 0.01	5.91 ± 0.05
$y_\mu/10^{-3}$	3.45 ± 0.03	12.49 ± 0.12
$y_\tau/10^{-2}$	5.89 ± 0.05	22.21 ± 0.22
$\lvert V_{us}\rvert/10^{-2}$	22.53 ± 0.07	22.53 ± 0.07
$\lvert V_{cb}\rvert/10^{-2}$	3.74 ± 0.05	3.47 ± 0.05
$\lvert V_{ub}\rvert/10^{-3}$	3.24 ± 0.11	3.00 ± 0.10
η_W	0.35 ± 0.01	0.35 ± 0.01

Table 4.4: Input values at $\mathrm{M_{GUT}}$ used in our fits. Central values and 1 σ errors are quoted. For Yukawa couplings, these numbers are found with the help of Tables 5.2 and 4.3 and by using the equations $y_{u_i}^{\mathrm{MSSM}}(\mathrm{M_{GUT}}) = y_{u_i}^{\mathrm{SM}}(\mathrm{M_Z})\eta_{u_i}/\sin\beta$ for up-type quarks and $y_{d_i,e_i}^{\mathrm{MSSM}}(\mathrm{M_{GUT}}) = y_{d_i,e_i}^{\mathrm{SM}}(\mathrm{M_Z})\eta_{d_i,e_i}/\cos\beta$ for down-type quarks and charged leptons. For the charged lepton Yukawa couplings, a relative uncertainty of 1% is assumed, instead of smaller experimental statistical errors, in order to take into account the theoretical uncertainties from threshold effects. For the CKM mixing parameters, we evolve the quantities from low scale to $\mathrm{M_{GUT}}$ by using the RGEs provided in Ref. [75, 111].

tends to be a little higher than the experimentally measured value, but it is still within acceptable range. In the eigenvalue spectrum of charged leptons, which is shown in pink in Fig. 5.2, the theoretical mean value for the muon Yukawa coupling tends to be a little lower than the experimental central value. The reason for these small discrepancies can be understood from the approximate relations $\frac{y_s}{y_b} \sim \epsilon_2$ and $\frac{\mathrm{y}_\mu}{\mathrm{y}_\tau} \sim \epsilon_2$ present in the model. At the GUT scale one has roughly $y_b \sim y_\tau$, which implies within the model $y_s \sim y_\mu$. This is why the histograms of Yukawa couplings for both strange-quark and muon Yukawa couplings are almost identical with approximately the same theoretical mean values, but observation dictates, $y_s \sim 4y_\mu$ at the GUT scale. This small discrepancy, inherent to these models, is still not major and is within acceptable range.

The probability distributions of the CKM parameters are shown in purple in Fig. 5.2. Overlaid on these

$\tan\beta$	10	50
ϵ_1	0.00181±0.00010	0.00169±0.00009
ϵ_2	0.0388±0.00222	0.03659±0.00215
ϵ_4	0.04055±0.00229	0.15716±0.00894

Table 4.5: Model parameters determined by χ^2 minimization for the $SU(5)$-based GUTs defined in Eqs. (4.2.4)-(4.2.8).

Observables	TMV±TSD		$\frac{\text{TMV}}{\text{ECV}}$		pull	
	$\tan\beta = 10$	$\tan\beta = 50$	$\tan\beta = 10$	$\tan\beta = 50$	$\tan\beta = 10$	$\tan\beta = 50$
$y_u/10^{-6}$	7.23±7.76	6.39±6.93	2.81	2.54	0.59	0.55
$y_c/10^{-3}$	2.55±2.53	2.26±2.37	1.85	1.64	0.46	0.37
y_t	0.88±0.46	0.89±0.46	1.67	1.63	0.77	0.74
$y_d/10^{-4}$	0.64±0.33	2.3±1.23	1.61	1.62	0.73	0.73
$y_s/10^{-3}$	2.10±0.77	7.59±2.79	2.83	2.67	1.75	1.69
$y_b/10^{-1}$	0.67±0.19	2.61±0.76	1.50	1.51	1.13	1.15
$y_e/10^{-4}$	0.64±0.34	2.34±1.22	3.96	3.96	1.42	1.42
$y_\mu/10^{-3}$	2.10±0.75	7.63±2.74	0.60	0.61	-1.79	-1.76
$y_\tau/10^{-1}$	0.67±0.19	2.59±0.76	1.14	1.16	0.42	0.48
$\lvert V_{us}\rvert/10^{-2}$	8.17±7.80	8.07±7.87	0.36	0.35	-1.83	-1.83
$\lvert V_{cb}\rvert/10^{-2}$	6.15±6.37	5.99±6.34	1.64	1.72	0.37	0.39
$\lvert V_{ub}\rvert/10^{-3}$	3.42±3.67	3.23±3.75	1.05	1.07	0.04	0.06
η_W	0.05±3.13	0.05±2.59	0.14	0.14	-0.09	-0.11

Table 4.6: χ^2 best fit values of the observables for the $SU(5)$-based GUTs defined in Eqs. (4.2.4)-(4.2.8) with the fixed model parameters given in Table 4.5. The best fit values shown in this table correspond to $\chi^2/n_{obs} = 1.13$ and 1.12 for $\tan\beta = 10$ and 50 respectively. Here TMV=theoretical mean value, TSD=theoretical standard deviation, ECV=experimental central value and pull is defined in Eq. (4.3.50).

distributions are the experimental values of these observables. These distributions [2] are also in very good agreement with data. The theoretical distribution for V_{us} has a mean value that tends to be somewhat smaller than the experimental value. This feature may be understood since the model has $V_{us} \sim \epsilon_1/\epsilon_2$. It also predicts $y_d/y_s \sim 0.05 \sim \epsilon_1/\epsilon_2$, which makes V_{us} to peak around 0.05, rather than the observed value of ~ 0.2. But there is still acceptable agreement.

[2]Similar distributions for the CKM parameters are obtained in Ref. [160] from a completely different statistical approach.

We can do a consistency check for the value of $\tan\beta$ used. From Eq. (4.2.43) we have, $\tan\beta \simeq \epsilon_4\ m_t/m_b\ \frac{|(\vec{d_0})_3|}{(Y_U^0)_{33}}$. Since $O(1)$ random variables are present in this equation, $\tan\beta$ in these models follows a distribution shown in Fig. 5.4. Both histograms have a long tail behaviour with the mean values of the distributions being $\tan\beta = 14$ and 71.4 respectively. For histograms with such behaviour, median may be a better measure, which are $\tan\beta =$ 9.4 and 48.3 respectively. We see broad consistency with the input values of $\tan\beta$ used in each case.

Since the small parameters ϵ_i do not enter into the neutrino sector, in the optimization process we did not include the neutrino observables. Once the model parameters are fixed as in Table 4.5, one can include the neutrino sector in the sampling process and investigate how well the observed quantities in this sector are reproduced by these models. Since the matrix structure is the same as the ones considered in earlier works assuming anarchical hypothesis only in the neutrino sector [127,128], the histogram distributions of the neutrino observables should be similar, which is what we find. In Figs. 4.3 and 4.4 we present plots for the theoretical predictions of the neutrino observables. The theoretical average values of these observables resulting from the Monte Carlo analysis are shown in Table 4.7. The input values for neutrino observables are taken from Ref. [76] corresponding to the case of normal ordering of the neutrino mass spectrum. We restrict our analysis to normal ordering, since the random matrix structure for the neutrinos strongly prefers this over inverted ordering. In our Monte Carlo simulations we found a 95.6% probability for normal ordering and a 4.4% probability for inverted ordering, which is similar to the results of Ref. [139]). To ensure normal ordering, we assume $m_1 \leq m_2 < m_3$ and we put the constraint $r < 1$ ($r \equiv \Delta m^2_{\rm sol}/\Delta m^2_{\rm atm}$ with $\Delta m^2_{\rm sol} = m_2^2 - m_1^2$ and $\Delta m^2_{\rm atm} = m_3^2 - m_2^2$) in the sampling procedure.

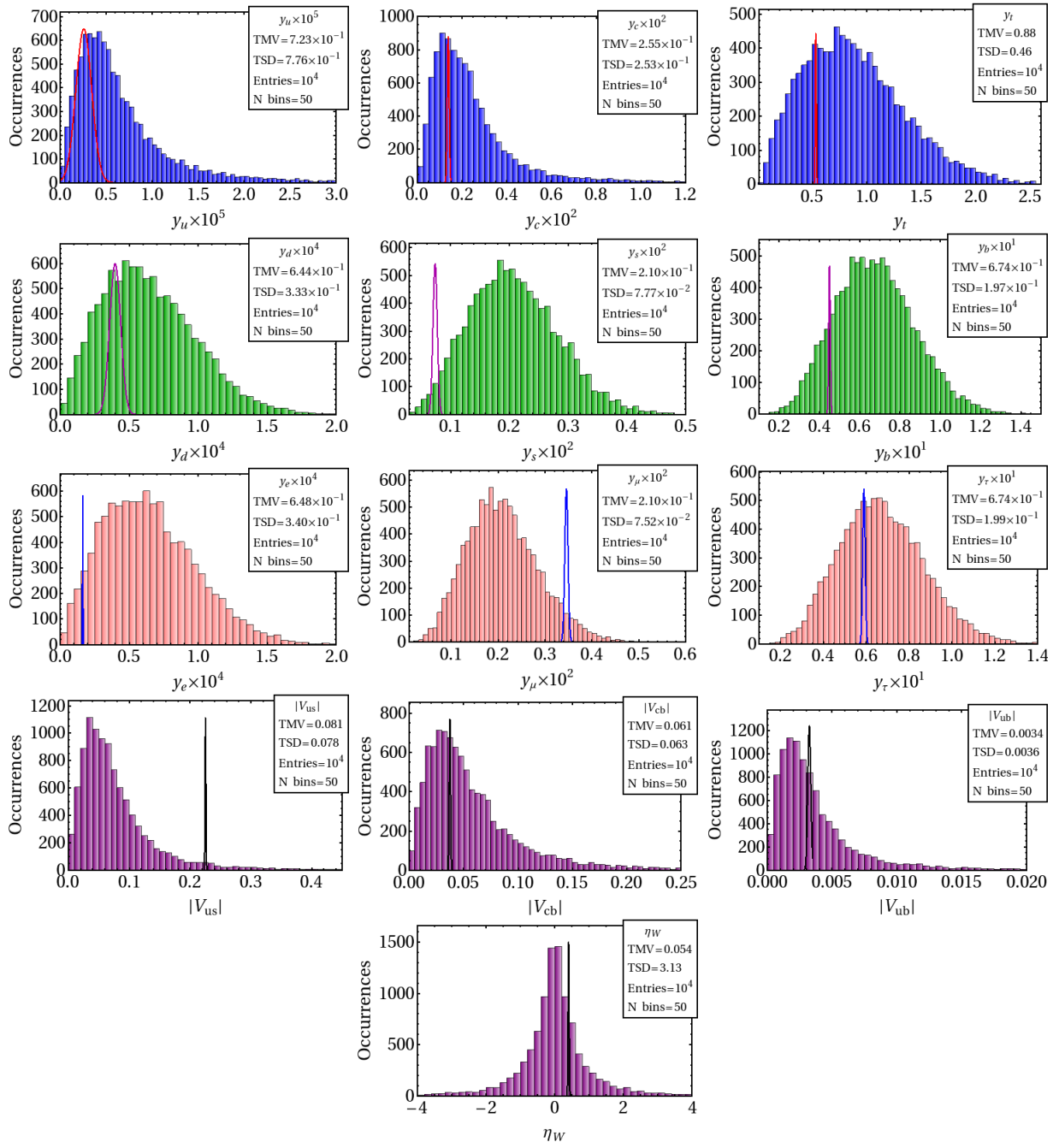

Figure 4.1: Histogram plots showing the distributions of the observables in the charged fermion sector. Blue (green, pink and purple) plots are the theoretical distributions of the up-type quarks (down-type quarks, charged leptons and CKM mixing parameters) according to the $SU(5)$-based GUTs with 10^4 occurrences for the case of $\tan\beta = 10$ corresponding to the model parameters given in Table 4.5. Red (magenta, blue and black) curves represent the corresponding experimental 1σ uncertainty range. For the charged leptons, a relative uncertainty of 1% is assumed in order to take into account theoretical uncertainties arising from SUSY and GUT scale threshold effects. The number of bins (N bins) is chosen to be 50.

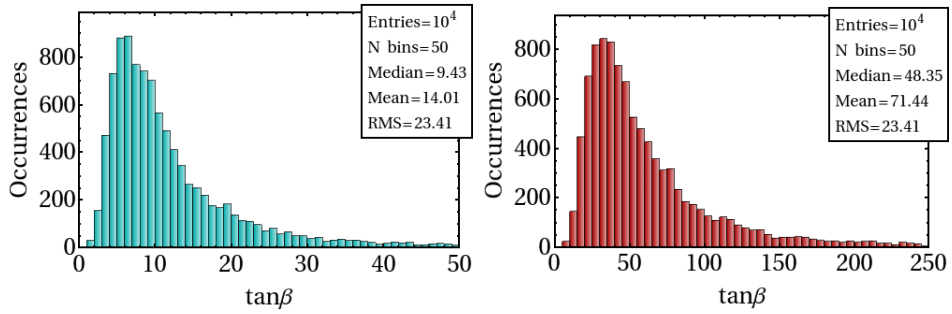

Figure 4.2: Histograms showing theoretical distributions of $\tan\beta$ given by Eq. (4.2.43) for the $SU(5)$-based GUTs with sample size of 10^4. Left plot corresponds to the case where $\tan\beta = 10$ and the right plot for $\tan\beta = 50$. The number of bins (N bins) is chosen to be 50.

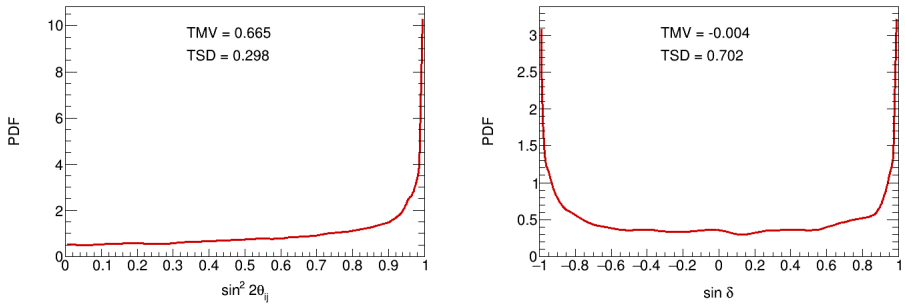

Figure 4.3: Probability density plots for the neutrino mixing parameters for $SU(5)$-based GUTs. The left plot is for the mixing angles, $\sin^2 2\theta_{ij}$ for $(ij) = (12), (23)$ and (13), and the right plot is for the CP-violating parameter $\sin\delta$. In these probability density plots, the area under the curve within a certain range represents the probability of finding the quantity within that particular range. Here TMV=theoretical mean value, TSD=theoretical standard deviation.

Observables	ECV	1σ exp	TMV	TSD	$\frac{\text{TMV}}{\text{EMV}}$	pull
$\frac{\Delta m^2_{sol}}{\Delta m^2_{atm}}$	0.031	0.001	0.135	0.186	4.37	0.56
$\sin^2\theta_{12}$	0.308	0.017	0.504	0.287	1.63	0.68
$\sin^2\theta_{23}$	0.3875	0.0225	0.501	0.290	1.29	0.39
$\sin^2\theta_{13}$	0.0241	0.0025	0.334	0.235	13.8	1.31

Table 4.7: Theoretical sampling results of the $SU(5)$-based model obtained from Monte Carlo simulation in the neutrino sector. Experimental central values with associated one sigma uncertainties are also quoted taken from Ref. [76]. Here TMV=theoretical mean value, TSD=theoretical standard deviation, ECV=experimental central value and pull is defined in Eq. (4.3.50). The theoretical results presented here are for sample size of 10^4. The best fit values shown in this table correspond to $\chi^2/n_{obs} = 0.66$.

In Fig. 4.3 we plot the probability density for the neutrino mixing parameters. The area under the curve in a probability density plot between any two values of the observable represents the probability of finding the observable within that particular range and the total area is normalized to unity. From these plots it is clear that for this class of models all the mixing parameters $\sin^2 2\theta_{ij}$ in the neutrino sector take preferentially large values. The CP-violating parameter $\sin\delta$ is peaked at its maximal values of ± 1. Preference of all the mixing parameters to be large is a consequence of the complete anarchical form of the neutrino mass matrix as their distributions are uniquely fixed by the invariant Haar measure.

In Fig. 4.4 we plot theoretical distributions of $\log_{10}(\Delta m^2_{\rm sol}/\Delta m^2_{\rm atm})$ and $\log_{10}(m_i/m_j)$. The upper left plot in Fig. 4.4 shows that the anarchic structure of the neutrino mass matrix prefers small values of the ratio of the two mass squared differences, r and the theoretical mean value is quite close to the experimental central value. The upper right plot reveals that anarchy predicts mild hierarchy in the neutrino mass spectrum. The lower plots in Fig. 4.4 exhibits the probability densities for the two different neutrino mass ratios, m_1/m_3 and m_1/m_2. As can be seen, the ratio m_1/m_2 peaks around 0.3. Extreme small values of m_1 are strongly disfavored in this model. For example, $m_1/m_2 < 0.01$ will be favored only with a 4% probability.

4.3.1 Monte Carlo analysis of $SU(5)$-inspired $U(1)$ flavor models

Models with two parameters $\{\epsilon, \epsilon_4\}$

In this subsection, we present our Monte Carlo results for the $SU(5)$-inspired $U(1)$ flavor models with $U(1)$ charges chosen to be $\{q_1 = 1, q_2 = 0, p = 0\}$ as explained in Sec. 4.2.2. Models of this type have two parameters, $\{\epsilon, \epsilon_4\}$. The only modification needed compared to our general setup is in the charged fermions sector where the

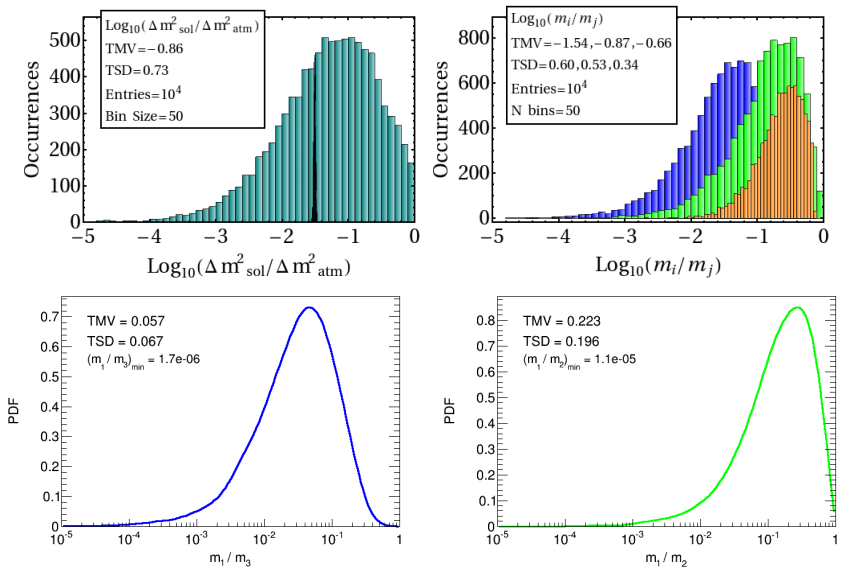

Figure 4.4: Two histogram plots showing the theoretical distributions of $\log_{10}(\Delta m^2_{\rm sol}/\Delta m^2_{\rm atm})$ (upper left) and $\log_{10}(m_{ij}) = \log_{10}(m_i/m_j)$ (upper right; blue, green and orange histograms are for $\log_{10}(m_1/m_3)$, $\log_{10}(m_1/m_2)$ and $\log_{10}(m_2/m_3)$ respectively). The black curve in the upper left plot represents the experimental 1σ uncertainty range. The two bottom plots are the probability density functions for the neutrino mass ratios m_i/m_j (blue and green plots are for m_1/m_3 and m_1/m_2). In these probability density plots, the area under the curve within a certain range represents the probability of finding the quantity within that particular range. These plots are the results from our Monte Carlo analysis for the anarchical neutrino mass models with normal mass ordering. Here TMV=theoretical mean value, TSD=theoretical standard deviation. For the two histogram distributions the number of bins is chosen to be 50 and for all the plots the sample size is taken to be 10^4.

matrix H is given by Eq. (4.2.45). This set of models has one less parameter compared to the general model. We have performed a fit as before in this two parameter case and the fitted model parameters are presented in Table 4.8. From this Table one finds, $\epsilon \sim \lambda^2$, where $\lambda \sim 0.22$. With this fixed parameters, the corresponding best fit values of the observables are shown in Table 4.9 and the theoretical distributions of these quantities are presented in Fig. 4.5. By comparing the fit results of Tables 4.6 and 4.9 one sees that a slightly better fit is obtained for the three parameter case compared to the analysis done here with one less parameter. In Table 4.6, all the observables are reproduced within 2σ error on average, whereas in Table 4.9, with one less parameter, two of the observables are in the $(2-3)\sigma$ range for the case of $\tan\beta = 10$ and for the case of $\tan\beta = 50$, one of the observables is little above 2σ error on average. Since the neutrino sector is exactly the same for all these models belonging to $SU(5)$-based GUTs, the analysis in the previous subsection remains unchanged.

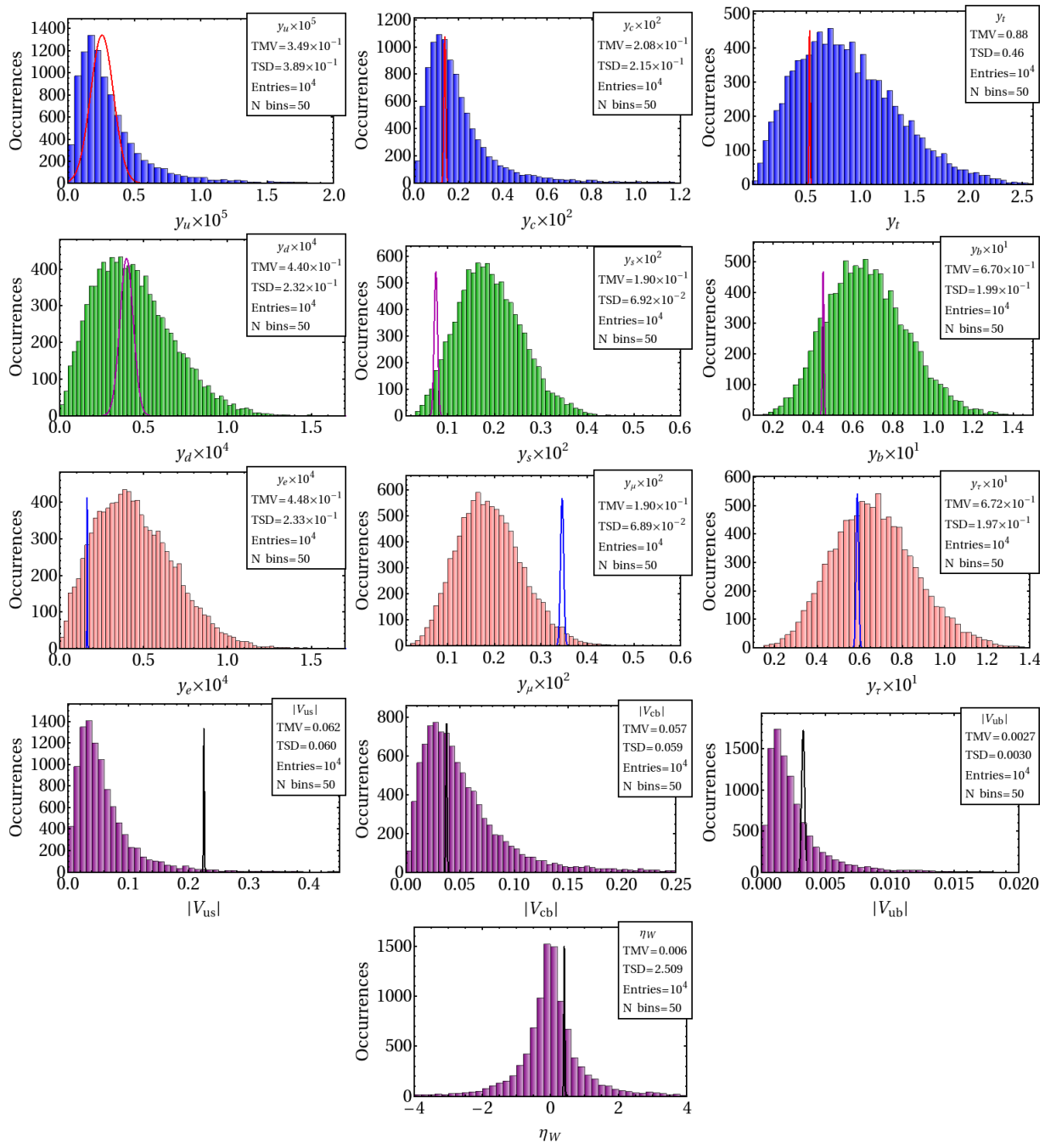

Figure 4.5: Histograms showing the theoretical distributions of the observables in the charged fermion sector in the $SU(5)$-inspired $U(1)$ flavor symmetric models with the charge assignment $\{q_1 = 1, q_2 = 0, p = 0\}$ defined by Eqs. (4.2.4)-(4.2.8) and (4.2.45) ($\tan\beta = 10$). The color code is the same as in Fig. 5.2.

Monte Carlo analysis of $U(1)$ model with one parameter $\{\epsilon\}$

In this subsection we apply a Monte Carlo analysis to the $SU(5)$-inspired flavor symmetry model with the $U(1)$-flavor charge assignment of $\{q_1 = 2, q_2 = 1, p = 0, 1, 2\}$ as discussed in Sec. 4.2.2. As explained there, the matrix

$\tan\beta$	10	50
ϵ	0.02855±0.00150	0.03847±0.00215
ϵ_4	0.03909±0.00220	0.14537±0.00826

Table 4.8: Model parameters determined by χ^2 minimization for the $SU(5)$-inspired $U(1)$ flavor symmetry models with two parameters.

Observables	TMV±TSD		$\frac{\text{TMV}}{\text{ECV}}$		pull	
	$\tan\beta = 10$	$\tan\beta = 50$	$\tan\beta = 10$	$\tan\beta = 50$	$\tan\beta = 10$	$\tan\beta = 50$
$y_u/10^{-6}$	3.49±3.89	4.96±5.55	1.35	1.97	0.23	0.43
$y_c/10^{-3}$	2.08±2.15	2.50±2.57	1.51	1.82	0.32	0.43
y_t	0.88±0.46	0.88±0.46	1.65	1.63	0.76	0.74
$y_d/10^{-4}$	0.44±0.23	1.92±1.00	1.10	1.32	0.17	0.46
$y_s/10^{-3}$	1.90±0.69	7.45±2.71	2.56	2.62	1.67	1.69
$y_b/10^{-1}$	0.67±0.19	2.42±0.71	1.49	1.40	1.11	0.96
$y_e/10^{-4}$	0.44±0.23	1.90±1.00	2.69	3.21	1.41	1.31
$y_\mu/10^{-3}$	1.90±0.75	7.38±2.71	0.55	0.59	-2.24	-1.87
$y_\tau/10^{-1}$	0.68±0.19	2.42±0.70	1.15	1.09	0.42	0.28
$\lvert V_{us}\rvert/10^{-2}$	8.17±7.80	6.81±6.86	0.36	0.30	-2.68	-2.29
$\lvert V_{cb}\rvert/10^{-2}$	5.75±5.93	6.19±6.30	1.53	1.78	0.33	0.43
$\lvert V_{ub}\rvert/10^{-3}$	2.73±3.03	2.81±2.96	0.84	0.93	-0.16	-0.06
η_W	0.006±2.509	0.003±2.30	0.01	0.006	-0.15	-1.13

Table 4.9: χ^2 best fit values of the observables for the $SU(5)$-inspired $U(1)$ flavor symmetry models with two parameters. The fixed model parameters are given in Table 4.8. The best fit values shown in this table correspond to $\chi^2/n_{obs} = 1.44$ and 1.41 for $\tan\beta = 10$ and 50 respectively.

elements in Eqs. (4.2.46)-(4.2.48) have order one complex coefficients c^f_{ij}. We assume that the coefficients are random complex variables with Gaussian distribution of variance 0.5 for both real and imaginary parts. For the off-diagonal terms of the complex symmetric matrix Y_R the coefficients have variance of 0.25. We generate this unbiased set of random variables following Gaussian distribution in a manner similar to the one described earlier. By taking the sample size to be 10^4, we study the theoretical probability distributions of the observables in the fermion sector. We carry out the Monte Carlo analysis for three cases with $p = 0, 1, 2$ (corresponding to $\tan\beta = 55, 25, 5$ respectively) and present the values of the parameter ϵ that minimizes the χ^2 for each case. For these values of $\tan\beta$ the RGE running factors are not given in Ref. [73] and hence we run the two loop

MSSM RGEs [74, 75] from low scale to the GUT scale [3]. We take the low scale central values of the observables from Table 2 of Ref. [72] at $\mu = 1$ TeV where the observables are converted to the $\overline{\rm DR}$ scheme, use the SUSY matching formula (without taking into account the threshold corrections) for the Yukawa couplings and evolve them upto the GUT scale and use these values as inputs (shown in Table 4.10) during the optimization. Like before, for the charged leptons, we assume a relative 1% uncertainty in order to take into account the theoretical uncertainties such as SUSY and GUT scale threshold effects.

Yukawa Couplings and CKM mixing parameters	$\tan\beta = 5$ (at $\mu = \mathrm{M_{GUT}}$)	$\tan\beta = 25$ (at $\mu = \mathrm{M_{GUT}}$)	$\tan\beta = 55$ (at $\mu = \mathrm{M_{GUT}}$)
$y_u/10^{-6}$	2.98 ± 1.00	2.88 ± 0.96	2.96 ± 0.99
$y_c/10^{-3}$	1.45 ± 0.04	1.4 ± 0.04	1.44 ± 0.04
$y_t/10^{-1}$	5.43 ± 0.04	5.23 ± 0.04	5.85 ± 0.05
$y_d/10^{-4}$	0.24 ± 0.02	1.24 ± 0.12	3.55 ± 0.36
$y_s/10^{-3}$	0.48 ± 0.024	2.47 ± 0.12	7.04 ± 0.35
$y_b/10^{-2}$	2.73 ± 0.02	14.33 ± 0.12	49.61 ± 0.44
$y_e/10^{-4}$	0.10 ± 0.001	0.51 ± 0.005	1.45 ± 0.01
$y_\mu/10^{-2}$	0.21 ± 0.002	1.08 ± 0.01	3.07 ± 0.03
$y_\tau/10^{-1}$	0.36 ± 0.003	1.89 ± 0.01	6.53 ± 0.06
$\lvert V_{us}\rvert/10^{-2}$	22.53 ± 0.07	22.53 ± 0.07	22.53 ± 0.07
$\lvert V_{cb}\rvert/10^{-2}$	3.72 ± 0.05	3.70 ± 0.05	3.37 ± 0.05
$\lvert V_{ub}\rvert/10^{-3}$	3.22 ± 0.11	3.21 ± 0.11	2.92 ± 0.10
η_W	0.35 ± 0.01	0.35 ± 0.01	0.35 ± 0.01

Table 4.10: Experimental central values with associated 1σ uncertainties at $\mathrm{M_{GUT}}$ scale used in our fits. The low scale central values of the observables are taken from the Table 2 of Ref. [72] at $\mu = 1$ TeV. For the charged leptons, a relative uncertainty of 1% is assumed in order to take into account the theoretical uncertainties as for example SUSY threshold and GUT scale effects.

p	2	1	0
$\tan\beta$	5	25	55
ϵ	0.1956±0.0097	0.1985±0.0105	0.1755±0.0098

Table 4.11: Model parameters fixed by minimization for the flavor symmetry based models defined in Eqs. (4.2.46)-(4.2.48) by employing Monte Carlo analysis with different values of p.

[3] We also performed the running for the cases with $\tan\beta = 10$ and 50 and found consistency with Ref. [73] and hence the values presented in Table 5.3.

The numerical values of the model parameter determined by χ^2-minimization are presented in Table 4.11. These values are similar to the ones computed in Table 2 of Ref. [145]. The best fit values resulting from the χ^2 minimization for the three cases with $p = 0, 1, 2$ are presented in Table 4.12. From this Table one sees that, for this class of models with a single parameter, the fit to the charged fermion observables is not very different from that of the models with 3 parameters. For V_{us}, the pull is greater than 2σ, but the rest of the observables are in good agreement. The main difference of this model compared to the previous two models is in the neutrino mixing parameters. In the $SU(5)$-based GUTs, the set of models where the left-handed light neutrino Yukawa coupling matrix elements are all $\sim O(1)$, large values of mixing angles are preferred for all three mixing parameters $\sin^2 2\theta_{ij}$ (see Fig. 4.3). On the other hand, the present model which is described by the Yukawa matrices given in Eqs. (4.2.46)-(4.2.48), $O(1)$ entries exist only in the 2-3 sector that give rise to large $\sin^2 2\theta_{23}$. But due to a suppression factor ϵ in the 1-3 sector, $\sin^2 2\theta_{13}$ naturally comes out to be smaller than unity. The probability density plots of $\sin^2 2\theta_{ij}$ are shown in Fig. 4.7, the patterns remain the same for different values of p for this set of models (Fig. 4.8) compared to the previous set analyzed before (Fig. 4.4). Except for the three mixing parameters, the theoretical distributions of the observables in the fermion sector remain similar in pattern and are shown in Figs. 4.6 for the case of $p = 2$ (histograms for other values of p's are similar, and are not shown).

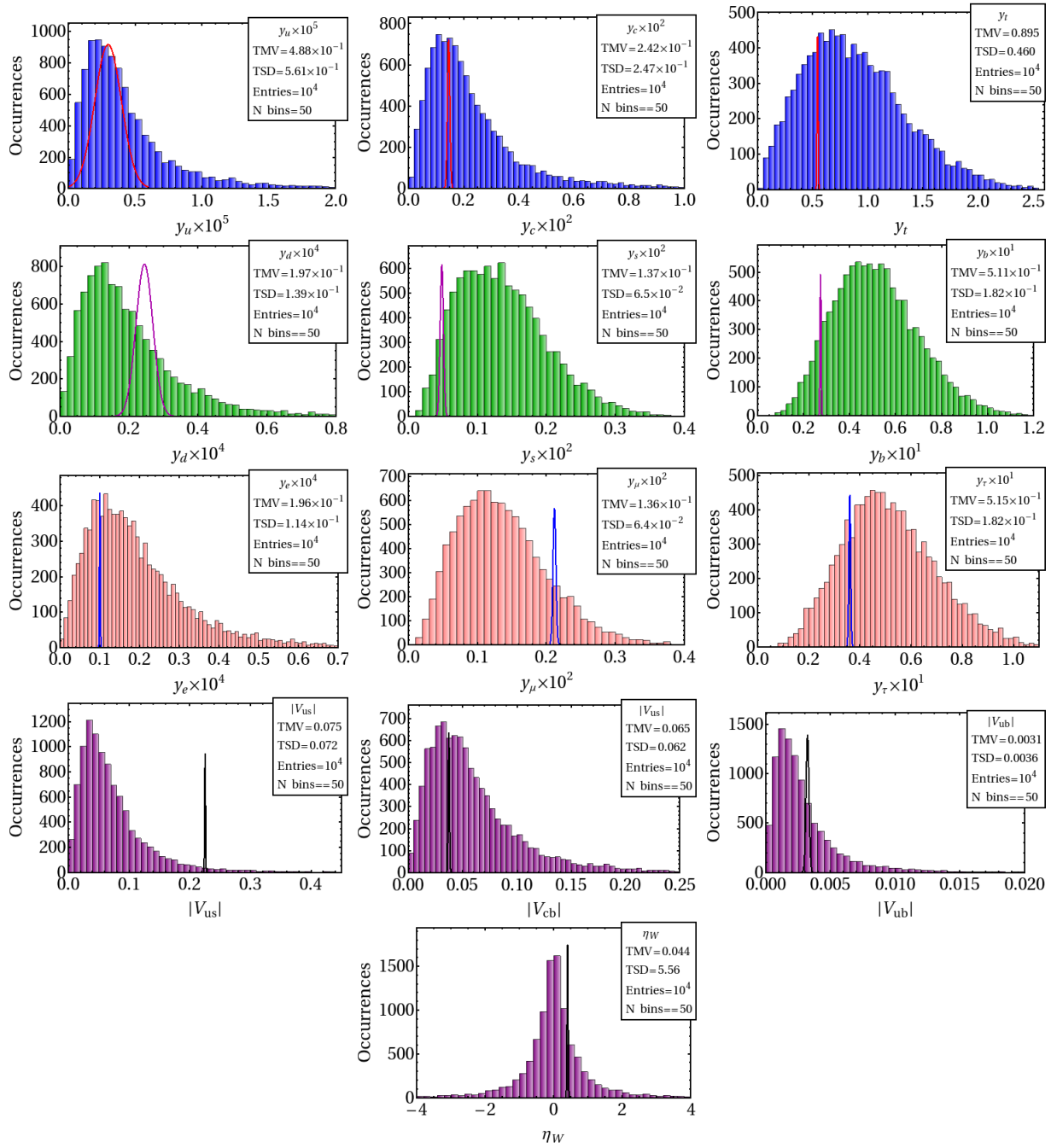

Figure 4.6: Histograms showing the theoretical distributions of the observables in the charged fermion sector according to the $SU(5)$-inspired $U(1)$ flavor symmetry based models with the charge assignment $\{q_1 = 2, q_2 = 1, p = 2\}$ defined by Eqs. (4.2.46)-(4.2.48) ($\tan\beta = 5$). The color code is the same as in Fig. 5.2.

Observables	TMV±TSD			$\frac{\text{TMV}}{\text{ECV}}$			pull		
	$\tan\beta = 5$	$\tan\beta = 25$	$\tan\beta = 55$	$\tan\beta = 5$	$\tan\beta = 25$	$\tan\beta = 55$	$\tan\beta = 5$	$\tan\beta = 25$	$\tan\beta = 55$
$y_u/10^{-6}$	4.88±5.61	5.42±6.06	2.00±2.26	1.63	1.88	0.67	0.33	0.41	-0.38
$y_c/10^{-3}$	2.42±2.47	2.59± 2.66	1.62±1.76	1.66	1.84	1.12	0.39	0.44	0.10
y_t	0.89±0.46	0.89±0.46	0.88±0.46	1.64	1.70	1.51	0.76	0.79	0.64
$y_d/10^{-5}$	1.97±1.39	11.0±7.78	30.8±22.6	0.80	0.88	0.86	-0.33	-0.18	-0.20
$y_s/10^{-3}$	1.37±0.65	7.31±3.49	28.4±13.6	2.83	2.95	4.04	1.36	1.38	1.57
$y_b/10^{-1}$	0.51±0.18	2.65±0.94	13.4±4.77	1.86	1.85	2.71	1.30	1.29	1.77
$y_e/10^{-5}$	1.96±1.14	11.10±7.88	31.06±22.69	1.95	2.16	2.13	0.67	0.75	0.72
$y_\mu/10^{-3}$	1.36±0.64	7.24±3.45	28.42±13.85	0.64	0.67	0.92	-1.16	-1.02	-0.16
$y_\tau/10^{-1}$	0.51±0.18	2.66±0.93	13.40±4.75	1.43	1.40	2.05	0.85	0.82	1.44
$\lvert V_{us}\rvert/10^{-1}$	0.75±0.72	0.77±0.69	0.61±0.59	0.33	0.34	0.27	-2.05	-2.11	-2.75
$\lvert V_{cb}\rvert/10^{-1}$	0.65±0.62	0.66± 0.65	0.53±0.54	1.74	1.79	1.57	0.44	0.45	0.35
$\lvert V_{ub}\rvert/10^{-2}$	0.31±0.36	0.32±0.36	0.20±0.24	0.98	1.01	0.69	-0.01	0.01	-0.36
η_W	0.04±5.56	0.01±2.49	0.04±2.72	0.11	0.02	0.11	-0.05	-0.13	-0.11
$\frac{\Delta m^2_{sol}}{\Delta m^2_{atm}}$	0.09±0.16	0.10± 0.16	0.09±0.16	3.17	3.27	3.21	0.42	0.43	0.41
$sin^2\theta_{12}^{PMNS}$	0.17±0.19	0.17±0.19	0.15±0.18	0.56	0.57	0.50	-0.70	-0.66	-0.84
$sin^2\theta_{23}^{PMNS}$	0.47±0.29	0.47±0.29	0.48±0.29	1.22	1.24	1.22	0.31	0.30	0.30
$sin^2\theta_{13}^{PMNS}$	0.09±0.12	0.10±0.12	0.08±0.11	3.97	4.14	3.44	0.57	0.58	0.51

Table 4.12: χ^2 best fit values of the observables for the $SU(5)$-inspired flavor symmetry based models defined in Eqs. (4.2.46)-(4.2.48) with fixed values of the model parameters given in Table 4.11. The best fit values shown in this table correspond to $\chi^2/n_{obs} = 0.73$, 0.74 and 1.05 for $p = 2$, 1 and 0 respectively. Here TMV=theoretical mean value, TSD=theoretical standard deviation, ECV=experimental central value and pull is defined in Eq. (4.3.50).

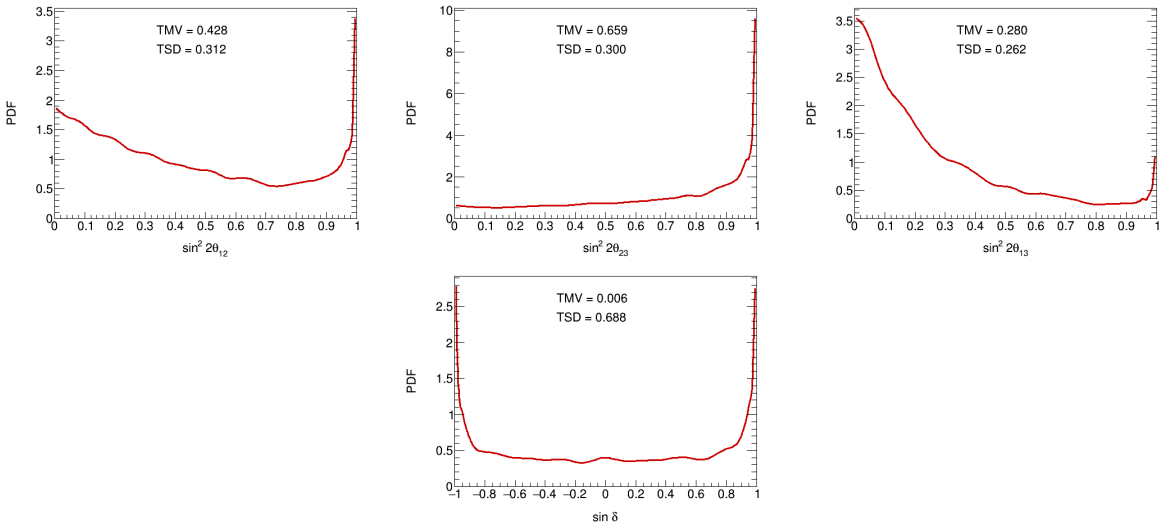

Figure 4.7: Probability density plots for the neutrino mixing parameters for the $SU(5)$-inspired flavor symmetry based models defined in Eqs. (4.2.46)-(4.2.48). The upper plots are for the mixing angles, $\sin^2 2\theta_{ij}$ and the lower plot is for CP-violating parameter $\sin\delta$.

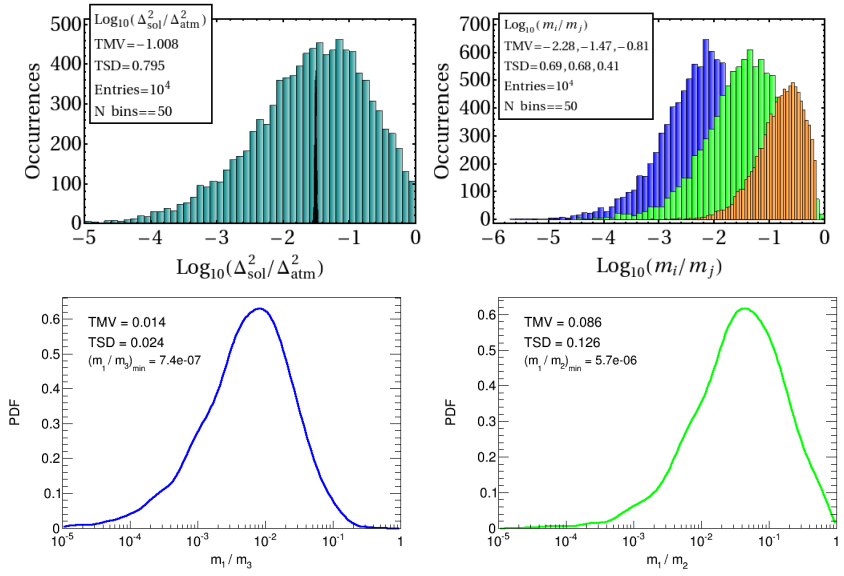

Figure 4.8: The theoretical distributions and the probability density plots of the observables in the neutrino sector for the $SU(5)$-inspired flavor symmetry based models defined in Eqs. (4.2.46)-(4.2.48). The notation is the same as in Fig. 4.4.

4.4 A Variant Monte Carlo Analysis of the $SU(5)$-based Models

The Monte Carlo analysis of Sec. 4.3 treats the random variables as unbiased set with Gaussian distribution and investigates the likelihood of these models to procreate the experimental values. The results presented in the previous section show that, on average, the agreement of the theoretical mean values with the experimental central values is very good, except for few observables for which the theoretical mean values do not coincide with the experimental central values but still the experimental central values lie within the range of values predicted by the theory. Since we have no control over the random variables, the theoretical standard deviations of each observables are quite large (as can be seen from columns 4 and 5 of Table 4.6) and of the same order as the theoretical mean values. In this section, we present a modified version of the Monte Carlo analysis, where the model parameters, ϵ_i are not fixed but rather treated as constrained random parameters. As before, we start with the set of uncorrelated random variables having Gaussian distribution and analyze the class of models with Yuwaka coupling matrices given by Eqs. (4.2.4)-(4.2.8). We consider a projection of these distributions onto a subspace of the original space of random parameters defined by the experimental constraints. These constraints create correlations between the random parameters, and therefore their distributions in the constrained subspace are in general different from the original (unconstrained) distributions. We optimize the model parameters by minimizing the difference between the complete set $\{\boldsymbol{r}\}$ of random parameters describing a given class of models, and the subset $\{\boldsymbol{r^*}\}$ of random parameters describing the models that satisfy the experimental constraints $O_{i\,\mathrm{th}} = E_{i\,\mathrm{exp}}$, which we call the distortion and denote by $D\left(\{\boldsymbol{r}^*\},\{\boldsymbol{r}\}\right)$. The condition of optimization is then

$$\boldsymbol{\epsilon}_{\mathrm{best}} = \underset{\boldsymbol{\epsilon}}{\mathrm{argmin}}\, D\left(\{\boldsymbol{r}^*\},\{\boldsymbol{r}\}\right). \tag{4.4.51}$$

To implement the optimization procedure, we modify the χ^2 minimization approach described in the previous sections by introducing an additional step which, starting from initial set of random parameters $\{\boldsymbol{r}_0\}$, tries to update the current set of random parameters $\{\boldsymbol{r}\}$ by minimizing $D = D(O,E) + D\left(\{\boldsymbol{r}\},\{\boldsymbol{r}_0\}\right)$, where

$$D(O,E) = \sum \left(\frac{O_{i\,\mathrm{th}} - E_{i\,\mathrm{exp}}}{\sigma_{i\,\mathrm{exp}}}\right)^2 \tag{4.4.52}$$

accounts for discrepancy between the model prediction and experiment, and the measure of distortion is chosen to be

$$D\left(\{\boldsymbol{r}\},\{\boldsymbol{r}_0\}\right) = \sum \frac{\left(C_{jk} - \mathbf{E}\left[C_{jk}\right]\right)^2}{\mathbf{E}\left[C_{jk}\right]}, \tag{4.4.53}$$

where C_{jk} is the number of occurrences of the binned value of the expected cumulative distribution function (cdf) of random variable r_j, and the sum is taken over all cdf bins k and all elements of all random matrices j in the model. The method we use is an iterative procedure that alternates the χ^2 minimization and $\{\boldsymbol{r}\}$ optimization steps. The best fit results of this procedure obtained for the $SU(5)$-based GUTs defined in Eqs.

Observables	TMV±TSD	$\frac{\text{TMV}}{\text{ECV}}$	pull
$y_u/10^{-6}$	2.57±0.09	1.00	0.00
$y_c/10^{-3}$	1.40±0.03	1.02	0.39
y_t	0.545±0.053	1.02	0.25
$y_d/10^{-4}$	0.39±0.04	0.99	-0.05
$y_s/10^{-3}$	0.75±0.03	1.02	0.28
$y_b/10^{-2}$	4.49±0.22	0.99	-0.02
$y_e/10^{-5}$	1.64±0.001	1.00	0.18
$y_\mu/10^{-3}$	3.46±0.002	1.00	0.11
$y_\tau/10^{-1}$	0.589±0.001	0.99	-0.09
$\|V_{us}\|$	0.225±0.0009	0.99	-0.29
$\|V_{cb}\|/10^{-2}$	3.75±0.017	1.00	0.04
$\|V_{ub}\|/10^{-3}$	3.24±0.03	0.99	-0.01
η_W	0.35±0.004	1.00	0.00

Table 4.13: Best fit values of the observables for the $SU(5)$-based GUTs defined in Eqs. (4.2.4)-(4.2.8) by employing the modified Monte Carlo analysis. Here we have considered the case with $\tan\beta = 10$ as input. As explained in the text, this results correspond to minimization of the function $D = D(O,E) + D\left(\{\boldsymbol{r}^*\},\{\boldsymbol{r}\}\right)$. This fit corresponds to $D(O,E)/n_{obs} = 0.03$. Here TMV=theoretical mean value, TSD=theoretical standard deviation, ECV=experimental central value and pull is defined in Eq. (4.3.50).

(4.2.4)-(4.2.8) is presented in Table 4.13. Here we have considered the case with $\tan\beta = 10$ as input. The models parameters that are extracted from this procedure are given in Eq. (4.4.54).

$$\begin{aligned} \varepsilon_1 &= 0.00106 \pm 0.00001, \\ \varepsilon_2 &= 0.08023 \pm 0.00044, \\ \varepsilon_4 &= 0.03294 \pm 0.00024. \end{aligned} \tag{4.4.54}$$

Observables	TMV±TSD	$\frac{\text{TMV}}{\text{ECV}}$	pull
$\frac{\Delta m^2_{sol}}{\Delta m^2_{atm}}$	0.031 ± 0.0002	1.0	0.01
$\sin^2\theta_{12}$	0.31 ± 0.02	0.99	0.17
$\sin^2\theta_{23}$	0.39 ± 0.03	0.99	0.23
$\sin^2\theta_{13}$	0.024 ± 0.001	1.0	0.12

Table 4.14: Best fit values of observables using the modified approach of Monte Carlo analysis in the neutrino sector for $SU(5)$-based GUTs defined in Eqs. (4.2.4)-(4.2.8). The best fit values shown in this table correspond to $\chi^2/n_{obs} = 0.1$. Here TMV=theoretical mean value, TSD=theoretical standard deviation, ECV=experimental central value and pull is defined in Eq. (4.3.50).

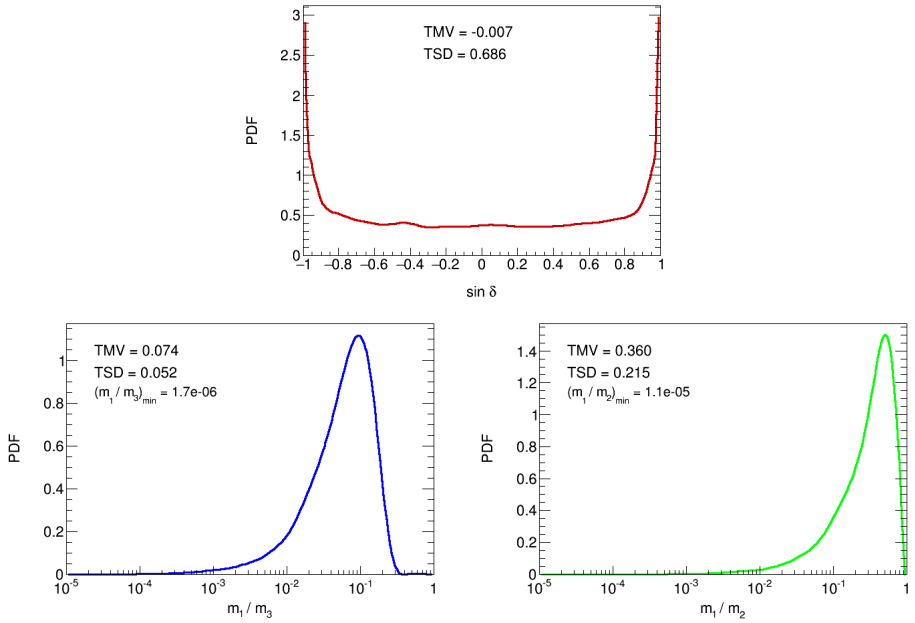

Figure 4.9: Probability density plots of the experimentally unmeasured quantities in the neutrino sector, the sine of the Dirac type phase (upper) and neutrino mass ratios m_1/m_3 (lower left) and m_1/m_2 (lower right) by employing the modified Monte Carlo analysis for $SU(5)$-based GUTs defined in Eqs. (4.2.4)-(4.2.8).

The best fit values presented in Table 4.13 corresponds to $D(O, E) = 0.43$. In this modified approach, all the theoretically predicted values of the observables almost coincide with the experimental measured values. Compared to the approach explained in the previous sections, theoretical errors are greatly reduced and comparable to the experimental uncertainties. Histogram distributions of the observables in the charged fermion sector corresponding to this result are presented in Fig. 4.10 and the distributions of the restricted set $\{\boldsymbol{r}^*\}$ are shown in Figs. 4.11, 4.12 and 4.13 for the matrices Y^0_U, Y^0_D and Y^0_L respectively. We also employ this approach in

the neutrino sector Eq. (4.2.10) separately, where the model parameters ϵ_i are absent. The results are presents in Table 4.14 that correspond to $D(O, E) = 0.1$. The histogram distributions of the theoretical predictions of these quantities in the neutrino sector are shown in Fig. 4.14 and the modified set $\{\boldsymbol{r}^*\}$ in Figs. 4.15 and 4.16. The $\sin\delta$ and the two neutrino mass ratios m_1/m_3 and m_1/m_2 are shown in Fig. 4.9. This variant of the Monte Carlo analysis shows that with the subspace $\{\boldsymbol{r}^*\}$ which does not have much deviation from the original landscape $\boldsymbol{r}$, excellent agreement of the observables to the experimental measured values can be achieved. One can in principle apply this modified approach to the special cases of the $SU(5)$-based GUTs explained in Sec. 4.2.2 but we do not include those analysis here.

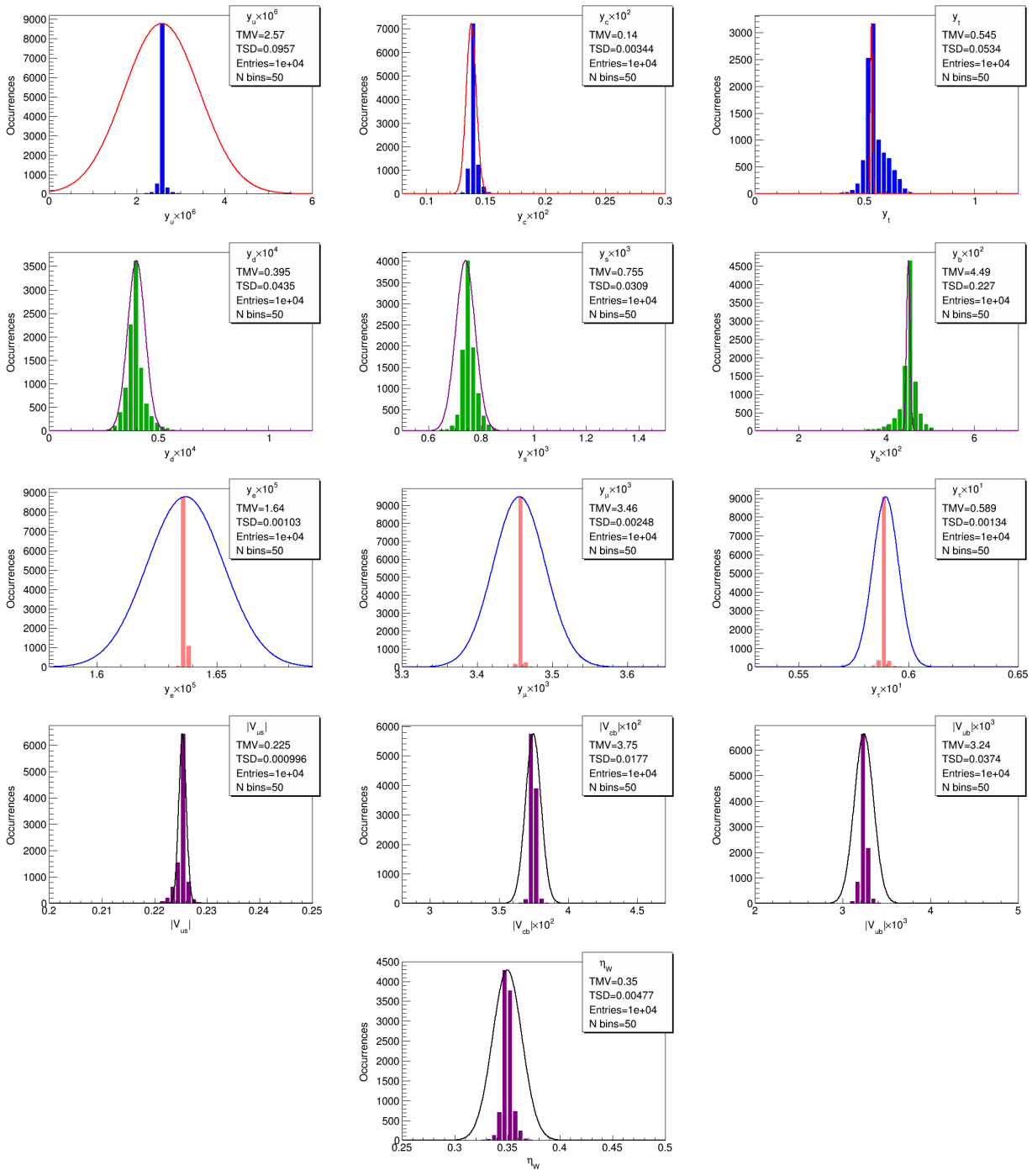

Figure 4.10: Histogram distributions of the observables in the charged fermion sector according to the modified Monte Carlo method for $SU(5)$-based GUTs defined in Eqs. (4.2.4)-(4.2.8) with $\tan\beta = 10$. Color code is the same as Fig. 5.2. Note the change of scales compared to Fig. 5.2 for few of the plots ($y_u \times 10^5 \to y_u \times 10^6$, $y_s \times 10^2 \to y_s \times 10^3$, $y_e \times 10^4 \to y_e \times 10^5$, $y_\mu \times 10^2 \to y_\mu \times 10^3$, $|V_{cb}| \to |V_{cb}| \times 10^2$, $|V_{ub}| \to |V_{ub}| \times 10^3$).

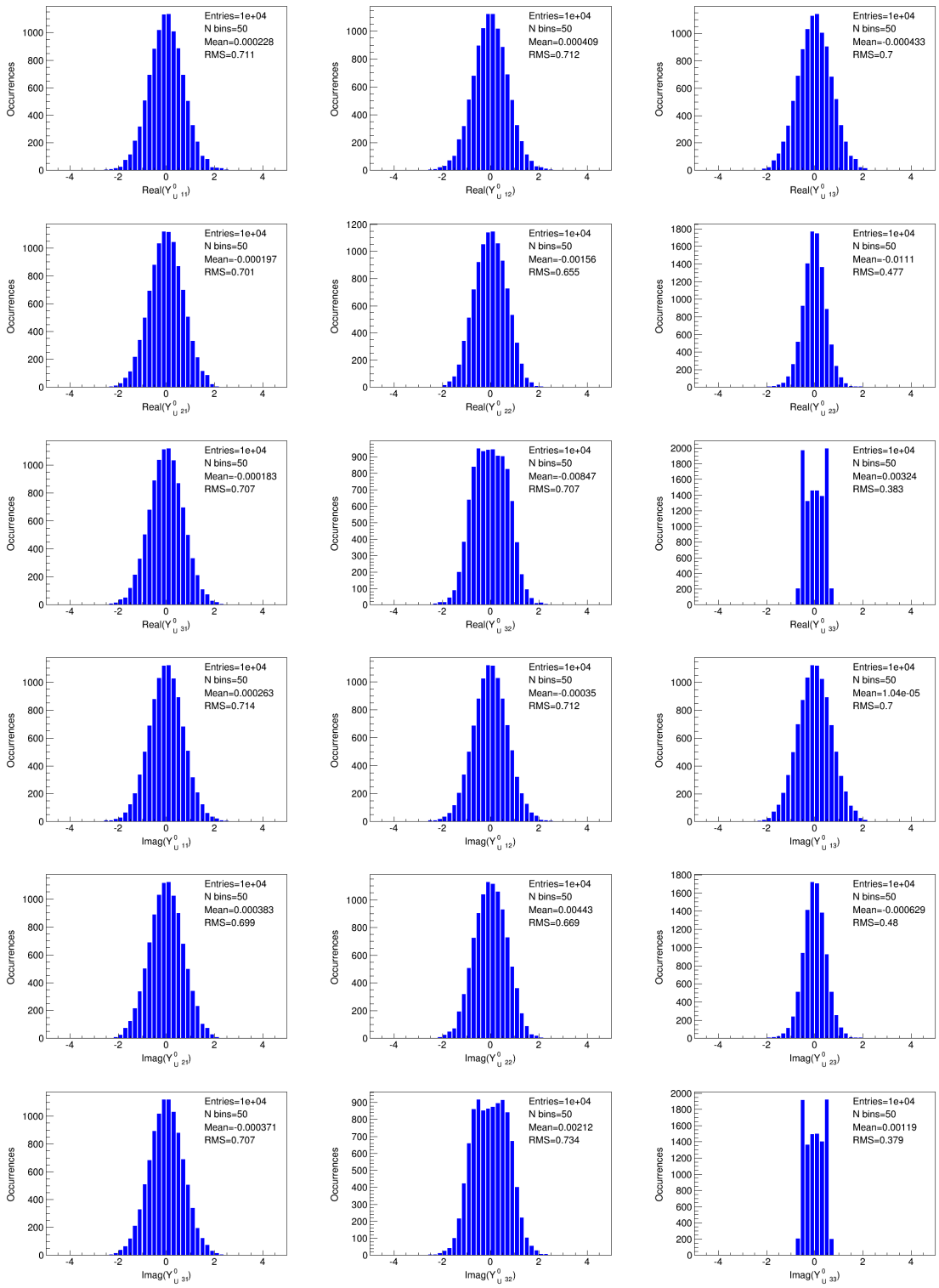

Figure 4.11: Distributions of the $O(1)$ random entries in the matrix Y_U^0 from the modified Monte Carlo analysis that produce the observables in Fig.4.10 for $\tan\beta = 10$. The first nine of the plots are for the real parts and the next nine for imaginary parts of the matrix, Y_U^0. For all these plots sample size and number of bins are taken to be 10^4 and 50 respectively.

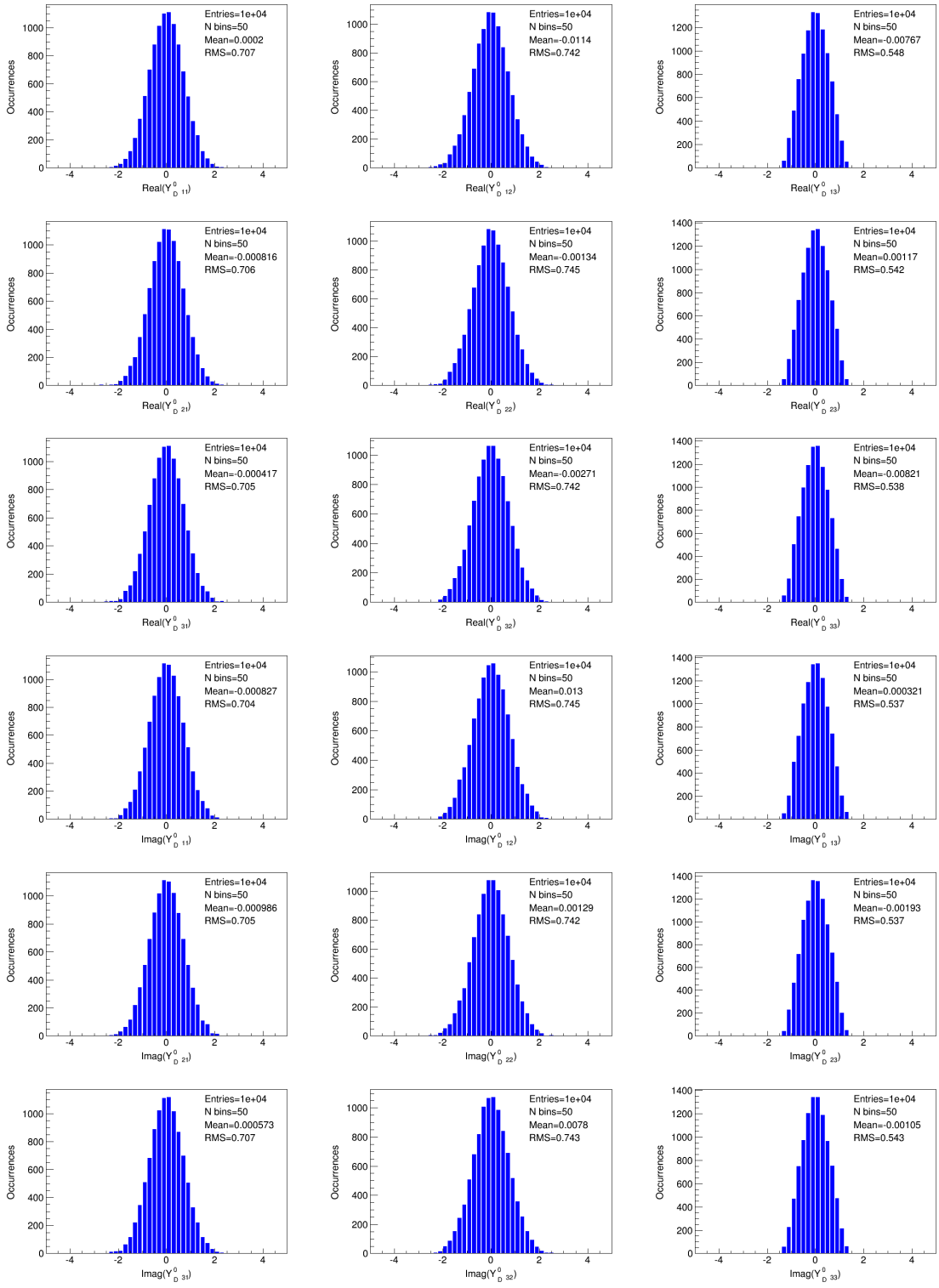

Figure 4.12: Distributions of the $O(1)$ random entries in the matrix Y_D^0 from the modified Monte Carlo analysis that produce the observables in Fig.4.10 for $\tan\beta = 10$. The first nine of the plots are for the real parts and the next nine for imaginary parts of the matrix, Y_D^0. For all these plots sample size and number of bins are taken to be 10^4 and 50 respectively.

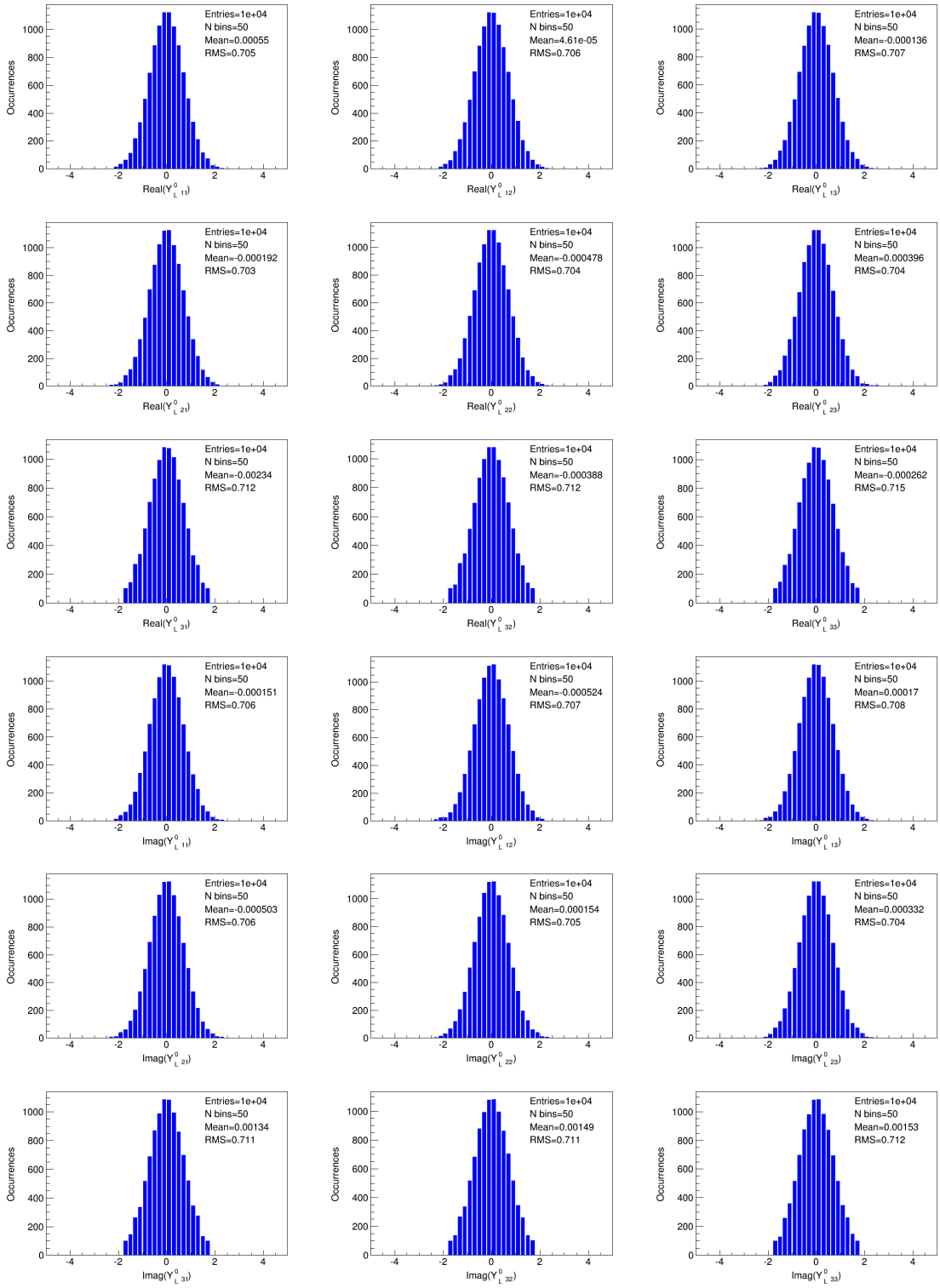

Figure 4.13: Distributions of the $O(1)$ random entries in the matrix Y_L^0 from the modified Monte Carlo analysis that produce the observables in Fig.4.10 for $\tan\beta = 10$. The first nine of the plots are for the real parts and the next nine for imaginary parts of the matrix, Y_L^0. For all these plots sample size and number of bins are taken to be 10^4 and 50 respectively.

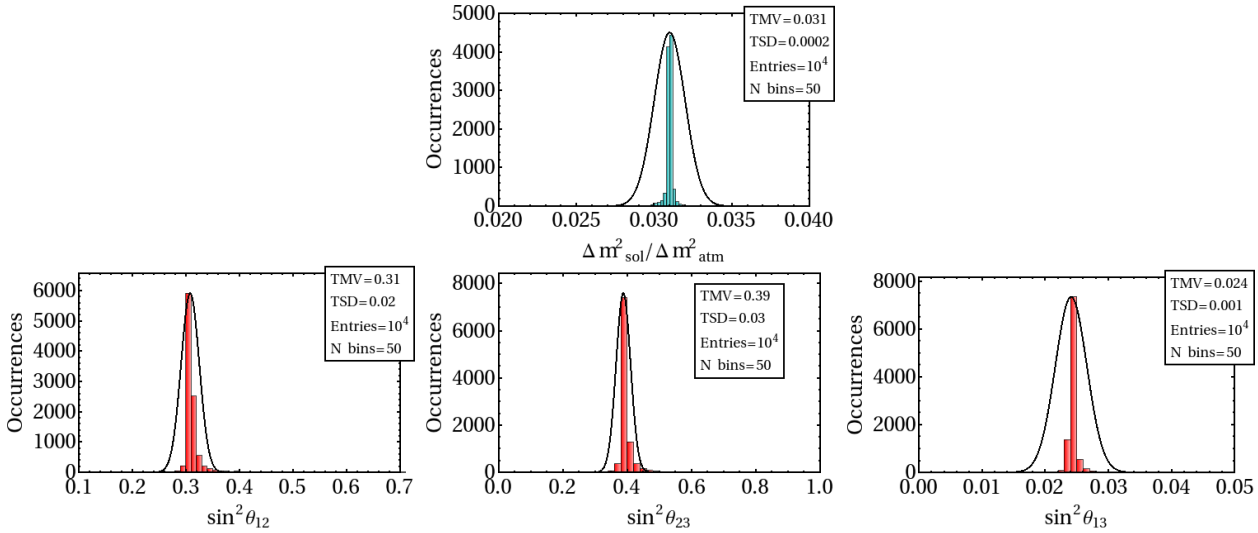

Figure 4.14: Histogram distributions of the observables in the neutrino sector according to the modified Monte Carlo approach for $SU(5)$-based GUTs with structure-less neutrino mass matrix. The top histogram plot (dark cyan) shows the theoretical distribution of the quantity $\Delta m^2_{\rm sol}/\Delta m^2_{\rm atm}$ and the bottom three plots (red) are for the mixing parameters $\sin^2\theta_{ij}$. The black curves represent the experimental 1σ ranges. The sample size is taken to be 10^4 and number of bins is taken to be 50.

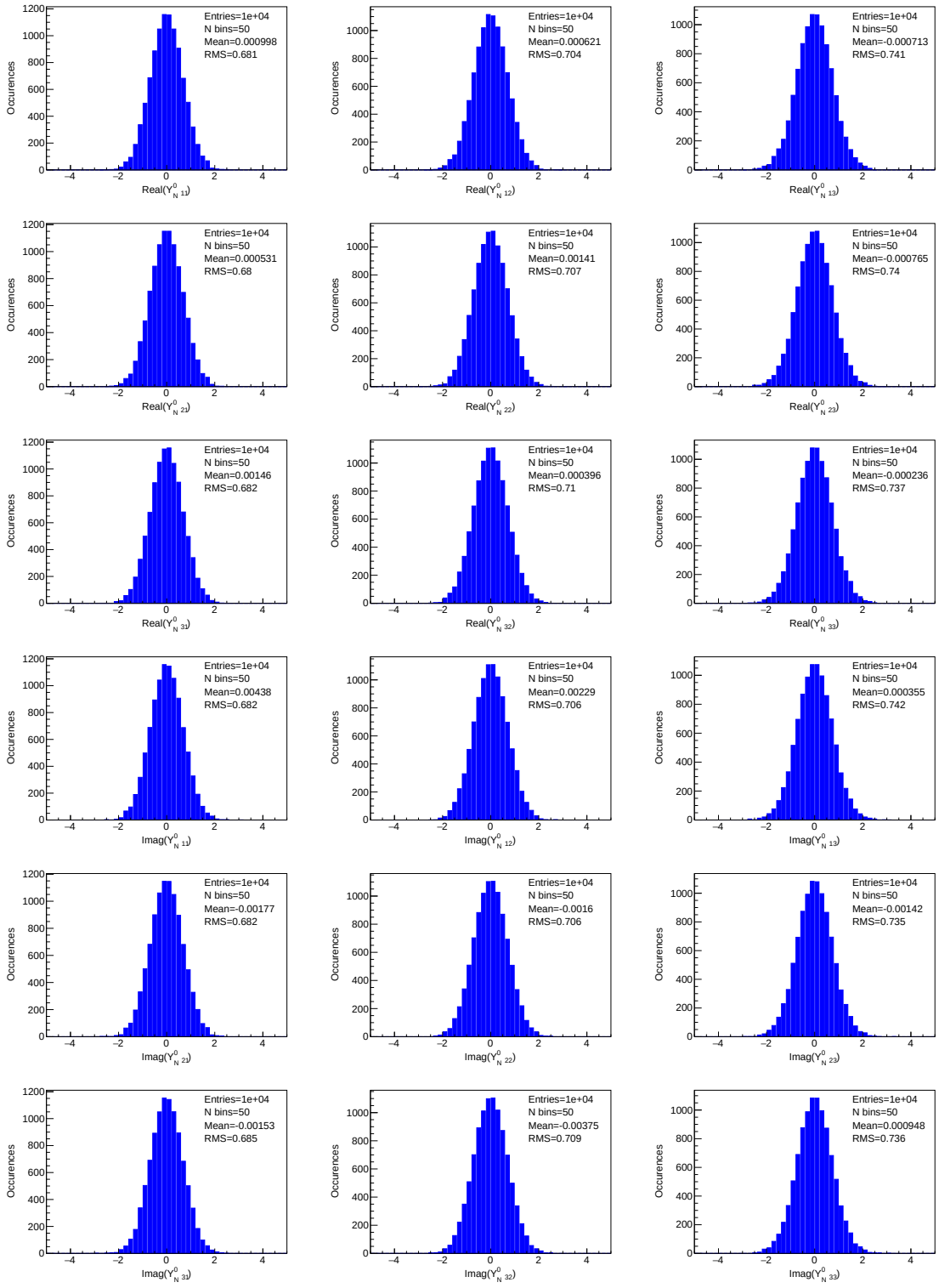

Figure 4.15: Distributions of the $O(1)$ random entries in the matrix Y_N^0 from the modified Monte Carlo approach that produce the observables in Fig.4.14.

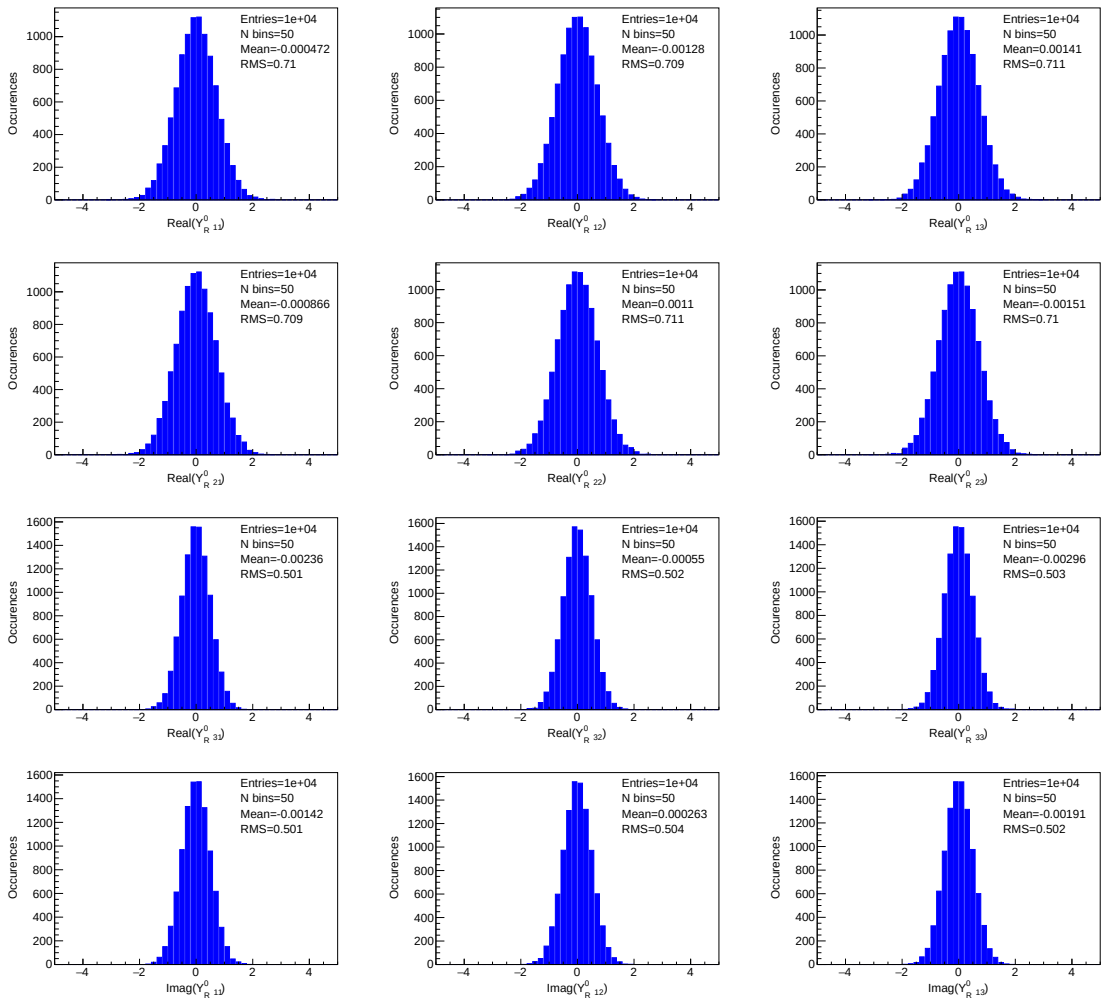

Figure 4.16: Distributions of the $O(1)$ random entries in the matrix Y_R^0 from the modified Monte Carlo approach that produce the observables in Fig.4.14.

4.5 Conclusion

In this paper we have extended the idea of anarchy from the neutrino sector to the quark and charged lepton sectors. This is made possible in the context of $SU(5)$ unified theories where the 10_i fermions mix with vector-like $10_\alpha + \overline{10}_\alpha$ fermions having GUT scale masses. While all the Yukawa couplings in these models are of order one, these mixings provide three hierarchical parameters which explain all the hierarchies in the charged fermion masses and quark mixing angles. The neutrino sector is immune to such mixings, and remain anarchical. We have also studied special cases of this general $SU(5)$ setup with smaller number of input parameters – either 2 or 1 – by introducing a flavor $U(1)$ symmetry that distinguishes the three families of 10_i fermions.

We have presented detailed quantitative analysis of these models following a probabilistic approach. The

Quantity		Structureless Neutrino Matrix	Hierarchical Neutrino Matrix
m_1/m_2	$\leq$0.01	4.24%	20.38%
	$\leq$0.1	33.77%	74.57%
	$\leq$0.2	56.23%	88.33%
$\sin\delta$	[0,0.25]	8.15%	8.9%
	(0.25,0.5]	8.79%	9.82%
	(0.5,0.75]	9.68%	10.16%
	(0.75,1.0]	23.87%	21.18%

Table 4.15: Comparison of probabilities of the two unmeasured quantities in the neutrino sector for the $SU(5)$-based GUTs with different neutrino mass matrix structures. For the quantity $\sin\delta$, these probabilities in the negative side remain roughly the same in the separate domains as for the positive side. Square bracket represents the end points are included in the set whereas for the round bracket the end points are not included.

Yukawa couplings of the model are assumed to be uncorrelated random variables obeying Gaussian distributions. Our Monte Carlo analysis shows that the combined anarchy-hierarchy scenario gives very good fit to all the fermion masses and mixings. We have also presented a variant Monte Carlo method where the model parameters are not kept fixed but have certain distributions constrained by the phenomenological considerations. This approach is proposed to systematically explore the subspace of the original Gaussian landscape that becomes consistent with all experimental constraints with greater accuracy. A figure of merit in this approach is the distortion of the distributions compared to the original Gaussian distributions. The framework is found to provide a good quality fit.

The theoretical distributions of the observables in the charged fermion sector remain roughly the same for the various models studied here. There is one important difference in the neutrino mixing parameters in the flavor $U(1)$ model that distinguishes the $\overline{5}_1$ from $\overline{5}_{2,3}$ fields: The mixing parameter $\sin\theta_{13}$ comes out to be somewhat smaller than $\sin\theta_{23}$. Anarchy prefers normal ordering of neutrino mass spectrum with a mild hierarchy in the masses. A comparison of the two experimentally unmeasured quantities in the neutrino sector, the mass ratio m_1/m_2 and the CP-violating parameter $\sin\delta$ predicted by our statistical analysis for the two different sets of models studied here is presented in Table 4.15.

CHAPTER 5

FERMION MASSES, LEPTOGENESIS AND BARYON NUMBER VIOLATION IN PATI-SALAM MODEL

5.1 Introduction

Despite being a very successful theory, the Standard Model (SM) has many shortcomings. The SM does not provide any insights for understanding the hierarchical pattern of the masses and mixings of the charged fermions. Also the origin of the neutrino oscillations is unexplained in the SM. In addition, it is also not obvious the observed quantization of electric charge in the SM. To explain these shortcoming of the SM, extensive search for finding new physics beyond the SM has been carried out. One of the most attractive extensions of the SM proposed in Refs. [79, 161, 162] are based on partial unification with gauge group $G_{224} = SU(2)_L \times SU(2)_R \times SU(4)_C$. This Pati-Salam (PS) group is the minimal quark-lepton symmetry model based on the $SU(4)_C$ group with the lepton number as the fourth color [79]. The minimal gauge group respecting symmetry between the left and right representations and that contains $SU(4)$-color and ensures electric charge quantization is the PS group. Due to quark-lepton unification, one can hope to understand the flavor puzzle in the PS model. The fermion multiplets of this theory contain the right-handed neutrino, this is why seesaw mechanism [38] is a natural candidate in PS model to explain the tiny neutrino masses. Furthermore, our Universe does not show symmetry between matter and antimatter. The origin of this matter-antimatter asymmetry may have link with the origin of neutrino mass. In seesaw scenario, the Majorana mass term violates the lepton number conservation, so employing the seesaw mechanism in this PS framework, the observed baryon asymmetry of the Universe can be incorporated by the Baryogenesis via Leptogenesis mechanism. In such a framework, the lepton asymmetry that is generated dynamically, later converted into the baryon asymmetry by the $(B + L)$-violating sphaleron interactions that exist in the SM. In the SM conservation of baryon number and lepton number are accidental, however, violation of these quantum numbers are natural in the PS model and baryon number violation induces interesting processes like nucleon decay and neutron-antineutron oscillation.

In this paper, we construct a minimal realistic model based on PS gauge group in the non-supersymetric framework. In addition to unifying quarks and leptons, seesaw mechanism arises in G_{224} framework naturally due to the automatic presence of the right-handed neutrinos. Assuming an economical Higgs sector, we construct

the complete Higgs potential and analyse it. This minimal set is required not only to realize successful symmetry breaking of the PS group down to the SM and further down to $SU_C(3) \times U_{\rm em}(1)$, but also to reproduce realistic fermion masses and mixings. We discuss the possibility of baryon violating processes such as nucleon decay and $n - \overline{n}$ oscillation in this set-up. Nucleon decay processes in this framework are, nucleon $\rightarrow$ lepton + meson, nucleon $\rightarrow$ antilepton + meson and nucleon $\rightarrow$ lepton + antilepton + antilepton. Relative branching fractions of different modes of nucleon decay processes arising in this theory are computed in certain approximations.

We also analyze the predictions of this model for quark and lepton masses and mixings. Our numerical study shows full consistency with the experimental data. To solve the matter-antimatter asymmetry of the Universe, we implement the novel idea of Baryogenesis via Leptogenesis. Utilizing the type-I seesaw scenario, the Baryogenesis via Leptogenesis mechanism can link between the matter-antimatter asymmetry and the CP violation in the neutrino sector. In search of successful baryon asymmetry, we scan over the relevant parameter space. In this work, on top of the PS gauge symmetry, we impose a global $U(1)_{PQ}$ Peccei-Quinn (PQ) symmetry, that solves the strong CP problem. If the PQ symmetry is broken at the high scale $\sim 10^{11-12}$ GeV, then the pseudo-scalar Goldstone boson associate with this breaking can explain the observed dark matter relic density of the universe. The presence of this global $U(1)$ symmetry puts some additional restrictions on the Higgs potential and hence reduce the number of parameters in the theory. With the economic choice of Higgs multiplets, we do a general study in $SU(2)_L \times SU(2)_R \times SU(4)_C \times U(1)_{PQ}$ set-up; a special case with the imposed parity symmetry is also considered and additional restrictions due to the consequence of the discrete symmetry are mentioned explicitly through out the text. We also explore another interesting possibility, where with the absence of the parity symmetry and low scale PS breaking, $g_L = g_R$ unification can be realized at the PQ breaking scale.

5.2 The model

5.2.1 The gauge group and spontaneous symmetry breaking chain

Breaking chain and particle content

We work on a left-right symmetric partial unification theory based on the PS gauge group, $SU(2)_L \times SU(2)_R \times SU(4)_C$. $SU(4)_C$ is an extension of the QCD gauge group, $SU(3)_C$ with lepton as the fourth color and $SU(2)_R$ is right-handed gauge group similar to the SM $SU(2)_L$ weak interactions. Starting from this group, to reach the SM group, several different breaking chains are possible, but in this paper we assume the one step spontaneous symmetry breaking (SSB) of the PS group to that of the SM group,

$$G_{224} \xrightarrow{M_X} SU(2)_L \times U(1)_Y \times SU(3)_C \tag{5.2.1}$$

$$\xrightarrow{M_{EW}} U(1)_{em} \times SU(3)_C. \tag{5.2.2}$$

In our model, we assume the existence of the following Higgs multiplets (under the PS group):

$$\mathbf{\Phi} = (2,2,1), \quad \mathbf{\Sigma} = (2,2,15), \quad \mathbf{\Delta}_R = (1,3,10). \tag{5.2.3}$$

Instead of G_{224}, if parity symmetry is also preserved (in this case we denote the group as G_{224P}), the existence of the Higgs field $\mathbf{\Delta}_L = (3,1,10)$ is needed due to the presence of the initial left-right parity symmetry. This choice of the Higgs multiplets is minimal. This one step breaking of PS group to the SM can be achieved by the VEV, $v_R = \langle \mathbf{\Delta}_R \rangle$ [163]. If the group is G_{224P} then breaking of the parity scale may not coincide with the breaking of the PS symmetry. Breaking the G_{224P} group by the VEV of $(1,3,10)$ automatically breaks the parity symmetry. The multiplet $\mathbf{\Delta}_R$, breaking $SU(4)_C$, $B-L$ and left-right symmetry spontaneously also provides masses to the heavy right-handed neutrinos. In an alternative approach the parity symmetry can be broken before breaking the PS group by a parity odd singlet Higgs and then the PS symmetry can be broken by the usual $(1,3,10)$ VEV. The SM group can be broken by the scalar field $\mathbf{\Phi}$ that contains the SM doublet. The VEV of $\mathbf{\Phi}$ field,

$$\langle \mathbf{\Phi} \rangle = \begin{bmatrix} k_1 & 0 \\ 0 & k_1' \end{bmatrix} \otimes diag(1,1,1,1) \tag{5.2.4}$$

is responsible for generating Dirac mass terms for the SM fermions. But if only $\mathbf{\Phi}$ is responsible for generating fermion masses, one gets the unacceptable relations, $m_e = m_d$, $m_\mu = m_s$ and $m_\tau = m_b$. These lead to $m_e/m_\mu = m_d/m_s$, which are certainly not in agreement with experimental measured values. These bad relations are the consequence of the multiplet $\mathbf{\Phi}$ being color singlet (in the $SU(4)_C$ space the fourth entry is also 1) and cannot differentiate fermions with different colors. To cure these bad relations, the existence of the Higgs multiplet $\mathbf{\Sigma}$ is assumed which is not color singlet, and by acquiring VEV of the form

$$\langle \mathbf{\Sigma} \rangle = \begin{bmatrix} k_2 & 0 \\ 0 & k_2' \end{bmatrix} \otimes diag(1,1,1,-3) \tag{5.2.5}$$

can correct the bad mass relations [79,162,163], $m_e = m_e^\Phi - 3m_e^\Sigma$, $m_d = m_d^\Phi + m_d^\Sigma$ and so on. Even though the field $\mathbf{\Phi}$ treats quarks and lepton on the same footing, $\mathbf{\Sigma}$ field being color non-singlet, distinguishes them and brings additional (-3) Clebsch factor for the leptons.

Renormalization group equations and the v_R scale

According to phenomenological consideration, the required hierarchical pattern of the VEVs is:

$$\langle \mathbf{\Delta}_R \rangle >> \langle \mathbf{\Phi} \rangle \sim \langle \mathbf{\Sigma} \rangle >> \langle \mathbf{\Delta}_L \rangle. \tag{5.2.6}$$

As previously mentioned, in the model without the parity symmetry $\mathbf{\Delta}_L$ field need not to be present. Even when this field is present, we assume that this field does not get any explicit VEV. However, this field does get small VEV due to the presence of specific types of quartic terms in the Higgs potential that are linear in $\mathbf{\Delta}_L$. After the EW symmetry breaking such acquired VEV is of the form, $\langle \mathbf{\Delta}_L \rangle \sim \lambda\, v_{ew}^2/v_R$ (where λ is the relevant quartic coupling). If parity is assumed to be a good symmetry, v_R can be fixed by the renormalization group equations (RGEs) running of the gauge coupling constants by using low energy data. This additional discrete symmetry on top of the PS symmetry demands $g_L = g_R$. The one-loop RGEs for the gauge couplings are given by [**?**]

$$\frac{d\alpha_i^{-1}(\mu)}{dln\mu} = \frac{a_i}{2\pi}. \tag{5.2.7}$$

For the SM group, G_{321} $b_i = (-7, -19/6, 41/10)$ [116]. Applying proper matching condition for the coupling constants

$$\alpha_{1Y}^{-1}(M_X) = \frac{3}{5}\alpha_{2R}^{-1}(M_X) + \frac{2}{5}\alpha_4^{-1}(M_X),\;\; \alpha_{2R}^{-1}(M_X) = \alpha_{2L}^{-1}(M_X),\;\; \alpha_{4C}^{-1}(M_X) = \alpha_{3C}^{-1}(M_X), \tag{5.2.8}$$

and using the low energy data, $\alpha_s(M_Z) = 0.1184$, $\alpha^{-1}(M_Z) = 127.944$ and $s^2_{\theta_W} = 0.23116$ taken from Ref. [72] (only the central values are quoted here), we find $M_X = 10^{13.71}$ GeV. From now on, for models with parity symmetry broken by the $\mathbf{\Delta}_R$ VEV, we set $v_R = 10^{14}$ GeV for the rest of the analysis. Specially when we will discuss the Baryogenesis via Leptogenesis, we stick to this value of v_R. On the other hand, If parity is absent, then the scale v_R is not fixed by the RGEs running. The differences in results for the cases with G_{224} and G_{224P} are mentioned explicitly through out the text when needed.

Left-right gauge coupling unification at the Peccei-Quinn scale

Breaking the parity symmetry that demands $g_L = g_R$ along with the breaking of the PS symmetry by the $(1, 3, 10)$ multiplet restricts the PS breaking scale to be high $\sim 10^{14}$ GeV. If parity symmetry is absent, this scale is not determined by the RGEs running from the low energy experimental data and the PS breaking can happen at much lower scale. The experimental limits on the branching ratio for $K_L^0 \to \mu^{\pm} e^{\mp}$ processes, mediated by the new gauge bosons X_a (a is the Lorentz index) with $(B - L)$ charge of $(4/3)$, implies that the v_R scale that breaks the $SU(4)_C$ must be greater than 1000 TeV [164, 165]. Here we explore the possibility of low scale PS scale breaking where $g_L = g_R$ unification can still be realized at the PQ scale $\sim 10^{11-13}$ GeV. For example, by including an extra $(1, 3, 10)$ multiplet and a real $(1, 3, 15)$ multiplet on top of the minimal Higgs content that are a complex $(2, 2, 1)$, a complex $(2, 2, 15)$ and a $(1, 3, 10)$ multiplet, left-right unification can happen at the

PQ scale as presented in Fig. 5.1. For this set of scalars, the RGE coefficients are $b_i = (2, 61/3, 8/3)$ for the group G_{224}.

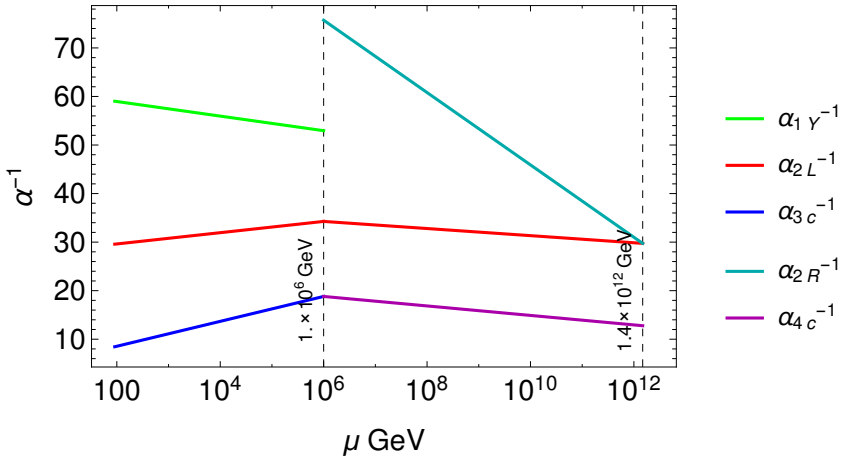

Figure 5.1: One-loop gauge coupling running of PS model without parity symmetry. By including an extra $(1, 3, 10)$ multiplet and a real $(1, 3, 15)$ multiplet on the top of the minimal Higgs content that are a complex $(2, 2, 1)$, a complex $(2, 2, 15)$ and a $(1, 3, 10)$ multiplet, $g_L = g_R$ unification at the PQ scale $\sim 10^{11-13}$ GeV can be realized.

Notation

Our notation for indices is as follows: the indices for $SU(2)_L$ group are $\alpha, \beta, \gamma, \delta, \kappa = 1, 2$, for $SU(2)_R$ group $\dot{\alpha}, \dot{\beta}, \dot{\gamma}, \dot{\delta}, \dot{\kappa} = \dot{1}, \dot{2}$ and for $SU(4)_C$ group $\mu, \nu, \rho, \tau, \lambda, \chi = 1, 2, 3, 4$. For $SU_C(3)_C \subset SU(4)_C$ we use the same symbols as for $SU(4)_C$ as indices but with a bar on them, for example, $\bar{\mu}, \bar{\nu} = 1, 2, 3$. While writing the gauge bosons and the covariant derivatives, we use index a as the Lorentz index.

In the PS model, the fermions belong to the representations $\mathbf{\Psi}_{L\,\mu\alpha} = (2, 1, 4)_k$ and $\mathbf{\Psi}_{R\,\mu\dot{\alpha}} = (1, 2, 4)_k$ with

$$\mathbf{\Psi}_{L,R} = \begin{pmatrix} u_r & u_g & u_b & \nu \\ d_r & d_g & d_b & e \end{pmatrix}_{L,R} \tag{5.2.9}$$

and $k\ (= 1, 2, 3)$ is the generation index. In group index notation the scalar fields can be written as:

$$\begin{aligned} (2, 2, 1) &= \mathbf{\Phi}^{\dot{\alpha}}_{\alpha}, \qquad (2, 2, 15) = \mathbf{\Sigma}^{\nu\ \dot{\alpha}}_{\mu\ \alpha}, \\ (1, 3, 10) &= \mathbf{\Delta}_{R\ \mu\nu\ \dot{\alpha}}^{\ \ \ \dot{\beta}}, \quad (3, 1, 10) = \mathbf{\Delta}_{L\ \mu\nu\ \alpha}^{\ \ \ \beta}. \end{aligned} \tag{5.2.10}$$

The SM decomposition of these fields are as follows:

$$(2,2,1) = (1,2,\frac{1}{2}) + (1,2,-\frac{1}{2}), \tag{5.2.11}$$

$$\begin{aligned}(2,2,15) = {} & (1,2,\frac{1}{2}) + (1,2,-\frac{1}{2}) + (3,2,\frac{1}{6}) + (\overline{3},2,-\frac{1}{6}) + (3,2,\frac{7}{6}) + (\overline{3},2,-\frac{7}{6}) \\ & + (8,2,\frac{1}{2}) + (8,2,-\frac{1}{2}),\end{aligned} \tag{5.2.12}$$

$$\begin{aligned}(1,3,10) = {} & (1,1,0) + (1,1,-1) + (1,1,-2) + (3,1,\frac{2}{3}) + (3,1,-\frac{1}{3}) + (3,1,-\frac{4}{3}) \\ & + (6,1,\frac{4}{3}) + (6,1,\frac{1}{3}) + (6,1,-\frac{2}{3}),\end{aligned} \tag{5.2.13}$$

$$(3,1,10) = (1,3,-1) + (3,3,-\frac{1}{3}) + (6,3,\frac{1}{3}). \tag{5.2.14}$$

5.2.2 Gauge boson mass spectrum

In the PS model, there are in total 21 gauge bosons, $W_{L\,a} \equiv$(3,1,1) of $SU(2)_L$, $W_{R\,a} \equiv$(1,3,1) of $SU(2)_R$ and $V_a \equiv$(1,1,15) of $SU(4)_C$. The decomposition of these fields under the SM are:

$$(3,1,1) = (1,3,0), \tag{5.2.15}$$

$$(1,3,1) = (1,1,1) + (1,1,0) + (1,1,-1), \tag{5.2.16}$$

$$(1,1,15) = (1,1,0) + (3,1,\frac{2}{3}) + (\overline{3},1,-\frac{2}{3}) + (8,1,0). \tag{5.2.17}$$

The gauge bosons W_R are the right-handed analogue of the three SM $SU(2)_L$ gauge bosons, W_L. The decomposition of $15 \subset SU(4)_C$ under the group $SU(3)_C \times U(1)_{B-L} \subset SU(4)_C$ is $15 = 1(0)+3(+4/3)+\overline{3}(-4/3)+8(0)$, where $8(0)$ are the massless gluons of $SU(3)_C$. The triplets, $X_a \equiv 3(+4/3)$ and $X_a^* \equiv \overline{3}(-4/3)$ with non-zero $B-L$ quantum numbers are the exotic particles (leptoquark gauge bosons). Contrary to the Grand Unified Theories (GUT) based on simple groups, the leptoquark gauge bosons of the PS model do not mediate proton decay as explained below. The transition between quarks and leptons are given by the following interactions that is part of the total Lagrangian

$$\mathcal{L}_X \supset \frac{g_4}{\sqrt{2}}\{X_a(\overline{u}\gamma^a\nu + \overline{d}\gamma^a e) + X_a^*(\overline{u}^c\gamma^a\nu^c + \overline{d}^c\gamma^a e^c)\}. \tag{5.2.18}$$

Since $U(1)_{B-L}$ is already a part of the gauge symmetry, $B-L$ is a conserved quantity. In addition to this, the above gauge interactions of the leptoquarks Eq. (5.2.18) has the accidental global $B+L$ symmetry, these two conserved quantities ensure the conservation of both B and L separately, this is why the gauge bosons of PS group do not mediate proton decay. On the other hand, minimal $SU(5)$ GUT model is ruled out due to too rapid proton decay mediated by the gauge leptoquarks. Since one can assign specific baryon and lepton numbers to these gauge bosons, in contrast to $SO(10)$ model, proton decay does not take place via these gauge bosons. Unification scale in $SO(10)$ model needs to be really high $> 10^{15}$ GeV to save the theory from too rapid proton decay.

The breaking $G_{224} \to G_{213}$, that does not break the $SU(2)_L$ group, the $W_{L\,a}$ gauge bosons remain massless. Due to this breaking, among the 18 (15 of $SU(4)_C$ and 3 of $SU(2)_R$) massless gauge bosons, 9 of them become massive after eating up the 9 Goldstone bosons (will be identified at the later part of the text), from the field $\mathbf{\Delta}_R$ and the other 9 of them (8 of $SU(3)_C$ and 1 of $U(1)_Y$) remain massless. Here we compute the mass spectrum of the gauge bosons. Following Ref. [166] the covariant derivative can be written as

$$\begin{aligned} D_a \mathbf{\Delta}_R = \partial_a \mathbf{\Delta}_{R\mu\nu\ \dot{\alpha}}^{\ \ \ \dot{\beta}} - ig_R W_{aR\dot{\alpha}}^{\ \ \ \dot{\gamma}} \mathbf{\Delta}_{R\mu\nu\ \dot{\gamma}}^{\ \ \ \dot{\beta}} + ig_R W_{aR\dot{\gamma}}^{\ \ \ \dot{\beta}} \mathbf{\Delta}_{R\mu\nu\ \dot{\alpha}}^{\ \ \ \dot{\gamma}} \\ - ig_C X^{\rho}_{a\ \mu} \mathbf{\Delta}_{R\rho\nu\ \dot{\alpha}}^{\ \ \ \dot{\beta}} - ig_C X^{\rho}_{a\ \nu} \mathbf{\Delta}_{R\rho\mu\ \dot{\alpha}}^{\ \ \ \dot{\beta}}, \end{aligned} \tag{5.2.19}$$

where a represents the Lorentz index. When the PS symmetry gets broken by the VEV of the $\mathbf{\Delta}_R$ field, using this covariant derivative, the gauge boson mass spectrum can be computed

$$M_{W_R^{\pm}} = \sqrt{2} g_R v_R, \tag{5.2.20}$$

$$M_{V^{(i)}} = \sqrt{2} g_C v_R. \tag{5.2.21}$$

Here $i = 9-14$ and their electric charge are $\pm 2/3$. The third component, $W_R^{(3)}$ of the (1,3,1) gauge boson mixes with the $V^{(15)}$ component from (1,1,15), then in the basis $\{W_R^{(3)}, V^{(15)}\}$ the mass squared matrix is given by

$$M^2 = 2 \begin{pmatrix} g_R^2 v_R^2 & -g_R \overline{g}_C v_R^2 \\ -g_R \overline{g}_C v_R^2 & \overline{g}_C^2 v_R^2 \end{pmatrix}, \tag{5.2.22}$$

where we have defined $\overline{g}_c = \sqrt{3/2}\ g_C$. One can easily calculate the two eigenvalues, one of the eigenvalues is zero and the corresponding eigenstate is given by

$$A_a = \frac{1}{\sqrt{g_R^2 + \overline{g}_C^2}} \left(\overline{g}_C W_{R\,a}^{(3)} + g_R X_a^{(15)} \right). \tag{5.2.23}$$

This is the massless gauge boson of $U(1)_Y$ group. Its orthogonal eigenstate acquires mass given by $\sqrt{2} v_R \sqrt{g_R^2 + \overline{g}_C^2}$. In addition, for the unbroken $SU(3)_C$ group, the massless gauge bosons are identified with $V^{(i)}$ $(i = 1-8)$ fields.

5.2.3 Peccei-Quinn symmetry

On top of the PS gauge symmetry we assume the existence of global Peccei-Quinn (PQ) symmetry, $U(1)_{PQ}$ [167–170] (for a relation between leptonic CP violation with strong CP phase in the context of left-right symmetric models see Ref. [171]). The PQ symmetry naturally solves the strong CP problem and simultaneously provides the axion solution to the dark matter problem [172, 173]. So the complete symmetry of our theories are either $G_{224} \times U_{PQ}(1)$ or $G_{224P} \times U_{PQ}(1)$. The SM singlet present in $\mathbf{\Delta}_R$ that break the PS symmetry and the singlet $\mathcal{S}$, each can break one $U(1)$ symmetry. If the VEV of the singlet, $\langle \mathcal{S} \rangle = v_S > v_R$, then this VEV breaks the

$U(1)_{PQ}$. On the contrary, if $v_R > v_S$, it leaves $U(1)_{B-L+PQ}$ group unbroken since it carries a PQ charge, which is then further broken via $U(1)_{B-L+PQ} \to U(1)_{B-L}$ by the $\mathcal{S}$ VEV. Due to the presence of the $U(1)_{PQ}$ symmetry, the complex scalar fields carry PQ charge which consequently puts additional restrictions on the Higgs potential, this reduces the number of parameters in the Higgs potential.

The VEV of the singlet field, $\langle \mathcal{S} \rangle$ breaks the PQ symmetry at the scale M_{PQ} and phenomenological requirement of this scale is $M_{PQ} \sim 10^{11-13}$ GeV. The miltiplets (2,2,1) and (2,2,15) are assumed to be complex and have non-zero charges under the PQ group. We choose the following charge assignment of the Higgs fields under $U(1)_{PQ}$:

fields	$\mathbf{\Phi}$(2,2,1)	$\mathbf{\Sigma}$(2,2,15)	$\mathbf{\Delta}_R$(1,3,10)	$\mathbf{\Delta}_L$(3,1,10)	$\mathbf{\Psi}_L$(2,1,4)	$\mathbf{\Psi}_R$(1,2,4)	$\mathcal{S}$(1,1,1)
Q_{PQ}	+2	+2	-2	+2	+1	-1	+4

Table 5.1: $U(1)_{PQ}$ charge assignment of the scalars.

5.3 Fermion masses and mixings

In this section we discuss the fermion masses and mixings in the PS model. The model under consideration is very predictive in explaining the data in the fermion sector. The Yukawa part of the Lagrangian is given by:

$$\mathcal{L}_{\mathcal{Y}} = Y_{1ij}\, \overline{\mathbf{\Psi}}_{Li} \mathbf{\Phi} \mathbf{\Psi}_{Rj} + Y_{15ij}\, \overline{\mathbf{\Psi}}_{Li} \mathbf{\Sigma} \mathbf{\Psi}_{Rj} + \{ Y^R_{10\,ij} \mathbf{\Psi}^T_{Ri} C \mathbf{\Delta}^*_R \mathbf{\Psi}_{Rj} + R \leftrightarrow L \} + h.c \tag{5.3.24}$$

where, Y_1, Y_{15} and $Y^{R,L}_{10}$ are the Yukawa coupling matrices resulting due to the interactions of the fermions with the (2,2,1), (2,2,15), (1,3,10) and (3,1,10) multiplets respectively. Generically Y_1 and Y_{15} are general complex matrices and due to Majorana nature, $Y^{R,L}_{10}$ are complex symmetric. When parity is imposed (see Eq. (5.6.64)) the matrices Y_1 and Y_{15} become Hermitian and $Y^{R,L}$ become identical, i.e,

$$Y_1 = Y_1^\dagger, \;\; Y_{15} = Y_{15}^\dagger, \;\; Y^R_{10} = Y^L_{10} = Y_{10} = Y^T_{10}. \tag{5.3.25}$$

For the analysis of the fermion masses and mixings we restrict ourselves to the case when parity summery is realized since this significantly reduces the number of parameters in the fermion sector due to constraints mentioned in Eq. (5.3.25), so the model becomes very predictive. The VEV of the (1,3,10) multiplet $\langle \mathbf{\Delta}_R \rangle$, breaks the G_{224} group down to the SM group and generates the right-handed Majorana neutrino masses given by $v_R Y_{10}$. The Higgs fields $\mathbf{\Phi}$ and $\mathbf{\Sigma}$ each contains two doublets of the SM acquire non-zero VEVs and are responsible for generating charged fermion masses. From the Lagrangian one can write down the fermion mass

matrices as:

$$M_u = k_u Y_1 + v_u Y_{15}, \quad M_d = k_d Y_1 + v_d Y_{15}, \tag{5.3.26}$$

$$M_D = k_u Y_1 - 3v_u Y_{15}, \;\; M_e = k_d Y_1 - 3v_d Y_{15}, \tag{5.3.27}$$

$$M_R = v_R Y_{10}. \tag{5.3.28}$$

M_u, M_d are the up-type and down-type quark mass matrices, M_e is the charged lepton mass matrix, M_D is the neutrino Dirac mass matrix and M_R is the right-handed Majorana neutrino mass matrix. $k_{u,d}$, $v_{u,d}$ are the VEVs of the four doublets. In general these VEVs are complex and there is one common phase for k_u and k_d and different phases for each of v_u and v_d. Only two relative phases will be physical and we bring these phases ($\theta_{1,2}$) with v_u and v_d. The analysis done in Sec. 5.6.2 shows that the VEV ratios are complex and can not be made real. One can absorb the VEVs into the coupling matrices and redefine them, leaving two relevant VEV ratios ($r_{1,2}$). Following these arguments, we can rewrite the mass matrices as,

$$M_u = M_1 + e^{i\theta_1} M_{15}, \quad M_d = r_1 M_1 + r_2 e^{i\theta_2} M_{15}, \tag{5.3.29}$$

$$M_D = M_1 - 3e^{i\theta_1} M_{15}, \;\; M_e = r_1 M_1 - 3r_2 e^{i\theta_2} M_{15}, \tag{5.3.30}$$

$$M_R = v_R Y_{10}, \tag{5.3.31}$$

where we have defined $M_1 = k_u Y_1$, $M_{15} = v_u Y_{15}$, $r_1 = k_d/k_u$ and $r_2 = v_d/v_u$. As mentioned earlier, due to parity symmetry the matrices M_1 and M_{15} are Hermitian, so without loss of generality one can take the M_1 matrix to be diagonal and real (3 real parameters) and one can also rotate away the two phases from the M_{15} matrix leaving only one phase in it (5 real and 1 complex parameters). So in total there are 11 magnitudes and 3 phases i.e, 14 free parameters in the charged fermion sector to fit 13 observables for the case of hard CP-violation. The fit result in the charged fermion sector is presented in Sec. 5.5.1 [1].

Let us now discuses the neutrino sector. The right-handed Majorana mass matrix is complex symmetric matrix and the corresponding Yukawa coupling matrix Y_{10} is arbitrary since it decouples from the charged fermion sector which is unlike the case of $SO(10)$ models. In unified theories due to the presence of right-handed neutrinos seesaw mechanism is a very good candidate to explain the extremely small observed light neutrino masses. One should note that due to the presence of terms linear in $\mathbf{\Delta}_L$ in the Higgs potential (Eq. (5.6.55)), this field will acquire a small VEV, v_L as mentioned above, that would be responsible for generating left-handed Majorana neutrino mass, $M_L = v_L Y_{10}$. In this paper, we assume the dominance of type-I seesaw scenario, then the light neutrino mass matrix is given by the type-I seesaw [38] formula,

[1] For spontaneous CP-violation scenario, the Yukawa coupling matrices are real, so there are 11 magnitudes and 2 phases i.e, 13 free parameters to fit 13 observables. In the next section we will perform numerical study to fit the fermion masses and mixings in the charged fermion sector. Our finding is that the spontaneous CP-violation case is unable to reproduce the observables (we found large total $\chi^2 \sim 125$), so from now on we will only consider the hard CP-violation case.

$$\mathcal{M}_\nu = -M_D M_R^{-1} M_D^T. \tag{5.3.32}$$

Inverting the type-I seesaw formula one can write M_R as ,

$$M_R = -M_D^T \mathcal{M}_\nu^{-1} M_D. \tag{5.3.33}$$

There is no new parameter in the M_D matrix and is completely fixed by the charged fermion sector. The light neutrino mass matrix, $\mathcal{M}_\nu$ can be diagonalized as

$$\mathcal{M}_\nu = U_\nu \Lambda_\nu U_\nu^T, \tag{5.3.34}$$

with

$$\Lambda_\nu = \mathrm{diag}(\mathrm{m}_1, \mathrm{m}_2, \mathrm{m}_3), \tag{5.3.35}$$

with m_i's being real and in the basis where the charged lepton mass matrix is diagonal,

$$U_\nu = U_{\mathrm{PMNS}}\ \mathrm{diag}(\mathrm{e}^{-\mathrm{i}\alpha}, \mathrm{e}^{-\mathrm{i}\beta}, 1) \tag{5.3.36}$$

where α and β are Majorana phases and U_{PMNS} is the CKM type mixing matrix with only one Dirac type phase δ in it.

We assume normal hierarchy [2] in the light neutrino sector, which leads upto a good approximation, $m_2 \sim \sqrt{\Delta m^2_{sol}}$ and $m_3 \sim \sqrt{\Delta m^2_{atm}}$ [3] . The quantities (Δm^2_{sol}, Δm^2_{atm}, $\theta_{ij}^{\mathrm{fermionfitPMNS}}$) in the neutrino sector have already been measured experimentally with good accuracy. The quantities m_1, α, β and δ are yet to be determined experimentally. So in Eq. (5.3.33), using the experimentally measured quantities in the neutrino sector, the right-handed Majorana mass matrix can be determined as a function of these four unknown quantities. In Sec. 5.5.2, we will explain the algorithm we follow while searching for the allowed parameter space to reproduce successful Leptogenesis in this model and also present our results. In addition to normal ordering of neutrino mass, we also investigated the case of inverted ordering following the similar algorithm but have not found any solution for the later case.

5.4 Baryogenesis via Leptogenesis

In unified theories the Baryogenesis via Leptogenesis [174] is a natural candidate to explained the observed matter-antimatter asymmetry [21]. This simple mechanism can be implemented in theories where light neutrino mass is generated via seesaw mechanism. For previous studies on Leptogenesis in the framework of $G_{224}/SO(10)$ see for example Refs. [27,33,175–179]. In this mechanism, the baryon asymmetry of the Universe is generated by

[2] For inverted ordering we have not found any solution that can generate successful baryon asymmetry, so we only concentrate on normal ordering.

[3] As we have assumed normal hierarchy, the lightest left-handed neutrino mass gets restricted as $0 \leq m_1 \lesssim 70\%\ m_2$.

the lepton asymmetry which is initially produced dynamically and later converted into the baryon asymmetry via the $(B + L)$-violating sphaleron process [180] that exist in the SM. Computing the baryon-asymmetric parameter involves solving the coupled Boltzmann equations. The asymmetry is generated when the decay rates of the heavy neutrinos $< H$ (H being the Hubble expansion rate), so Leptogenesis is expected to occur at a temperature of order of the mass of the lightest right-handed heavy neutrino, M_1. For hierarchical spectrum of the right-handed neutrinos, i.e, $M_1 \ll M_2 < M_3$, the lightest heavy neutrino is responsible for generating the baryon asymmetry and known as N_1-dominated Leptogenesis. In this work we concentrate on N_1-dominated Leptogenesis. It is showed that flavor can play significant role in the mechanism of Leptogenesis. Flavored Leptogenesis has been studied with great details, see for example Refs. [181–186].

The minimum required reheat temperature of the universe depends on the details of the flavor structure of the lepton asymmetry. Without taking into account the flavor effects, the lower bound to produce successful baryon asymmetry is $M_1 > 10^9$ GeV [187]. Including the flavor effects relaxes this lower bound a little bit (for details see Ref. [182]). Approximate analytical solutions of the Boltzman equations have been derived that are in good agreement with the exact solutions (see for example Ref. [183]). While scanning over the parameter space in search for successful Leptogenesis we apply these analytical solutions to compute the baryon asymmetry. The analytical formula depends on the interaction rate of the charged lepton Yukawa couplings [186]. We are interested in the two different regions, first, when only the tau Yukawa coupling is in equilibrium which corresponds to range $10^9\text{GeV} \lesssim \text{M}_1 \lesssim 10^{12}$ GeV. In this first case, the flavor effects are important. The second region where no charged lepton Yukawa couplings are in equilibrium that corresponds to the case $M_1 \gtrsim 10^{12}$ GeV. In this second case all flavors are indistinguishable and is no different than the one flavor scenario.

Here we briefly mention the approximate analytical solutions that are derived in the literature as mentioned above. In the regime where flavors are indistinguishable, the CP asymmetry generated by the N_1 decay is

$$\epsilon_1 = \frac{1}{8\pi} \sum_{j\neq 1} \frac{Im[(Y_D^\dagger Y_D)^2_{j1}]}{(Y_D^\dagger Y_D)_{11}}\, g\left(\frac{M_j^2}{M_1^2}\right), \tag{5.4.37}$$

where,

$$g(x) = \sqrt{x}\left[\frac{1}{1-x} + 1 - (1+x) ln\left(\frac{1+x}{x}\right)\right]. \tag{5.4.38}$$

Beside the CP parameter ϵ_1, the final asymmetry depends on the wash-out parameter,

$$K = \frac{\widetilde{m}_1}{\widetilde{m}^*}, \tag{5.4.39}$$

with $\widetilde{m}^* \sim 10^{-3}$ eV and

$$\widetilde{m}_1 = \frac{(Y_D^\dagger Y_D)_{11} v^2}{M_1}. \tag{5.4.40}$$

In the strong wash-out regime, i.e, for $K >> 1$, the lepton asymmetry is given by the following approximate formula

$$Y_{\mathcal{L}} \simeq 0.3 \frac{\epsilon_1}{g^*} \left(\frac{0.55 \times 10^{-3}\text{eV}}{\widetilde{m}_1} \right)^{1.16}, \tag{5.4.41}$$

with g^* being the effective number of spin-degrees of freedom in thermal equilibrium, which is ~ 108 in the SM with a single generation of right-handed neutrinos. With these the baryon asymmetry is given by $Y_{\mathcal{B}} \simeq 12/37\, Y_{\mathcal{L}}$. Another useful relation is $\eta_B = 7.04\, Y_{\mathcal{B}}$, where η_B is the number of baryons and anti-baryons normalized to the number of photons. On the other hand, in the weak wash-out regime, the approximate analytical formula is,

$$Y_{\mathcal{L}} \simeq 0.3 \frac{\epsilon_1}{g^*} \left(\frac{\widetilde{m}_1}{3.3 \times 10^{-3}\text{eV}} \right). \tag{5.4.42}$$

On the contrary, the regime where the flavor effects are important, the CP asymmetry in the α-th flavor is given by

$$\epsilon_{\alpha\alpha} = \frac{1}{8\pi (Y_D^\dagger Y_D)_{11}} \sum_{j \neq 1} Im[(Y_D^\dagger)_{1\alpha} (Y_D^\dagger Y_D)_{1j} (Y_D^T)_{j\alpha}]\; g\left(\frac{M_j^2}{M_1^2} \right). \tag{5.4.43}$$

And the wash-out parameter is

$$K_{\alpha\alpha} \simeq \frac{\widetilde{m}_{\alpha\alpha}}{10^{-3}\text{eV}}, \;\; \widetilde{m}_{\alpha 1} = \frac{|(Y_D)_{\alpha 1}|^2 v^2}{M_1} \tag{5.4.44}$$

that parametrizes the decay rate of N_1 to the α-th flavor. In the strong wash-out regime for all flavor, i.e, $K_{\alpha\alpha} >> 1$, the total asymmetry is $Y_{\mathcal{L}} = \sum_\alpha Y_{\alpha\alpha}$, where the approximate analytical formula for $Y_{\alpha\alpha}$ is

$$Y_{\alpha\alpha} \simeq 0.3 \frac{\epsilon_{\alpha\alpha}}{g^*} \left(\frac{0.55 \times 10^{-3}\text{eV}}{\widetilde{m}_{\alpha\alpha}} \right)^{1.16}. \tag{5.4.45}$$

And in the weak wash-out regime the formula is,

$$Y_{\alpha\alpha} \simeq 1.5 \frac{\epsilon_{\alpha\alpha}}{g^*} (\frac{\widetilde{m}_1}{3.3 \times 10^{-3}\text{eV}}) (\frac{\widetilde{m}_{\alpha\alpha}}{3.3 \times 10^{-3}\text{eV}}). \tag{5.4.46}$$

The Baryon asymmetric parameter has been measure experimentally, $\eta_B = (5.7 \pm 0.6) \times 10^{-10}$ [4] [19, 20]. Since this scenario of generating baryon asymmetry requires the right-handed neutrino mass scale to be high, for this analysis we fix this scale to be $v_R = 10^{14}$ GeV as discussed before in the text.

5.5 Fit to fermion masses and mixings and parameter space for successful Leptogenesis

5.5.1 Numerical analysis of the charged fermion sector

In this sub-section we show our fit results of the fermion masses and mixings in the charged fermion sector. For optimization purpose we do χ^2-analysis. The pull and χ^2-function are defined as:

[4] 90% CL - deuterium only.

Masses (in GeV) and CKM parameters	Inputs (at $\mu = M_{PS}$)	Best fit values	Pulls
$m_u/10^{-3}$	0.48 ± 0.16	0.48	0.009
m_c	0.26 ± 0.008	0.26	-0.03
m_t	80.78 ± 0.69	80.78	0.001
$m_d/10^{-3}$	1.24 ± 0.12	1.26	0.020
$m_s/10^{-3}$	23.50 ± 1.23	22.21	-1.04
m_b	1.09 ± 0.009	1.09	0.11
$m_e/10^{-3}$	0.482669 ± 0.004826	0.482645	-0.05
$m_\mu/10^{-3}$	101.8943 ± 1.0189	101.898	0.03
m_τ	1.732205 ± 0.017322	1.73223	0.01
$\theta_{12}^{\rm CKM}/10^{-2}$	22.543 ± 0.071	22.541	-0.02
$\theta_{23}^{\rm CKM}/10^{-2}$	4.783 ± 0.072	4.799	0.22
$\theta_{13}^{\rm CKM}/10^{-2}$	0.413 ± 0.014	0.412	-0.01
$\delta^{\rm CKM}$	1.207 ± 0.054	1.198	-0.15

Table 5.2: χ^2 fit of the observables in the charged fermion sector. This best fit correspond to $\chi^2 = 1.2$ for 13 observables. For charged leptons, a relative uncertainty of 0.1% is assumed to take into account the uncertainties, for example threshold corrections at the PS scale.

$$P_i = \frac{O_{i\ \rm th} - E_{i\ \rm exp}}{\sigma_i}, \tag{5.5.47}$$

$$\chi^2 = \sum_i P_i^2, \tag{5.5.48}$$

where σ_i represent experimental 1σ uncertainty and $O_{i\ \rm th}$, $E_{i\ \rm exp}$ and P_i represent the theoretical prediction, experimental central value and pull of an observable i. We fit the values of the observables at the PS breaking scale, $M_{PS} = 10^{14}$ GeV. To get the PS scale values of the observables, we take the central values at the M_Z scale from Table-1 of Ref. [72] and run the RGEs [110] to get the inputs at the high scale. For the associated one sigma uncertainties of the observables at the PS scale, we keep the same percentage uncertainty with respect to the central value of each quantity as that of the M_Z scale. For the charged lepton Yukawa couplings, a relative uncertainty of 0.1% is assumed in order to take into account the theoretical uncertainties, for example threshold effects at the PS scale. The inputs are shown in the Table 5.2 where the fit results are presented.

As noted before, for this case, we have 14 parameters, 11 magnitudes and 3 phases. We perform the χ^2 function minimization and the best minimum corresponds to total $\chi^2 = 1.2$ is obtained for 13 observables which

is a good fit [5]. The result corresponding to the best fit is shown in Table 5.2. The values of the parameters corresponding to the best fit are:

$$\theta_1 = 7.83759 \cdot 10^{-4},\ \theta_2 = -3.131385,\ r_1 = 1.29347 \cdot 10^{-2},\ r_2 = -9.13047 \cdot 10^{-3}, \tag{5.5.49}$$

$$M_1 = \begin{pmatrix} 0.2988234 & 0. & 0. \\ 0. & 5.066234 & 0. \\ 0. & 0. & 94.801891 \end{pmatrix} \text{GeV}, \tag{5.5.50}$$

$$M_{15} = \begin{pmatrix} -0.212786 & 0.367673 & -2.85309 \\ 0.367673 & -3.53464 & -11.8404 - 0.699369i \\ -2.85309 & -11.8404 + 0.699369i & -15.8963 \end{pmatrix} \text{GeV}. \tag{5.5.51}$$

5.5.2 Parameter space for successful Leptogenesis

Using the seesaw formula Eq. (5.3.32), one can in principle fit all the neutrino observables since the matrix M_R which is in general a complex symmetric matrix contains 6 complex parameters. Instead, we will follow an alternative procedure. The right-handed neutrino mass matrix is given by inverting the seesaw formula Eq. (5.3.33). After the fitting of the fermion masses and mixings has been done, the Dirac neutrino mass matrix gets fixed. For our fit, this Dirac neutrino mass matrix is

$$M_D = \begin{pmatrix} 0.937182 + 0.00050032i & -1.10302 - 0.000864501i & 8.55928 + 0.00670841i \\ -1.10302 - 0.000864501i & 15.6702 + 0.00831092i & 35.5195 + 2.12595i \\ 8.55928 + 0.00670841i & 35.5228 - 2.07027i & 142.491 + 0.0373765i \end{pmatrix} \text{GeV}. \tag{5.5.52}$$

Then for observed known values of $\Delta m^2_{sol,atm}$ and $\sin^2\theta_{ij}^{\rm PMNS}$, we are left with 4 unknown parameters m_1, α, β and δ, so one can express the right-handed Majorana mass matrix as a function of these free parameters, $M_R = M_R(m_1, \alpha, \beta, \delta)$, this is why the baryon asymmetric parameter in Leptogenesis mechanism is also become a function of these, i.e, $\eta_B = \eta_B(m_1, \alpha, \beta, \delta)$. We search the parameter space of these parameters that correspond to successful Leptogenesis. While hunting for the parameter space, the algorithm we follow is, we vary the experimentally measured quantities $(\Delta m^2_{sol,atm}, \sin^2\theta_{ij}^{\rm PMNS})$ in the neutrino sector within the 2σ allowed range. In Eq. (5.3.36) the Dirac phase δ is varied in the range $[0,\ 2\pi]$ whereas the Majorana phases α, β are varied within $[0,\ \pi]$, these are the physical ranges for these phases (for details see Ref. [188]). Baryon asymmetric parameter is computed in a basis where both the charged lepton and the right-handed neutrino mass matrices

[5] Note that the total $\chi^2 \neq 0$ even though the number of parameters is 1 more than the number of observables, it is because among the 14 parameters 3 of them are phases that can only be varied between 0 to 2π.

are real and diagonal. We diagonalize these mass matrices as,

$$M_e = U_{e_L} \Lambda_e U_{e_R}^{\dagger} \ , \quad M_R = U_{\nu_R} \Lambda_R U_{\nu_R}^T, \tag{5.5.53}$$

with $\Lambda_e = \mathrm{diag}(\mathrm{m_e}, \mathrm{m}_\mu, \mathrm{m}_\tau)$ and $\Lambda_R = \mathrm{diag}(\mathrm{M}_1, \mathrm{M}_2, \mathrm{M}_3)$. In this basis, the Dirac neutrino mass matrix is given by $U_{e_L}^{\dagger} M_D U_{\nu_R}^T$ where

$$U_{e_L} = \begin{pmatrix} 0.964706 & -0.259692 + 0.00589944i & 0.0432075 + 0.00025877i \\ 0.246127 + 0.00525722i & 0.947897 & 0.201767 + 0.0132524i \\ -0.0934313 + 0.00250479i & -0.184011 + 0.0125101i & 0.97839 \end{pmatrix}, \tag{5.5.54}$$

which is fixed from the fit parameters in the charged fermions and U_{ν_R} can be computed as a function of the free parameters $m_1, \alpha, \beta, \delta$. The inputs in the neutrino sector are taken from [76] and shown in Table 5.3.

While scanning over the parameter space, if $10^9 \mathrm{GeV} \lesssim \mathrm{M}_1 \lesssim 10^{12}$ GeV, we compute the baryon asymmetric parameter by taking into account the flavor effects and for $M_1 \gtrsim 10^{12}$ GeV, calculating η_B involving the case where flavors are indistinguishable. For perturbitivity reason, we put a cut-off of $M_3 \lesssim 2 \cdot 10^{14}$ GeV. For both the scenarios, unflavored or flavored, we use the formula for the strong wash-out regime when the wash-out parameter > 1 (K and $K_{\alpha\alpha}$) and the formula for weak wash-out regime when it is < 1 (instead of $\gg 1$ and $\ll 1$ respectively). It is to be mentioned that our investigation shows that the parameter space only permits solution in the strong wash-out regime.

In Fig. 5.2, η_B is plotted against α, β and δ phases respectively for the two different values of $m_1 = 1, 2$ meV where the other quantities are varied over the whole range as mentioned before. Whether or not flavor effects are involved, depending on that, the allowed region in the parameter space is pretty much different. In Fig. 5.3, the permitted region for m_β and $m_{\beta\beta}$ to have successful Leptogenesis is shown, where $m_\beta = \sum_i |U_{\nu\ ei}|^2 m_i$ is the effective mass parameter for the beta-decay and $m_{\beta\beta} = |\sum_i U_{\nu\ ei}^2 m_i|$ is the effective mass parameter for neutrinoless double beta decay. The correlations between the phase δ and the angle θ_{13} is presented in Fig. 5.4. The relations between the heavy right-handed neutrino mass spectrum permitted by successfully reproducing η_B is shown in Fig. 5.5. The plots presented here are the result of 10^8 iterations.

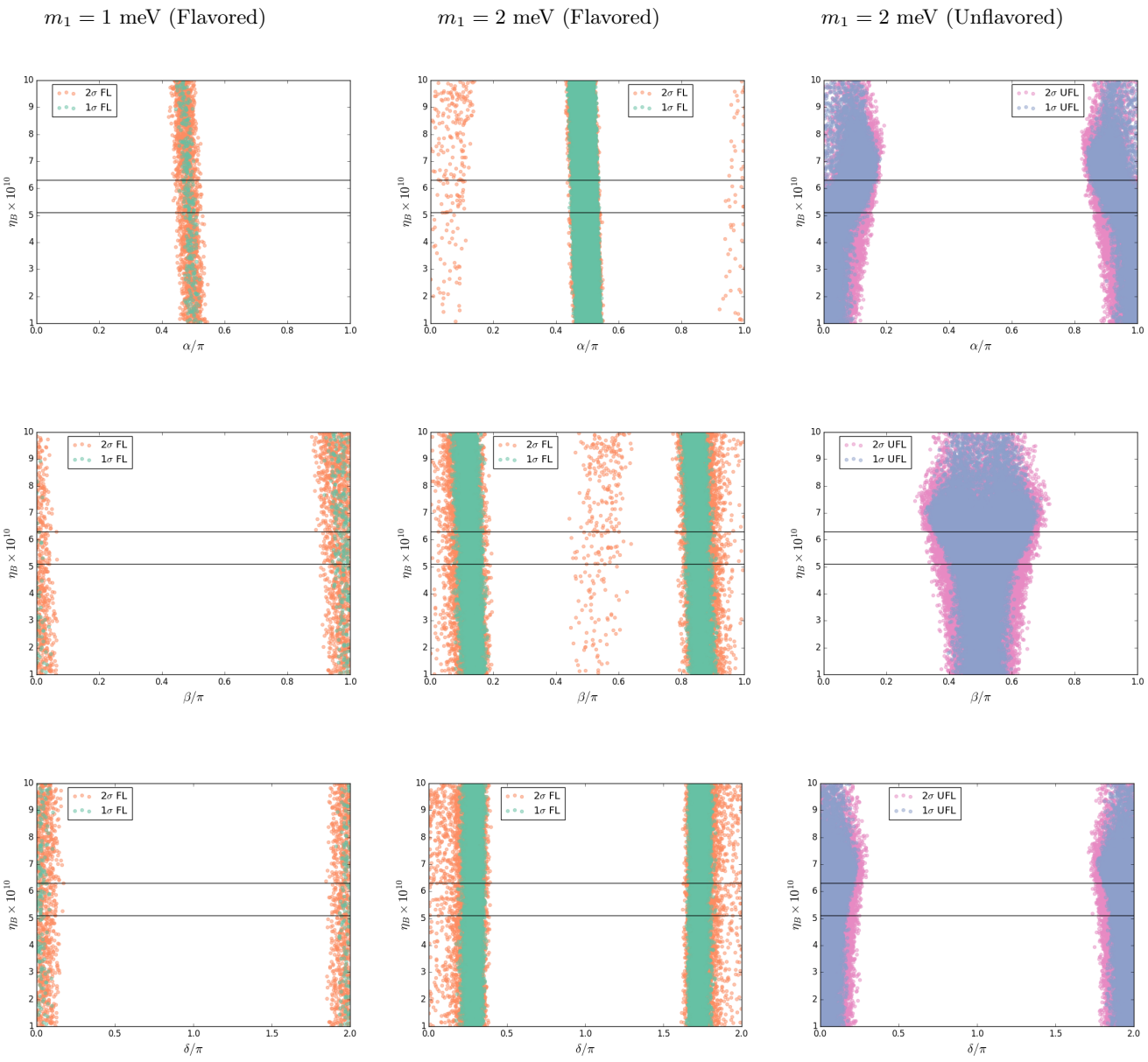

Figure 5.2: As mentioned in the text, the baryon asymmetric parameter is function of the four unknown quantities, $\eta_B = \eta_B(m_1, \alpha, \beta, \delta)$. Allowed parameter space for η_B corresponding to these unknown quantities α, β, δ for two different values of $m_1 = 1, 2$ meV are presented here. While searching for the parameter space, the other quantities in the neutrino sector, $\Delta m^2_{sol,atm}, \sin^2\theta^{\rm PMNS}_{ij}$ that have been measured experimentally, are varied within their 2σ experimental allowed range. The horizontal black lines represent the experimental 1σ range of η_B. The green and orange set correspond to Leptogenesis scenario where flavor effects are important, whereas, the blue and pink set is the flavor blind solutions. For these two different scenarios, green and blue represent solutions where $\Delta m^2_{sol,atm}, \sin^2\theta^{\rm PMNS}_{ij}$ are varied within experimental 1σ range and orange and pink within 2σ range.

Quantity	1σ range	2σ range
$\Delta m^2_{sol}/10^{-5}eV^2$	7.32-7.80	7.15-8.00
$\Delta m^2_{atm}/10^{-3}eV^2$	2.33-2.49	2.27-2.55
$\sin^2\theta_{12}^{\rm PMNS}/10^{-1}$	2.91-3.25	2.75-3.42
$\sin^2\theta_{23}^{\rm PMNS}/10^{-1}$	3.65-4.10	3.48-4.48
$\sin^2\theta_{13}^{\rm PMNS}/10^{-2}$	2.16-2.66	1.93-2.90

Table 5.3: Observables in the neutrino sector taken from [76].

parameters	10^9GeV $\lesssim$ M$_1$ $\lesssim 10^{12}$ GeV		$M_1 \gtrsim 10^{12}$ GeV
	$m_1 = 1$ meV	$m_1 = 2$ meV	$m_1 = 2$ meV
α	1.52000	1.58856	2.98463
β	3.05225	0.41436	1.20953
δ	-0.03128	0.96204	5.70804
$\Delta m^2_{sol}/10^{-5}eV^2$	7.60680	7.62805	7.71611
$\Delta m^2_{atm}/10^{-3}eV^2$	2.37437	2.33256	2.30159
$\sin^2\theta_{12}^{\rm PMNS}$	0.29188	0.29219	0.29036
$\sin^2\theta_{23}^{\rm PMNS}$	0.36578	0.39725	0.38922
$\sin^2\theta_{13}^{\rm PMNS}$	0.02581	0.02213	0.02642
$\eta_B/10^{-10}$	5.65	5.74	6.27

Table 5.4: Benchmark points for computing baryon asymmetric parameter is presented. η_B is computed by taking into account the flavor effects if 10^9GeV $\lesssim$ M$_1$ $\lesssim 10^{12}$ GeV or in the flavor indistinguishable regime if $M_1 \gtrsim 10^{12}$ GeV. Two different values of the lightest left-handed neutrino masses are considered, $m_1 = 1$ and 2 meV, where for the second case, solutions exists for both flavored and unflavored scenarios.

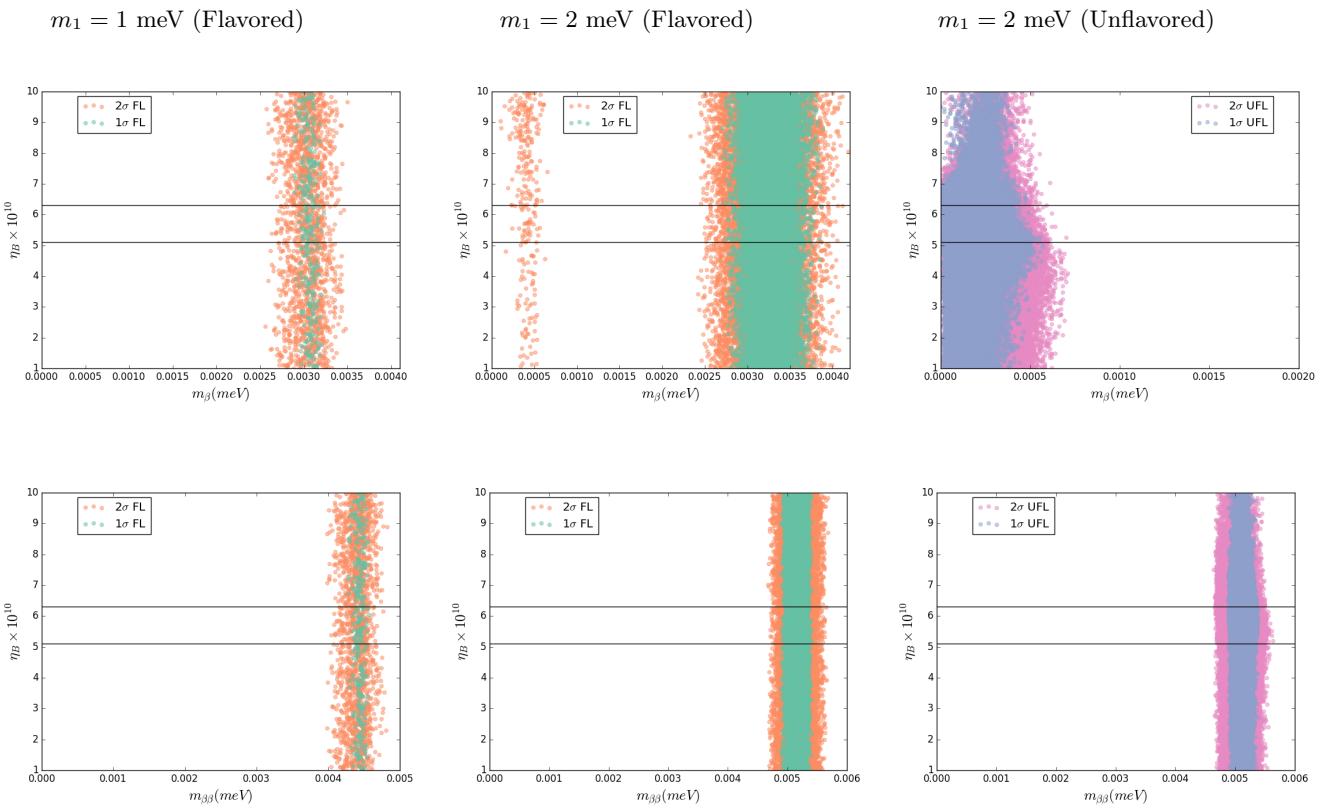

Figure 5.3: The correspondence between the baryon asymmetry and $m_{\beta,\beta\beta}$ are plotted, where $m_\beta = \sum_i |U_{\nu\ ei}|^2 m_i$ is the effective mass parameter for the beta-decay and $m_{\beta\beta} = |\sum_i U^2_{\nu\ ei} m_i|$ is the effective mass parameter for neutrinoless double beta decay. Color code is the same as in Fig. 5.2.

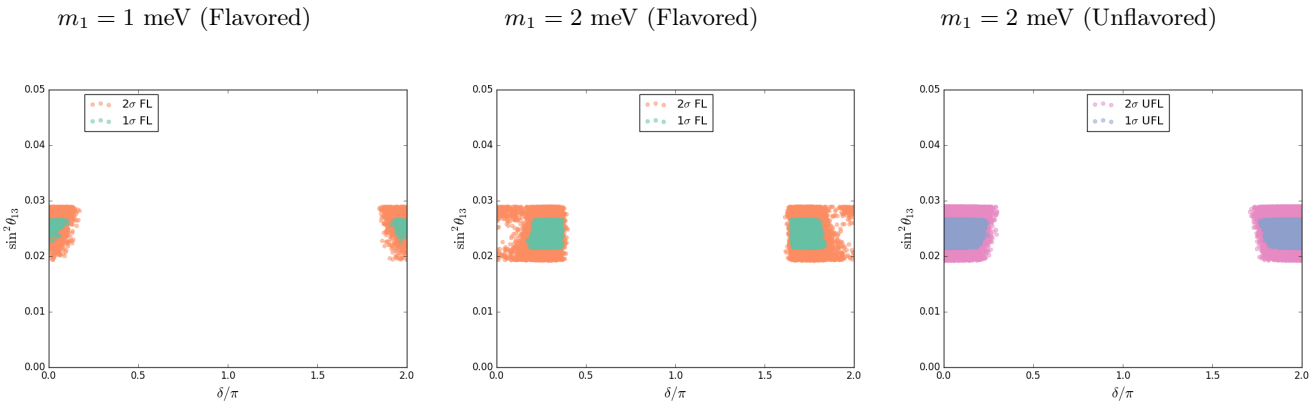

Figure 5.4: Correlation between the quantities δ and $\sin^2_{\theta^{PMNS}_{13}}$ is plotted for three different values of $m_1 = 0.8, 1, 2$ meV. Color code is the same as in Fig. 5.2.

The general behaviour is, for larger values of m_1, the parameter space gets more populated. For smaller values of m_1, the parameter space is mostly preferred by flavored Leptogenesis scenario. For example, setting $m_1 = 0.8$ meV, we found that a very small portion of the parameter space permits baryon asymmetry in the right range. Only flavored Leptogenesis scenario is allowed in this case provided that not all the varied quantities are restricted within 1σ range. The plots for this case are presented in Fig. 5.7. If m_1 is set to a higher value, for example $m_1 = 1$ meV, again only solutions exits for flavored Leptogenesis case but in this case solutions are permitted even if all the varied quantities are within 1σ range. For even higher value of the lightest left-handed neutrino mass, parameter space allows solutions for both flavored and unflavored Leptogenesis scenarios. We demonstrate such case by setting $m_1 = 2$ meV. Our investigation shows that, when m_1 is set to higher and higher values, the parameter space gets even more and more crowded. For example with $m_1 = 2$ meV, we see that the regions corresponding to these different settings are distinct. Higher the value of m_1, more the overlapping in the parameter space for the two distinct scenarios. As a demonstration, plots corresponding to this scenario with $m_1 = 4$ meV are presented in Fig. 5.7.

In the neutrino sector, among the four different experimentally unmeasured quantities, particularly the Dirac type phase δ is the most important one, since it has the potential to be measured in the upcoming neutrino experiments. In Fig. 5.6, we present the allowed values for this CP violating phase to have successful Leptogenesis is presented for different values of the lightest neutrino mass m_1. For the readers convenience, benchmark points corresponding to few different cases are presented in Table 5.4.

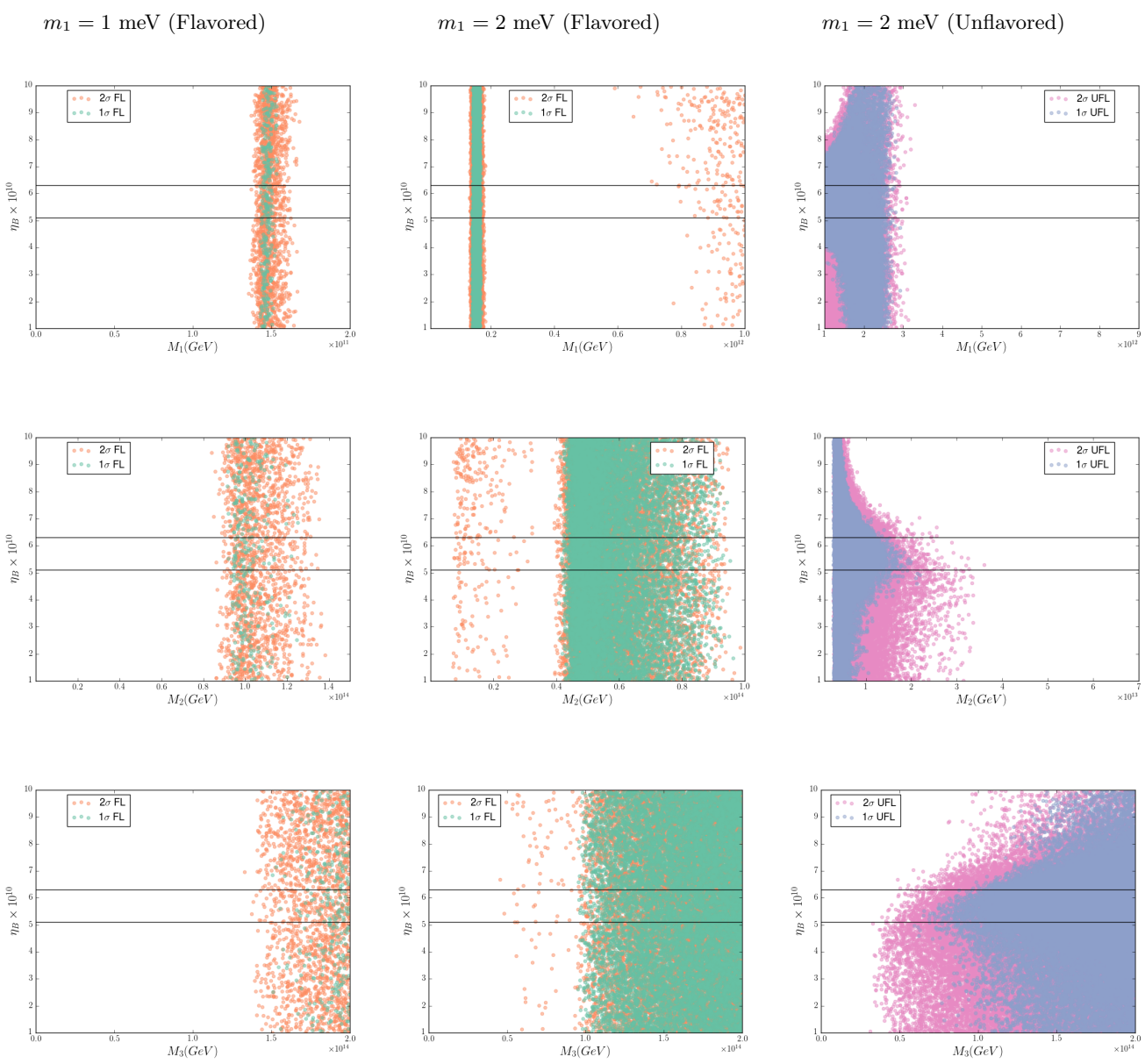

Figure 5.5: The correspondence between the baryon asymmetry and the heavy right-handed neutrino mass spectrum M_i are plotted. Color code is the same as in Fig. 5.2.

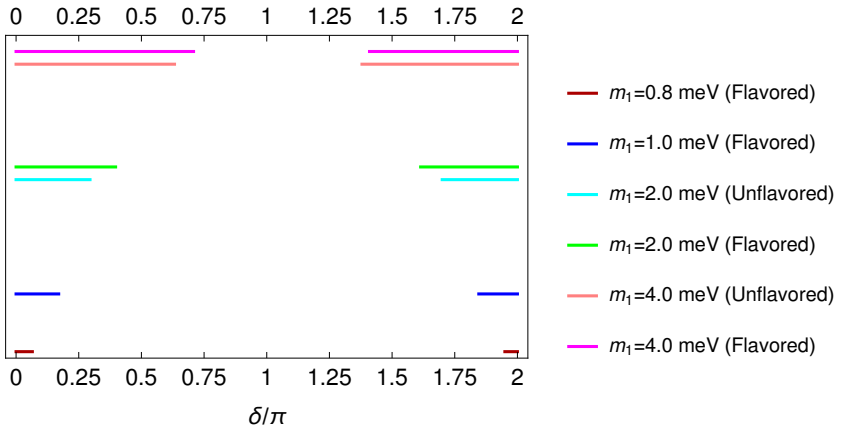

Figure 5.6: Allowed range of the CP violating phase δ for successful Leptogenesis for different values of m_1.

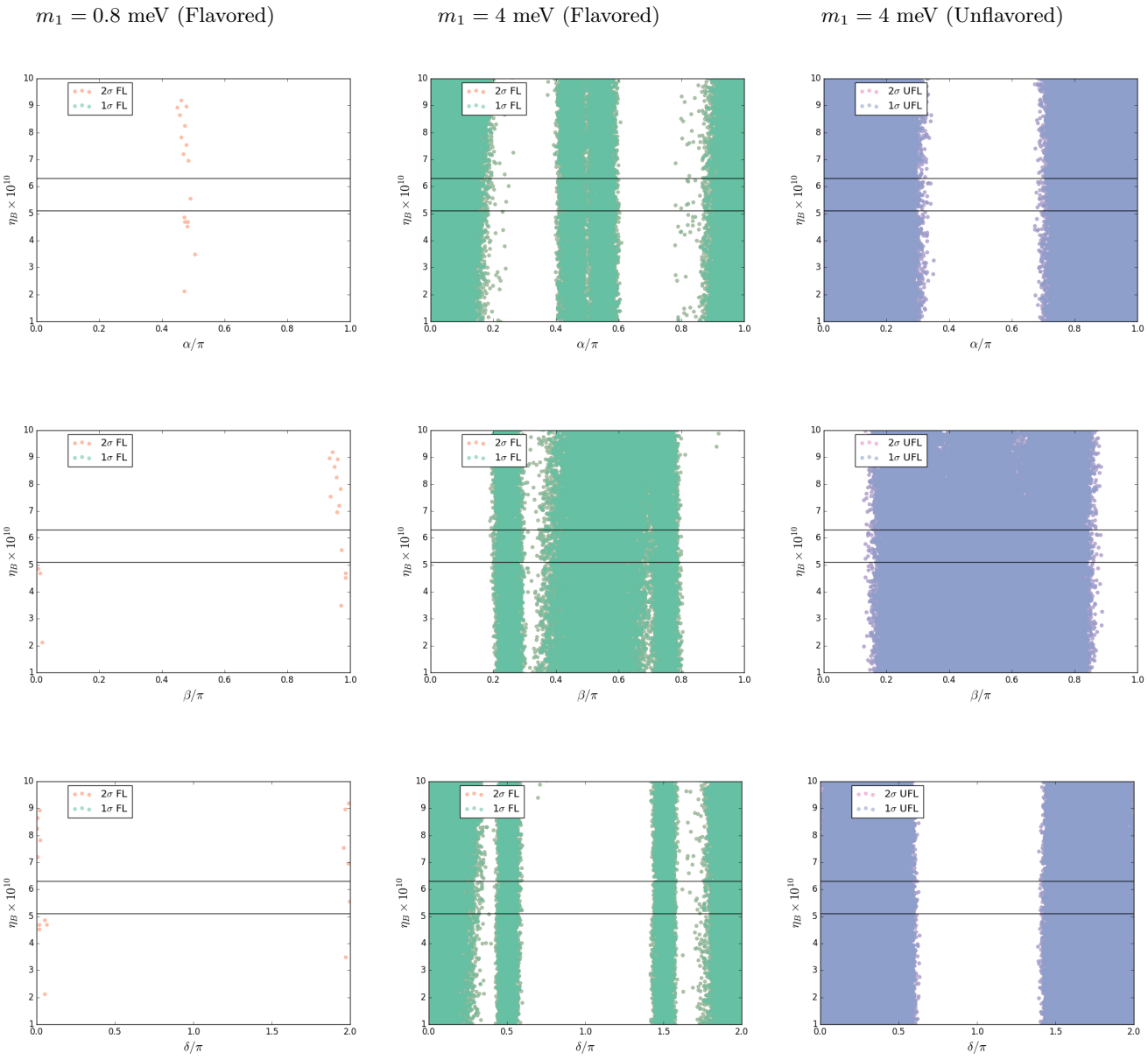

Figure 5.7: Allowed parameter space for η_B corresponding to the unknown quantities α, β, δ for two different values of $m_1 = 0.8, 4$ meV are presented here. Color code is the same as in Fig. 5.2.

5.6 The Higgs potential and scalar mass spectrum

5.6.1 The Higgs potential

In this sub-section we construct the complete scalar potential with $G_{224} \times U(1)_{PQ}$ symmetry. As mentioned earlier, the field $\mathbf{\Delta}_L$ which is present if the group is G_{224P} but need not be present if the gauge group is

G_{224} instead. But for generality, we construct the scalar potential containing $(2,2,1),(2,2,15),(1,3,10)$ and $(3,1,10)$ fields that respects $G_{224}\times U(1)_{PQ}$ symmetry and then discuss the constraints introduced by imposing the parity symmetry. For G_{224} with the absence of $(3,1,10)$ one can set $\mathbf{\Delta}_L=0$ to attain the relevant terms in the potential. The most general Higgs potential respecting $G_{224}\times U(1)_{PQ}$ symmetry with the scalars given in Eq. (5.2.10) is:

$$V=V_{\mathbf{\Phi}}+V_{\mathbf{\Sigma}}+V_{\mathbf{\Delta}}+V_{\mathbf{\Phi\Sigma}}+V_{\mathbf{\Phi\Delta}}+V_{\mathbf{\Sigma\Delta}}+V_{\mathbf{\Phi\Sigma\Delta}}+V_{\mathcal{S}}, \tag{5.6.55}$$

with,

$$V_{\mathbf{\Phi}}=-\mu_{\Phi}^2\ \mathbf{\Phi}_{\alpha}^{\dot{\alpha}}\mathbf{\Phi}_{\dot{\alpha}}^{*\alpha}+\lambda_{1\Phi}\ \mathbf{\Phi}_{\alpha}^{\dot{\alpha}}\mathbf{\Phi}_{\dot{\alpha}}^{*\alpha}\mathbf{\Phi}_{\beta}^{\dot{\beta}}\mathbf{\Phi}_{\dot{\beta}}^{*\beta}+\lambda_{2\Phi}\ \mathbf{\Phi}_{\alpha}^{\dot{\alpha}}\mathbf{\Phi}_{\dot{\beta}}^{*\alpha}\mathbf{\Phi}_{\beta}^{\dot{\beta}}\mathbf{\Phi}_{\dot{\alpha}}^{*\beta}, \tag{5.6.56}$$

$$\begin{aligned}V_{\mathbf{\Sigma}}=&-\mu_{\Sigma}^2\ \mathbf{\Sigma}_{\mu\ \alpha}^{\nu\ \dot{\alpha}}\mathbf{\Sigma}_{\nu\ \dot{\alpha}}^{*\mu\ \alpha}+\lambda_{1\Sigma}\ \mathbf{\Sigma}_{\mu\ \alpha}^{\nu\ \dot{\alpha}}\mathbf{\Sigma}_{\nu\ \dot{\alpha}}^{*\mu\ \alpha}\mathbf{\Sigma}_{\rho\ \beta}^{\tau\ \dot{\beta}}\mathbf{\Sigma}_{\tau\ \dot{\beta}}^{*\rho\ \beta}+\lambda_{2\Sigma}\ \mathbf{\Sigma}_{\mu\ \alpha}^{\nu\ \dot{\alpha}}\mathbf{\Sigma}_{\tau\ \dot{\alpha}}^{*\rho\ \alpha}\mathbf{\Sigma}_{\nu\ \beta}^{\mu\ \dot{\beta}}\mathbf{\Sigma}_{\rho\ \dot{\beta}}^{*\tau\ \beta}\\&+\lambda_{3\Sigma}\ \mathbf{\Sigma}_{\mu\ \alpha}^{\nu\ \dot{\alpha}}\mathbf{\Sigma}_{\rho\ \dot{\alpha}}^{*\tau\ \alpha}\mathbf{\Sigma}_{\tau\ \beta}^{\rho\ \dot{\beta}}\mathbf{\Sigma}_{\nu\ \dot{\beta}}^{*\mu\ \beta}+\lambda_{4\Sigma}\ \mathbf{\Sigma}_{\mu\ \alpha}^{\nu\ \dot{\alpha}}\mathbf{\Sigma}_{\nu\ \dot{\alpha}}^{*\rho\ \alpha}\mathbf{\Sigma}_{\rho\ \beta}^{\tau\ \dot{\beta}}\mathbf{\Sigma}_{\tau\ \dot{\beta}}^{*\mu\ \beta}+\lambda_{5\Sigma}\ \mathbf{\Sigma}_{\mu\ \alpha}^{\nu\ \dot{\alpha}}\mathbf{\Sigma}_{\tau\ \dot{\alpha}}^{*\mu\ \alpha}\mathbf{\Sigma}_{\nu\ \beta}^{\rho\ \dot{\beta}}\mathbf{\Sigma}_{\rho\ \dot{\beta}}^{*\tau\ \beta}\\&+\lambda_{6\Sigma}\ \mathbf{\Sigma}_{\mu\ \alpha}^{\nu\ \dot{\alpha}}\mathbf{\Sigma}_{\rho\ \dot{\alpha}}^{*\tau\ \alpha}\mathbf{\Sigma}_{\tau\ \beta}^{\mu\ \dot{\beta}}\mathbf{\Sigma}_{\nu\ \dot{\beta}}^{*\rho\ \beta}+\lambda_{7\Sigma}\ \mathbf{\Sigma}_{\mu\ \alpha}^{\nu\ \dot{\alpha}}\mathbf{\Sigma}_{\nu\ \dot{\beta}}^{*\mu\ \alpha}\mathbf{\Sigma}_{\rho\ \beta}^{\tau\ \dot{\beta}}\mathbf{\Sigma}_{\tau\ \dot{\alpha}}^{*\rho\ \beta}+\lambda_{8\Sigma}\ \mathbf{\Sigma}_{\mu\ \alpha}^{\nu\ \dot{\alpha}}\mathbf{\Sigma}_{\tau\ \dot{\beta}}^{*\rho\ \alpha}\mathbf{\Sigma}_{\nu\ \beta}^{\mu\ \dot{\beta}}\mathbf{\Sigma}_{\rho\ \dot{\alpha}}^{*\tau\ \beta}\\&+\lambda_{9\Sigma}\ \mathbf{\Sigma}_{\mu\ \alpha}^{\nu\ \dot{\alpha}}\mathbf{\Sigma}_{\nu\ \dot{\beta}}^{*\rho\ \alpha}\mathbf{\Sigma}_{\rho\ \beta}^{\tau\ \dot{\beta}}\mathbf{\Sigma}_{\tau\ \dot{\alpha}}^{*\mu\ \beta}+\lambda_{10\Sigma}\ \mathbf{\Sigma}_{\mu\ \alpha}^{\nu\ \dot{\alpha}}\mathbf{\Sigma}_{\tau\ \dot{\beta}}^{*\mu\ \alpha}\mathbf{\Sigma}_{\nu\ \beta}^{\rho\ \dot{\beta}}\mathbf{\Sigma}_{\rho\ \dot{\alpha}}^{*\tau\ \beta}+\lambda_{11\Sigma}\ \mathbf{\Sigma}_{\mu\ \alpha}^{\nu\ \dot{\alpha}}\mathbf{\Sigma}_{\nu\ \gamma}^{\mu\ \dot{\gamma}}\epsilon^{\alpha\gamma}\epsilon_{\ \dot{\alpha}\dot{\gamma}}\mathbf{\Sigma}_{\rho\ \beta\dot{\beta}}^{*\tau\ \rho\ \kappa}\epsilon_{\ \beta\kappa}\epsilon^{\dot{\beta}\dot{\kappa}}\\&+\lambda_{12\Sigma}\ \mathbf{\Sigma}_{\mu\ \alpha}^{\nu\ \dot{\alpha}}\mathbf{\Sigma}_{\tau\ \gamma}^{\rho\ \dot{\gamma}}\epsilon^{\alpha\gamma}\epsilon_{\ \dot{\alpha}\dot{\gamma}}\mathbf{\Sigma}_{\nu\ \dot{\beta}}^{*\mu\ \beta}\mathbf{\Sigma}_{\rho\ \dot{\kappa}}^{*\tau\ \kappa}\epsilon_{\ \beta\kappa}\epsilon^{\dot{\beta}\dot{\kappa}}+\lambda_{13\Sigma}\ \mathbf{\Sigma}_{\mu\ \alpha}^{\nu\ \dot{\alpha}}\mathbf{\Sigma}_{\nu\ \gamma}^{\rho\ \dot{\gamma}}\epsilon^{\alpha\gamma}\epsilon_{\ \dot{\alpha}\dot{\gamma}}\mathbf{\Sigma}_{\rho\ \dot{\beta}}^{*\tau\ \beta}\mathbf{\Sigma}_{\tau\ \dot{\kappa}}^{*\mu\ \kappa}\epsilon_{\ \beta\kappa}\epsilon^{\dot{\beta}\dot{\kappa}}\\&+\lambda_{14\Sigma}\ \mathbf{\Sigma}_{\mu\ \alpha}^{\nu\ \dot{\alpha}}\mathbf{\Sigma}_{\rho\ \gamma}^{\tau\ \dot{\gamma}}\epsilon^{\alpha\gamma}\epsilon_{\ \dot{\alpha}\dot{\gamma}}\mathbf{\Sigma}_{\tau\ \dot{\beta}}^{*\mu\ \beta}\mathbf{\Sigma}_{\nu\ \dot{\kappa}}^{*\rho\ \kappa}\epsilon_{\ \beta\kappa}\epsilon^{\dot{\beta}\dot{\kappa}},\end{aligned} \tag{5.6.57}$$

$$\begin{aligned}V_{\mathbf{\Delta}}=\{&-\mu_{\Delta_R}^2\ \mathbf{\Delta}_{R\mu\nu\ \dot{\alpha}}^{\ \ \ \dot{\beta}}\mathbf{\Delta}_{R\ \dot{\beta}}^{*\mu\nu\ \dot{\alpha}}+\lambda_{1R}\ \mathbf{\Delta}_{R\mu\nu\ \dot{\alpha}}^{\ \ \ \dot{\beta}}\mathbf{\Delta}_{R\ \dot{\beta}}^{*\mu\nu\ \dot{\alpha}}\mathbf{\Delta}_{R\rho\tau\ \dot{\gamma}}^{\ \ \ \dot{\kappa}}\mathbf{\Delta}_{R\ \dot{\kappa}}^{*\rho\tau\ \dot{\gamma}}+\lambda_{2R}\ \mathbf{\Delta}_{R\mu\nu\ \dot{\alpha}}^{\ \ \ \dot{\beta}}\mathbf{\Delta}_{R\ \dot{\kappa}}^{*\mu\nu\ \dot{\gamma}}\mathbf{\Delta}_{R\rho\tau\ \dot{\beta}}^{\ \ \ \dot{\alpha}}\mathbf{\Delta}_{R\ \dot{\gamma}}^{*\rho\tau\ \dot{\kappa}}\\&+\lambda_{3R}\ \mathbf{\Delta}_{R\mu\nu\ \dot{\alpha}}^{\ \ \ \dot{\beta}}\mathbf{\Delta}_{R\ \dot{\gamma}}^{*\mu\nu\ \dot{\kappa}}\mathbf{\Delta}_{R\rho\tau\ \dot{\kappa}}^{\ \ \ \dot{\gamma}}\mathbf{\Delta}_{R\ \dot{\beta}}^{*\rho\tau\ \dot{\alpha}}+\lambda_{4R}\ \mathbf{\Delta}_{R\mu\nu\ \dot{\alpha}}^{\ \ \ \dot{\beta}}\mathbf{\Delta}_{R\ \dot{\beta}}^{*\nu\rho\ \dot{\alpha}}\mathbf{\Delta}_{R\rho\tau\ \dot{\gamma}}^{\ \ \ \dot{\kappa}}\mathbf{\Delta}_{R\ \dot{\kappa}}^{*\tau\mu\ \dot{\gamma}}\\&+\lambda_{5R}\ \mathbf{\Delta}_{R\mu\nu\ \dot{\alpha}}^{\ \ \ \dot{\beta}}\mathbf{\Delta}_{R\ \dot{\kappa}}^{*\nu\rho\ \dot{\gamma}}\mathbf{\Delta}_{R\rho\tau\ \dot{\beta}}^{\ \ \ \dot{\alpha}}\mathbf{\Delta}_{R\ \dot{\gamma}}^{*\tau\mu\ \dot{\kappa}}+\ R\leftrightarrow L\}+\lambda_6\ \mathbf{\Delta}_{R\mu\nu\ \dot{\alpha}}^{\ \ \ \dot{\beta}}\mathbf{\Delta}_{R\ \dot{\beta}}^{*\mu\nu\ \dot{\alpha}}\mathbf{\Delta}_{L\rho\tau\ \alpha}^{\ \ \ \beta}\mathbf{\Delta}_{L\ \beta}^{*\rho\tau\ \alpha}\\&+\lambda_7\ \mathbf{\Delta}_{R\mu\nu\ \dot{\alpha}}^{\ \ \ \dot{\beta}}\mathbf{\Delta}_{R\ \dot{\beta}}^{*\nu\rho\ \dot{\alpha}}\mathbf{\Delta}_{L\rho\tau\ \alpha}^{\ \ \ \beta}\mathbf{\Delta}_{L\ \beta}^{*\tau\mu\ \alpha}+\lambda_8\ \mathbf{\Delta}_{R\mu\nu\ \dot{\alpha}}^{\ \ \ \dot{\beta}}\mathbf{\Delta}_{R\ \dot{\beta}}^{*\rho\tau\ \dot{\alpha}}\mathbf{\Delta}_{L\rho\tau\ \alpha}^{\ \ \ \beta}\mathbf{\Delta}_{L\ \beta}^{*\mu\nu\ \alpha}\\&+(\widetilde{\lambda_9}\ \mathbf{\Delta}_{R\mu\nu\ \dot{\alpha}}^{\ \ \ \dot{\beta}}\mathbf{\Delta}_{R\rho\tau\ \dot{\beta}}^{\ \ \ \dot{\alpha}}\mathbf{\Delta}_{L\lambda\chi\ \alpha}^{\ \ \ \beta}\mathbf{\Delta}_{L\zeta\omega\ \beta}^{\ \ \ \alpha}\epsilon^{\mu\rho\lambda\zeta}\epsilon^{\nu\tau\chi\omega}+\widetilde{\lambda_9}^*\ \mathbf{\Delta}_{R\dot{\alpha}}^{*\mu\nu\ \dot{\beta}}\mathbf{\Delta}_{R\dot{\beta}}^{*\rho\tau\ \dot{\alpha}}\mathbf{\Delta}_{L\alpha}^{*\lambda\chi\ \beta}\mathbf{\Delta}_{L\beta}^{*\zeta\omega\ \alpha}\epsilon_{\mu\rho\lambda\zeta}\epsilon_{\nu\tau\chi\omega}),\end{aligned} \tag{5.6.58}$$

and the mix terms,

$$V_{\mathbf{\Phi\Sigma}} = \alpha_1\ \mathbf{\Phi}^{\dot\alpha}_{\alpha}\mathbf{\Phi}^{*\alpha}_{\dot\alpha}\mathbf{\Sigma}^{\nu\ \dot\beta}_{\mu\ \beta}\mathbf{\Sigma}^{*\mu\ \beta}_{\nu\ \dot\beta} + \alpha_2\ \mathbf{\Phi}^{\dot\alpha}_{\alpha}\mathbf{\Phi}^{*\alpha}_{\dot\beta}\mathbf{\Sigma}^{\nu\ \dot\beta}_{\mu\ \beta}\mathbf{\Sigma}^{*\mu\ \beta}_{\nu\ \dot\alpha} + \alpha_3\ \mathbf{\Phi}^{\dot\alpha}_{\alpha}\mathbf{\Phi}^{*\beta}_{\dot\alpha}\mathbf{\Sigma}^{\nu\ \dot\beta}_{\mu\ \beta}\mathbf{\Sigma}^{*\mu\ \alpha}_{\nu\ \dot\beta} + \alpha_4\ \mathbf{\Phi}^{\dot\alpha}_{\alpha}\mathbf{\Phi}^{*\beta}_{\dot\beta}\mathbf{\Sigma}^{\nu\ \dot\beta}_{\mu\ \beta}\mathbf{\Sigma}^{*\mu\ \alpha}_{\nu\ \dot\alpha}$$
$$+ (\widetilde{\alpha}_5\ \mathbf{\Phi}^{\dot\alpha}_{\alpha}\mathbf{\Phi}^{\dot\beta}_{\beta}\mathbf{\Sigma}^{*\nu\ \alpha}_{\mu\ \dot\alpha}\mathbf{\Sigma}^{*\mu\ \beta}_{\nu\ \dot\beta} + \widetilde{\alpha}^*_5\ \mathbf{\Phi}^{*\alpha}_{\dot\alpha}\mathbf{\Phi}^{*\beta}_{\dot\beta}\mathbf{\Sigma}^{\nu\ \dot\alpha}_{\mu\ \alpha}\mathbf{\Sigma}^{\mu\ \dot\beta}_{\nu\ \beta}) + (\widetilde{\alpha}_6\ \mathbf{\Phi}^{\dot\alpha}_{\alpha}\mathbf{\Phi}^{\dot\beta}_{\beta}\mathbf{\Sigma}^{*\nu\ \alpha}_{\mu\ \dot\beta}\mathbf{\Sigma}^{*\mu\ \beta}_{\nu\ \dot\alpha} + \widetilde{\alpha}^*_6\ \mathbf{\Phi}^{*\alpha}_{\dot\alpha}\mathbf{\Phi}^{*\beta}_{\dot\beta}\mathbf{\Sigma}^{\nu\ \dot\beta}_{\mu\ \alpha}\mathbf{\Sigma}^{\mu\ \dot\alpha}_{\nu\ \beta}),$$
(5.6.59)

$$V_{\mathbf{\Phi\Delta}} = \{\beta_{1R}\ \mathbf{\Phi}^{\dot\alpha}_{\alpha}\mathbf{\Phi}^{*\alpha}_{\dot\alpha}\mathbf{\Delta}_{R\mu\nu\dot\beta}{}^{\dot\gamma}\mathbf{\Delta}^{*\mu\nu\dot\beta}_{R\ \dot\gamma} + \beta_{2R}\ \mathbf{\Phi}^{\dot\alpha}_{\alpha}\mathbf{\Phi}^{*\alpha}_{\dot\beta}\mathbf{\Delta}_{R\mu\nu\dot\alpha}{}^{\dot\gamma}\mathbf{\Delta}^{*\mu\nu\dot\beta}_{R\ \dot\gamma} + \ R\leftrightarrow L\}$$
$$+ (\widetilde{\beta}_3\mathbf{\Phi}^{\dot\alpha}_{\alpha}\mathbf{\Phi}^{\dot\beta}_{\beta}\epsilon_{\alpha\kappa}\epsilon^{\dot\alpha\dot\kappa}\mathbf{\Delta}^{*\mu\nu\ \dot\beta}_{R\dot\kappa}\mathbf{\Delta}_{L\mu\nu\ \kappa}{}^{\beta} + \widetilde{\beta}^*_3\mathbf{\Phi}^{*\alpha}_{\dot\alpha}\mathbf{\Phi}^{*\beta}_{\dot\beta}\epsilon^{\beta\kappa}\epsilon_{\dot\beta\dot\kappa}\mathbf{\Delta}_{R\mu\nu\ \dot\beta}{}^{\dot\kappa}\mathbf{\Delta}^{*\mu\nu\ \beta}_{L\kappa}),$$
(5.6.60)

$$V_{\mathbf{\Sigma\Delta}} = \{\gamma_{1R}\ \mathbf{\Sigma}^{\tau\ \dot\alpha}_{\rho\ \alpha}\mathbf{\Sigma}^{*\rho\ \alpha}_{\tau\ \dot\alpha}\mathbf{\Delta}_{R\mu\nu\dot\beta}{}^{\dot\gamma}\mathbf{\Delta}^{*\mu\nu\dot\beta}_{R\dot\gamma} + \gamma_{2R}\ \mathbf{\Sigma}^{\tau\ \dot\alpha}_{\rho\ \alpha}\mathbf{\Sigma}^{*\mu\ \alpha}_{\tau\ \dot\alpha}\mathbf{\Delta}_{R\mu\nu\dot\beta}{}^{\dot\gamma}\mathbf{\Delta}^{*\nu\rho\dot\beta}_{R\dot\gamma} + \gamma_{3R}\ \mathbf{\Sigma}^{\tau\ \dot\alpha}_{\rho\ \alpha}\mathbf{\Sigma}^{*\rho\ \alpha}_{\mu\ \dot\alpha}\mathbf{\Delta}_{R\tau\nu\dot\beta}{}^{\dot\gamma}\mathbf{\Delta}^{*\nu\mu\dot\beta}_{R\dot\gamma}$$
$$+ \gamma_{4R}\ \mathbf{\Sigma}^{\tau\ \dot\alpha}_{\rho\ \alpha}\mathbf{\Sigma}^{*\nu\ \alpha}_{\mu\ \dot\alpha}\mathbf{\Delta}_{R\tau\nu\dot\beta}{}^{\dot\gamma}\mathbf{\Delta}^{*\rho\mu\dot\beta}_{R\dot\gamma} + \gamma_{5R}\ \mathbf{\Sigma}^{\tau\ \dot\alpha}_{\rho\ \alpha}\mathbf{\Sigma}^{*\rho\ \alpha}_{\tau\ \dot\beta}\mathbf{\Delta}_{R\mu\nu\dot\alpha}{}^{\dot\gamma}\mathbf{\Delta}^{*\mu\nu\dot\beta}_{R\dot\gamma} + \gamma_{6R}\ \mathbf{\Sigma}^{\tau\ \dot\alpha}_{\rho\ \alpha}\mathbf{\Sigma}^{*\mu\ \alpha}_{\tau\ \dot\beta}\mathbf{\Delta}_{R\mu\nu\dot\alpha}{}^{\dot\gamma}\mathbf{\Delta}^{*\nu\rho\dot\beta}_{R\dot\gamma}$$
$$+ \gamma_{7R}\ \mathbf{\Sigma}^{\tau\ \dot\alpha}_{\rho\ \alpha}\mathbf{\Sigma}^{*\rho\ \alpha}_{\mu\ \dot\beta}\mathbf{\Delta}_{R\tau\nu\dot\alpha}{}^{\dot\gamma}\mathbf{\Delta}^{*\nu\mu\dot\beta}_{R\dot\gamma} + \gamma_{8R}\ \mathbf{\Sigma}^{\tau\ \dot\alpha}_{\rho\ \alpha}\mathbf{\Sigma}^{*\nu\ \alpha}_{\mu\ \dot\beta}\mathbf{\Delta}_{R\tau\nu\dot\alpha}{}^{\dot\gamma}\mathbf{\Delta}^{*\rho\mu\dot\beta}_{R\dot\gamma} + \ R\leftrightarrow L\}$$
$$+ (\widetilde{\gamma}_{9R}\ \mathbf{\Sigma}^{\nu\ \dot\alpha}_{\mu\ \alpha}\mathbf{\Sigma}^{\tau\ \dot\beta}_{\rho\ \beta}\epsilon^{\alpha\beta}\epsilon_{\dot\alpha\dot\beta}\mathbf{\Delta}_{R\nu\lambda\ \dot\kappa}{}^{\dot\gamma}\mathbf{\Delta}_{R\tau\chi\ \dot\gamma}{}^{\dot\kappa}\epsilon^{\mu\rho\lambda\chi} + \widetilde{\gamma}^*_{9R}\ \mathbf{\Sigma}^{*\mu\ \alpha}_{\nu\ \dot\alpha}\mathbf{\Sigma}^{*\rho\ \beta}_{\tau\ \dot\beta}\epsilon_{\alpha\beta}\epsilon^{\dot\alpha\dot\beta}\mathbf{\Delta}^{*\nu\lambda\dot\gamma}_{R\ \dot\kappa}\mathbf{\Delta}^{*\tau\chi\ \dot\kappa}_{R\ \dot\gamma}\epsilon_{\mu\rho\lambda\chi})$$
$$+ (\widetilde{\gamma}_{10R}\ \mathbf{\Sigma}^{\nu\ \dot\alpha}_{\mu\ \alpha}\mathbf{\Sigma}^{\tau\ \dot\beta}_{\rho\ \beta}\epsilon^{\alpha\beta}\epsilon_{\dot\alpha\dot\kappa}\mathbf{\Delta}_{R\nu\lambda\ \dot\beta}{}^{\dot\gamma}\mathbf{\Delta}_{R\tau\chi\ \dot\gamma}{}^{\dot\kappa}\epsilon^{\mu\rho\lambda\chi} + \widetilde{\gamma}^*_{10R}\ \mathbf{\Sigma}^{*\mu\ \alpha}_{\nu\ \dot\alpha}\mathbf{\Sigma}^{*\rho\ \beta}_{\tau\ \dot\beta}\epsilon_{\alpha\beta}\epsilon^{\dot\alpha\dot\kappa}\mathbf{\Delta}^{*\nu\lambda\ \dot\beta}_{R\ \dot\gamma}\mathbf{\Delta}^{*\tau\chi\ \dot\gamma}_{R\ \dot\kappa}\epsilon_{\mu\rho\lambda\chi})$$
$$+ (\widetilde{\gamma}_{9L}\ \mathbf{\Sigma}^{*\mu\ \alpha}_{\nu\ \dot\alpha}\mathbf{\Sigma}^{*\rho\ \beta}_{\tau\ \dot\beta}\epsilon_{\alpha\beta}\epsilon^{\dot\alpha\dot\beta}\mathbf{\Delta}_{L\mu\lambda\ \kappa}{}^{\gamma}\mathbf{\Delta}_{L\rho\chi\gamma}{}^{\kappa}\epsilon^{\nu\tau\lambda\chi} + \widetilde{\gamma}^*_{9L}\ \mathbf{\Sigma}^{\nu\ \dot\alpha}_{\mu\ \alpha}\mathbf{\Sigma}^{\tau\ \dot\beta}_{\rho\ \beta}\epsilon^{\alpha\beta}\epsilon_{\dot\alpha\dot\beta}\mathbf{\Delta}^{*\mu\lambda\ \gamma}_{L\ \kappa}\mathbf{\Delta}^{*\rho\chi\ \kappa}_{L\ \gamma}\epsilon_{\nu\tau\lambda\chi})$$
$$+ (\widetilde{\gamma}_{10L}\ \mathbf{\Sigma}^{*\mu\ \alpha}_{\nu\ \dot\alpha}\mathbf{\Sigma}^{*\rho\ \beta}_{\tau\ \dot\beta}\epsilon_{\alpha\kappa}\epsilon^{\dot\alpha\dot\beta}\mathbf{\Delta}_{L\mu\lambda\ \gamma}{}^{\kappa}\mathbf{\Delta}_{L\rho\chi\beta}{}^{\gamma}\epsilon^{\nu\tau\lambda\chi} + \widetilde{\gamma}^*_{10L}\ \mathbf{\Sigma}^{\nu\ \dot\alpha}_{\mu\ \alpha}\mathbf{\Sigma}^{\tau\ \dot\beta}_{\rho\ \beta}\epsilon^{\alpha\kappa}\epsilon_{\dot\alpha\dot\beta}\mathbf{\Delta}^{*\mu\lambda\ \gamma}_{L\ \kappa}\mathbf{\Delta}^{*\rho\chi\ \beta}_{L\ \gamma}\epsilon_{\nu\tau\lambda\chi})$$
$$+ (\widetilde{\eta}_1\ \mathbf{\Sigma}^{\nu\ \dot\alpha}_{\mu\ \alpha}\mathbf{\Sigma}^{*\tau\ \beta}_{\rho\ \dot\beta}\mathbf{\Delta}_{R\nu\lambda\ \dot\alpha}{}^{\dot\beta}\mathbf{\Delta}_{L\tau\chi\ \beta}{}^{\alpha}\epsilon^{\mu\rho\lambda\chi} + \widetilde{\eta}^*_1\ \mathbf{\Sigma}^{*\nu\ \alpha}_{\mu\ \dot\alpha}\mathbf{\Sigma}^{\tau\ \dot\beta}_{\rho\ \beta}\mathbf{\Delta}^{*\mu\lambda\dot\alpha}_{R\ \dot\beta}\mathbf{\Delta}^{*\rho\chi\beta}_{L\ \alpha}\epsilon_{\nu\tau\lambda\chi})$$
$$+ (\widetilde{\eta}_2\ \mathbf{\Sigma}^{\nu\ \dot\alpha}_{\mu\ \alpha}\mathbf{\Sigma}^{\mu\ \dot\beta}_{\nu\ \beta}\epsilon^{\alpha\kappa}\epsilon_{\dot\alpha\dot\kappa}\mathbf{\Delta}_{R\lambda\chi\ \dot\beta}{}^{\dot\kappa}\mathbf{\Delta}^{*\lambda\chi\ \beta}_{L\ \kappa} + \widetilde{\eta}^*_2\ \mathbf{\Sigma}^{*\mu\ \alpha}_{\nu\ \dot\alpha}\mathbf{\Sigma}^{*\nu\ \beta}_{\mu\ \dot\beta}\epsilon_{\alpha\kappa}\epsilon^{\dot\alpha\dot\kappa}\mathbf{\Delta}^{*\lambda\chi\ \dot\beta}_{R\ \dot\kappa}\mathbf{\Delta}_{L\lambda\chi\ \beta}{}^{\kappa})$$
$$+ (\widetilde{\eta}_3\ \mathbf{\Sigma}^{\nu\ \dot\alpha}_{\mu\ \alpha}\mathbf{\Sigma}^{\mu\ \dot\beta}_{\rho\ \beta}\epsilon^{\alpha\kappa}\epsilon_{\dot\alpha\dot\kappa}\mathbf{\Delta}^{\dot\kappa}_{R\nu\tau\ \dot\beta}\mathbf{\Delta}^{*\tau\rho\ \beta}_{L\ \kappa} + \widetilde{\eta}^*_3\ \mathbf{\Sigma}^{*\mu\ \alpha}_{\nu\ \dot\alpha}\mathbf{\Sigma}^{*\rho\ \beta}_{\mu\ \dot\beta}\epsilon_{\alpha\kappa}\epsilon_{\dot\alpha\dot\kappa}\mathbf{\Delta}^{*\nu\tau\ \dot\beta}_{R\ \dot\kappa}\mathbf{\Delta}_{L\tau\rho\ \beta}{}^{\kappa})$$
$$+ (\widetilde{\eta}_4\ \mathbf{\Sigma}^{\nu\ \dot\alpha}_{\mu\ \alpha}\mathbf{\Sigma}^{\tau\ \dot\beta}_{\rho\ \beta}\epsilon^{\alpha\kappa}\epsilon_{\dot\alpha\dot\kappa}\mathbf{\Delta}_{R\ \nu\tau\ \dot\beta}{}^{\dot\kappa}\mathbf{\Delta}^{*\mu\rho\beta}_{L\ \kappa} + \widetilde{\eta}^*_4\ \mathbf{\Sigma}^{*\mu\ \alpha}_{\nu\ \dot\alpha}\mathbf{\Sigma}^{*\rho\ \beta}_{\tau\ \dot\beta}\epsilon_{\alpha\kappa}\epsilon^{\dot\alpha\dot\kappa}\mathbf{\Delta}^{*\nu\tau\ \dot\beta}_{R\ \dot\kappa}\mathbf{\Delta}_{L\mu\rho\ \beta}{}^{\kappa}),$$
(5.6.61)

$$V_{\mathbf{\Phi\Sigma\Delta}} = \{(\widetilde{\chi}_{1R}\ \mathbf{\Phi}^{*\alpha}_{\dot\alpha}\mathbf{\Sigma}^{\nu\ \dot\alpha}_{\mu\ \alpha}\mathbf{\Delta}_{R\nu\rho\dot\beta}{}^{\dot\gamma}\mathbf{\Delta}^{*\rho\mu\dot\beta}_{R\dot\gamma} + \widetilde{\chi}^*_{1R}\ \mathbf{\Phi}^{\dot\alpha}_{\alpha}\mathbf{\Sigma}^{*\nu\ \alpha}_{\mu\ \dot\alpha}\mathbf{\Delta}_{R\nu\rho\dot\beta}{}^{\dot\gamma}\mathbf{\Delta}^{*\rho\mu\dot\beta}_{R\dot\gamma})$$
$$+ (\widetilde{\chi}_{2R}\ \mathbf{\Phi}^{*\alpha}_{\dot\alpha}\mathbf{\Sigma}^{\nu\ \dot\beta}_{\mu\ \alpha}\mathbf{\Delta}_{R\nu\rho\dot\beta}{}^{\dot\gamma}\mathbf{\Delta}^{*\rho\mu\dot\alpha}_{R\dot\gamma} + \widetilde{\chi}^*_{2R}\ \mathbf{\Phi}^{\dot\alpha}_{\alpha}\mathbf{\Sigma}^{*\nu\ \alpha}_{\mu\ \dot\beta}\mathbf{\Delta}_{R\nu\rho\dot\alpha}{}^{\dot\gamma}\mathbf{\Delta}^{*\rho\mu\dot\beta}_{R\dot\gamma}) + \ R\leftrightarrow L\}$$
$$+ (\widetilde{\chi}_3\ \mathbf{\Phi}^{\dot\alpha}_{\alpha}\mathbf{\Sigma}^{\nu\ \dot\beta}_{\mu\ \beta}\epsilon^{\alpha\kappa}\epsilon_{\dot\alpha\dot\kappa}\mathbf{\Delta}_{R\nu\tau\ \dot\beta}{}^{\dot\kappa}\mathbf{\Delta}^{*\tau\mu\ \beta}_{L\ \kappa} + \widetilde{\chi}^*_3\ \mathbf{\Phi}^{*\alpha}_{\dot\alpha}\mathbf{\Sigma}^{*\mu\ \beta}_{\nu\ \dot\beta}\epsilon_{\alpha\kappa}\epsilon^{\dot\alpha\dot\kappa}\mathbf{\Delta}^{*}_{R\nu\tau\ \dot\kappa}{}^{\dot\beta}\mathbf{\Delta}_{L\tau\mu\ \beta}{}^{\kappa}),$$
(5.6.62)

$$V_{\mathcal{S}} = -\mu^2_{\mathcal{S}}\ \mathcal{S}\mathcal{S}^* + \lambda_{\mathcal{S}}\ \mathcal{S}\mathcal{S}^*\mathcal{S}\mathcal{S}^* + (\xi_1\ \mathbf{\Phi}^{\dot\alpha}_{\alpha}\mathbf{\Phi}^{*\alpha}_{\dot\alpha} + \xi_2\ \mathbf{\Sigma}^{\nu\ \dot\alpha}_{\mu\ \alpha}\mathbf{\Sigma}^{*\mu\ \dot\alpha}_{\nu\ \alpha} + \{\xi_{3R}\ \mathbf{\Delta}_{R\mu\nu\dot\alpha}{}^{\dot\beta}\mathbf{\Delta}^{*\mu\nu\dot\alpha}_{R\ \dot\beta} + \ R\leftrightarrow L\})\mathcal{S}\mathcal{S}^*$$
$$+ (\widetilde{\zeta}\mathbf{\Phi}^{\dot\alpha}_{\alpha}\mathbf{\Phi}^{\dot\beta}_{\beta}\epsilon^{\alpha\beta}\epsilon_{\dot\alpha\dot\beta}\mathcal{S}^* + \widetilde{\zeta}^*\mathbf{\Phi}^{*\alpha}_{\dot\alpha}\mathbf{\Phi}^{*\beta}_{\dot\beta}\epsilon_{\alpha\beta}\epsilon^{\dot\alpha\dot\beta}\mathcal{S}) + (\widetilde{\omega}\mathbf{\Sigma}^{\nu\ \dot\alpha}_{\mu\ \alpha}\mathbf{\Sigma}^{\mu\ \dot\beta}_{\nu\ \beta}\epsilon^{\alpha\beta}\epsilon_{\dot\alpha\dot\beta}\mathcal{S}^* + \widetilde{\omega}^*\mathbf{\Sigma}^{*\nu\ \dot\alpha}_{\mu\ \alpha}\mathbf{\Sigma}^{*\mu\ \beta}_{\nu\ \dot\beta}\epsilon_{\alpha\beta}\epsilon^{\dot\alpha\dot\beta}\mathcal{S}).$$
(5.6.63)

To differentiate the complex couplings from the real ones in the potential we put tilde on the top of the complex ones. All the index contractions are shown explicitly. The parameters with dimension of mass are $\mu_\phi, \mu_\Sigma, \mu_\Delta, \mu_{\mathcal{S}}, \widetilde{\zeta}, \widetilde{\omega}$. To find the maximum possible number of invariants of each kind one needs to use the group theoretical rules of tensor product decomposition (for details see Ref. [189]). Note that in general there can be more gauge invariant terms in the Higgs potential, but those are absent in out theory due to the presence of the $U(1)_{PQ}$ symmetry. Below we discuss the constraints on the cubic and quartic couplings in the potential

due to additional left-right parity symmetry.

Scalar potential in the left-right parity symmetric limit

If the parity symmetry is assumed to be a good symmetry then there are further restrictions on the potential Eq. (5.6.55). Under left-right parity, the fermions and the scalar fields transform as

$$\mathbf{\Psi}_L \longleftrightarrow \mathbf{\Psi}_R,\ \ \mathbf{\Phi} \longleftrightarrow \mathbf{\Phi}^*,\ \ \mathbf{\Sigma} \longleftrightarrow \mathbf{\Sigma}^*,\ \ \mathbf{\Delta}_R \longleftrightarrow \mathbf{\Delta}_L,\ \ \mathcal{S} \longleftrightarrow \mathcal{S}^*. \tag{5.6.64}$$

The terms that are achieved by $R \leftrightarrow L$ in Eq. (5.6.55) have exactly the same coupling constants, for example, $\mu^2_{\Delta_L} = \mu^2_{\Delta_R}$, $\lambda_{iL} = \lambda_{iR}$ $(i = 1 - 5)$ and so on. Also due to the invariance under parity, some of the complex couplings in the potential will become real, they are,

$$\widetilde{\alpha}_{5,6},\ \widetilde{\beta}_3,\ \widetilde{\eta}_{4,5,6},\ \widetilde{\chi}_3,\ \widetilde{\zeta},\ \widetilde{\omega}\ \in \mathbb{R}. \tag{5.6.65}$$

The only six couplings in the potential that remain complex are

$$\widetilde{\lambda}_9,\ \widetilde{\gamma}_{9,10},\ \widetilde{\eta}_1,\ \widetilde{\chi}_{1,2} \in \mathbb{C}. \tag{5.6.66}$$

Note that, under parity, if the singlet field is odd, i.e, instead of $\mathcal{S} \longleftrightarrow \mathcal{S}^*$, if the transformation property is $\mathcal{S} \longleftrightarrow -\mathcal{S}^*$, then the cubic couplings $\widetilde{\zeta}$ and $\widetilde{\omega}$ become purely imaginary. If the VEV of the parity odd singlet is $v_S > v_R$, then the parity breaking scale and the $SU(2)_R$ breaking scale can be decoupled and in this scenario the PS breaking scale can be as low as 10^6 GeV as mentioned earlier.

5.6.2 The scalar mass spectrum

Mass spectrum of Δ_R scalar fields

The Yukawa Lagrangian of the theory is given in Eq. (5.3.24), where the first two terms are the Dirac type Yukawa couplings. The third term generates the right-handed neutrino Majorana masses when the PS symmetry is broken by the VEV $\langle(1,3,10)\rangle$. Expanding this term of the Yukawa coupling one gets (here $\mathbf{\Delta}$ represents $\mathbf{\Delta}_R$):

$$\begin{aligned}\mathcal{L}_{Majorana} = Y^R_{10_{ij}}\{&\nu^T_{Ri}C\nu_{Rj}\mathbf{\Delta}^*_{\nu\nu} - e^T_{Ri}Ce_{Rj}\mathbf{\Delta}^*_{ee} - (e^T_{Ri}\nu_{Rj} + \nu^T_{Ri}Ce_{Rj})\mathbf{\Delta}^*_{e\nu} + u^T_{Ri}Cu_{Rj}\mathbf{\Delta}^*_{uu}\\ &- d^T_{Ri}Cd_{Rj}\mathbf{\Delta}^*_{dd} - (u^T_{Ri}Cd_{Rj} + d^T_{Ri}Cu_{Rj})\mathbf{\Delta}^*_{ud} + (u^T_{Ri}C\nu_{Rj} + \nu^T_{Ri}Cu_{Rj})\mathbf{\Delta}^*_{u\nu}\\ &- (e^T_{Ri}Cd_{Rj} + d^T_{Ri}Ce_{Rj})\mathbf{\Delta}^*_{de} - (d^T_{Ri}C\nu_{Rj} + \nu^T_{Ri}Cd_{Rj} + e^T_{Ri}Cu_{Rj} + u^T_{Ri}Ce_{Rj})\mathbf{\Delta}^*_{ue}\} + h.c\end{aligned} \tag{5.6.67}$$

with the following identification

$$\mathbf{\Delta}^*_{\nu\nu}(1,1,0) = \mathbf{\Delta}^{*44\ \dot{1}}_{\dot{2}}; \qquad \mathbf{\Delta}^*_{ee}(1,1,2) = \mathbf{\Delta}^{*44\ \dot{2}}_{\dot{1}}; \quad \mathbf{\Delta}^*_{e\nu}(1,1,1) = \mathbf{\Delta}^{*44\ \dot{1}}_{\dot{1}}\ ; \tag{5.6.68}$$

$$\mathbf{\Delta}^*_{uu}(\overline{6},1,-\frac{4}{3}) = \mathbf{\Delta}^{*\bar{\mu}\bar{\nu}\ \dot{1}}_{\dot{2}}; \quad \mathbf{\Delta}^*_{dd}(\overline{6},1,\frac{2}{3}) = \mathbf{\Delta}^{*\bar{\mu}\bar{\nu}\ \dot{2}}_{\dot{1}}; \quad \mathbf{\Delta}^*_{ud}(\overline{6},1,-\frac{1}{3}) = \mathbf{\Delta}^{*\bar{\mu}\bar{\nu}\ \dot{1}}_{\dot{1}}\ ; \tag{5.6.69}$$

$$\mathbf{\Delta}^*_{u\nu}(\overline{3},1,-\frac{2}{3}) = \mathbf{\Delta}^{*\bar{\mu}4\ \dot{1}}_{\dot{2}}; \quad \mathbf{\Delta}^*_{de}(\overline{3},1,\frac{4}{3}) = \mathbf{\Delta}^{*\bar{\mu}4\ \dot{2}}_{\dot{1}}; \quad \mathbf{\Delta}^*_{ue}(\overline{3},1,\frac{1}{3}) = \mathbf{\Delta}^{*\bar{\mu}4\ \dot{1}}_{\dot{1}}. \tag{5.6.70}$$

Only the neutral component gets VEV, $v_R = \langle \mathbf{\Delta}_{\nu\nu} \rangle$. With this identification and by minimizing the potential Eq. (5.6.55), one can compute the mass spectrum of $\mathbf{\Delta}_R$. The PS breaking minimization conditions is

$$\frac{\partial V_\Delta}{\partial v_R} = v_R[2v_R^2(\lambda_{1R} + \lambda_{3R} + \lambda_{4R}) - \mu_\Delta^2] = 0. \tag{5.6.71}$$

Choosing the non-trivial solution with $v_R \neq 0$, this equation is used to eliminate μ_Δ^2 from the potential. Imposing this extremum condition back to the potential one gets the following mass spectrum for $\mathbf{\Delta}_R$:

$$m^2_{\Delta_{\nu\nu}} = 2\ v_R^2\ (\lambda_{1R} + \lambda_{3R} + \lambda_{4R}), \tag{5.6.72}$$

$$m^2_{\Delta_{ee}} = 4\ v_R^2\ (\lambda_{2R} + \lambda_{5R}), \tag{5.6.73}$$

$$m^2_{\Delta_{e\nu}} = 0, \tag{5.6.74}$$

$$m^2_{\Delta_{uu}} = -2\ v_R^2\ \lambda_{4R}, \tag{5.6.75}$$

$$m^2_{\Delta_{dd}} = 2\ v_R^2\ (\lambda_{2R} - \lambda_{3R} - \lambda_{4R}), \tag{5.6.76}$$

$$m^2_{\Delta_{ud}} = -2\ v_R^2\ (\lambda_{3R} + \lambda_{4R}), \tag{5.6.77}$$

$$m^2_{\Delta_{u\nu}} = 0, \tag{5.6.78}$$

$$m^2_{\Delta_{de}} = 2\ v_R^2\ (2\ \lambda_{2R} - 2\ \lambda_{3R} - \lambda_{4R} + 2\ \lambda_{5R}), \tag{5.6.79}$$

$$m^2_{\Delta_{ue}} = -2\ v_R^2\ (2\ \lambda_{3R} + \lambda_{4R}). \tag{5.6.80}$$

There is a mass relation which is given by

$$m^2_{\Delta_{ee}} = m^2_{\Delta_{de}} - m^2_{\Delta_{ud}} + m^2_{\Delta_{uu}}. \tag{5.6.81}$$

There exist seven physical Higgs states $\mathbf{\Delta}_{\nu\nu}, \mathbf{\Delta}_{ee}, \mathbf{\Delta}_{uu}, \mathbf{\Delta}_{dd}, \mathbf{\Delta}_{ud}, \mathbf{\Delta}_{de}, \mathbf{\Delta}_{ue}$ and three Nambu-Goldstone boson states $\mathbf{\Delta}_{e\nu}, \mathbf{\Delta}_{u\nu}$ and $i(\mathbf{\Delta}_{44\ \dot{1}}^{\ \ \dot{2}} - \mathbf{\Delta}^{*44\ \dot{1}}_{\dot{2}})/2 \equiv \mathbf{\Delta}_G$. As mentioned in Sec. 5.2.2, due to the $G_{224} \to G_{213}$ breaking, 9 of the gauge bosons become massive after eating up the 9 Goldstone bosons. These Goldstone bosons correspond to $\mathbf{\Delta}_{e\nu}$, $\mathbf{\Delta}_{u\nu}$ and $\mathbf{\Delta}_G$ (real field) fields. We note that these sextets can have rich phenomenology if their masses are relatively low, for example, these sextets can be responsible for generating baryon asymmetry after the sphaleron decoupling, see Ref. [190–193]. By considering the sextet masses at the TeV scale flavor physics constraints are also computed in Ref. [194].

If both the PS and PQ symmetry breaking are taken into account together, where the PQ symmetry is broken by the complex singlet VEV, $\langle \mathcal{S} \rangle = v_S$ the minimization conditions are

$$\frac{\partial V}{\partial v_R} = v_R[2v_R^2(\lambda_{1R} + \lambda_{3R} + \lambda_{4R} + v_S^2\xi_{3R}) - \mu_\Delta^2] = 0 \text{ and} \tag{5.6.82}$$

$$\frac{\partial V}{\partial v_S} = v_S[2v_S^2\lambda_{\mathcal{S}} + v_R^2\xi_{3R} - \mu_{\mathcal{S}}^2] = 0. \tag{5.6.83}$$

Assuming the general symmetry breaking solutions $v_S \neq 0$ and $v_R \neq 0$, these equations can be used to solve for μ_Δ^2 and $\mu_{\mathcal{S}}^2$. Using these minimization conditions like before one can easily derive the mass spectrum for the $\mathbf{\Delta}_R$ and $\mathcal{S}$ fields. The mass spectrum essentially remain unchanged except $\mathbf{\Delta}_{\nu\nu}$ mixes with the real part of the singlet field. The two by two mass squared matrix of this mixing in the basis $\{\mathbf{\Delta}_{\nu\nu}, Re[\mathcal{S}]\}$ is given by

$$\begin{pmatrix} 2\ v_R^2\ (\lambda_{1R} + \lambda_{3R} + \lambda_{4R}) & 2v_S v_R \xi_{3R} \\ 2v_S v_R \xi_{3R} & 4v_S^2\lambda_{\mathcal{S}} \end{pmatrix}. \tag{5.6.84}$$

The imaginary part of $\mathcal{S}$ remains massless after the PQ symmetry breaking. After EW symmetry breaking, this field will eventually mix with the components from the four doublets coming from $\mathbf{\Phi}$ and $\mathbf{\Sigma}$ and receive a mass of the order of v_{ew}/v_S. Since $v_{ew} \ll v_S$, this field will remain essentially massless and can be identified as the axion field.

The doublet $(1, 2, \pm 1/2)$ mass square matrix

In the model, there are two complex bidoublets (2,2,1) and (2,2,15) that contain four $SU_L(2)$ doublets. Among them, two of them are $\mathbf{\Phi}_\alpha^{\dot{1}}$ and $\mathbf{\Sigma}_\alpha^{\dot{1}} \equiv -\frac{2}{\sqrt{3}}\mathbf{\Sigma}_4^{4\ \dot{1}}{}_\alpha$ that have the quantum number $(1, 2, -1/2)$ under the SM and the other two are $\mathbf{\Phi}_\alpha^{\dot{2}}$ and $\mathbf{\Sigma}_\alpha^{\dot{2}} \equiv -\frac{2}{\sqrt{3}}\mathbf{\Sigma}_4^{4\ \dot{2}}{}_\alpha$ which have quantum number of $(1, 2, +1/2)$ under the SM. Writing as,

$$h_\alpha^{(i)} = \{\mathbf{\Phi}_\alpha^{\dot{1}}, \mathbf{\Sigma}_\alpha^{\dot{1}}, \mathbf{\Phi}_{\dot{2}}^{*\beta}\epsilon_{\beta\alpha}, \mathbf{\Sigma}_{\dot{2}}^{*\beta}\epsilon_{\beta\alpha}\} \tag{5.6.85}$$

and similarly

$$\bar{h}^{(i)\alpha} = \{\mathbf{\Phi}_{\dot{1}}^{*\alpha}, \mathbf{\Sigma}_{\dot{1}}^{*\alpha}, \mathbf{\Phi}_{\dot{\beta}}^{\dot{2}}\epsilon^{\beta\alpha}, \mathbf{\Sigma}_{\dot{\beta}}^{\dot{2}}\epsilon^{\beta\alpha}\} \tag{5.6.86}$$

the doublet mass squared matrix, $\mathcal{D}$ in the flavor basis can be found from the potential as

$$\bar{h}^{\alpha(j)}\mathcal{D}_{ij}h_\alpha^{(i)}. \tag{5.6.87}$$

It is straightforward to compute this doublet mass square matrix,

$$\mathcal{D} = \begin{pmatrix} -\mu_\phi^2 + v_R^2\ (\beta_1 + \beta_2) + v_S^2\ \xi_1 & -\frac{\sqrt{3}}{2}v_R^2\ (\tilde{\chi}_1^* + \tilde{\chi}_2^*) & 2\ v_S\ \tilde{\zeta} & 0 \\ -\frac{\sqrt{3}}{2}v_R^2\ (\tilde{\chi}_1 + \tilde{\chi}_2) & -\mu_\Sigma^2 + v_R^2\ A_2 + v_S^2\ \xi_2 & 0 & 2\ v_S\ \tilde{\omega} \\ 2\ v_S\ \tilde{\zeta}^* & 0 & -\mu_\phi^2 + v_R^2\ \beta_1 + v_S^2\xi_1 & -\frac{\sqrt{3}}{2}v_R^2\ \tilde{\chi}_1 \\ 0 & 2\ v_S\ \tilde{\omega}^* & -\frac{\sqrt{3}}{2}v_R^2\ \tilde{\chi}_1^* & -\mu_\Sigma^2 + v_R^2\ A_1 + v_S^2\ \xi_2 \end{pmatrix} \tag{5.6.88}$$

where we have defined

$$A_1 = \gamma_1 + \frac{3}{4}(\gamma_2 + \gamma_3 + \gamma_4),\ A_2 = A_1 + \gamma_5 + \frac{3}{4}(\gamma_6 + \gamma_7 + \gamma_8). \tag{5.6.89}$$

Recall that if parity symmetry is imposed, $\widetilde{\zeta}$ and $\widetilde{\omega}$ will be real but $\widetilde{\chi}_{1,2}$ entering in this matrix will remain complex, so in general $\mathcal{D}$ will have two independent phases entering in this matrix.

The Hermitian matrix, $\mathcal{D}$ can be diagonalized as $\mathcal{D} = U\Lambda U^\dagger$ where U is an unitary matrix (Λ is the diagonal matrix) that relates the flavor basis, $h_\alpha^{(i)}$ and mass basis, $h_\alpha^{\prime(i)}$ states as,

$$\bar{h}^{\alpha(i)}\mathcal{D}_{ij}h_\alpha^{(j)} = \bar{h}^{\alpha(i)}U_{il}\Lambda_{lk}U^*_{jk}h_\alpha^{(j)} = \bar{h}^{\alpha\prime(i)}\Lambda_{ij}h_\alpha^{\prime(j)}. \tag{5.6.90}$$

So

$$h_\alpha^{\prime(k)} = U^*_{jk}h_\alpha^{(j)}. \tag{5.6.91}$$

The doublet mass matrix written here is before the EW phase transition, so the SM Higgs doublet will correspond to the zero eigenvalue solution, which can be found by imposing the fine tuning condition $det(\mathcal{D}) = 0$. One can write the SM Higgs doublet that is a linear combination of the four doublets as,

$$H \equiv h_\alpha^{\prime(1)} = U^*_{j1}h_\alpha^{(j)}, \quad \text{that gives,} \quad h_\alpha^{(i)} = U_{ji}h_\alpha^{\prime(j)}. \tag{5.6.92}$$

When the SM doublet acquires VEV, $\langle H\rangle = v_{\rm EW}$, the EW phase transition takes place and one gets,

$$\langle h_\alpha^{(1)}\rangle = U_{11}v_{\rm EW} \equiv \alpha\ v_{\rm EW}, \quad \langle h_\alpha^{(2)}\rangle = U_{12}v_{\rm EW} \equiv \beta\ v_{\rm EW}, \tag{5.6.93}$$

$$\langle h_\alpha^{(3)}\rangle = U_{13}v_{\rm EW} \equiv \gamma\ v_{\rm EW}, \quad \langle h_\alpha^{(4)}\rangle = U_{14}v_{\rm EW} \equiv \delta\ v_{\rm EW}. \tag{5.6.94}$$

By finding the matrix elements U_{ij} it can be shown that the combinations $\alpha\gamma^*$ and $\beta\delta^*$ will remain complex and so all the VEVs in Eq. (5.6.93) cannot be taken to be real. This is why the VEV ratios of the doublets that appears in the fermion mass matrices are in general complex. This conclusion is also applicable for the case with parity symmetry imposed, since $\widetilde{\chi}_{1,2}$ that are complex couplings will introduce two independent phases in $\mathcal{D}$.

The triplet $(3, 2, \pm\frac{1}{6})$ mass square matrix

The color triplets are $\mathbf{\Sigma}_{\bar{\mu}\ \alpha}^{4\ \dot{1}}$ and $\mathbf{\Sigma}_{4\ \alpha}^{\bar{\mu}\ \dot{2}}$ that are $(3, 2, +1/6)$ and $(\overline{3}, 2, -1/6)$ under the SM group respectively. The mass square matrix is given as follows

$$\begin{pmatrix} \mathbf{\Sigma}_{\bar{\mu}\ \alpha}^{4\ \dot{1}} & \mathbf{\Sigma}_{\bar{\mu}\ \dot{2}}^{*4\ \beta}\epsilon_{\beta\alpha} \end{pmatrix} \begin{pmatrix} -\mu_\Sigma^2 + v_R^2(\gamma_1 + \gamma_3 + \gamma_5 + \gamma_7) + v_\mathcal{S}^2\xi_2 & 2\ v_\mathcal{S}\ \widetilde{\omega} \\ 2\ v_\mathcal{S}\ \widetilde{\omega}^* & -\mu_\Sigma^2 + v_R^2(\gamma_1 + \gamma_2) + v_\mathcal{S}^2\ \xi_2 \end{pmatrix} \begin{pmatrix} \mathbf{\Sigma}_{4\ \dot{1}}^{*\bar{\mu}\ \alpha} \\ \mathbf{\Sigma}_{4\ \sigma}^{\bar{\mu}\ \dot{2}}\epsilon^{\sigma\alpha} \end{pmatrix}. \tag{5.6.95}$$

Note that if the parity symmetry is imposed, all the matrix elements in this mass squared matrix will become real.

The triplet $(3,2,\pm\frac{7}{6})$ mass square matrix

The color triplets are $\mathbf{\Sigma}^{4\ \dot{2}}_{\bar{\mu}\ \alpha}$ and $\mathbf{\Sigma}^{\bar{\mu}\ \dot{1}}_{4\ \alpha}$ that are $(3,2,+7/6)$ and $(\overline{3},2,-7/6)$ under the SM group respectively. The mass square matrix is given as follows

$$\begin{pmatrix} \mathbf{\Sigma}^{4\ \dot{2}}_{\bar{\mu}\ \alpha} & \mathbf{\Sigma}^{*4\ \beta}_{\bar{\mu}\ \dot{1}}\epsilon_{\beta\alpha} \end{pmatrix} \begin{pmatrix} -\mu_\Sigma^2 + v_R^2(\gamma_1+\gamma_3) + v_{\mathcal{S}}^2\xi_2 & -2\ v_{\mathcal{S}}\ \widetilde{\omega} \\ -2\ v_{\mathcal{S}}\ \widetilde{\omega}^* & -\mu_\Sigma^2 + v_R^2(\gamma_1+\gamma_2+\gamma_5+\gamma_6) + v_{\mathcal{S}}^2\ \xi_2 \end{pmatrix} \begin{pmatrix} \mathbf{\Sigma}^{*\bar{\mu}\ \alpha}_{4\ \dot{2}} \\ \mathbf{\Sigma}^{\bar{\mu}\ \dot{1}}_{4\ \sigma}\epsilon^{\sigma\alpha} \end{pmatrix}. \tag{5.6.96}$$

Again if the parity symmetry is imposed, all the matrix elements in this mass squared matrix will become real.

The octet $(8,2,\pm\frac{1}{2})$ mass square matrix

The color octets are $\mathbf{\Sigma}^{\bar{\nu}\ \dot{1}}_{\bar{\mu}\ \alpha}$ and $\mathbf{\Sigma}^{\bar{\nu}\ \dot{2}}_{\bar{\mu}\ \alpha}$ that are (8,2,-1/2) and (8,2,+1/2) under the SM group respectively. The mass square matrix is given as follows

$$\begin{pmatrix} \mathbf{\Sigma}^{\bar{\nu}\ \dot{1}}_{\bar{\mu}\ \alpha} & \mathbf{\Sigma}^{*\bar{\nu}\ \beta}_{\bar{\mu}\ \dot{2}}\epsilon_{\beta\alpha} \end{pmatrix} \begin{pmatrix} -\mu_\Sigma^2 + v_R^2(\gamma_1+\gamma_5) + v_{\mathcal{S}}^2\xi_2 & 2\ v_{\mathcal{S}}\ \widetilde{\omega} \\ 2\ v_{\mathcal{S}}\ \widetilde{\omega}^* & -\mu_\Sigma^2 + v_R^2\ \gamma_1 + v_{\mathcal{S}}^2\ \xi_2 \end{pmatrix} \begin{pmatrix} \mathbf{\Sigma}^{*\bar{\mu}\ \alpha}_{\bar{\nu}\ \dot{1}} \\ \mathbf{\Sigma}^{\bar{\mu}\ \dot{2}}_{\bar{\nu}\ \sigma}\epsilon^{\sigma\alpha} \end{pmatrix}. \tag{5.6.97}$$

Just like the previous cases, if parity is a good symmetry, this mass squared matrix will become real.

The mass spectrum of $\mathbf{\Delta}_L$ field

The identification of the $(3,1,10^*)$ field under the SM multiplets is (here $\mathbf{\Delta}$ represents $\mathbf{\Delta}_L$):

$$\mathbf{\Delta}^*_{qq}(\overline{6},3,-\frac{1}{3}) = \mathbf{\Delta}^{*\overline{\mu\nu}\ \beta}_{\alpha}, \quad \mathbf{\Delta}^*_{ql}(\overline{3},3,\frac{1}{3}) = \mathbf{\Delta}^{*\overline{\mu}4\ \beta}_{\alpha}, \quad \mathbf{\Delta}^*_{ll}(1,3,-1) = \mathbf{\Delta}^{*44\ \beta}_{\alpha}. \tag{5.6.98}$$

The mass spectrum of these fields are given as follows:

$$m^2_{\Delta_{ll}} = -\mu^2_{\Delta_L} + v_R^2\ (\lambda_{6L} + \lambda_{7L} + \lambda_{8L}) + v_{\mathcal{S}}^2\ \xi_{L3} \tag{5.6.99}$$

$$m^2_{\Delta_{qq}} = -\mu^2_{\Delta_L} + v_R^2\ \lambda_{6L} + v_{\mathcal{S}}^2\ \xi_{L3} \tag{5.6.100}$$

$$m^2_{\Delta_{ql}} = -2\mu^2_{\Delta_L} + v_R^2\ (2\lambda_{6L} + \lambda_{7L}) + 2v_{\mathcal{S}}^2\ \xi_{L3}. \tag{5.6.101}$$

5.7 Baryon number violation

5.7.1 Nucleon decay

Though nucleon decay is not mediated by the gauge bosons of the PS group, depending on the detail of the scalar sector, nucleon may decay. A PS model with scalars (2,2,1), (1,3,10) and (3,1,10) nucleon is absolutely stable. The reason of the stability is due to the existence of a hidden discrete symmetry [195] in the model $q_\mu \to e^{i\pi/3} q_\mu$, $\mathbf{\Delta}_{\mu\nu} \to e^{-2i\pi/3}\mathbf{\Delta}_{\mu\nu}$, $\mathbf{\Delta}_{\mu 4} \to e^{i\pi/3}\mathbf{\Delta}_{\mu 4}$. The Lagrangian is invariant under the discrete symmetry even after SSB. But the scalar sector Eq. (5.2.3) that we are considering which also contains (2,2,15) multiplet, in principle can lead to baryon(B) and lepton(L) violating processes by nucleon decay [163, 196], due to the presence of some specific quartic terms in the scalar potential Eq. (5.6.55). In our model, the part of the potential $V_{\Sigma\Delta}$ in Eq. (5.6.61) contains terms that can cause the nucleon to decay. The terms with coupling coefficients $\widetilde{\gamma}_9, \widetilde{\gamma}_{10}, \widetilde{\eta}_1$ in Eq. (5.6.61) in combination with Yukawa interactions Eq. (5.3.24) are responsible for $|\Delta(B-L)| = 2$ processes when the symmetry gets broken spontaneously by $\langle \mathbf{\Delta}_R \rangle$. These $(B+L)$ conserving processes cause the proton to decay into leptons and mesons. The feynman diagrams corresponding to such quartic terms involving processes like $3q \to q\overline{q}l$ ($p, n \to l+$ mesons, with $l = e^-, \mu^-, \nu_e, \nu_\mu$; meson= π, K, etc.) contain $SU(3)_C$ triplets, $\mathbf{\Sigma}_3$ and octets, $\mathbf{\Sigma}_8$ originating from the multiplet (2,2,15). The feynman diagram corresponding to this processes are as shown in Fig. 5.8 (left diagram).

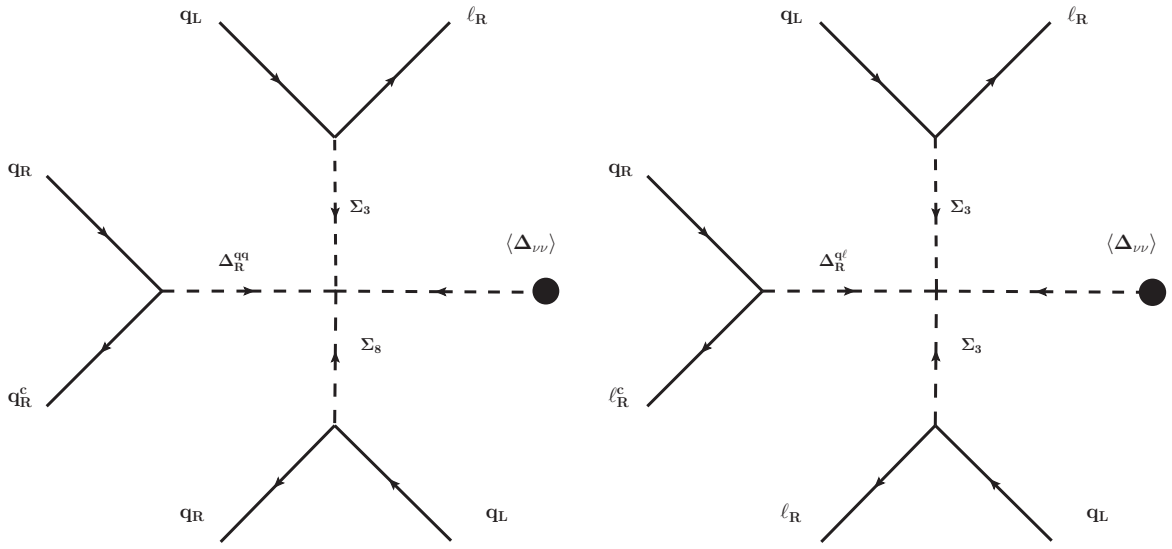

Figure 5.8: Feynman diagrams for nucleon decay with the $v_R = \langle \mathbf{\Delta}_R \rangle$ VEV insertions. The left diagram induces nucleon decay processes like nucleon → lepton + mesons and the right digram nucleon → lepton + lepton + antilepton processes.

For PS model with this minimal set of scalars, another feynman digram that contributes to the nucleon

decay can be constructed by replacing the color octet Σ_8 by a color triplet Σ_3 and the sextet Δ_6 by color triplet Δ_3 as shown in Fig. 5.8 (right diagram). This kind of diagrams will lead to nucleon decay $3q \to ll\bar{l}$. The processes shown in Fig. 5.8 are generated by the dimension nine ($d = 9$) operators. Shortly we will show that in our set-up $d = 9$ operators only give rise to the decay processes of the type nucleon$\to$ lepton+ meson(s) but not nucleon $\to$ lepton + lepton + antilepton processes since these three lepton decays always involve ν_R in the final state and hence are extremely suppressed.

However, three lepton decay processes of nucleon can take place in our model via the $d = 10$ operators [197–199]. The feynman diagrams corresponding to nucleon decay processes mediated by $d = 10$ operators are shown in Fig. 5.9. These decay modes are: nucleon$\to$ antilepton + meson and nucleon$\to$ lepton + antilepton+ antilepton. Below we present the effective Lagrangians corresponding to $d = 9$ and $d = 10$ and discuss the different nucleon decay modes and compute the branching fractions in certain approximations. For operator analysis regarding baryon and lepton number violation see Ref. [200–203].

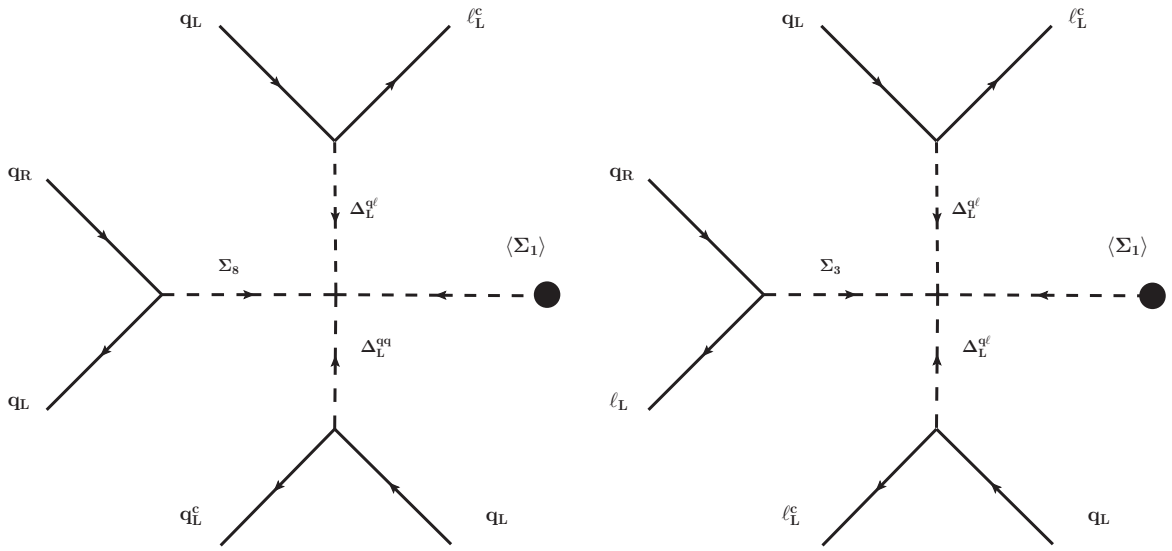

Figure 5.9: Feynman diagrams for nucleon decay with the SM doublet VEV insertions. The left diagram induces nucleon decay processes like nucleon $\to$ lepton + mesons and the right digram nucleon $\to$ lepton + antilepton + antilepton processes.

$d = 9$ **proton decay**

The effective Lagrangian describing these $d = 9$ six-fermion vertex that corresponds to nucleon decay can be written down by using Eqs. (5.3.24) and (5.6.61),

$$\mathcal{L}_{eff}^{d=9} = \mathcal{L}_{eff}^{(a)} + \mathcal{L}_{eff}^{(b)} + \mathcal{L}_{eff}^{(c)}, \tag{5.7.102}$$

with,

$$\mathcal{L}^{(a)}_{eff} = -(2\widetilde{\gamma}_{9R}v_R)\epsilon^{\overline{\mu\rho}\overline{\lambda}}Y^*_{15pq}Y^*_{15kl}Y^R_{10mn}\left(\frac{d^T_{Rm\overline{\chi}}Cd_{Rn\overline{\lambda}}}{m^2_{\Delta_{R(\overline{6},1,\frac{2}{3})}}}\right)\Bigg\{\left(\frac{\overline{u}^{\overline{\chi}}_{Rp}u_{Lq\overline{\mu}}}{m^2_{\Sigma_{(8,2,\frac{1}{2})}}}\right)\left(\frac{\overline{e}_{Rk}d_{Ll\overline{\rho}}}{m^2_{\Sigma_{(\overline{3},2,-\frac{7}{6})}}}\right)$$
$$-\left(\frac{\overline{d}^{\overline{\chi}}_{Rp}u_{Lq\overline{\mu}}}{m^2_{\Sigma_{(8,2,-\frac{1}{2})}}}\right)\left(\frac{\overline{\nu}_{Rk}d_{Ll\overline{\rho}}}{m^2_{\Sigma_{(\overline{3},2,-\frac{1}{6})}}}\right)-\left(\frac{\overline{u}^{\overline{\chi}}_{Rp}d_{Lq\overline{\mu}}}{m^2_{\Sigma_{(8,2,\frac{1}{2})}}}\right)\left(\frac{\overline{e}_{Rk}u_{Ll\overline{\rho}}}{m^2_{\Sigma_{(\overline{3},2,-\frac{7}{6})}}}\right)+\left(\frac{\overline{d}^{\overline{\chi}}_{Rp}d_{Lq\overline{\mu}}}{m^2_{\Sigma_{(8,2,-\frac{1}{2})}}}\right)\left(\frac{\overline{\nu}_{Rk}u_{Ll\overline{\rho}}}{m^2_{\Sigma_{(\overline{3},2,-\frac{1}{6})}}}\right)\Bigg\}, \tag{5.7.103}$$

$$\begin{aligned}\mathcal{L}^{(b)}_{eff} = &-(2\widetilde{\gamma}_{10R}v_R)\epsilon^{\overline{\mu\rho}\overline{\lambda}}Y^*_{15pq}Y^*_{15kl}Y^R_{10mn}\times\\
&\Bigg\{\left(\frac{\overline{u}^{\overline{\chi}}_{Rp}u_{Lq\overline{\mu}}}{m^2_{\Sigma_{(8,2,\frac{1}{2})}}}\right)\left[\left(\frac{\overline{\nu}_{Rk}d_{Ll\overline{\rho}}}{m^2_{\Sigma_{(\overline{3},2,-\frac{1}{6})}}}\right)\left(\frac{d^T_{Rm\overline{\chi}}Cu_{Rn\overline{\lambda}}}{m^2_{\Delta_{R(\overline{6},1,-\frac{1}{3})}}}\right)+\left(\frac{\overline{e}_{Rk}d_{Ll\overline{\rho}}}{m^2_{\Sigma_{(\overline{3},2,-\frac{7}{6})}}}\right)\left(\frac{d^T_{Rm\overline{\chi}}Cd_{Rn\overline{\lambda}}}{m^2_{\Delta_{R(\overline{6},1,\frac{2}{3})}}}\right)\right]\\
&-\left(\frac{\overline{u}^{\overline{\chi}}_{Rp}d_{Lq\overline{\mu}}}{m^2_{\Sigma_{(8,2,\frac{1}{2})}}}\right)\left[\left(\frac{\overline{\nu}_{Rk}u_{Ll\overline{\rho}}}{m^2_{\Sigma_{(\overline{3},2,-\frac{1}{6})}}}\right)\left(\frac{d^T_{Rm\overline{\chi}}Cu_{Rn\overline{\lambda}}}{m^2_{\Delta_{R(\overline{6},1,-\frac{1}{3})}}}\right)+\left(\frac{\overline{e}_{Rk}u_{Ll\overline{\rho}}}{m^2_{\Sigma_{(\overline{3},2,-\frac{7}{6})}}}\right)\left(\frac{d^T_{Rm\overline{\chi}}Cd_{Rn\overline{\lambda}}}{m^2_{\Delta_{R(\overline{6},1,\frac{2}{3})}}}\right)\right]\\
&+\left(\frac{\overline{\nu}_{Rp}u_{Lq\overline{\mu}}}{m^2_{\Sigma_{(\overline{3},2,-\frac{1}{6})}}}\right)\left[\left(\frac{\overline{\nu}_{Rk}d_{Ll\overline{\rho}}}{m^2_{\Sigma_{(\overline{3},2,-\frac{1}{6})}}}\right)\left(\frac{e^T_{Rm}Cu_{Rn\overline{\lambda}}}{m^2_{\Delta_{R(\overline{3},1,\frac{1}{3})}}}\right)+\left(\frac{\overline{e}_{Rk}d_{Ll\overline{\rho}}}{m^2_{\Sigma_{(\overline{3},2,-\frac{7}{6})}}}\right)\left(\frac{e^T_{Rm}Cd_{Rn\overline{\lambda}}}{m^2_{\Delta_{R(\overline{3},1,\frac{4}{3})}}}\right)\right]\\
&-\left(\frac{\overline{\nu}_{Rp}d_{Lq\overline{\mu}}}{m^2_{\Sigma_{(\overline{3},2,-\frac{1}{6})}}}\right)\left[\left(\frac{\overline{\nu}_{Rk}u_{Ll\overline{\rho}}}{m^2_{\Sigma_{(\overline{3},2,-\frac{1}{6})}}}\right)\left(\frac{e^T_{Rm}Cu_{Rn\overline{\lambda}}}{m^2_{\Delta_{R(\overline{3},1,\frac{1}{3})}}}\right)+\left(\frac{\overline{e}_{Rk}u_{Ll\overline{\rho}}}{m^2_{\Sigma_{(\overline{3},2,-\frac{7}{6})}}}\right)\left(\frac{e^T_{Rm}Cd_{Rn\overline{\lambda}}}{m^2_{\Delta_{R(\overline{3},1,\frac{4}{3})}}}\right)\right]\Bigg\},\end{aligned} \tag{5.7.104}$$

$$\begin{aligned}\mathcal{L}^{(c)}_{eff} = &-(\widetilde{\eta}_1 v_R)\epsilon^{\overline{\zeta}\overline{\tau\chi}}Y^*_{15pq}Y_{15kl}Y^L_{10mn}\frac{1}{m^2_{\Sigma_{(\overline{3},2,-\frac{1}{6})}}}\Bigg\{\left(\overline{\nu}_{Rp}u_{Lq\overline{\zeta}}\right)\left(\frac{\overline{u}^{\overline{\rho}}_{Lk}d_{Rl\overline{\tau}}}{m^2_{\Sigma_{(8,2,\frac{1}{2})}}}\right)\left(\frac{d^T_{Lm\overline{\rho}}Cu_{Ln\overline{\chi}}}{m^2_{\Delta_{L(\overline{6},1,-\frac{1}{3})}}}\right)\\
&+\left(\overline{\nu}_{Rp}u_{Lq\overline{\zeta}}\right)\left(\frac{\overline{d}^{\overline{\rho}}_{Lk}d_{Rl\overline{\tau}}}{m^2_{\Sigma_{(8,2,\frac{1}{2})}}}\right)\left(\frac{d^T_{Lm\overline{\rho}}Cd_{Ln\overline{\chi}}}{m^2_{\Delta_{L(\overline{6},1,-\frac{1}{3})}}}\right)-\left(\frac{\overline{\nu}_{Rp}d_{Lq\overline{\zeta}}}{m^2_{\Sigma_{(\overline{3},2,-\frac{1}{6})}}}\right)\left(\frac{\overline{u}^{\overline{\rho}}_{Lk}d_{Rl\overline{\tau}}}{m^2_{\Sigma_{(8,2,\frac{1}{2})}}}\right)\left(\frac{u^T_{Lm\overline{\rho}}Cu_{Ln\overline{\chi}}}{m^2_{\Delta_{L(\overline{6},1,-\frac{1}{3})}}}\right)\\
&+\left(\overline{\nu}_{Rp}u_{Lq\overline{\zeta}}\right)\left(\frac{\overline{\nu}_{Lk}d_{Rl\overline{\tau}}}{m^2_{\Sigma_{(\overline{3},2,-\frac{1}{6})}}}\right)\left(\frac{e^T_{Lm\overline{\rho}}Cu_{Ln\overline{\chi}}}{m^2_{\Delta_{L(\overline{3},1,\frac{1}{3})}}}\right)+\left(\frac{\overline{\nu}_{Rp}u_{Lq\overline{\zeta}}}{m^2_{\Sigma_{(\overline{3},2,-\frac{1}{6})}}}\right)\left(\frac{\overline{e}_{Lk}d_{Rl\overline{\tau}}}{m^2_{\Sigma_{(\overline{3},2,-\frac{1}{6})}}}\right)\left(\frac{e^T_{Lm\overline{\rho}}Cd_{Ln\overline{\chi}}}{m^2_{\Delta_{L(\overline{3},1,\frac{1}{3})}}}\right)\\
&-\left(\overline{\nu}_{Rp}d_{Lq\overline{\zeta}}\right)\left(\frac{\overline{\nu}_{Lk}d_{Rl\overline{\tau}}}{m^2_{\Sigma_{(\overline{3},2,-\frac{1}{6})}}}\right)\left(\frac{\nu^T_{Lm\overline{\rho}}Cu_{Ln\overline{\chi}}}{m^2_{\Delta_{L(\overline{3},1,\frac{1}{3})}}}\right)\Bigg\},\end{aligned} \tag{5.7.105}$$

here k, l, m, n, p, q are the generation indices. The terms involving color octets mediate nutron decay via the channels $n \to \pi^+ e^-_R, K^+ e^-_R, \pi^+\mu^-_R, K^+\mu^-_R, \pi^0\nu_R, K^0\nu_R$ and proton decay via $p \to \pi^+\nu_R, K^+\nu_R$. And the terms where the color triplets replacing color octets, the decay modes are, $n \to \nu_L{}^c\nu_L\nu_R$, $e^+_R e^-_R\nu_R$, $\mu^+_R e^-_R\nu_R$, $e^+_R\mu^-_R\nu_R$, $\mu^+_R\mu^-_R\nu_R$, $e^+_L e^-_L\nu_R$, $e^+_L\mu^-_L\nu_R$, $\mu^+_L e^-_L\nu_R$, $\mu^+_L\mu^-_L\nu_R$ and $p \to e^+_R\nu_R\nu_R$, $\mu^+_R\nu_R\nu_R$, $e^+_L\nu_L\nu_R$, $\mu^+_L\nu_L\nu_R$.

Note that for all the three lepton decays of the nucleon as well as some of the two body decay modes with the lepton being the neutrino, these decays can not be observed due to the additional suppressions of large right-handed neutrino mass. For the three lepton decay channels, always one of the leptons is a right-handed neutrino

and for the two body decay channels with neutrino as the lepton, it is always the right-handed neutrino. This is not true in general within the PS framework. But in our model due to the $U(1)_{PQ}$ symmetry, $\mathbf{\Sigma}$ has coupling with $\overline{\boldsymbol{\psi}}_L \boldsymbol{\psi}_R$ and $\mathbf{\Sigma}^*$ has coupling with $\overline{\boldsymbol{\psi}}_R \boldsymbol{\psi}_L$, see Eq. (5.3.24). Also PQ charge conservation does not allow quartic terms of the form $\mathbf{\Sigma}^2 {\mathbf{\Delta}_R^*}^2$ rather allowed term is of the form $\mathbf{\Sigma}^2 {\mathbf{\Delta}_R}^2$. The combined effect of these two facts restricts some of the modes of nucleon decay in our model as mentioned above. However, neutron decay into a lepton and a meson ($n \to e_R^- \pi^+, e_R^- K^+, \mu_R^- \pi^+, \mu_R^- K^+$) can be within the observable range with specific choice of the parameter space. There will be similar modes of proton decay ($p \to e_R^- \pi^+ \pi^+, e_R^- K^+ \pi^+, \mu_R^- \pi^+ \pi^+, \mu_R^- K^+ \pi^+$) with an additional pion in the final state and hence will be suppressed compared to neutron decay.

On the dimensional ground the decay rate of these $n \to$ lepton + meson processes is given by

$$\Gamma^{d=9}_{n \to \ell + \text{meson}} \sim \frac{1}{8\pi} \left| \frac{v_R \, \Lambda_{QCD}^5}{M^6} \right|^2 m_p. \tag{5.7.106}$$

Here m_p is the mass of the proton and the mass of the Higgs bosons involved are taken to be of the same order and is denoted by M. While computing this, the amplitude of such processes get multiplied by the factor Λ_{QCD}^5, here a factor of Λ_{QCD}^3 enters due to the hadronization of 3 quarks into a nucleon and a factor of Λ_{QCD}^2 comes into play due to the hadronization of $q\overline{q}$ to a meson (for numerical computations, we take $\Lambda_{QCD} = 170$ MeV). Assuming the Higgs bosons masses equal to the PS breaking scale, i.e, $M = v_R$, the decay rate ($\tau = \Gamma^{-1}$) of such processes to be within the observables range ($\tau \sim 10^{34}$ yrs) requires the PS breaking scale to be as low as $v_R \sim 3.5 \times 10^5$ GeV.

For high scale breaking of PS group $v_R \sim 10^{14}$ GeV required for the case with imposed parity symmetry makes the nucleon decay completely unobservable. On the other hand if the parity symmetry gets broken at the high scale by the VEV of the singlet, odd under parity that breaks the PQ symmetry, v_R scale can be much lowered ∼1000 TeV as explained earlier. Though the mentioned required v_R scale for the nucleon decay to be observable is computed in the naive dimensional ground, by choosing right values of the quartic couplings involved in these processes, nucleon decay can be within the observable range while simultaneously satisfying the lower bound of the PS scale breaking. Certainly the Higgs bosons masses are not degenerate and the parameters can be choose in such a way that their masses can be significantly lower than the PS breaking scale and hence nucleon decay can happen in the interesting observable range in our theory.

On the other hand, decay rate of the $p \to$ lepton + mesons processes is given by

$$\Gamma^{d=9}_{p \to \ell + \text{mesons}} \sim \frac{1}{8\pi} \left| \frac{v_R \, \Lambda_{QCD}^7}{M^6} \right|^2 m_p^{-3}. \tag{5.7.107}$$

The additional factor of Λ_{QCD}^2 is due to the presence of an extra pion in the final state. By a similar computation one finds that $v_R \sim 9.5 \times 10^4$ GeV is required for such processes to be within the observable range. Again this required v_R is computed naively. Even though additional suppression factor is present due to an extra

pion in the final state, appropriate choice of the model parameters can make this proton decay modes observable.

$d = 10$ **proton decay**

The effective Lagrangian describing the $d = 10$ six-fermion vertex that correspond to nucleon decay can be written down by using Eqs. (5.3.24) and (5.6.61),

$$\mathcal{L}_{eff}^{d=10} = \mathcal{L}_{eff}^{(d)} + \mathcal{L}_{eff}^{(e)}, \tag{5.7.108}$$

$$\begin{aligned}
\mathcal{L}_{eff}^{(d)} = (\widetilde{\gamma}_{9L} v_{ew}) \epsilon^{\overline{\tau}\overline{\lambda}\overline{\chi}} Y_{15_{pq}} Y^L_{10_{kl}} Y^L_{10_{mn}} \Bigg\{ & \frac{1}{m^2_{\Delta_{L(\overline{3},3,\frac{1}{3})}} m^2_{\Delta_{L(\overline{6},3,-\frac{1}{3})}}} \left[\left(\frac{\overline{u}^{\overline{\rho}}_{Lp} u_{Rq\overline{\tau}}}{m^2_{\Sigma_{(8,2,-\frac{1}{2})}}} \right) + \left(\frac{\overline{d}^{\overline{\rho}}_{Lp} d_{Rq\overline{\tau}}}{m^2_{\Sigma_{(8,2,\frac{1}{2})}}} \right) \right] \\
& \left[\left(e^T_{Lk} C u_{Ll\overline{\lambda}} \right) \left(d^T_{Lm\overline{\rho}} C u_{Ln\overline{\chi}} \right) + \left(e^T_{Lk} C d_{Ll\overline{\lambda}} \right) \left(u^T_{Lm\overline{\rho}} C u_{Ln\overline{\chi}} \right) + \left(\nu^T_{Lk} C d_{Ll\overline{\lambda}} \right) \left(d^T_{Lm\overline{\rho}} C d_{Ln\overline{\chi}} \right) \right. \\
& \left. + \left(\nu^T_{Lk} C d_{Ll\overline{\lambda}} \right) \left(u^T_{Lm\overline{\rho}} C d_{Ln\overline{\chi}} \right) \right] + \frac{1}{m^4_{\Delta_{L(\overline{3},3,\frac{1}{3})}}} \left[\left(\frac{\overline{\nu}_{Lp} u_{Rq\overline{\tau}}}{m^2_{\Sigma_{(\overline{3},2,-\frac{7}{6})}}} \right) + \left(\frac{\overline{e}_{Lp} d_{Rq\overline{\tau}}}{m^2_{\Sigma_{(\overline{3},2,-\frac{1}{6})}}} \right) \right] \\
& \left[\left(e^T_{Lk} C u_{Ll\overline{\lambda}} \right) \left(e^T_{Lm} C u_{Ln\overline{\chi}} \right) + \left(e^T_{Lk} C d_{Ll\overline{\lambda}} \right) \left(\nu^T_{Lm} C u_{Ln\overline{\chi}} \right) + \left(\nu^T_{Lk} C d_{Ll\overline{\lambda}} \right) \left(\nu^T_{Lm\overline{\rho}} C d_{Ln\overline{\chi}} \right) \right] \Bigg\},
\end{aligned} \tag{5.7.109}$$

$$\begin{aligned}
\mathcal{L}_{eff}^{(e_1)} = & (\widetilde{\gamma}_{10L} v_{ew}) \epsilon^{\overline{\tau}\overline{\lambda}\overline{\chi}} Y_{15_{pq}} Y^L_{10_{kl}} Y^L_{10_{mn}} \times \\
& \Bigg\{ \frac{1}{m^2_{\Sigma_{(8,2,\frac{1}{2})}} m^2_{\Delta_{L(\overline{3},3,\frac{1}{3})}} m^2_{\Delta_{L(\overline{6},3,-\frac{1}{3})}}} \{ \left(\overline{u}^{\overline{\rho}}_{Lp} d_{Rq\overline{\tau}} \right) \left[\left(\nu^T_{Lk} C u_{Ll\overline{\lambda}} \right) \left(d^T_{Lm\overline{\rho}} C u_{Ln\overline{\chi}} \right) + \left(\nu^T_{Lk} C d_{Ll\overline{\lambda}} \right) \left(u^T_{Lm\overline{\rho}} C u_{Ln\overline{\chi}} \right) \right] \\
& + \left(\overline{d}^{\overline{\rho}}_{Lp} d_{Rq\overline{\tau}} \right) \left[\left(\nu^T_{Lk} C u_{Ll\overline{\lambda}} \right) \left(d^T_{Lm\overline{\rho}} C d_{Ln\overline{\chi}} \right) + \left(\nu^T_{Lk} C d_{Ll\overline{\lambda}} \right) \left(u^T_{Lm\overline{\rho}} C d_{Ln\overline{\chi}} \right) \right] \} \\
& + \frac{1}{m^2_{\Sigma_{(\overline{3},2,-\frac{1}{6})}} m^4_{\Delta_{L(\overline{3},3,\frac{1}{3})}}} \{ (\overline{\nu}_{Lp} d_{Rq\overline{\tau}}) \left[\left(\nu^T_{Lk} C u_{Ll\overline{\lambda}} \right) \left(e^T_{Lk} C u_{Ll\overline{\lambda}} \right) + \left(\nu^T_{Lk} C d_{Ll\overline{\lambda}} \right) \left(\nu^T_{Lk} C u_{Ll\overline{\lambda}} \right) \right] \\
& + (\overline{e}_{Lp} d_{Rq\overline{\tau}}) \left[\left(\nu^T_{Lk} C u_{Ll\overline{\lambda}} \right) \left(e^T_{Lk} C d_{Ll\overline{\lambda}} \right) + \left(\nu^T_{Lk} C d_{Ll\overline{\lambda}} \right) \left(\nu^T_{Lk} C d_{Ll\overline{\lambda}} \right) \right] \} \Bigg\},
\end{aligned} \tag{5.7.110}$$

$$\begin{aligned}
\mathcal{L}_{eff}^{(e_2)} = & (\widetilde{\gamma}_{10L} v_{ew}) \epsilon^{\overline{\tau}\overline{\lambda}\overline{\chi}} Y_{15_{pq}} Y^L_{10_{kl}} Y^L_{10_{mn}} \times \\
& \Bigg\{ \frac{1}{m^2_{\Sigma_{(8,2,-\frac{1}{2})}} m^2_{\Delta_{L(\overline{3},3,\frac{1}{3})}} m^2_{\Delta_{L(\overline{6},3,-\frac{1}{3})}}} \{ \left(\overline{u}^{\overline{\rho}}_{Lp} u_{Rq\overline{\tau}} \right) \left[\left(e^T_{Lk} C u_{Ll\overline{\lambda}} \right) \left(d^T_{Lm\overline{\rho}} C u_{Ln\overline{\chi}} \right) + \left(e^T_{Lk} C d_{Ll\overline{\lambda}} \right) \left(u^T_{Lm\overline{\rho}} C u_{Ln\overline{\chi}} \right) \right] \\
& + \left(\overline{d}^{\overline{\rho}}_{Lp} u_{Rq\overline{\tau}} \right) \left[\left(e^T_{Lk} C u_{Ll\overline{\lambda}} \right) \left(d^T_{Lm\overline{\rho}} C d_{Ln\overline{\chi}} \right) + \left(e^T_{Lk} C d_{Ll\overline{\lambda}} \right) \left(u^T_{Lm\overline{\rho}} C d_{Ln\overline{\chi}} \right) \right] \} \\
& + \frac{1}{m^2_{\Sigma_{(\overline{3},2,-\frac{7}{6})}} m^4_{\Delta_{L(\overline{3},3,\frac{1}{3})}}} \{ (\overline{\nu}_{Lp} u_{Rq\overline{\tau}}) \left[\left(e^T_{Lk} C u_{Ll\overline{\lambda}} \right) \left(e^T_{Lk} C u_{Ll\overline{\lambda}} \right) + \left(e^T_{Lk} C d_{Ll\overline{\lambda}} \right) \left(\nu^T_{Lk} C u_{Ll\overline{\lambda}} \right) \right] \\
& + (\overline{e}_{Lp} u_{Rq\overline{\tau}}) \left[\left(e^T_{Lk} C u_{Ll\overline{\lambda}} \right) \left(e^T_{Lk} C d_{Ll\overline{\lambda}} \right) + \left(e^T_{Lk} C d_{Ll\overline{\lambda}} \right) \left(\nu^T_{Lk} C d_{Ll\overline{\lambda}} \right) \right] \} \Bigg\},
\end{aligned} \tag{5.7.111}$$

$$\mathcal{L}^{(e_3)}_{eff} = (\widetilde{\gamma}_{10L} v_{ew}) \epsilon^{\overline{\tau}\overline{\lambda}\overline{\chi}} Y_{15pq} Y^L_{10kl} Y^L_{10mn} \times$$
$$\Bigg\{ \frac{1}{m^2_{\Sigma_{(8,2,\frac{1}{2})}} m^2_{\Delta_{L(\overline{3},3,\frac{1}{3})}} m^2_{\Delta_{L(\overline{6},3,-\frac{1}{3})}}} \{ \left(\overline{u}^{\overline{\rho}}_{Lp} d_{Rq\overline{\tau}}\right) \left[\left(e^T_{Lk} C u_{Ll\overline{\lambda}}\right) \left(u^T_{Lm\overline{\rho}} C u_{Ln\overline{\chi}}\right) + \left(\nu^T_{Lk} C u_{Ll\overline{\lambda}}\right) \left(u^T_{Lm\overline{\rho}} C d_{Ln\overline{\chi}}\right) \right]$$
$$- \left(\overline{d}^{\overline{\rho}}_{Lp} d_{Rq\overline{\tau}}\right) \left[\left(e^T_{Lk} C u_{Ll\overline{\lambda}}\right) \left(d^T_{Lm\overline{\rho}} C u_{Ln\overline{\chi}}\right) + \left(\nu^T_{Lk} C u_{Ll\overline{\lambda}}\right) \left(d^T_{Lm\overline{\rho}} C d_{Ln\overline{\chi}}\right) \right] \}$$
$$+ \frac{1}{m^2_{\Sigma_{(\overline{3},2,-\frac{1}{6})}} m^4_{\Delta_{L(\overline{3},3,\frac{1}{3})}}} \{ (\overline{\nu}_{Lp} d_{Rq\overline{\tau}}) \left[\left(\nu^T_{Lk} C u_{Ll\overline{\lambda}}\right) \left(e^T_{Lk} C u_{Ll\overline{\lambda}}\right) + \left(\nu^T_{Lk} C d_{Ll\overline{\lambda}}\right) \left(\nu^T_{Lk} C u_{Ll\overline{\lambda}}\right) \right]$$
$$+ (\overline{e}_{Lp} d_{Rq\overline{\tau}}) \left[\left(e^T_{Lk} C u_{Ll\overline{\lambda}}\right) \left(e^T_{Lk} C u_{Ll\overline{\lambda}}\right) + \left(e^T_{Lk} C d_{Ll\overline{\lambda}}\right) \left(\nu^T_{Lk} C u_{Ll\overline{\lambda}}\right) \right] \} \Bigg\}, \tag{5.7.112}$$

$$\mathcal{L}^{(e_4)}_{eff} = (\widetilde{\gamma}_{10L} v_{ew}) \epsilon^{\overline{\tau}\overline{\lambda}\overline{\chi}} Y_{15pq} Y^L_{10kl} Y^L_{10mn} \times$$
$$\Bigg\{ \frac{1}{m^2_{\Sigma_{(8,2,-\frac{1}{2})}} m^2_{\Delta_{L(\overline{3},3,\frac{1}{3})}} m^2_{\Delta_{L(\overline{6},3,-\frac{1}{3})}}} \{ \left(\overline{u}^{\overline{\rho}}_{Lp} u_{Rq\overline{\tau}}\right) \left[\left(e^T_{Lk} C d_{Ll\overline{\lambda}}\right) \left(u^T_{Lm\overline{\rho}} C u_{Ln\overline{\chi}}\right) + \left(\nu^T_{Lk} C d_{Ll\overline{\lambda}}\right) \left(u^T_{Lm\overline{\rho}} C d_{Ln\overline{\chi}}\right) \right]$$
$$- \left(\overline{d}^{\overline{\rho}}_{Lp} u_{Rq\overline{\tau}}\right) \left[\left(e^T_{Lk} C d_{Ll\overline{\lambda}}\right) \left(d^T_{Lm\overline{\rho}} C u_{Ln\overline{\chi}}\right) + \left(e^T_{Lk} C u_{Ll\overline{\lambda}}\right) \left(d^T_{Lm\overline{\rho}} C d_{Ln\overline{\chi}}\right) \right] \}$$
$$+ \frac{1}{m^2_{\Sigma_{(\overline{3},2,-\frac{7}{6})}} m^4_{\Delta_{L(\overline{3},3,\frac{1}{3})}}} \{ (\overline{\nu}_{Lp} u_{Rq\overline{\tau}}) \left[\left(\nu^T_{Lk} C u_{Ll\overline{\lambda}}\right) \left(e^T_{Lk} C d_{Ll\overline{\lambda}}\right) + \left(\nu^T_{Lk} C d_{Ll\overline{\lambda}}\right) \left(\nu^T_{Lk} C d_{Ll\overline{\lambda}}\right) \right]$$
$$+ (\overline{e}_{Lp} u_{Rq\overline{\tau}}) \left[\left(e^T_{Lk} C u_{Ll\overline{\lambda}}\right) \left(e^T_{Lk} C d_{Ll\overline{\lambda}}\right) + \left(e^T_{Lk} C d_{Ll\overline{\lambda}}\right) \left(\nu^T_{Lk} C d_{Ll\overline{\lambda}}\right) \right] \} \Bigg\}, \tag{5.7.113}$$

where $\mathcal{L}^{(e)} = \sum_i \mathcal{L}^{(e_i)}$ with $i = 1 - 4$. The terms involving color octets mediate neutron decay via the channels $n \to \nu_L{}^c \pi^0, e^+_L \pi^-, \mu^+_L \pi^-, \nu_L{}^c K^0, K^- e^+_L, K^- \mu^+_L$ and proton decay via $p \to \nu_L{}^c \pi^+, e^+_L \pi^0, \nu_L{}^c K^+, e^+_L K^0, \mu^+_L \pi^0, \mu^+_L K^0$. And the terms where the color triplets replacing color octets, the decay modes are, $n \to \nu_L \nu_L{}^c \nu_L{}^c, e^-_L e^+_L \nu_L{}^c$, $e^-_L \mu^+_L \nu_L{}^c$, $\mu^-_L e^+_L \nu_L{}^c$, $\mu^-_L \mu^+_L \nu_L{}^c$ and $p \to e^+_L \nu_L \nu_L{}^c$, $\mu^+_L \nu_L \nu_L{}^c$, $e^-_L e^+_L e^+_L$, $\mu^-_L e^+_L e^+_L$, $\mu^-_L \mu^+_L e^+_L$, $\mu^-_L \mu^+_L \mu^+_L$.

Six fermion vertex $d = 9$ nucleon decay operators mediate processes like $n \to$ lepton + meson and $p \to$ lepton + mesons, whereas, $n \to$ antilepton + meson and $p \to$ antilepton + meson processes arise through $d = 10$ six fermion vertex operators. $d = 10$ operators also induce processes with three lepton final state, which is not the case with $d = 9$. The decay width for processes like $n, p \to$ antilepton + meson is

$$\Gamma^{d=10}_{n,p \to \ell^c + \text{meson}} \sim \frac{1}{8\pi} \left| \frac{v_{ew}\ \Lambda^5_{QCD}}{M^6} \right|^2 m_p, \tag{5.7.114}$$

and for the three lepton final state processes

$$\Gamma^{d=10}_{n,p \to \ell \ell^c \ell^c} \sim \frac{1}{256\pi^3} \left| \frac{v_{ew}\ \Lambda^3_{QCD}}{M^6} \right|^2 m^5_p. \tag{5.7.115}$$

For $n, p \to$ antilepton + meson to be within the observable range ($\tau \sim 10^{34}$ yrs [117]), the requirement on the PS scale is $v_R \sim 10^5$ GeV. The three lepton final state also requires $v_R \sim 10^5$ GeV (here $\tau \sim 10^{33}$ yrs [204]).

Again, as mentioned above, by appropriate choice of the quartic couplings involved in these decay rate of these processes can simultaneously satisfy the lower bound of the PS breaking but still be in the interesting observable range. As mentioned earlier, if the parity symmetry is not imposed, the presence of $\mathbf{\Delta}_L$ is not required. It is to be noted that in the absence of this field, only the nucleon decay mode allowed is nucleon$\rightarrow$ lepton + mesons via the $d = 9$ operators.

Nucleon decay relative branching fractions

By using the formulae as mentioned above one can compare the decay widths of the different modes. A naive estimation of the relative branching fractions reveal

$$\frac{\Gamma^{d=9}_{p\rightarrow \ell+mesons}}{\Gamma^{d=9}_{n\rightarrow \ell+meson}} \sim \frac{\Lambda^4_{QCD}}{m_p^4} \sim 10^{-3}, \tag{5.7.116}$$

$$\frac{\Gamma^{d=10}_{n,p\rightarrow \ell^c+meson}}{\Gamma^{d=9}_{n\rightarrow \ell+meson}} \sim \frac{v^2_{ew}}{v^2_R} \sim 10^{-8}, \tag{5.7.117}$$

$$\frac{\Gamma^{d=10}_{n,p\rightarrow \ell\ell^c\ell^c}}{\Gamma^{d=9}_{n\rightarrow \ell+meson}} \sim \frac{1}{32\pi^2}\frac{v^2_{ew}}{v^2_R}\frac{m_p^4}{\Lambda^4_{QCD}} \sim 10^{-7}, \tag{5.7.118}$$

$$\frac{\Gamma^{d=10}_{n,p\rightarrow \ell^c+meson}}{\Gamma^{d=9}_{p\rightarrow \ell+mesons}} \sim \frac{v^2_{ew}}{v^2_R}\frac{m_p^4}{\Lambda^4_{QCD}} \sim 10^{-5}, \tag{5.7.119}$$

$$\frac{\Gamma^{d=10}_{n,p\rightarrow \ell\ell^c\ell^c}}{\Gamma^{d=9}_{p\rightarrow \ell+mesons}} \sim \frac{1}{32\pi^2}\frac{v^2_{ew}}{v^2_R}\frac{m_p^8}{\Lambda^8_{QCD}} \sim 10^{-4}, \tag{5.7.120}$$

$$\frac{\Gamma^{d=10}_{n,p\rightarrow \ell^c+meson}}{\Gamma^{d=10}_{n,p\rightarrow \ell\ell^c\ell^c}} \sim 32\pi^2\frac{\Lambda^4_{QCD}}{m_p^4} \sim 0.34. \tag{5.7.121}$$

Here we have chosen $v_R = 10^6$ GeV. This estimation shows that for the $d = 9$ case, neutron decay will be dominating over the proton decay due the the presence of extra pion in the final state. Again $d = 10$ processes are suppressed compared to the $d = 9$ processes due to the extra suppression factor of v^2_{ew}/v^2_R. We remind the readers that this may not be true in general, since the Higgs boson mass spectrum is non-degenerate and appropriate hierarchical pattern can be realized to make these two processes comparable.

Since nucleon decay processes involve more than one quartic coupling, definite predictions about the relative branching fractions of different decay channels can not be firmly predicted. However, they are calculable in certain approximations. Here for the purpose of illustration we set $\gamma_{L9} = \gamma_{R9}$ and the rest of the couplings responsible for nucleon decay to be zero. $\gamma_{L9} = \gamma_{R9}$ can be realised if parity symmetry is imposed. For the nucleon decay to be within the observable range v_R scale also needs to be low. If the parity symmetry gets broken by the singlet VEV that is odd under parity, $\gamma_{L9} \approx \gamma_{R9}$ can be realized and still the PS breaking scale can be as low as $v_R \sim 10^6$ GeV. Recall that with the parity symmetry imposed, $Y^L_{10} = Y^R_{10}$ is also realized. Note than in these decay width formulae the dimensionless Yukawa couplings are ignored. However, they may play

significant role in the branching ratios and one needs to include them when comparing specific decay channels.

Comment on $d = 7$ B-violating operators

In unified theories, another interesting B-violating operators involving Higgs bosons that can mediate nucleon decay correspond to the case of $d = 7$. In addition to the leptoquark color triplets present in our theory, if also diquark color triplets exist, then $d = 7$ operators can mediate nucleon decay. For example, quartic terms in the Higgs potential involving a triplet leptoquark, a triplet diquark, a Higgs doublet and the neutral component from $\mathbf{\Delta}_R$ is responsible for generating nucleon decay processes [205] when the $B - L$ violating VEV of $\mathbf{\Delta}_R$ is inserted. In our minimal model due to the absence of diquark color triplets, $d = 7$ operators are not present. Due to many uncertainties, here we do not have definite predictions on the branching rations.

5.7.2 $n - \overline{n}$ Oscillation

Another phenomenologically interesting process that can take place in PS model is the $\Delta B = 2$ interactions that leads to $n-\overline{n}$ oscillation. A PS model with the presence of only (1,3,10) scalar can have nucleon transition at the tree level that includes six-fermion $\Delta B = 2$ vertex [195, 206] as shown in Fig. 5.10. Such transitions are again lead by a specific type of term in the scalar potential with the help of the Majorana type mass term in the Yukawa coupling. The term in the potential responsible for such processes has the form $\mathbf{\Delta}^4$. The only such existing term in our potential is

$$V_\Delta \supset \widetilde{\lambda_9}\, \mathbf{\Delta}_{R\mu\nu\ \dot{\alpha}}^{\ \ \dot{\beta}} \mathbf{\Delta}_{R\rho\tau\ \dot{\beta}}^{\ \ \dot{\alpha}} \mathbf{\Delta}_{L\lambda\chi\ \alpha}^{\ \ \beta} \mathbf{\Delta}_{L\zeta\omega\ \beta}^{\ \ \alpha} \epsilon^{\mu\rho\lambda\zeta} \epsilon^{\nu\tau\chi\omega} + h.c. \tag{5.7.122}$$

Interactions generated by Eq. (5.7.122) and Eq. (5.3.24) after the spontaneous PS symmetry breaking by $\langle \Delta_R \rangle$ cause $n - \overline{n}$ oscillation. The existing term is of the form $\mathbf{\Delta}_R^2 \mathbf{\Delta}_L^2$, which indicates that if parity is not imposed which does not demand the need of $\mathbf{\Delta}_L$ field, $n-\overline{n}$ transition is forbidden due to the added $U(1)_{PQ}$ symmetry. In PS model without $U(1)_{PQ}$ symmetry, $n-\overline{n}$ transition takes place via terms of the form $\mathbf{\Delta}_R^4$, such terms are forbidden in our theory since this field carries non-zero PQ charge.

The effective Lagrangian describing the six-fermion vertex ($d = 9$ operators) that corresponds to $n - \overline{n}$ oscillation can be written down by using Eqs. (5.3.24) and (5.6.58),

$$\mathcal{L}_{eff}^{n-\overline{n}} = -\widetilde{\lambda}_9 (2v_R) \epsilon^{\overline{\rho}\overline{\lambda\zeta}} \epsilon^{\overline{\tau}\overline{\chi\omega}} Y^R_{10\,kl} Y^L_{10\,mn} Y^L_{10\,pq} \quad \frac{\left(d^T_{Rk\overline{\rho}} C d_{Rl\overline{\tau}}\right)}{m^2_{\Delta_{R(\overline{6},1,\frac{2}{3})}} m^4_{\Delta_{L(\overline{6},3,-\frac{1}{3})}}}$$
$$\left\{ \left(d^T_{Lm\overline{\lambda}} C u_{Ln\overline{\chi}}\right) \left(d^T_{Lp\overline{\zeta}} C u_{Lq\overline{\omega}}\right) - \left(d^T_{Lm\overline{\lambda}} C d_{Ln\overline{\chi}}\right) \left(u^T_{Lp\overline{\zeta}} C u_{Lq\overline{\omega}}\right) - \left(u^T_{Lm\overline{\lambda}} C u_{Ln\overline{\chi}}\right) \left(d^T_{Lp\overline{\zeta}} C d_{Lq\overline{\omega}}\right) \right\}, \tag{5.7.123}$$

here k, l, m, n, p, q are the generation indices.

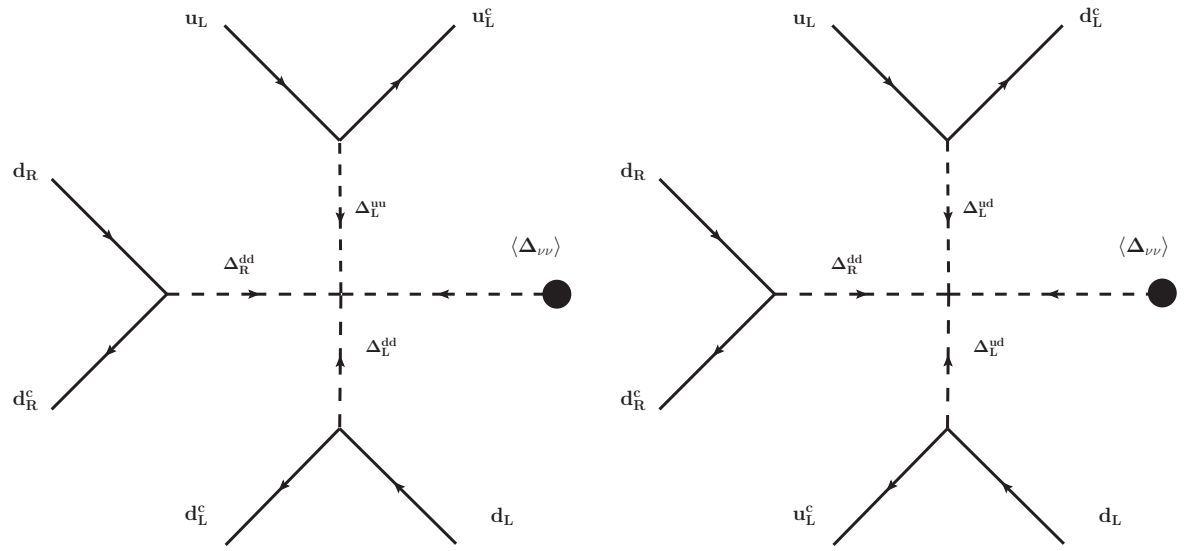

Figure 5.10: Feynman diagrams for $n - \overline{n}$ oscillation.

Again on the dimensional ground, the $n - \overline{n}$ oscillation transition time can be computed as

$$\tau_{n-\overline{n}} = \frac{M^6}{v_R \, \Lambda_{QCD}^6}. \tag{5.7.124}$$

The present limit on this transition time is constraint by the matter disintegration, which is $\tau_{n-\overline{n}} \geq 2 \times 10^8$ sec. [207]. A slightly weaker bound but with less uncertainty is obtained from the free neutron oscillation search, $\tau_{n-\overline{n}} \geq 10^8$ sec. [208]. By taking $\tau_{n-\overline{n}} = 10^8$ sec. one can find the lower bound on the scale $v_R \sim 3.2 \times 10^5$ GeV (like before $M = v_R$ is assumed). Certainly by choosing the relevant parameters of the model one can have $n - \overline{n}$ transition time within the interesting observable range.

5.8 Conclusion

In this work, we have presented a minimal renormalizable nonsupersymmetric model based on the Pati-Salam group, $SU(2)_L \times SU(2)_R \times SU(4)_C$ that unifies quark and leptons by treating leptons as the fourth color. We extend the symmetry of our theory by imposing global Peccei-Quinn symmetry, $U(1)_{PQ}$, that automatically solves the strong CP problem and provides axion as a dark matter candidate. This economic choice of the Higgs set makes the theory very predictive and with only 14 parameters in the Yukawa sector a good fit to the charged fermion masses and mixings are obtained. The origin of the baryon asymmetry of the Universe is linked to the seesaw mechanism that is responsible for neutrino oscillations. Detail search of the parameter space for successful generation of matter-antimatter asymmetry is carried out. The complete Higgs potential with minimal scalar content is constructed and the full mass spectrum of the fields are computed. Possible nucleon decay modes arising from dimension 9 and dimension 10 operators are discussed and branching fractions of

different channels are computed with certain approximations. Neutron-antineutron oscillation via dimension 9 operators in this framework is also analysed. Both the nucleon lifetime and neutron-antineutron transition time can be within the observable range.

CHAPTER 6

SUMMARY AND CONCLUSIONS

As mentioned throughout the text, the Standard Model (SM) of particle physics, even though highly successful, fails to explain many observed phenomena, hence, this theory needs to be extended. A dedicated study in search of the physics beyond the SM has been the main focus of this dissertation. Here, we presented various well motivated new unified models to resolve some of the shortcoming of the SM. Each model presented in this dissertation, has its own distinct features, hence can be experimentally distinguished.

In chapter 2 we present a new class of unified models based on $SO(10)$ symmetry which provides insights into the masses and mixings of quarks and leptons, including the neutrinos. The key feature of our proposal is the absence of Higgs boson 10_H belonging to the fundamental representation that is normally employed. Flavor mixing is induced via vector-like fermions in the $16 + \overline{16}$ representation. A variety of scenarios, both supersymmetric and otherwise, are analyzed involving a $\overline{126}_H$ along with either a 45_H or a 210_H of Higgs boson employed for symmetry breaking. It is shown that this framework, with only a limited number of parameters, provides an excellent fit to the full fermion spectrum, utilizing either type-I or type-II seesaw mechanism. These flavor models can be potentially tested and distinguished in their predictions for proton decay branching ratios, which are analyzed.

In chapter 3 we show that in $SO(10)$ models, a Yukawa sector consisting of a real 10_H, a real 120_H and a complex 126_H of Higgs fields can provide a realistic fit to all fermion masses and mixings, including the neutrino sector. Although the group theory of $SO(10)$ demands that the 10_H and 120_H be real, most constructions complexify these fields and impose symmetries exterior to $SO(10)$ to achieve predictivity. The proposed new framework with *real* 10_H and *real* 120_H relies only on $SO(10)$ gauge symmetry, and yet has a limited number of Yukawa parameters. Our analysis shows that while there are restrictions on the observables, a good fit to the entire fermion spectrum can be realized. Unification of gauge couplings is achieved with an intermediate scale Pati-Salam gauge symmetry. Proton decay branching ratios are calculable, with the leading decay modes being $p \to \overline{\nu}\pi^+$ and $p \to e^+\pi^0$.

As mentioned repeatedly throughout the text, the masses of the charged fermion and the mixing angles among quarks are observed to be strongly hierarchical, while analogous parameters in the neutrino sector appear to be structure-less or anarchical. In chapter 4 we develop a class of unified models based on $SU(5)$

symmetry that explains these differing features probabilistically. With the aid of three input parameters that are hierarchical, and with the assumption that all the Yukawa couplings are uncorrelated random variables described by Gaussian distributions, we show by Monte Carlo simulations that the observed features of the entire fermion spectrum can be nicely reproduced. We extend our analysis to an $SU(5)$-based flavor $U(1)$ model making use of the Froggatt-Nielsen mechanism where the order one Yukawa couplings are modeled as random variables, which also shows good agreement with observations.

In chapter 5, a predictive model based on an unified theory possessing the gauge symmetry of the Pati-Salam group, $SU(2)_L \times SU(2)_R \times SU(4)_C$ is studied. A detail analysis of the Higgs potential and the Yukawa couplings is carried out in this partially unified theory, which is one of the most attractive extensions of the Standard Model. The minimal Pati-Salam model can successfully incorporate the hierarchies in the charged fermion masses and mixings and seesaw mechanism is a natural way to explain the extremely small neutrino masses in this framework. Seesaw mechanism together with Baryogenesis via Leptogenesis scenario can account for the observed cosmological baryon asymmetry of the Universe. Along with solving the strong CP problem, the assumed $U(1)_{PQ}$ Peccei-Quinn symmetry can provide the ingredient for Dark Matter candidate. Even though the nucleon decay is not mediated by the gauge bosons in Pati-Salam theory, the scalar diquarks and leptoquarks together can cause nucleon to decay. Nucleon decay processes in this framework are, nucleon $\rightarrow$ lepton + meson, nucleon $\rightarrow$ antilepton + meson and nucleon $\rightarrow$ lepton + antilepton + antilepton. With appropriate choice of the parameters of theory, these processes can be within the observable range. In this theory neutron-antineutron oscillation takes place that can also be observed in the ongoing experiments.

REFERENCES

[1] P. W. Higgs, "Broken symmetries, massless particles and gauge fields," Phys. Lett. **12**, 132 (1964).

[2] P. W. Higgs, "Broken Symmetries and the Masses of Gauge Bosons," Phys. Rev. Lett. **13**, 508 (1964).

[3] F. Englert and R. Brout, "Broken Symmetry and the Mass of Gauge Vector Mesons," Phys. Rev. Lett. **13**, 321 (1964).

[4] G. S. Guralnik, C. R. Hagen and T. W. B. Kibble, "Global Conservation Laws and Massless Particles," Phys. Rev. Lett. **13**, 585 (1964).

[5] S. Weinberg, "A Model of Leptons," Phys. Rev. Lett. **19**, 1264 (1967).

[6] A. Salam, "Weak and Electromagnetic Interactions," Conf. Proc. C **680519**, 367 (1968).

[7] S. L. Glashow, "Partial Symmetries of Weak Interactions," Nucl. Phys. **22**, 579 (1961).

[8] Y. Nambu, "Axial vector current conservation in weak interactions," Phys. Rev. Lett. **4**, 380 (1960).

[9] Y. Nambu and G. Jona-Lasinio, "Dynamical Model of Elementary Particles Based on an Analogy with Superconductivity. 1.," Phys. Rev. **122**, 345 (1961).

[10] Y. Nambu and G. Jona-Lasinio, "Dynamical Model Of Elementary Particles Based On An Analogy With Superconductivity. Ii," Phys. Rev. **124**, 246 (1961).

[11] J. Goldstone, "Field Theories with Superconductor Solutions," Nuovo Cim. **19**, 154 (1961).

[12] G. Aad *et al.* [ATLAS Collaboration], "Observation of a new particle in the search for the Standard Model Higgs boson with the ATLAS detector at the LHC," Phys. Lett. B **716**, 1 (2012) [arXiv:1207.7214 [hep-ex]].

[13] S. Chatrchyan *et al.* [CMS Collaboration], "Observation of a new boson at a mass of 125 GeV with the CMS experiment at the LHC," Phys. Lett. B **716**, 30 (2012) [arXiv:1207.7235 [hep-ex]].

[14] Y. Fukuda *et al.* [Super-Kamiokande Collaboration], "Evidence for oscillation of atmospheric neutrinos," Phys. Rev. Lett. **81**, 1562 (1998) [hep-ex/9807003].

[15] Q. R. Ahmad *et al.* [SNO Collaboration], "Direct evidence for neutrino flavor transformation from neutral current interactions in the Sudbury Neutrino Observatory," Phys. Rev. Lett. **89**, 011301 (2002) [nucl-ex/0204008].

[16] K. Abe *et al.* [T2K Collaboration], "Indication of Electron Neutrino Appearance from an Accelerator-produced Off-axis Muon Neutrino Beam," Phys. Rev. Lett. **107**, 041801 (2011) [arXiv:1106.2822 [hep-ex]].

[17] V. C. Rubin and W. K. Ford, Jr., "Rotation of the Andromeda Nebula from a Spectroscopic Survey of Emission Regions," Astrophys. J. **159**, 379 (1970).

[18] P. A. R. Ade *et al.* [Planck Collaboration], "Planck 2013 results. I. Overview of products and scientific results," Astron. Astrophys. **571**, A1 (2014) [arXiv:1303.5062 [astro-ph.CO]].

[19] F. Iocco, G. Mangano, G. Miele, O. Pisanti and P. D. Serpico, "Primordial Nucleosynthesis: from precision cosmology to fundamental physics," Phys. Rept. **472** (2009) 1 [arXiv:0809.0631 [astro-ph]].

[20] C. S. Fong, M. C. Gonzalez-Garcia and E. Nardi, "Leptogenesis from Soft Supersymmetry Breaking (Soft Leptogenesis)," Int. J. Mod. Phys. A **26**, 3491 (2011) [arXiv:1107.5312 [hep-ph]].

[21] A. D. Sakharov, "Violation of CP Invariance, c Asymmetry, and Baryon Asymmetry of the Universe," Pisma Zh. Eksp. Teor. Fiz. **5**, 32 (1967) [JETP Lett. **5**, 24 (1967)] [Sov. Phys. Usp. **34**, 392 (1991)] [Usp. Fiz. Nauk **161**, 61 (1991)].

[22] J. C. Pati and A. Salam, "Lepton Number as the Fourth Color," Phys. Rev. D **10**, 275 (1974) Erratum: [Phys. Rev. D **11**, 703 (1975)].

[23] H. Georgi and S. L. Glashow, "Unity of All Elementary Particle Forces," Phys. Rev. Lett. **32**, 438 (1974).

[24] H. Georgi, H. R. Quinn and S. Weinberg, "Hierarchy of Interactions in Unified Gauge Theories," Phys. Rev. Lett. **33**, 451 (1974).

[25] H. Georgi, in Particles and Fields (edited by C.E. Carlson), A.I.P. (1975); H. Fritzch and P. Minkowski, Ann. Phys. **93**, 193 (1975).

[26] K. S. Babu and R. N. Mohapatra, "Predictive neutrino spectrum in minimal SO(10) grand unification," Phys. Rev. Lett. **70**, 2845 (1993) [hep-ph/9209215].

[27] T. Fukuyama and N. Okada, "Neutrino oscillation data versus minimal supersymmetric SO(10) model," JHEP **0211**, 011 (2002) [hep-ph/0205066].

[28] H. S. Goh, R. N. Mohapatra and S. P. Ng, "Minimal SUSY SO(10), b tau unification and large neutrino mixings," Phys. Lett. B **570**, 215 (2003) [hep-ph/0303055].

[29] H. S. Goh, R. N. Mohapatra and S. P. Ng, "Minimal SUSY SO(10) model and predictions for neutrino mixings and leptonic CP violation," Phys. Rev. D **68**, 115008 (2003) [hep-ph/0308197].

[30] S. Bertolini, M. Frigerio and M. Malinsky, "Fermion masses in SUSY SO(10) with type II seesaw: A Non-minimal predictive scenario," Phys. Rev. D **70**, 095002 (2004) [hep-ph/0406117].

[31] K. S. Babu and C. Macesanu, "Neutrino masses and mixings in a minimal SO(10) model," Phys. Rev. D **72**, 115003 (2005) [hep-ph/0505200].

[32] A. S. Joshipura and K. M. Patel, "Fermion Masses in SO(10) Models," Phys. Rev. D **83**, 095002 (2011) [arXiv:1102.5148 [hep-ph]].

[33] G. Altarelli and D. Meloni, "A non supersymmetric SO(10) grand unified model for all the physics below M_{GUT}," JHEP **1308**, 021 (2013) [arXiv:1305.1001 [hep-ph]].

[34] A. Dueck and W. Rodejohann, "Fits to SO(10) Grand Unified Models," JHEP **1309**, 024 (2013) [arXiv:1306.4468 [hep-ph]].

[35] C. S. Aulakh and R. N. Mohapatra, "Implications of Supersymmetric SO(10) Grand Unification," Phys. Rev. D **28**, 217 (1983).

[36] T. E. Clark, T. K. Kuo and N. Nakagawa, "A So(10) Supersymmetric Grand Unified Theory," Phys. Lett. B **115**, 26 (1982).

[37] C. S. Aulakh, B. Bajc, A. Melfo, G. Senjanovic and F. Vissani, "The Minimal supersymmetric grand unified theory," Phys. Lett. B **588**, 196 (2004) [hep-ph/0306242].

[38] P. Minkowski, Phys. Lett. B **67** (1977) 421; T. Yanagida, proceedings of the *Workshop on Unified Theories and Baryon Number in the Universe*, Tsukuba, 1979, eds. A. Sawada, A. Sugamoto; S. Glashow, in *Cargese 1979, Proceedings, Quarks and Leptons* (1979); M. Gell-Mann, P. Ramond, R. Slansky, proceedings of the *Supergravity Stony Brook Workshop*, New York, 1979, eds. P. Van Niewenhuizen, D. Freeman; R. Mohapatra, G. Senjanović, "Neutrino Mass and Spontaneous Parity Violation," Phys.Rev.Lett. **44** (1980) 912.

[39] M. Magg and C. Wetterich, "Neutrino Mass Problem and Gauge Hierarchy," Phys. Lett. B **94**, 61 (1980); J. Schechter and J. W. F. Valle, "Neutrino Masses in SU(2) x U(1) Theories," Phys. Rev. D **22**, 2227 (1980); G. Lazarides, Q. Shafi and C. Wetterich, "Proton Lifetime and Fermion Masses in an SO(10) Model," Nucl.

Phys. B **181**, 287 (1981); R. N. Mohapatra and G. Senjanovic, "Neutrino Masses and Mixings in Gauge Models with Spontaneous Parity Violation," Phys. Rev. D **23**, 165 (1981).

[40] R. N. Mohapatra, "Limits on the Mass of the Right-handed Majorana Neutrino," Phys. Rev. D **34**, 909 (1986); A. Font, L. E. Ibanez and F. Quevedo, "Does Proton Stability Imply the Existence of an Extra Z0?," Phys. Lett. B **228**, 79 (1989); S. P. Martin, "Some simple criteria for gauged R-parity," Phys. Rev. D **46**, 2769 (1992) [hep-ph/9207218].

[41] C. S. Aulakh, K. Benakli and G. Senjanovic, "Reconciling supersymmetry and left-right symmetry," Phys. Rev. Lett. **79**, 2188 (1997) [hep-ph/9703434].

[42] C. S. Aulakh, A. Melfo and G. Senjanovic, "Minimal supersymmetric left-right model," Phys. Rev. D **57**, 4174 (1998) [hep-ph/9707256].

[43] C. S. Aulakh, A. Melfo, A. Rasin and G. Senjanovic, "Seesaw and supersymmetry or exact R-parity," Phys. Lett. B **459**, 557 (1999) [hep-ph/9902409].

[44] C. S. Aulakh, B. Bajc, A. Melfo, A. Rasin and G. Senjanovic, "SO(10) theory of R-parity and neutrino mass," Nucl. Phys. B **597**, 89 (2001) [hep-ph/0004031].

[45] B. Bajc, G. Senjanovic and F. Vissani, "How neutrino and charged fermion masses are connected within minimal supersymmetric SO(10)," PoS HEP **2001**, 198 (2001) [hep-ph/0110310].

[46] B. Bajc, G. Senjanovic and F. Vissani, "b - tau unification and large atmospheric mixing: A Case for noncanonical seesaw," Phys. Rev. Lett. **90**, 051802 (2003) [hep-ph/0210207].

[47] B. Bajc, G. Senjanovic and F. Vissani, "Probing the nature of the seesaw in renormalizable SO(10)," Phys. Rev. D **70**, 093002 (2004) [hep-ph/0402140].

[48] C. S. Aulakh, "MSGUTs from germ to bloom: Towards falsifiability and beyond," hep-ph/0506291.

[49] B. Bajc, A. Melfo, G. Senjanovic and F. Vissani, "Fermion mass relations in a supersymmetric SO(10) theory," Phys. Lett. B **634**, 272 (2006) [hep-ph/0511352].

[50] C. S. Aulakh and S. K. Garg, "MSGUT : From bloom to doom," Nucl. Phys. B **757**, 47 (2006) [hep-ph/0512224].

[51] S. Bertolini, T. Schwetz and M. Malinsky, "Fermion masses and mixings in SO(10) models and the neutrino challenge to SUSY GUTs," Phys. Rev. D **73**, 115012 (2006) [hep-ph/0605006].

[52] G. F. Giudice and A. Romanino, "Split supersymmetry," Nucl. Phys. B **699**, 65 (2004), Erratum: [Nucl. Phys. B **706**, 487 (2005)] [hep-ph/0406088].

[53] N. Arkani-Hamed, S. Dimopoulos, G. F. Giudice and A. Romanino, "Aspects of split supersymmetry," Nucl. Phys. B **709**, 3 (2005) [hep-ph/0409232].

[54] B. Bajc, I. Dorsner and M. Nemevsek, "Minimal SO(10) splits supersymmetry," JHEP **0811**, 007 (2008) [arXiv:0809.1069 [hep-ph]].

[55] T. Fukuyama, K. Ichikawa and Y. Mimura, "Revisiting fermion mass and mixing fits in the minimal SUSY $SO(10)$ GUT," Phys. Rev. D **94**, no. 7, 075018 (2016) [arXiv:1508.07078 [hep-ph]].

[56] G. F. Giudice and A. Strumia, "Probing High-Scale and Split Supersymmetry with Higgs Mass Measurements," Nucl. Phys. B **858**, 63 (2012) [arXiv:1108.6077 [hep-ph]].

[57] E. Bagnaschi, G. F. Giudice, P. Slavich and A. Strumia, "Higgs Mass and Unnatural Supersymmetry," JHEP **1409**, 092 (2014) [arXiv:1407.4081 [hep-ph]].

[58] C. S. Aulakh, I. Garg and C. K. Khosa, "Baryon stability on the Higgs dissolution edge: threshold corrections and suppression of baryon violation in the NMSGUT," Nucl. Phys. B **882**, 397 (2014) [arXiv:1311.6100 [hep-ph]].

[59] K. S. Babu, B. Bajc and S. Saad, "New Class of SO(10) Models for Flavor," Phys. Rev. D **94**, no. 1, 015030 (2016) [arXiv:1605.05116 [hep-ph]].

[60] K. S. Babu and S. M. Barr, "An SO(10) solution to the puzzle of quark and lepton masses," Phys. Rev. Lett. **75**, 2088 (1995) [hep-ph/9503215].

[61] M. Yasue, "Symmetry Breaking of SO(10) and Constraints on Higgs Potential. 1. Adjoint (45) and Spinorial (16)," Phys. Rev. D **24**, 1005 (1981).

[62] S. M. Barr, "A New Symmetry Breaking Pattern for SO(10) and Proton Decay," Phys. Lett. B **112**, 219 (1982).

[63] G. Anastaze, J. P. Derendinger and F. Buccella, Z. Phys. C **20**, 269 (1983).

[64] S. Bertolini, L. Di Luzio and M. Malinsky, "On the vacuum of the minimal nonsupersymmetric SO(10) unification," Phys. Rev. D **81**, 035015 (2010) [arXiv:0912.1796 [hep-ph]].

[65] S. Bertolini, L. Di Luzio and M. Malinsky, "The quantum vacuum of the minimal SO(10) GUT," J. Phys. Conf. Ser. **259**, 012098 (2010) [arXiv:1010.0338 [hep-ph]].

[66] M. Yasue, "HOW TO BREAK SO(10) VIA SO(4) x SO(6) DOWN TO SU(2)(L) x SU(3)(C) x U(1)," Phys. Lett. B **103**, 33 (1981).

[67] K. S. Babu and E. Ma, "Symmetry Breaking in SO(10): Higgs Boson Structure," Phys. Rev. D **31**, 2316 (1985).

[68] K. S. Babu and S. Khan, "Minimal nonsupersymmetric $SO(10)$ model: Gauge coupling unification, proton decay, and fermion masses," Phys. Rev. D **92**, no. 7, 075018 (2015) [arXiv:1507.06712 [hep-ph]].

[69] K. S. Babu, I. Gogoladze, P. Nath and R. M. Syed, "A Unified framework for symmetry breaking in SO(10)," Phys. Rev. D **72**, 095011 (2005) [hep-ph/0506312].

[70] D. Chang and A. Kumar, "Symmetry Breaking of SO(10) by 210-dimensional Higgs Boson and the Michel's Conjecture," Phys. Rev. D **33**, 2695 (1986).

[71] T. Fukuyama, A. Ilakovac, T. Kikuchi, S. Meljanac and N. Okada, "SO(10) group theory for the unified model building," J. Math. Phys. **46**, 033505 (2005) [hep-ph/0405300].

[72] S. Antusch and V. Maurer, "Running quark and lepton parameters at various scales," JHEP **1311**, 115 (2013) [arXiv:1306.6879 [hep-ph]].

[73] Z. z. Xing, H. Zhang and S. Zhou, "Updated Values of Running Quark and Lepton Masses," Phys. Rev. D **77**, 113016 (2008) [arXiv:0712.1419 [hep-ph]].

[74] V. D. Barger, M. S. Berger and P. Ohmann, "Supersymmetric grand unified theories: Two loop evolution of gauge and Yukawa couplings," Phys. Rev. D **47**, 1093 (1993) [hep-ph/9209232].

[75] V. D. Barger, M. S. Berger and P. Ohmann, "Universal evolution of CKM matrix elements," Phys. Rev. D **47**, 2038 (1993) [hep-ph/9210260].

[76] G. L. Fogli, E. Lisi, A. Marrone, D. Montanino, A. Palazzo and A. M. Rotunno, "Global analysis of neutrino masses, mixings and phases: entering the era of leptonic CP violation searches," Phys. Rev. D **86**, 013012 (2012) [arXiv:1205.5254 [hep-ph]].

[77] K. S. Babu and S. M. Barr, "Proton decay and realistic models of quark and lepton masses," Phys. Lett. B **381**, 137 (1996) [hep-ph/9506261].

[78] Y. Aoki, E. Shintani and A. Soni, "Proton decay matrix elements on the lattice," Phys. Rev. D **89**, no. 1, 014505 (2014) [arXiv:1304.7424 [hep-lat]].

[79] J. C. Pati and A. Salam, "Lepton Number as the Fourth Color," Phys. Rev. D **10**, 275 (1974) Erratum: [Phys. Rev. D **11**, 703 (1975)].

[80] H. Georgi and S. L. Glashow, "Unity of All Elementary Particle Forces," Phys. Rev. Lett. **32**, 438 (1974).

[81] H. Georgi, H. R. Quinn and S. Weinberg, "Hierarchy of Interactions in Unified Gauge Theories," Phys. Rev. Lett. **33**, 451 (1974).

[82] J. Schechter and J. W. F. Valle, "Neutrino Masses in SU(2) x U(1) Theories," Phys. Rev. D **22**, 2227 (1980); G. Lazarides, Q. Shafi and C. Wetterich, "Proton Lifetime and Fermion Masses in an SO(10) Model," Nucl. Phys. B **181**, 287 (1981); R. N. Mohapatra and G. Senjanović, "Neutrino Masses and Mixings in Gauge Models with Spontaneous Parity Violation," Phys. Rev. D **23**, 165 (1981); C. Wetterich, "Neutrino Masses and the Scale of B-L Violation," Nucl. Phys. B **187**, 343 (1981); J. Schechter and J. W. F. Valle, "Neutrino Decay and Spontaneous Violation of Lepton Number," Phys. Rev. D **25**, 774 (1982).

[83] T. G. Rizzo and G. Senjanović, "Can There Be Low Intermediate Mass Scales in Grand Unified Theories?," Phys. Rev. Lett. **46**, 1315 (1981); T. G. Rizzo and G. Senjanović, "Grand Unification and Parity Restoration at Low-Energies. 1. Phenomenology," Phys. Rev. D **24**, 704 (1981) [Phys. Rev. D **25**, 1447 (1982)]; T. G. Rizzo and G. Senjanović, "Grand Unification and Parity Restoration at Low-energies. 2. Unification Constraints," Phys. Rev. D **25**, 235 (1982).

[84] W. E. Caswell, J. Milutinović, and G. Senjanović, "Predictions of Left-right Symmetric Grand Unified Theories," Phys. Rev. D **26**, 161 (1982).

[85] D. Chang, R. N. Mohapatra and M. K. Parida, "Decoupling Parity and SU(2)-R Breaking Scales: A New Approach to Left-Right Symmetric Models," Phys. Rev. Lett. **52**, 1072 (1984).

[86] J. M. Gipson and R. E. Marshak, "Intermediate Mass Scales in the New SO(10) Grand Unification in the One Loop Approximation," Phys. Rev. D **31**, 1705 (1985).

[87] D. Chang, R. N. Mohapatra, J. Gipson, R. E. Marshak and M. K. Parida, "Experimental Tests of New SO(10) Grand Unification," Phys. Rev. D **31**, 1718 (1985).

[88] N. G. Deshpande, E. Keith and P. B. Pal, "Implications of LEP results for SO(10) grand unification," Phys. Rev. D **46**, 2261 (1993).

[89] N. G. Deshpande, E. Keith and P. B. Pal, "Implications of LEP results for SO(10) grand unification with two intermediate stages," Phys. Rev. D **47**, 2892 (1993) [hep-ph/9211232].

[90] S. Bertolini, L. Di Luzio and M. Malinský, "Intermediate mass scales in the non-supersymmetric SO(10) grand unification: A Reappraisal," Phys. Rev. D **80**, 015013 (2009) [arXiv:0903.4049 [hep-ph]].

[91] L. Gráf, M. Malinský, T. Mede and V. Susič, "One-Loop Pseudo-Goldstone Masses in the Minimal $SO(10)$ Higgs Model," arXiv:1611.01021 [hep-ph].

[92] S. Dimopoulos, S. Raby and F. Wilczek, "Supersymmetry and the Scale of Unification," Phys. Rev. D **24**, 1681 (1981); L. E. Ibáñez and G. G. Ross, "Low-Energy Predictions in Supersymmetric Grand Unified Theories," Phys. Lett. B **105**, 439 (1981); M. B. Einhorn and D. R. T. Jones, "The Weak Mixing Angle and Unification Mass in Supersymmetric SU(5)," Nucl. Phys. B **196**, 475 (1982); W. J. Marciano and G. Senjanović, "Predictions of Supersymmetric Grand Unified Theories," Phys. Rev. D **25**, 3092 (1982).

[93] K. S. Babu, B. Bajc and S. Saad, "Yukawa Sector of Minimal SO(10) Unification," JHEP **1702**, 136 (2017) [arXiv:1612.04329 [hep-ph]].

[94] K. S. Babu and S. M. Barr, "An SO(10) solution to the puzzle of quark and lepton masses," Phys. Rev. Lett. **75**, 2088 (1995) [hep-ph/9503215].

[95] G. Lazarides, Q. Shafi and C. Wetterich, "Proton Lifetime and Fermion Masses in an SO(10) Model," Nucl. Phys. B **181**, 287 (1981).

[96] A. Davidson, V. P. Nair and K. C. Wali, "Mixing Angles and CP Violation in the $SO(10) \times U(1)_{(pq)}$ Model," Phys. Rev. D **29**, 1513 (1984).

[97] G. Lazarides and Q. Shafi, "Fermion masses and mixings in SO(10)," Nucl. Phys. B **350**, 179 (1991).

[98] D. G. Lee and R. N. Mohapatra, "An SO(10) x S(4) scenario for naturally degenerate neutrinos," Phys. Lett. B **329**, 463 (1994) [hep-ph/9403201].

[99] B. Bajc, A. Melfo, G. Senjanović and F. Vissani, "Yukawa sector in non-supersymmetric renormalizable SO(10)," Phys. Rev. D **73**, 055001 (2006) [hep-ph/0510139].

[100] W. M. Yang and Z. G. Wang, "Fermion masses and flavor mixing in a supersymmetric SO(10) model," Nucl. Phys. B **707**, 87 (2005) [hep-ph/0406221].

[101] B. Dutta, Y. Mimura and R. N. Mohapatra, "Suppressing proton decay in the minimal SO(10) model," Phys. Rev. Lett. **94**, 091804 (2005) [hep-ph/0412105].

[102] C. S. Aulakh and S. K. Garg, "The New Minimal Supersymmetric GUT : Spectra, RG analysis and Fermion Fits," Nucl. Phys. B **857**, 101 (2012) [arXiv:0807.0917 [hep-ph]].

[103] M. C. Chen and K. T. Mahanthappa, "Fermion masses and mixing and CP violation in SO(10) models with family symmetries," Int. J. Mod. Phys. A **18**, 5819 (2003) [hep-ph/0305088].

[104] W. Grimus and H. Kuhbock, "Fermion masses and mixings in a renormalizable $SO(10) \times Z(2)$ GUT," Phys. Lett. B **643**, 182 (2006) [hep-ph/0607197].

[105] Y. Cai and H. B. Yu, "A SO(10) GUT Model with S4 Flavor Symmetry," Phys. Rev. D **74**, 115005 (2006) [hep-ph/0608022].

[106] A. Albaid, "Flavor Violation in a Minimal $SO(10) \times A_4$ SUSY GUT," Int. J. Mod. Phys. A **27**, 1250005 (2012) [arXiv:1106.4070 [hep-ph]].

[107] P. M. Ferreira, W. Grimus, D. Jurčiukonis and L. Lavoura, "Flavour symmetries in a renormalizable SO(10) model," Nucl. Phys. B **906**, 289 (2016) [arXiv:1510.02641 [hep-ph]].

[108] E. Witten, "Neutrino Masses in the Minimal O(10) Theory," Phys. Lett. **91B**, 81 (1980).

[109] B. Bajc and G. Senjanović, "Radiative seesaw: A Case for split supersymmetry," Phys. Lett. B **610**, 80 (2005) [hep-ph/0411193].

[110] M. E. Machacek and M. T. Vaughn, "Two Loop Renormalization Group Equations in a General Quantum Field Theory. 2. Yukawa Couplings," Nucl. Phys. B **236**, 221 (1984); H. Arason, D. J. Castaño, B. Keszthelyi, S. Mikaelian, E. J. Piard, P. Ramond and B. D. Wright, "Renormalization group study of the standard model and its extensions. 1. The Standard model," Phys. Rev. D **46**, 3945 (1992).

[111] K. S. Babu, "Renormalization Group Analysis of the Kobayashi-Maskawa Matrix," Z. Phys. C **35**, 69 (1987).

[112] K. S. Babu, C. N. Leung and J. T. Pantaleone, "Renormalization of the neutrino mass operator," Phys. Lett. B **319**, 191 (1993) [hep-ph/9309223]; S. Antusch, M. Drees, J. Kersten, M. Lindner and M. Ratz, "Neutrino mass operator renormalization revisited," Phys. Lett. B **519**, 238 (2001) [hep-ph/0108005].

[113] H. Georgi, "Towards a Grand Unified Theory of Flavor," Nucl. Phys. B **156**, 126 (1979).

[114] F. del Aguila and L. E. Ibáñez, "Higgs Bosons in SO(10) and Partial Unification," Nucl. Phys. B **177**, 60 (1981).

[115] R. N. Mohapatra and G. Senjanović, "Higgs Boson Effects in Grand Unified Theories," Phys. Rev. D **27**, 1601 (1983).

[116] D. R. T. Jones, "The Two Loop beta Function for a G(1) x G(2) Gauge Theory," Phys. Rev. D **25**, 581 (1982).

[117] H. Nishino *et al.* [Super-Kamiokande Collaboration], "Search for Nucleon Decay into Charged Anti-lepton plus Meson in Super-Kamiokande I and II," Phys. Rev. D **85**, 112001 (2012) [arXiv:1203.4030 [hep-ex]].

[118] M. Machacek, "The Decay Modes of the Proton," Nucl. Phys. B **159**, 37 (1979).

[119] P. Fileviez Perez, "Fermion mixings versus d = 6 proton decay," Phys. Lett. B **595**, 476 (2004) [hep-ph/0403286].

[120] P. Nath and P. Fileviez Perez, "Proton stability in grand unified theories, in strings and in branes," Phys. Rept. **441**, 191 (2007) [hep-ph/0601023].

[121] Y. Fukuda *et al.* [Super-Kamiokande Collaboration], "Evidence for oscillation of atmospheric neutrinos," Phys. Rev. Lett. **81**, 1562 (1998) [hep-ex/9807003].

[122] Q. R. Ahmad *et al.* [SNO Collaboration], "Direct evidence for neutrino flavor transformation from neutral current interactions in the Sudbury Neutrino Observatory," Phys. Rev. Lett. **89**, 011301 (2002) [nucl-ex/0204008].

[123] K. Abe *et al.* [T2K Collaboration], "Indication of Electron Neutrino Appearance from an Accelerator-produced Off-axis Muon Neutrino Beam," Phys. Rev. Lett. **107**, 041801 (2011) [arXiv:1106.2822 [hep-ex]]; P. Adamson *et al.* [MINOS Collaboration], "Improved search for muon-neutrino to electron-neutrino oscillations in MINOS," Phys. Rev. Lett. **107**, 181802 (2011) [arXiv:1108.0015 [hep-ex]].

[124] Y. Abe *et al.* [Double Chooz Collaboration], "Indication for the disappearance of reactor electron antineutrinos in the Double Chooz experiment," Phys. Rev. Lett. **108**, 131801 (2012) [arXiv:1112.6353 [hep-ex]]; F. P. An *et al.* [Daya Bay Collaboration], "Observation of electron-antineutrino disappearance at Daya Bay," Phys. Rev. Lett. **108**, 171803 (2012) [arXiv:1203.1669 [hep-ex]]; J. K. Ahn *et al.* [RENO Collaboration], "Observation of Reactor Electron Antineutrino Disappearance in the RENO Experiment," Phys. Rev. Lett. **108**, 191802 (2012) [arXiv:1204.0626 [hep-ex]].

[125] C. Patrignani *et al.* [Particle Data Group], "Review of Particle Physics," Chin. Phys. C **40**, no. 10, 100001 (2016).

[126] K. S. Babu, "TASI Lectures on Flavor Physics," arXiv:0910.2948 [hep-ph].

[127] L. J. Hall, H. Murayama and N. Weiner, "Neutrino mass anarchy," Phys. Rev. Lett. **84**, 2572 (2000) [hep-ph/9911341].

[128] N. Haba and H. Murayama, "Anarchy and hierarchy," Phys. Rev. D **63**, 053010 (2001) [hep-ph/0009174].

[129] G. Altarelli, F. Feruglio and I. Masina, "Models of neutrino masses: Anarchy versus hierarchy," JHEP **0301**, 035 (2003) [hep-ph/0210342].

[130] A. de Gouvea and H. Murayama, "Statistical test of anarchy," Phys. Lett. B **573**, 94 (2003) [hep-ph/0301050].

[131] J. R. Espinosa, "Anarchy in the neutrino sector?," hep-ph/0306019.

[132] A. de Gouvea and H. Murayama, "Neutrino Mixing Anarchy: Alive and Kicking," Phys. Lett. B **747**, 479 (2015) [arXiv:1204.1249 [hep-ph]].

[133] G. Altarelli, F. Feruglio, I. Masina and L. Merlo, "Repressing Anarchy in Neutrino Mass Textures," JHEP **1211**, 139 (2012) [arXiv:1207.0587 [hep-ph]].

[134] V. Brdar, M. Konig and J. Kopp, "Neutrino Anarchy and Renormalization Group Evolution," Phys. Rev. D **93**, no. 9, 093010 (2016) [arXiv:1511.06371 [hep-ph]].

[135] J. F. Fortin, N. Giasson and L. Marleau, "Probability density function for neutrino masses and mixings," Phys. Rev. D **94**, no. 11, 115004 (2016) [arXiv:1609.08581 [hep-ph]].

[136] M. L. Mehta, Random matrices, Vol. 142 (Academic press, 2004).

[137] Y. Bai and G. Torroba, "Large N (=3) Neutrinos and Random Matrix Theory," JHEP **1212**, 026 (2012) [arXiv:1210.2394 [hep-ph]].

[138] J. Bergstrom, D. Meloni and L. Merlo, "Bayesian comparison of U(1) lepton flavor models," Phys. Rev. D **89**, no. 9, 093021 (2014) [arXiv:1403.4528 [hep-ph]].

[139] X. Lu and H. Murayama, "Neutrino Mass Anarchy and the Universe," JHEP **1408**, 101 (2014) [arXiv:1405.0547 [hep-ph]].

[140] K. S. Babu and S. M. Barr, "Large neutrino mixing angles in unified theories," Phys. Lett. B **381**, 202 (1996) [hep-ph/9511446].

[141] K. S. Babu, A. Khanov and S. Saad, "Anarchy with Hierarchy: A Probabilistic Appraisal," Phys. Rev. D **95**, no. 5, 055014 (2017) [arXiv:1612.07787 [hep-ph]].

[142] M. J. Strassler, "Generating a fermion mass hierarchy in a composite supersymmetric standard model," Phys. Lett. B **376**, 119 (1996) [hep-ph/9510342].

[143] A. E. Nelson and M. J. Strassler, "A Realistic supersymmetric model with composite quarks," Phys. Rev. D **56**, 4226 (1997) [hep-ph/9607362].

[144] C. D. Froggatt and H. B. Nielsen, "Hierarchy of Quark Masses, Cabibbo Angles and CP Violation," Nucl. Phys. B **147**, 277 (1979).

[145] K. S. Babu, T. Enkhbat and I. Gogoladze, "Anomalous U(1) symmetry and lepton flavor violation," Nucl. Phys. B **678**, 233 (2004) [hep-ph/0308093].

[146] K. S. Babu and T. Enkhbat, "Fermion mass hierarchy and electric dipole moments," Nucl. Phys. B **708**, 511 (2005) [hep-ph/0406003].

[147] K. Agashe, T. Okui and R. Sundrum, "A Common Origin for Neutrino Anarchy and Charged Hierarchies," Phys. Rev. Lett. **102**, 101801 (2009) [arXiv:0810.1277 [hep-ph]].

[148] F. Feruglio, K. M. Patel and D. Vicino, "Order and Anarchy hand in hand in 5D SO(10)," JHEP **1409**, 095 (2014) [arXiv:1407.2913 [hep-ph]].

[149] F. Brummer, S. Fichet and S. Kraml, "The Supersymmetric flavour problem in 5D GUTs and its consequences for LHC phenomenology," JHEP **1112**, 061 (2011) [arXiv:1109.1226 [hep-ph]].

[150] K. Yoshioka, "On fermion mass hierarchy with extra dimensions," Mod. Phys. Lett. A **15**, 29 (2000) [hep-ph/9904433].

[151] C. H. Albright, K. S. Babu and S. M. Barr, "A Minimality condition and atmospheric neutrino oscillations," Phys. Rev. Lett. **81**, 1167 (1998) [hep-ph/9802314].

[152] J. Sato and T. Yanagida, "Large lepton mixing in a coset space family unification on E(7) / SU(5) x U(1)**3," Phys. Lett. B **430**, 127 (1998) [hep-ph/9710516].

[153] N. Irges, S. Lavignac and P. Ramond, "Predictions from an anomalous U(1) model of Yukawa hierarchies," Phys. Rev. D **58**, 035003 (1998) [hep-ph/9802334].

[154] N. Maekawa, "Neutrino masses, anomalous U(1) gauge symmetry and doublet - triplet splitting," Prog. Theor. Phys. **106**, 401 (2001) [hep-ph/0104200].

[155] H. Georgi and C. Jarlskog, "A New Lepton - Quark Mass Relation in a Unified Theory," Phys. Lett. B **86**, 297 (1979).

[156] See for e.g., I. Dorsner and P. Fileviez Perez, "Unification versus proton decay in SU(5)," Phys. Lett. B **642**, 248 (2006) [hep-ph/0606062].

[157] N. Haba, "Composite model with neutrino large mixing," Phys. Rev. D **59**, 035011 (1999) [hep-ph/9807552].

[158] S. M. Barr and H. Y. Chen, "A Simple Grand Unified Relation between Neutrino Mixing and Quark Mixing," JHEP **1211**, 092 (2012) [arXiv:1208.6546 [hep-ph]].

[159] S. M. Barr and H. Y. Chen, "Model of quark and lepton mixing and mass hierarchy," Phys. Rev. D **93**, no. 5, 053009 (2016) [arXiv:1511.05989 [hep-ph]].

[160] J. F. Donoghue, K. Dutta and A. Ross, "Quark and lepton masses and mixing in the landscape," Phys. Rev. D **73**, 113002 (2006) [hep-ph/0511219].

[161] J. C. Pati and A. Salam, "Unified Lepton-Hadron Symmetry and a Gauge Theory of the Basic Interactions," Phys. Rev. D **8**, 1240 (1973).

[162] J. C. Pati and A. Salam, "Is Baryon Number Conserved?," Phys. Rev. Lett. **31**, 661 (1973).

[163] J. C. Pati, A. Salam and U. Sarkar, "Delta B = - Delta L, neutron —> e- pi+, e- K+, mu- pi+ and mu- K+ DECAY modes in SU(2)-L X SU(2)-R X SU(4)-C or SO(10)," Phys. Lett. B **133**, 330 (1983).

[164] G. Valencia and S. Willenbrock, "Quark - lepton unification and rare meson decays," Phys. Rev. D **50**, 6843 (1994) [hep-ph/9409201].

[165] A. D. Smirnov, "Mass limits for scalar and gauge leptoquarks from K(L)0 —> e-+ mu+-, B0 —> e-+ tau+- decays," Mod. Phys. Lett. A **22**, 2353 (2007) [arXiv:0705.0308 [hep-ph]].

[166] L. F. Li, "Group Theory of the Spontaneously Broken Gauge Symmetries," Phys. Rev. D **9**, 1723 (1974).

[167] R. D. Peccei and H. R. Quinn, "CP Conservation in the Presence of Instantons," Phys. Rev. Lett. **38**, 1440 (1977).

[168] R. D. Peccei and H. R. Quinn, "Constraints Imposed by CP Conservation in the Presence of Instantons," Phys. Rev. D **16**, 1791 (1977).

[169] S. Weinberg, "A New Light Boson?," Phys. Rev. Lett. **40**, 223 (1978).

[170] F. Wilczek, "Problem of Strong p and t Invariance in the Presence of Instantons," Phys. Rev. Lett. **40**, 279 (1978).

[171] R. Kuchimanchi, "Leptonic CP problem in left-right symmetric model," Phys. Rev. D **91**, no. 7, 071901 (2015) [arXiv:1408.6382 [hep-ph]].

[172] J. E. Kim, "A Review on axions and the strong CP problem," AIP Conf. Proc. **1200**, 83 (2010) [arXiv:0909.3908 [hep-ph]].

[173] J. E. Kim and G. Carosi, "Axions and the Strong CP Problem," Rev. Mod. Phys. **82**, 557 (2010) [arXiv:0807.3125 [hep-ph]].

[174] M. Fukugita and T. Yanagida, "Baryogenesis Without Grand Unification," Phys. Lett. B **174**, 45 (1986).

[175] J. C. Pati, "Leptogenesis within a predictive G(224) / SO(10) framework," hep-ph/0209160.

[176] F. Buccella, D. Falcone and L. Oliver, "Baryogenesis via leptogenesis from quark-lepton symmetry and a compact heavy N_R spectrum," Phys. Rev. D **83**, 093013 (2011) [arXiv:1006.5698 [hep-ph]].

[177] N. Okada and Q. Shafi, "θ_{13}, CP Violation and Leptogenesis in Minimal Supersymmetric $SU(4)_c \times SU(2)_L \times SU(2)_R$" arXiv:1109.4963 [hep-ph].

[178] F. Buccella, D. Falcone, C. S. Fong, E. Nardi and G. Ricciardi, "Squeezing out predictions with leptogenesis from SO(10)," Phys. Rev. D **86**, 035012 (2012) [arXiv:1203.0829 [hep-ph]].

[179] P. Di Bari and S. F. King, "Successful N_2 leptogenesis with flavour coupling effects in realistic unified models," JCAP **1510**, no. 10, 008 (2015) [arXiv:1507.06431 [hep-ph]].

[180] V. A. Kuzmin, V. A. Rubakov and M. E. Shaposhnikov, "On the Anomalous Electroweak Baryon Number Nonconservation in the Early Universe," Phys. Lett. B **155**, 36 (1985).

[181] R. Barbieri, P. Creminelli, A. Strumia and N. Tetradis, "Baryogenesis through leptogenesis," Nucl. Phys. B **575**, 61 (2000) [hep-ph/9911315].

[182] A. Abada, S. Davidson, F. X. Josse-Michaux, M. Losada and A. Riotto, "Flavor issues in leptogenesis," JCAP **0604**, 004 (2006) [hep-ph/0601083].

[183] A. Abada, S. Davidson, A. Ibarra, F.-X. Josse-Michaux, M. Losada and A. Riotto, "Flavour Matters in Leptogenesis," JHEP **0609**, 010 (2006) [hep-ph/0605281].

[184] S. Blanchet and P. Di Bari, "Flavor effects on leptogenesis predictions," JCAP **0703**, 018 (2007) [hep-ph/0607330].

[185] S. Antusch, S. F. King and A. Riotto, "Flavour-Dependent Leptogenesis with Sequential Dominance," JCAP **0611**, 011 (2006) [hep-ph/0609038].

[186] E. Nardi, Y. Nir, E. Roulet and J. Racker, "The Importance of flavor in leptogenesis," JHEP **0601**, 164 (2006) [hep-ph/0601084].

[187] S. Davidson and A. Ibarra, "A Lower bound on the right-handed neutrino mass from leptogenesis," Phys. Lett. B **535**, 25 (2002) [hep-ph/0202239].

[188] A. de Gouvea and J. Jenkins, "The Physical Range of Majorana Neutrino Mixing Parameters," Phys. Rev. D **78**, 053003 (2008) [arXiv:0804.3627 [hep-ph]].

[189] R. Slansky, "Group Theory for Unified Model Building," Phys. Rept. **79**, 1 (1981).

[190] K. S. Babu, R. N. Mohapatra and S. Nasri, "Post-Sphaleron Baryogenesis," Phys. Rev. Lett. **97**, 131301 (2006) [hep-ph/0606144].

[191] K. S. Babu, R. N. Mohapatra and S. Nasri, "Unified TeV Scale Picture of Baryogenesis and Dark Matter," Phys. Rev. Lett. **98**, 161301 (2007) [hep-ph/0612357].

[192] K. S. Babu, P. S. Bhupal Dev and R. N. Mohapatra, "Neutrino mass hierarchy, neutron - anti-neutron oscillation from baryogenesis," Phys. Rev. D **79**, 015017 (2009) [arXiv:0811.3411 [hep-ph]].

[193] K. S. Babu, P. S. Bhupal Dev, E. C. F. S. Fortes and R. N. Mohapatra, "Post-Sphaleron Baryogenesis and an Upper Limit on the Neutron-Antineutron Oscillation Time," Phys. Rev. D **87**, no. 11, 115019 (2013) [arXiv:1303.6918 [hep-ph]].

[194] E. C. F. S. Fortes, K. S. Babu and R. N. Mohapatra, arXiv:1311.4101 [hep-ph].

[195] R. N. Mohapatra and R. E. Marshak, "Local B-L Symmetry of Electroweak Interactions, Majorana Neutrinos and Neutron Oscillations," Phys. Rev. Lett. **44**, 1316 (1980) [Phys. Rev. Lett. **44**, 1643 (1980)].

[196] J. C. Pati, "Nucleon Decays Into Lepton + Lepton + Anti-lepton + Mesons Within SU(4) of Color," Phys. Rev. D **29**, 1549 (1984).

[197] S. Rudaz, "Chiral symmetry, broken scale invariance and the nuclear equation of state," In *Paris 1992, Proceedings, QCD vacuum structure* 146-152, and Minnesota U. Minneapolis - UMN-TH-92-1124 (92/10,rec.Feb.93) 8 p.

[198] P. J. O'Donnell and U. Sarkar, "Three lepton decay mode of the proton," Phys. Lett. B **316**, 121 (1993) [hep-ph/9307254].

[199] B. Brahmachari, P. J. O'Donnell and U. Sarkar, "A Model for the three lepton decay mode of the proton," Z. Phys. C **74**, 171 (1997) [hep-ph/9406371].

[200] S. Weinberg, "Baryon and Lepton Nonconserving Processes," Phys. Rev. Lett. **43**, 1566 (1979).

[201] S. Weinberg, "Varieties of Baryon and Lepton Nonconservation," Phys. Rev. D **22**, 1694 (1980).

[202] F. Wilczek and A. Zee, "Operator Analysis of Nucleon Decay," Phys. Rev. Lett. **43**, 1571 (1979).

[203] H. A. Weldon and A. Zee, Nucl. Phys. B **173**, 269 (1980). doi:10.1016/0550-3213(80)90218-7

[204] V. Takhistov *et al.* [Super-Kamiokande Collaboration], "Search for Trilepton Nucleon Decay via $p \to e^+\nu\nu$ and $p \to \mu^+\nu\nu$ in the Super-Kamiokande Experiment," Phys. Rev. Lett. **113**, no. 10, 101801 (2014) [arXiv:1409.1947 [hep-ex]].

[205] K. S. Babu and R. N. Mohapatra, "B-L Violating Nucleon Decay and GUT Scale Baryogenesis in SO(10)," Phys. Rev. D **86**, 035018 (2012) [arXiv:1203.5544 [hep-ph]].

[206] D. G. Phillips, II *et al.*, "Neutron-Antineutron Oscillations: Theoretical Status and Experimental Prospects," Phys. Rept. **612**, 1 (2016) [arXiv:1410.1100 [hep-ex]].

[207] K. Abe *et al.* [Super-Kamiokande Collaboration], "The Search for $n - \bar{n}$ oscillation in Super-Kamiokande I," Phys. Rev. D **91**, 072006 (2015) [arXiv:1109.4227 [hep-ex]].

[208] M. Baldo-Ceolin *et al.*, Z. Phys. C **63**, 409 (1994). doi:10.1007/BF01580321

VITA

Shaikh Saad

Candidate for the Degree of

Doctor of Philosophy

Dissertation: **FERMION MASSES AND MIXINGS, LEPTOGENESIS AND BARYON NUMBER VIOLATION IN UNIFIED THEORIES**

Major Field: Physics

Biographical:

Education:

Completed the requirements for the degree of Doctor of Philosophy with a major in Physics at Oklahoma State University in July, 2017.
Received M.Sc. in Theoretical Physics, Department of Theoretical Physics, University of Dhaka, Dhaka, Bangladesh in 2010.
Received B.Sc. (Hons.), Department of Physics, University of Dhaka, Dhaka, Bangladesh in 2009.

Recognition:

Travel award (2017), "Phenomenology Symposium 2017", University of Pittsburgh, USA.
Outstanding Research Assistant (category: theoretical physics, 2016), Department of Physics, Oklahoma State University, USA.
Graduate Summer Research Fellowship (2016), Oklahoma State University, USA.
Travel award, "Phenomenology Symposium 2015", University of Pittsburgh, USA from GPSGA, Oklahoma State University, USA.
Travel award and Living allowance, CETUP* 2015; "Neutrino Physics and Beyond Standard Model", Lead, South Dakota, USA.